Safety in Mines Research Advisory Committee

Final Project Report

Coal pillar design procedures

G. York, I. Canbulat, B.W. Jack

Research agency: CSIR Mining Technology

Project number: COL 337

Date: March 2000

Executive Summary

Examination of collapsed pillar cases outside of the empirical limits of Salamon and Munro's *in situ* database has highlighted the need for additional parameters to be considered in the design of coal pillars. These include the influence of discontinuities, surrounding strata characteristics and the effects of deterioration and time.

An underground pillar monitoring exercise was successful, until the dynamic collapse failure of the pillar, which was not recorded due to the manual nature of the recording. A continuous logging system is vital for further such experiments. Increased certainty is required with respect to whether the pillar was confined by a goaf, before more definite conclusions can be made. This requires a different support strategy, such as long hole cable anchors.

Joint frequency, joint condition and joint orientation have an important effect on the strength of coal pillars. A new methodology has been developed to take these effects into account. An evaluation of the field data showed that pillars without any joint structures are likely to be about 10 per cent stronger than predicted by the empirical Salamon and Munro equation.

A simple and flexible technique to incorporate the effect of scaling, or time effects, into pillar design, has been produced. Pillars may be designed by specifying a probability of survival for a given number of years. Alternatively, it might be required that the probability of survival for an indefinite period should not be less than a specific value. Real rates of scaling for different geotechnical areas are required for the technique to become practical.

An analysis of geotechnical data according to the dimensions of discontinuity and roof rating from a substantial database allowed the identification of eight distinct geotechnical areas in South African collieries.

The size effect at the *in situ* scale, if present at all, is negligible. A representative value of *in situ* critical rock mass strength, Θ_c, is 6.3 MPa. It has been shown that significant (in the statistical sense) differences in coal material strength detected in the laboratory can lead to a modification of Θ_c.

The effect of variations of the pillar / roof or floor contact conditions on the width to height ratio (w/h) effect on pillar strength have been catered for by means of a design chart. The 99 per cent confidence interval for the *in situ* contact friction angle is 21.0° to 24.8°.

The results of these investigations have been put together to form the basis of a new methodology for pillar design. A pillar design flowchart has been produced. The modular approach to pillar design, with explicit quantification of the influence of Θ_c, jointing, w/h and

roof / floor contact conditions, allows scope for site or geotechnical area specific pillar design. However, this also requires site specific measurements of geotechnical parameters.

There are a number of issues not yet resolved. Among them are:

1) the proposed new design methodology requires underground verification

2) the effect of coaltopping has not been determined

3) the factors that form part of the pillar design methodology have been assumed to act in series; this is not necessarily the case.

A trial period is suggested in which rock engineers make use of the new methodology in different areas and compare results so that confidence is built up in their applicability in different geological settings.

Acknowledgements

This project has been funded by the Safety in Mines Research Advisory Committee. CSIR Miningtek extends grateful acknowledgement to Ingwe Rock Engineering for help extended.

CSIR Miningtek would like to extend appreciation to Dr B.J. Madden and Mr G.D. Prohaska for their work in this project while in the employ of CSIR Miningtek.

Table of Contents

List of Figures

List of Tables

Glossary

Abbreviations

APS	average pillar stress
l/w	ratio of length to width of a pillar
UCS	uniaxial compressive strength
w/h	w/h ratio

Symbols and technical terms

1-a	the slope of the strength – w/h straight line fit normalised to Θ
a	the intercept of the linear pillar strength function normalised to Θ
ϕ	angle of internal friction (in Chapter 6)
ϕ	peak joint friction angle (in Chapter 2)
ϕ_c	contact friction angle
c	cohesion
f_j	pillar strength reduction factor accounting for the joint sets on both orthogonal faces of the pillar: $f_j = f_1 \times f_2$
f_1, f_2	pillar strength reduction factors for each orthogonal face in turn
k ratio	ratio of horizontal to vertical virgin stresses
ρ	the density of rock
s	sample standard deviation
s_m	sample standard deviation / mean of the sample, expressed as a percentage
S	expected pillar strength based on laboratory testing
S_a	expected pillar strength taking contact conditions, the critical rock mass strength and jointing into account
S_c	expected pillar strength taking the contact conditions and the critical rock mass strength into account
Θ	the strength of a pillar or model pillar of w/h=1
Θ_c	the critical rock mass strength

1 Update of pillar failures and collate cases of instability or poor performance

1.1 Introduction

South Africa has led the world in pillar design research since the Coalbrook Colliery disaster of 1960, in which more than 7 000 pillars collapsed, 4 400 within a 5 minute period. Intensive research since this disaster has resulted in design formulae and guidelines which have provided the South African coal industry with methodologies for the safe extraction of a valuable resource.

Previous research has provided:

- a pillar design formula for permanent bord and pillar workings
- methods for the determination of pillar deformation characteristics
- squat pillar design formula
- pillar design when using a continuous miner
- barrier pillar design guidelines
- design of shallow workings
- pillar extraction guidelines
- multi-seam design guidelines
- pillar and rib pillar extraction guidelines

Early this century this more rational approach to the determination of coal pillar strength began with the testing of coal specimens in the laboratory. While general trends were quickly established, (such as a decrease in the specimen strength with increasing height and size and an increase in strength with increasing width), the wide scatter of results made the extrapolation of strength results to full size pillars extremely difficult. In order to overcome the limitations of the laboratory tests, testing of large in situ samples was initiated. These experiments had the advantage of being conducted in the underground environment and yielded valuable information regarding the stress-strain behaviour of coal pillars. However, these tests were time consuming,

expensive and did not overcome the problem of extrapolation of results to full size pillars nor to other seams or geological environments.

Current coal pillar research (in rock engineering) is focused on improving the understanding of both the behaviour of the surrounding strata and the application and limitations of the South African coal pillar design procedures. As virgin reserves are depleted, the extraction of existing pillars becomes more likely, pillars formed today could be extracted at a future date; in some cases, well into the 21st century. Therefore, the understanding of the long term stability of pillars becomes more critical in terms of both the safety of underground workers during extraction procedures and a valuable national resource.

A further consideration is that increasingly difficult mining conditions under increasing production cost pressures in a competitive world market will be the challenge of the future. To meet that challenge, understanding of the way that the strata behave around the coal seam will be crucial.

For a stable mining operation, three elements of the system need consideration: the roof strata, coal seam and floor strata. Since all are interrelated, failure of only one of these elements results in failure of the system, adversely affecting the mining operation and jeopardising the safety of the workers.

This chapter reviews the research into pillar design for the period 1965-1995 as well as the collapses that occurred in South Africa between 1965 - 1997.

1.2 Review of South African coal pillar design research

In South Africa an intensive investigation into the strength of coal pillars was initiated through the statistical analysis of 98 intact and 27 collapsed pillar geometries by Salamon and Munro (1967) using a probabilistic notion of safety factor, defined as:

$$\text{Safety factor} = \frac{\text{strength}}{\text{load}} \qquad \textit{Equation 1-1.}$$

The values for strength and load must be regarded as predictions which are subject to error.

Salamon (1967) thought it reasonable to suppose that the majority of mining engineers arrived at an acceptable compromise between safety and economic mining, with the optimum safety factor lying in the range where 50 per cent of the stable cases are most densely concentrated. This occurs between safety factors of 1.3 to 1.9 with the mean being 1.6 and it is this value that was recommended for the design of production pillars in South African bord and pillar workings.

Load is calculated using the modified cover load or Tributary Area Theory, where each individual pillar is assumed to carry the weight of the overburden immediately above it. This assumption applies where the pillars are of uniform size and the panel width is larger than the depth to the seam. These conditions are fulfilled by the majority of bord and pillar panels in South African collieries.

Strength is taken to mean the strength of a coal pillar as opposed to the strength of a coal specimen. The strength of a pillar was said to depend on the material strength as well as the pillar's volume and shape. The shape effect was said to be a result of constraints imposed on the pillar through friction or cohesion by the roof and floor.

The formula for strength was given as:

$$S = kh^{\alpha}w^{\beta} \qquad \textit{Equation 1-2}$$

where k = 7 176 kPa, α = -0.66 and β = 0.46. Figure 1-1 shows the intact and collapsed cases using these values. Salamon and Munro)1967) stated that the scatter of results was due to three major causes:

1) natural causes - that is, variations in coal strength, seam structure and the quality of the roof and floor;

2) the approximate nature of the strength formula; and

3) human error.

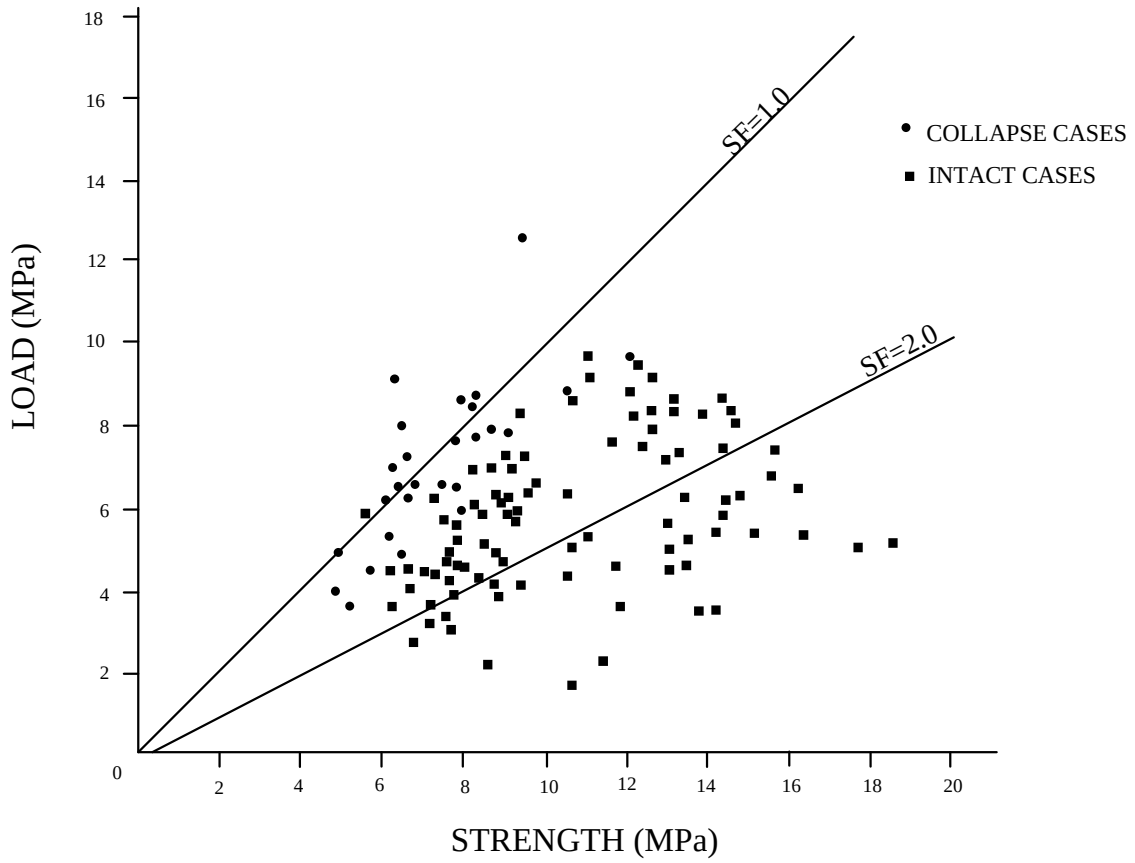

Figure 1-1 Tributary Area Loads as a function of calculated pillar strengths for collapsed and stable areas of mining. After Salamon and Munro (1967).

Salamon (1967) emphasised that the pillar strength formula was essentially empirical and therefore should not be extended beyond the range of data (Table 1-1) used to derive it. Furthermore, the assumption in the formula of one average strength for all coal seams was recognised by him as a possible limitation.

Salamon and Oravecz (1976) considered the strength formula to be conservative when the width to height exceeded five or six and that a pillar with a width to height of 10 was considered virtually indestructible.

Between 1963 and 1969 considerable effort was made to determine the strength of coal from the Witbank Coalfield. Coal strengths and material properties for Nos. 1, 2 and 4 Seam from the Wolvekrans Section of the Witbank Colliery in the Witbank Coalfield were recorded by Wiid (1963). While differences in seam strength were indicated by the results, there was considerable scatter and overlap of strength values between the three seams.

Results of tests conducted on the No. 2 Seam at Wolvekrans Section, Witbank Colliery, were reported in a CSIR report (1965). This testing programme was conducted underground in order to overcome the resulting effects on coal specimens from the difference between underground and laboratory temperatures and in humidity levels, which in turn affect the moisture content. In addition, the deterioration of the specimens through transportation would be eliminated

The effect of specimen size on strength is clearly seen in Figure 1-2, where a significant reduction in strength occurs with increasing specimen size.

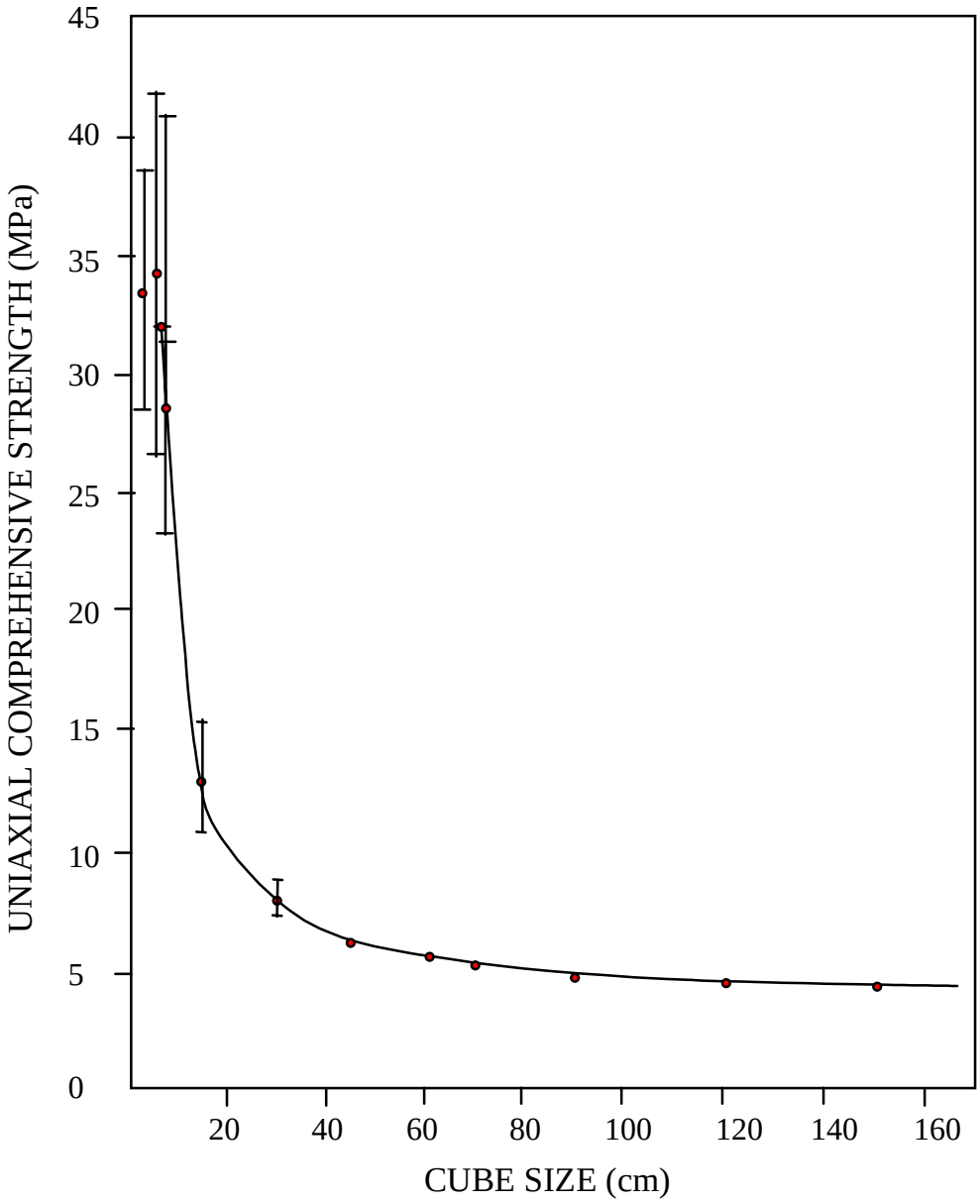

Figure 1-2 The effect of specimen size on the strength of coal. After Bieniawski (1968).

The laboratory investigations into the strengths of individual South African coal seams showed that, while quantitative differences occur, the determination of individual seam strength is

influenced by many factors including specimen transportation, preparation, moisture content, position in the seam and size. However, in the larger specimens there was less scatter in the test results obtained.

Extensive in situ testing was conducted in South Africa during the period 1966 to 1974. The feasibility of conducting large scale in situ tests in South Africa was investigated at the Wolvekrans Section, Witbank Colliery, in the No. 4 Seam by Hoek (1966). Following on from this report, a substantial in situ testing programme was conducted over an eight year period by the Chamber of Mines Research Organization (now Division of Mining Technology, CSIR) and the CSIR with 91 in situ tests being conducted which were summarised by Bieniawski and van Heerden (1975). Bieniawski and Mulligan (1967) concluded that there would be no decrease in the strength of a sample beyond a 5 foot cube.

Concurrent with the CSIR testing programme, in situ tests were conducted by Cook et al (1971) and Wagner (1974). A major finding of this work was the realisation that the centre portion of a pillar was capable of withstanding extremely high stresses, even when the pillar had been compressed beyond its maximum resistance, which is traditionally regarded as the strength of the pillar. Other important findings were that the strength of circumferential portions of a pillar were virtually independent of the sample width to height ratio, whereas the strength of its centre increases with an increasing width to height ratio, Figure 1-3 (after Wagner 1974). While the modulus of elasticity was found to be a true material property and independent of geometry, the post failure modulus was markedly affected by width to height ratio, which indicated the post-failure behaviour of a pillar is a structural or system property and not an inherent material property.

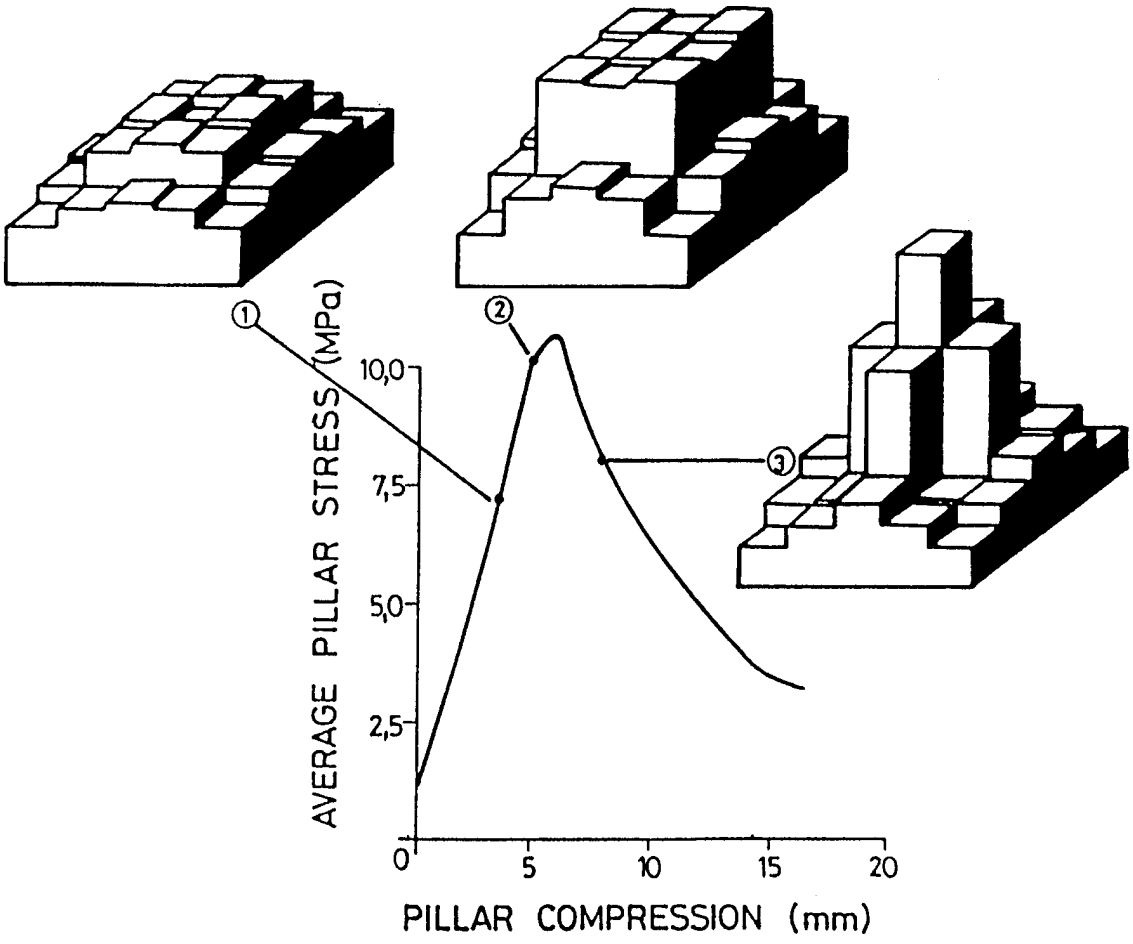

Figure 1-3 Stress in coal pillar versus pillar compression. After Wagner (1980).

The in situ testing of coal resulted in increased knowledge of the behaviour of coal pillars, particularly as far as the stress-strain behaviour is concerned. However, similarly to the laboratory investigations, a wide scatter of results was obtained. In addition, in situ experiments were limited by the capacity of the loading system applied to the pillar and proved to be time-consuming, elaborate and expensive.

The displacement of pillars induced by bord and pillar mining in two collieries at 11.6 m and 25.5 m depth to the seam were monitored by Salamon and Oravecz (1966). The findings were compared to theoretical results using both a homogeneous and a transversely isotropic elastic model. The former gave a good description of the observed displacement, and conclusions from the investigation showed that the in situ Young's modulus of coal measure strata was considerably lower at low stresses than values determined by laboratory experiments. Hence the stress concentration in the pillars could be smaller than previously suspected. These field measurements were invaluable because they showed that observed in situ results could be explained using elastic theory. Hence, in a low stress environment, the behaviour of coal pillars could be predetermined.

Oravecz (1973) investigated the load on coal pillars by field measurement, analytical analysis and use of the electrical resistance analogue. He concluded, on the basis of theoretical work and experimental investigation, that at the low levels of stress, as well as small displacements which occur in stable bord and pillar workings of coal mines, the theory of elasticity applies to coal measure strata.

Salamon in 1982 extended his pillar-strength formula to take cognisance of the increasing ability of a pillar to carry loads with increasing width-to-height ratio.

Laboratory tests on sandstone specimens were analysed by Wagner and Madden (1984) to examine the suitability of the new formula, known as the squat-pillar formula, to predict the strength increase with increasing width-to-height ratios. The squat-pillar formula was found to fit the laboratory results well, and although these laboratory results cannot be related directly to coal pillars because of the difference in the material, scale, and time taken to test the samples, the general trend can be assumed to be similar.

The strength of a pillar given by the squat-pillar formula is

$$\sigma_s = k\frac{R_0^b}{V^a}\left\{\frac{b}{\varepsilon}\left[\left(\frac{R}{R_0}\right)^{\varepsilon} - 1\right] + 1\right\} \qquad \textbf{\textit{Equation 1-3}}$$

where R_o = critical width-to height ratio

ε = rate of strength increase

a = 0.0667

b = 0.5933

V = volume of pillar.

Salamon and Wagner (1985) suggested that the squat-pillar formula could be used with the critical width-to-height ratio (R_o) taken as 5.0 and that ε could be taken as 2.5, although a realistic estimate was more difficult for the latter. The assumption of 5 for R_o is based on the fact that no pillar with a width-to height ratio of more than 3.75 was known to have collapsed.

Field investigations into the performance of squat pillars were conducted at Longridge, Hlobane and Piet Retief Collieries. Based on the field trials, as well as laboratory and theoretical results, the Government Mining Engineer accepted the use of the Squat Pillar formula for the design of Collieries.

In 1992 Madden and Hardman examined the South African pillar collapses, with the same criteria used by Salamon and Munro (1967), to select those cases that represented pillar failure

as a result of the strength of the coal pillar being exceeded by the load imposed upon it. A total of 31 pillar collapses were recorded after the introduction of the pillar design formula in South Africa. Of the 31 cases, 17 satisfied the criteria (Table 1-1). These collapses were analysed, together with Salamon and Munro's 27 collapses, to show whether there were any new trends in the collapse of bord and pillar workings. The new formula described the pillar strength, σ_p, as:

$$\sigma_p = 5.24 \frac{w^{0.63}}{h^{0.78}} \qquad \textbf{\textit{Equation 1-4.}}$$

Madden (1991) stated that, when the strength was calculated from both formulae, there was little variation (2 – 5 per cent) between formulae (Equation 1-2) and (Equation 1-4) over the empirical range covered by the formulae. This confirms that the strength formula of Salamon and Munro (1976) can successfully be used in the design of stable bord-and-pillar workings. When the data on individual seams were used, the statistical analysis showed that, although the strength of individual seams differs, there is no statistically significant difference between the strengths of individual seams so that the average strength should represent all seams. The results indicated that there is little variation between the later and the earlier collapses.

Two significant features emerged from the analysis of the collapsed pillars. Firstly, pillars at depths of less than 40.0 m with widths of less than 4.0 and a percentage extraction in excess of 75 per cent are prone to pillar collapse even when the designed safety factor is higher than 1.6. These three parameters are interrelated, and caution should be used in the designing of pillars at shallow depth. The effects of blast damage, geological discontinuities, weathering, or weak layers within the pillar influence the strength of small pillars more dramatically than they do larger pillars, and it is these factors that significantly weaken these small pillars . Salamon and Oravecz (1976), recognising the dramatic effect of a small reduction in pillar width when the pillar is less than 4.5 m in width, suggested that no pillar should be mined with a width of less than 3.0 m and that pillars between 3.0 m and 4.5 m in width should have a safety factor of at least 1.7.

Madden (1991) suggested that, at depths of less than 40.0 m, pillar widths should preferably be greater than 5.0 m, the width-to-height ratio should be in excess of 2.0 and the percentage extraction be less than 75 per cent. In addition, a safety factor of more than 1.6 should be maintained.

Of the 31 cases, for which the time period was known, 26 per cent of the collapse occurred within the first year, while 50 per cent occurred within four years of mining.

Because the Salamon and Munro pillar design formula was based on the designed mining dimensions of workings which were mined by the drill-and-blast method, the formula for pillar strength indirectly takes into account the weakening effect of blast damage. Therefore, the

effective width of a pillar designed according to the Salamon and Munro formula, but mined by a continuous miner, must be greater than that of a pillar formed by drilling and blasting, by an amount approaching the extent of the blast zone.

The depth of blast damage into the side of a pillar has been quantified as being between 0.25 and 0.3 m (Madden (1987)). The effect on the safety factor of a pillar formed by a continuous miner can be estimated on the assumption that effective pillar width increases by the depth of the fractured zone over that of a pillar mined by conventional methods. If the nominal pillar width, w, results in a safety factor η, then the safety factor of bord-and-pillar workings developed by means of a continuous miner, η_o, can be calculated from the following expression after Wagner and Madden (1984):

$$\eta_0 = \eta\left(1+\frac{2\Delta w_0}{w}\right)^{2,46} \qquad \textbf{\textit{Equation 1-5.}}$$

This expression calculated the increased safety factor of a pillar cut by a continuous miner in the absence of a blast-damage zone. Thus, if the pillar width, w, were 10 m, the designed safety factor 1.6 and the blast-damage zone 0.3 m, the safety factor of a pillar formed by a continuous miner would be 1.85.

Two important points should be noted.

(a) For a pillar formed by a continuous miner, there is a fixed increase in pillar width by the extent of the blast-damage zone, and not a fixed increase in safety factor.

(b) It is the strength calculation of the pillar formed by a continuous miner that is being adjusted by this method, not the safety-factor design formula.

Maximum benefit in terms of increased extraction from the use of continuous miners occurs between pillars greater in width than 5.0 m and at depths of less than 175 m. This is due to the fact that stress-induced sidewall slabbing can occur in very small pillars and at depths of more than 175 m.

Hill (1989) investigated the effects of multi seam mining through in situ experiments. Many collieries have more than one seam which are economical to mine, but, when these seams lie in close proximity to one another, stress concentrations may occur which can result in difficult mining and even impose restrictions on the type of mining. Current procedure is to follow guidelines established in 1970s, which tend to be conservative and in fact only apply to bord and pillar layouts. Studies in local collieries established that it is feasible to mine multi seams both safely and economically, using high extraction techniques, with criteria which were established. However, the effect on both the upper and lower seams must be determined in

terms of a caving mechanism. Where mining of an upper seam has taken place, the feasibility of mining the lower seam safely at a later date will depend on fracturing and subsidence that has taken place and more specifically, the ratio of the parting thickness to lower seam extraction height. Pillar extraction over lower seam bord and pillar workings produce dynamic changes in the lower seam. The study showed that caving conditions in South Africa collieries vary considerably with the overlying strata. The stability of the parting will depend on the magnitude and direction of stresses caused by the caving which can be determined using established failure criteria.

The multiseam guidelines are as follows:

(i) If parting > 1.5 x pillar centre distance, then no superimposition necessary. Pillar safety factor = 1.6.

(ii) If parting > 0.75 x centre distance, then only the barrier pillars are superimposed. Pillar safety factor = 1.6.

(iii) If the parting > 2 x bord width, then the pillars must be superimposed and designed to a safety factor of 1.7.

(iv) If the parting < 2 x bord width then panel pillars must be superimposed. The safety factor of the pillar must be 1.8 with a combined safety factor of 1.4.

Pillar extraction using handgot methods has been practised in South African collieries for many years. During the late sixties, pillar extraction with mechanised conventional equipment commenced, and, approximately a decade later, continuous miners were introduced into pillar and rib pillar extraction panels. During the years that these mining methods were practised, a vast amount of experience was gained on the various collieries. Problems were experienced by various mines. In response, the management of these mines made numerous alterations to the mining methods with varying degrees of success. Research was also conducted by COMRO and various mines and mining houses.

However, apart from the recommendations of Salamon and Oravecz (1976) on pillar design in stooping sections, little information had been published and, thus, little was generally available to mine managers, planners and operators to assist them in the layout and design for pillar and rib pillar extraction.

Beukes (1992) published design guidelines for pillar and rib pillar extraction which combined current rock mechanics practice with regard to pillar extraction, with experience developed from local mining conditions. A survey was conducted of all the pillar and rib pillar practices in South Africa as well as abroad and the successes, failures, problems experienced, changes made to the mining methods and the results of these changes were collated. Design guidelines relevant

to the various methods of pillar and rib pillar extraction were established to improve the safety and performance of pillar extraction operations. The guidelines were not intended to be prescriptive but were designed more to bring to the attention of the mine manager, planner and operator those factors which should be taken into consideration during the planning and operation of a pillar or rib pillar extraction panel.

Esterhuizen (1993) investigated barrier pillar design. Barrier pillars are required to prevent the possible collapse of underground coal workings in one area from spreading to adjacent workings so that they need to be capable of resisting increased loads imposed on them. The aim of this study was to address the need for methods of determining the strength and loading of barrier pillars. The following objectives were set:

- to estimate the strength of barrier pillars from cases which had collapsed in the past;
- to evaluate factors which affect the strength of barrier pillars;
- to assess the load carried by barrier pillars before and after the collapse of adjacent workings; and
- to develop a method which can be used to design barrier pillars in South African coal mines.

A study of collapsed barrier pillars showed that barrier pillars which were as wide as the adjacent panel pillars were able to arrest a collapse. Fallout of roof can increase the effective height of pillars. In one of the cases the increase in the effective height of the pillar due to bord failure was thought to be responsible for the collapse of a 30 m wide barrier.

The load on barrier pillars was found to depend largely on the behaviour of the overlying strata. When no collapse has taken place, the barrier pillars are at a lower stress level than the adjacent pillars in the workings. If the width of barriers is designed to be a constant multiple of the adjacent panel pillars they will be subject to approximately constant stresses, regardless of the depth. The results of the study were used to recommend a design method for barrier pillars.

Özbay (1994) investigated the laboratory strength of coal samples from Sigma and Delmas Collieries as part of the current SIMRAC project on pillar design conducted by Miningtek, CSIR. This project has concentrated on three areas of research, namely laboratory strength of individual seams, the geotechnical classification of coal pillars and in situ monitoring of coal pillar behaviour. The project motivation was due to the collapses of pillars, some with apparent high safety factors and at a relatively young age.

Esterhuizen (1995) suggested that considerable variations in the large scale strength of coal are likely to exist due to the variation in the intensity of discontinuities in the different coal seams,

which in South Africa varies from massive unjointed coal to highly jointed coal. The application of standard rock classification techniques supported this contention. Numerical model studies showed that the reduction in the strength of coal pillars due the presence of jointing is not constant for all width to height ratios, but the effect of jointing becomes less pronounced as the width to height ratio increases.

1.3 Update of collapse pillar data

The current pillar project has attempted to developed a design procedure to take cognisance of different geological and structural factors, as well as the influence of the surrounding strata. The initial procedure was on reviewing the coal pillar collapse database. A re-analysis of all available collapsed data was undertaken. This was done to examine where and why pillar collapses occurred.

Salamon and Munro included collapse data where the coal seam was the weakest element. Thus, in Salamon and Munro's coal strength formula, a strong roof and floor are assumed. In Madden's re-assessment of Salamon and Munro's strength formula in 1988, the same assumptions were applied and 14 collapse cases were excluded from the analysis.

As mining is taking place in all geotechnical environments, pillar design procedures must take cognisance of all factors than can influence stability. Data excluded by Salamon and Munro (1967) (23 cases) and Madden (1988) (14 cases) have been re-examined and included where appropriate.

The majority of collapses that were excluded from Salamon and Munro's database were not used because of unreliable information. Further investigations only allowed 4 of these cases to be included in the current analysis, while all 14 cases not included by Madden (1988) have been included together with the 21 cases of pillar collapses between 1988 to 1996. A total of 23 collapses that occurred between 1988 to 1996 have been recorded, however, only 21 of these collapses were used in the analysis, due to multiseam mining in two of the cases.

Table 1-1 gives the data from Salamon and Munro (1967), Madden (1988) and 23 additional collapses that had occurred since the analyses of 1988, as well as data not used Salamon and Munro and Madden. One case, No 171, appears to have been overlooked in both Salamon's original work and Madden's review in 1988.

Table 1-1 indicates that the seam at the colliery in the Klip River Coalfield does not conform to the current formula as shown by the safety factors of 2.0 to 2.8 and pillar width to mining height ratios of 2.5 to 4.17 at which collapses took place. One of the collapses occurred while mining was taking place. The Vaal Basin collapses have been highlighted previously (van der Merwe, 1993), however, the high pillar width to mining height ratio of 3.5 to 4.3 are of interest. The pillar collapse at Matla Colliery, No 5 Seam, was reported on in the final report SIMRAC project COL021 (Madden *et al*, 1995). Figure 1-4 and Figure 1-5 show the frequency of collapsed cases versus safety factor, and pillar width to mining height ratio for the three periods 1904-1965, 1966-1988, 1989 to 1996. The figures suggest that Salamon's original formula is applicable within the original range, however long term collapses are occurring with low safety factors pillars and that seam specific regional characteristics are influencing the pillar stability, e.g. the Vaal and Klip River Coalfields. In the Vaal Basin pillar deterioration occurs over time. At the colliery in the Klip River Coalfield, numerous discontinuities affected pillar stability causing pillar failure shortly after mining, despite high safety factors and pillar width to mining height ratios. It is also of concern that the collapses, which occurred within a few years of mining, usually involved a relatively large number of pillars. Of interest is the comparison between the pillar width to mining height ratios of intact cases from Salamon and Munro's data in 1967 to the pillar width to height ratios recorded by Madden and Özan during a survey of panels in 1991. The average width to height ratio of the pillar designs had increased from 3.7 to 6.14. It was also found that the width to height ratio of the pillar collapses had increased, although none of these new collapses were in the squat pillar range of greater than 5.0.

A pillar collapse case with a safety factor of 5.58 has been included in Figure 1-4. This case was not included in Salamon and Munro's original analysis as weak roof and extensive falls were thought to have induced the collapse, which occurred at very shallow depth (12.8 m).

Similarly the No 5 Seam collapse in the Witbank Coalfield had acceptable design parameters to account for the shallow depth of mining (less than 40 m). However, the collapse was due to a weak floor which resulted in foundation failure and pillars failing in tension.

In a large proportion (34 cases) of the above cases the designed factors of safety, based on a k value of 7.2 MPa, were higher than the industry accepted standards of 1.6 and 2.0, yet pillar collapses resulted. It is thought that these collapses occurred because the current design procedure does not take into account several important pillar system factors that ultimately effect the stability. Salamon and Munro's strength formula was developed from collapsed cases

where the coal was the weakest element within the pillar system. However, failure of any system element (the roof, pillar or floor) will result in instability. The current research aims to include all factors into the pillar design procedure.

It should be noted that the majority of coal produced underground in South Africa comes from the Witbank and Highveld Coalfields (approximately 75 – 85 per cent). In these coalfields Salamon and Munro's strength formula does perform well in the design of stable pillar systems.

Figure 1-6 indicates that, while some cases collapsed during mining, other cases collapsed 20 to 40 years after the mining. This highlights the long term stability aspect of pillar design, which has environmental implications and relevance to mine closure applications.

Figure 1-7 shows the number of pillars collapsed versus frequency. As can be seen from this Figure, in most of the cases (71 per cent) the number of pillars that collapsed was less than 200; however in some instances the number was much higher.

Figure 1-8 shows the depth of mining versus frequency of pillar collapse. This figure indicates that majority of the collapses occurred at a depth of less than 110 m.

1.4 Future research knowledge requirements

From this review (and the outcomes of this project) it is clear that to provide a comprehensive design methodology which takes into account all the significant factors which can lead to pillar system instability, further detailed research is required. Important issues requiring research are discussed below.

In 1993 van der Merwe attempted to re-analyse the pillar design formula for the Vaal Basin. He analysed pillar collapses that occurred only in the Vaal Basin Coalfield and identified these collapses as a separate group which were characterized by higher safety factors and shorter life spans than the other failures in other coalfields. This is collaborated by the grouping of pillar collapses as indicated in Figure 1-4.

The causes of pillar deterioration exemplified by the above example are not well known and require further investigation. The rate of deterioration may vary between coal seams, as suggested by van der Merwe; however, without an improved understanding of this phenomenon, the long term stability of coal pillar workings will not be understood. This can have an impact on future planning of civil infrastructure over old bord and pillar workings as well as on mine closure and the environmental effects on both the surface and ground water supplies. As part of this project the effect of pillar deterioration on pillar strength has been investigated for

Vaal Basin, however, this study requires further investigation into other coalfields in South Africa, (see Chapter 3).

A recent pillar collapse was attributed to foundation failure where the pillars were thought to have failed in tension. The design of the pillars was according to current practice. An issue of concern is that the current pillar design methodology does not account for weakness in the surrounding strata. Identification of potentially unstable layers beneath a coal seam may be achieved by index tests such as slake durability, or swell index tests, but this should be done during the pre-mining drilling phase. However, how to incorporate the affects of such weaknesses into a design methodology has not been established. This may involve limiting the stress over the pillar or designing for stable foundations. Further research is therefore required into foundation stability beneath coal pillars.

Another parameter that is highlighted in Figure 1-4 is the influence of discontinuities on coal pillar strength. Five collapses in the Klip River Coalfield are attributed to the numerous slips that occur in the pillars.

Research is currently being carried out to identify anomalous structures that will influence the stability of a coal pillar. This is being conducted by the University of Pretoria who are developing a pillar rating system for discontinuities. The effect of discontinuities on pillar strength has also been investigated as part of this project (see Chapter 2).

Other factors that will determine the stability of pillar workings include the loading of the pillars by the overburden strata. Currently each pillar is assumed to carry the weight of the super incumbent strata as determined by the tributary area theory. While this may be conservative with regard to bord and pillar workings, an understanding of the load carried by pillars during pillar extraction is essential for safe operation.

Beukes (1990) stated that in the past the safety factor was too often the only parameter used to determine the size of the pillars with critical factors being ignored. The critical factors affecting pillar size were summarized as: safety factor, behaviour of the overburden strata, mining method and mining equipment. It was also stated that the behaviour of the overburden strata is possibly the most critical factor as it also affects the mining method, the type of mining equipment that can be used and the support required during development and stooping. Beukes concluded that “the mining method should be pre-determined and the pillar should be designed to augment this method. The type and size of the mining equipment also have a major influence on the type of mining that can be practised and the pillar dimensions required for safe and effective extraction”. Further research to quantify these influences needs to be carried out.

1.5 Conclusions

Research into pillar strength is time consuming and costly. However, the benefits to the industry, workforce and country are the development of stable pillar systems, and therefore safe and economic extraction of coal reserves, research into pillar systems will be required due to the expanding nature of mining.

Previous research has resulted in:

- Pillar design formula for permanent bord and pillar workings
- Determination of pillar deformation characteristics
- Squat pillar design formula
- Pillar design when using a continuous miner
- Barrier pillar design guidelines
- Design of shallow workings
- Pillar extraction guidelines
- Multi-Seam design guidelines

Further improvement to the above can be made through continued applied research, in particular in the areas of the effect of time on pillar strength, weathering effects, strength of rectangular pillars and anomalies within the current design. Back analysis of previous mined areas holds the possible key to an improved understanding of pillar performance and design.

The current coal pillar design procedures are effective in designing stable bord and pillar workings in the vast majority of the South African coal mining areas.

However, examination of recent collapsed pillar cases has highlighted the need for additional parameters to be considered in the design of coal pillars. These include the influence of discontinuities, surrounding strata characteristics and the effects of deterioration and time. While further research into these phenomena is required, identification of the geotechnical areas where these parameters have resulted in pillar failure may provide the solution for incorporating these parameters into a stable design methodology.

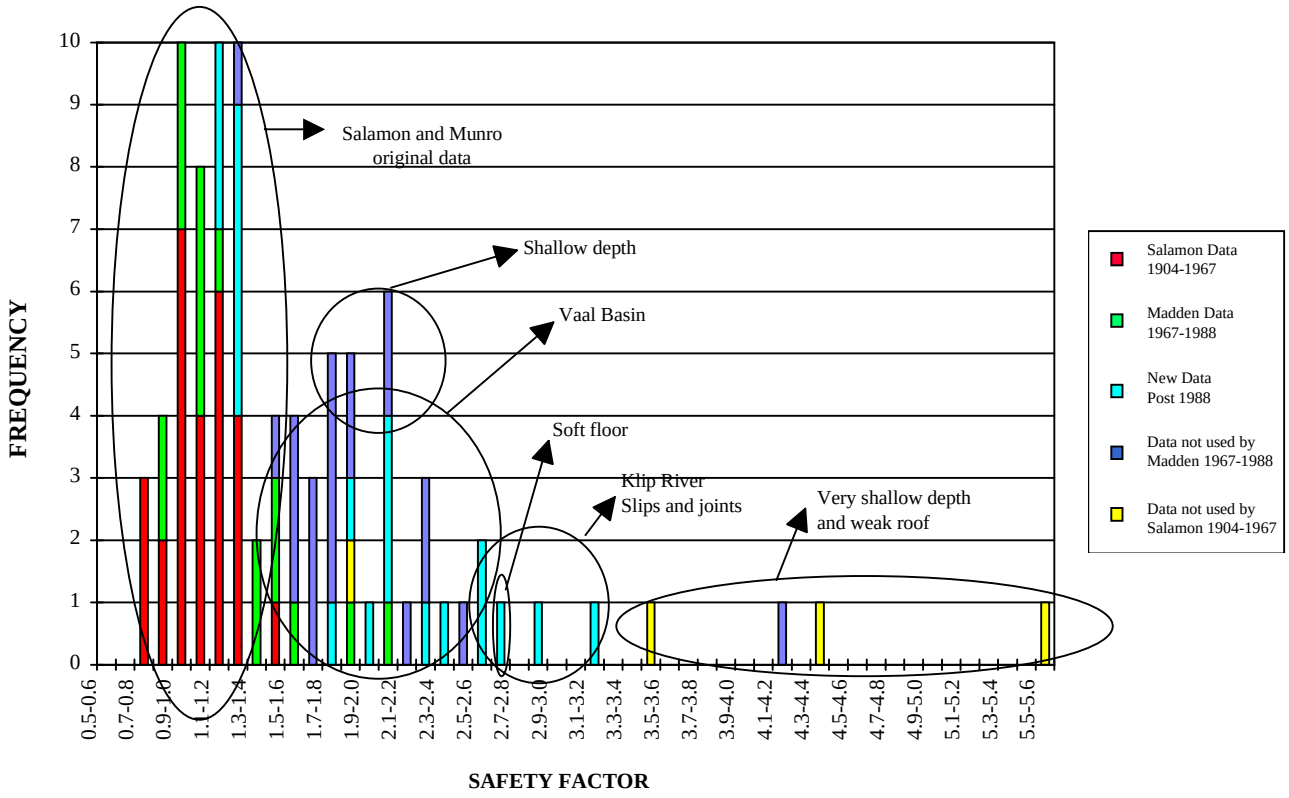

Figure 1-4 Frequency of pillar collapse versus the design safety factor.

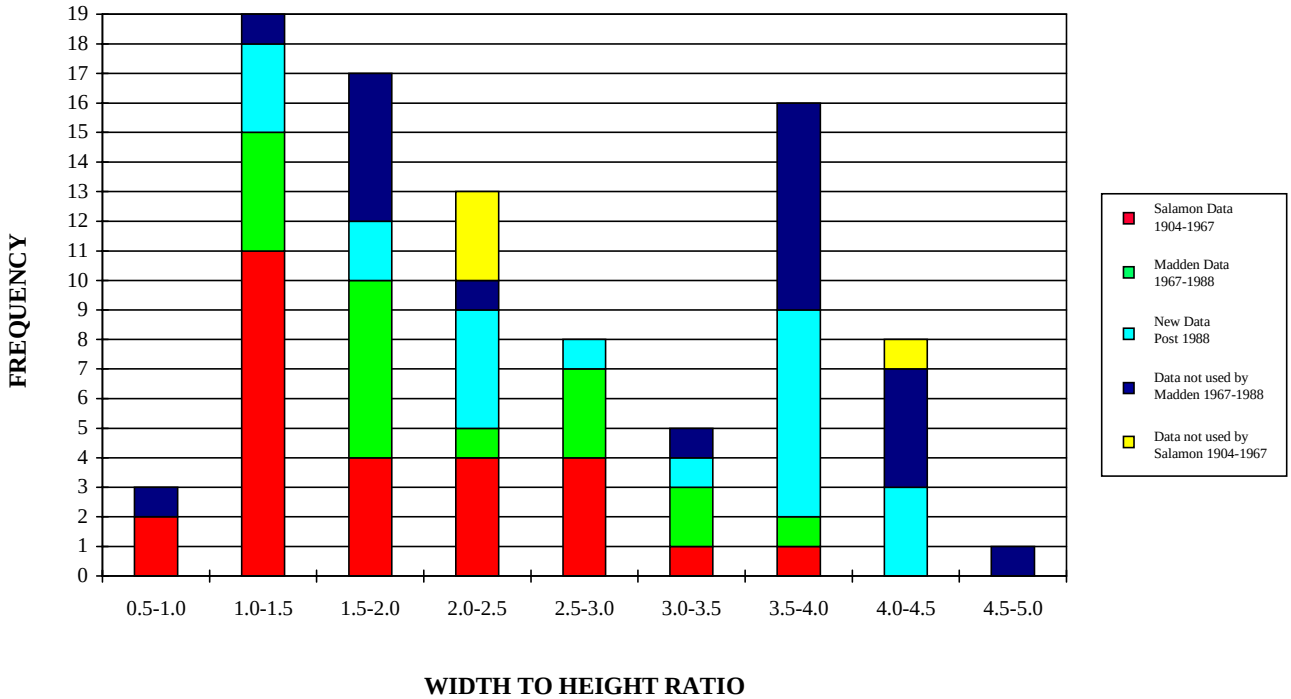

Figure 1-5 Frequency of pillar collapses versus pillar width to mining height ratio

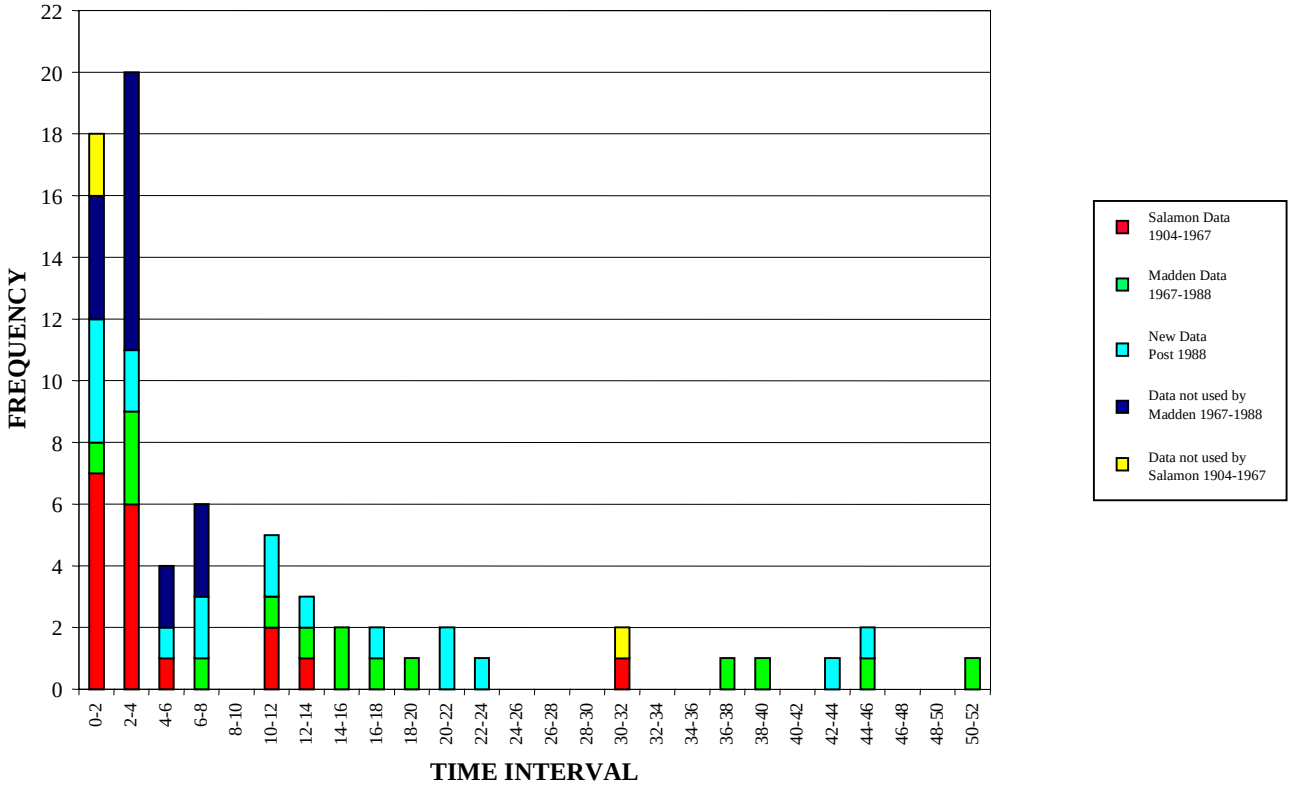

Figure 1-6 Time interval to collapse versus frequency

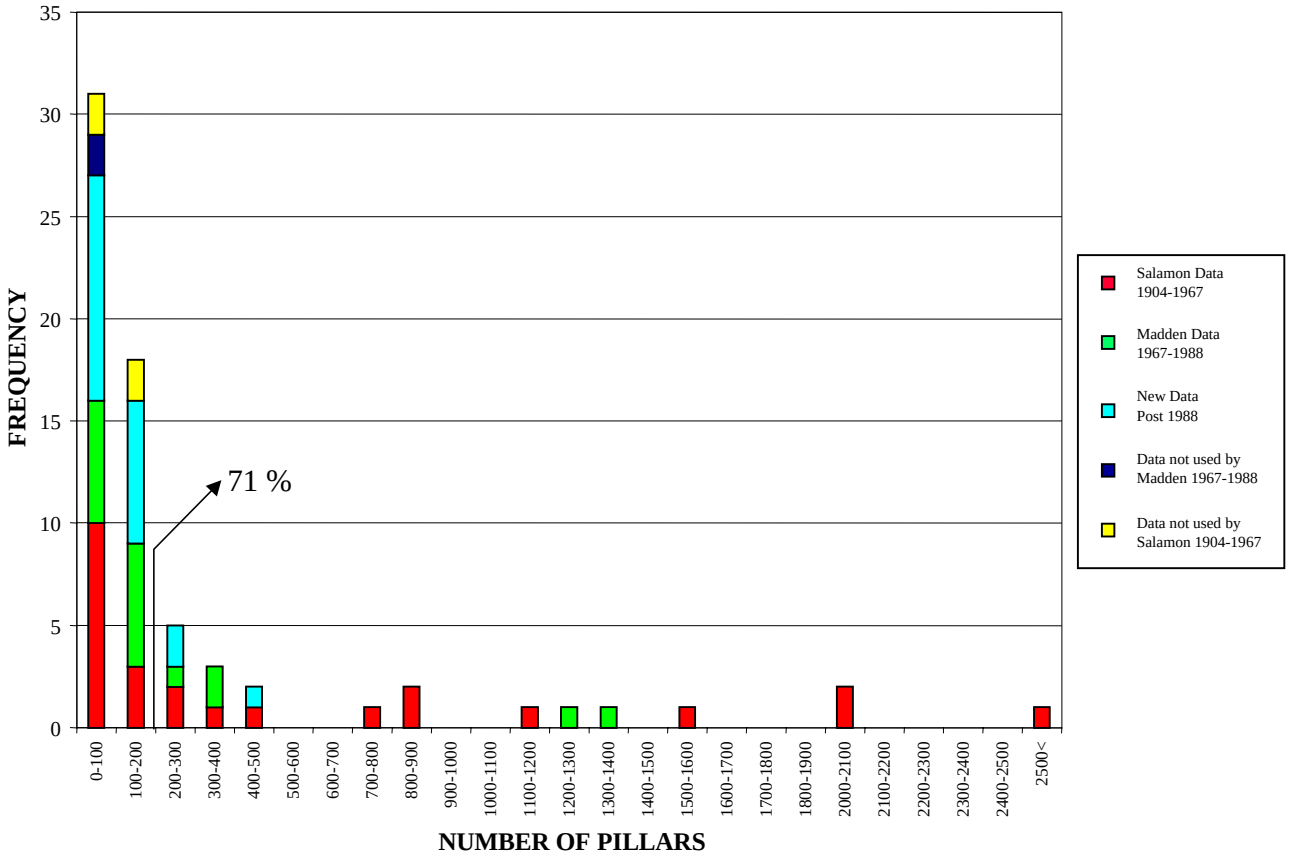

Figure 1-7 Number of pillars involved in collapse versus frequency

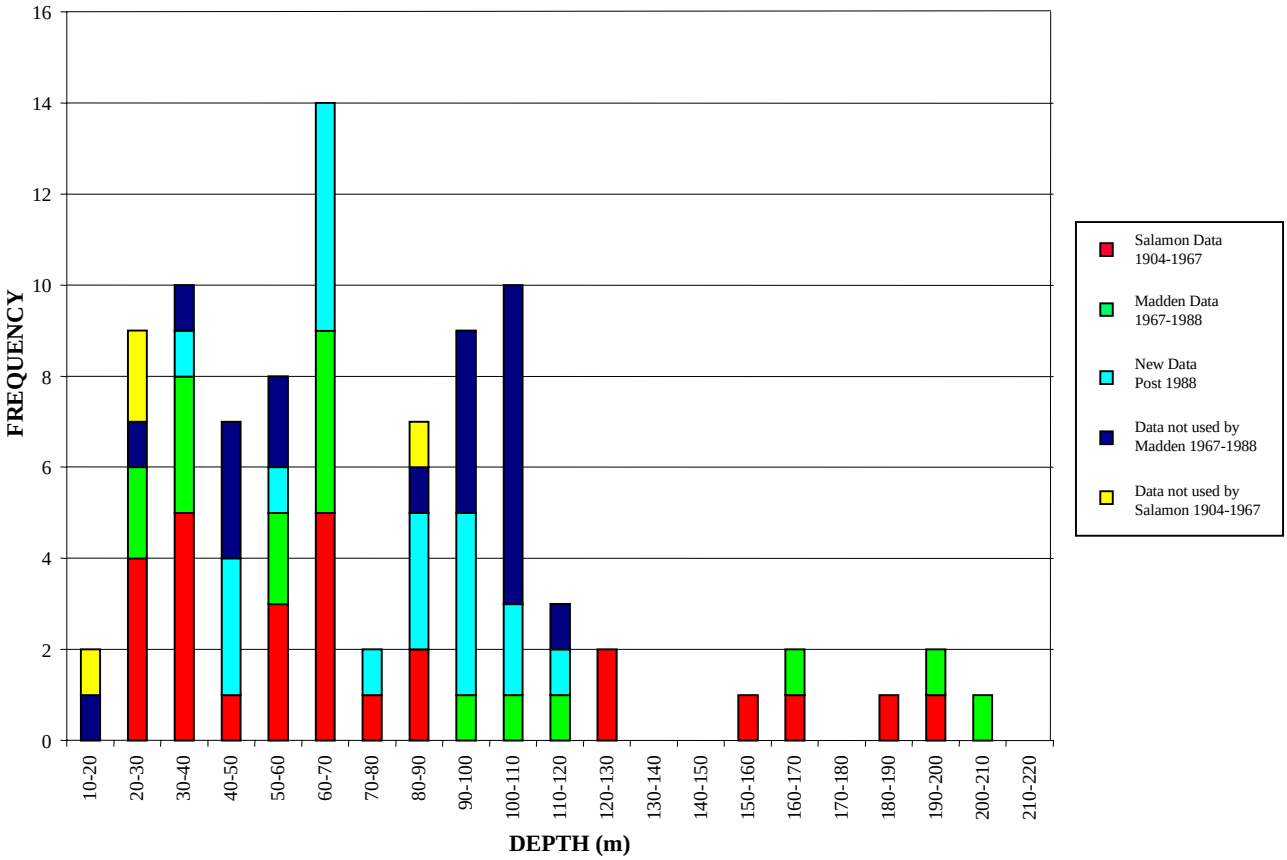

Figure 1-8 Depth of collapse versus frequency

Table 1-1 Collapse database; Salamon and Munro, 1967, Madden, 1991, New data, 1996.

Case No.	Colliery	Seam	Coalfiled	Depth (m)	Pillar Width (m)	Bord Width (m)	Mining Height (m)	Safety Factor	Date of Working	Date of subsidence	Time Interval (years)	Surface Area Affected (hectares)	No of Pillars	w/h	
9	New Largo	W 4	Witbank	30.5	3.35	6.40	2.59	1.04	1951-53	1963	12	7.53	831	1.29	
12	Coronation	W 1	Witbank	25.9	3.66	8.53	3.05	0.87	1917	1921	4	0.2	26	1.20	
16	M. Steam	W 2	Witbank	21.3	3.96	8.23	4.57	0.99	1922	1947	Current	?	?	0.87	
17	Wolvekrans	W 2	Witbank	29.6	5.18	7.01	5.49	1.22	1945	1959	14	0.61	64	0.94	
18	Witbank	W 2	Witbank	27.4	3.66	7.92	2.13	1.15	?	1904		0.61	68	1.71	
19	Apex	Springs	Springs-Witbank	36.6	6.10	7.62	4.88	1.26	?	?		2.43	172	1.25	
39	Kendal	W 5	Witbank	36.6	4.57	7.62	2.44	1.24	1941	1941	Current	0.81	87	1.88	
40	Wolvekrans	W 2	Witbank	33.5	6.10	6.71	5.49	1.46	1946	1950	4	1.01	91	1.11	
41	Crown Douglas	W 2	Witbank	30.5	4.57	7.62	3.66	1.14	1912-18	1919	1	0.4	47	1.25	
42	South Witbank	W 4	Witbank	53.3	5.18	6.40	3.66	0.98	1957	1962	5	24.28	2065	1.42	
54	Welgedacht	Springs	Springs-Witbank	62.5	6.10	7.62	2.44	1.16	?	1917		0.61	74	2.50	
55	Blesbok	W 5	Witbank	68.6	3.35	5.79	1.52	0.75	1954	1955	0.33	4.05	714	2.20	**SALAMON**
57	Koornfontein	W 2	Witbank	88.4	7.16	6.55	4.88	0.77	1958-59	1962	3	4.86	430	1.47	**DATA**
58	South Witbank	W 5	Witbank	128.0	12.80	5.49	5.49	1.16	1957	1959	1.5	3.64	348	2.33	
59	Cornelia	O F S No. 2	Vaal Basin	57.9	5.18	6.40	3.66	0.90	1961	1961	1	?	?	1.42	
60	Coalbrook	O F S No. 2	Vaal Basin	152.4	12.19	6.10	4.88	0.93	Current	1960	Current	308.79	7778	2.50	
64	South Witbank	W 4	Witbank	61.0	4.72	6.86	3.51	0.70	1957	1959	1.5	8.5	816	1.35	
66	Springfield	Main	South Rand	193.2	15.85	5.49	5.49	0.95	1954	1957	3	52.61	1578	2.89	
67	Springfield	Main	South Rand	184.7	15.85	5.49	5.49	1.00	1955	1956	1	4.45	238	2.89	
115	Union	Ermelo Dreyton	Eastern Transval	76.2	4.88	6.10	1.37	1.26	1937	1937	Current	20.64	2095	3.56	
116	Waterpan	W 2	Witbank	61.0	6.10	6.10	4.57	0.99	1932	1964	32	1.42	78	1.33	
117	Waterpan	W 2	Witbank	61.0	6.10	7.62	3.05	1.03	19.3	?		0.4	30	2.00	
118	Waterpan	W 2	Witbank	57.9	6.10	7.62	3.96	0.91	1932	1964	32	0.4	34	1.54	
119	W. Consolidated	W 4	Witbank	41.1	4.27	6.40	3.05	1.05	1955	1959	4	1.82	228	1.40	
120	Cornelia	O F S No 1	Vaal Basin	128.0	9.75	5.49	3.66	1.12	1952	1953	1	1.21	159	2.67	
122	Springfield	Main	South Rand	167.6	15.85	5.49	5.49	1.10	1954-8	1961	3	1.71	102	2.89	
126	Vierfontein	Main	Free State	87.8	6.10	6.10	1.98	1.20	1955-8	1959	1	12.14	1102	3.08	
148	New Largo	W 4	Witbank	28.5	3.8	5.8	2.7	1.52	1951-53	1968	15	3	179	1.41	
148A	New Largo	W 4	Witbank	34	3.5	6.7	2.7	0.92	1951-53	1968	15	3.6	312	1.30	
148B	New Largo	W 4	Witbank	34	3.5	6.7	2.7	0.92	1951-53	1971	18	1.8	126	1.30	
149	Koornfontein	W 2	Witbank	90	7.5	6	4.8	0.89	1958-59	1968	11	9	397	1.56	
150	Blesbok	W 5	Witbank	57	3.6	5.4	1.35	1.20	?	1969		0.65	96	2.67	
151	Tweefontein	W 2	Witbank	62	7.5	6.4	4	1.37	1931	1971	40	6.3	261	1.88	
157	Sigma	O F S No 2	Vaal Basin	112	10.55	6.45	2.82	1.48	1975-78	1980	2	4.8	122	3.74	
159	Sigma	O F S No 2	Vaal Basin	108	10.55	6.48	3.18	1.41	1972-75	1979	4	18	1312	3.32	
162	Tweefontein	W 2	Witbank	62	7.3	6.2	4	1.36	1930	1982	52	1.8	93	1.83	
163	South Witbank	W 4	Witbank	56	5.1	6.5	3.3	0.96	1957	1976	19	19.5	1256	1.55	**MADDEN**
164	Wolvekrans	W 2	Witbank	33	6.4	6.4	4.88	1.80	?	1983	?		56	1.31	**DATA**
165	Springbok	W 5	Witbank	22	3.5	6.5	1.6	2.09	1982	1985	3	0.5	40	2.19	
166	Tweefontein	W 2	Witbank	62	6.1	6.1	4	1.07	1930	1976	46	0.04	20	1.53	
167	Tweefontein	W 2	Witbank	62	6.1	6.1	4	1.07	1930	1968	38	1.3	165	1.53	
168	Springfield	Main	South Rand	165.7	15	5	5.94	1.05	1966	1970	4	5	106	2.53	
169	Springfield	Main	South Rand	195	17	6	4.88	1.04	1972	1980	8	0.5	27	3.48	
170	Springfield	Main	South Rand	205	17	6	5.88	0.88	1967	1980	13	11.9	193	2.89	
171	Wolvekrans	W 2	Witbank	41	6.4	6.4	6.2	1.24	1944	1966**	22	0.3	18	1.03	
172	Wolvekrans	W 2	Witbank	41	6.4	6.4	6.2	1.24	1944	1988	44	0.4	24	1.03	
173	Wolvekrans	W 2	Witbank	41	6.4	6.4	6.2	1.24	1944	1990	46	0.4	22	1.03	
174	Matla	W 5	Witbank	35.5	5.5	5.5	2.2	2.64	1981	1995	14	0.8	69	2.50	
175	Springlake	Bottom	Klip River	70	7.5	5	1.8	2.54	1987	1995	12	3	200	4.17	
176	Springlake	Bottom	Klip River	63.5	7.5	5	2.1	2.53	1988	1991	3.5	1.4	90	3.57	
177	Springlake	Bottom	Klip River	61	6	5	1.9	2.10	1995	1995	Current	2.5	200	3.16	
178	Springlake	Bottom	Klip River	61	7.5	5	1.9	2.81	1995	1995	0.25	2.8	200	3.95	
179	Ballengech		Klip River	74	10	5	4	2.00	1986	1986	0.042	2.8	95	2.50	
180	Sigma	O F S No 3	Vaal Basin	82	10	5	2.8	2.28	1987	1991	4	11.5	500	3.57	**NEW**
181	Sigma	O F S No 3	Vaal Basin	96	12	6	2.9	2.07	1982	1993	11	2.6	73	4.14	**DATA**
182	Sigma	O F S No 2b	Vaal Basin	70	12.5	5.5	2.9	3.14	1981			1.7	50	4.31	
183	Sigma	O F S No 2b	Vaal Basin	88	11	6	2.9	2.04				2	75	3.79	
184	Sigma	O F S No 2a	Vaal Basin	112	11.5	5.5	2.9	1.79	1978	1979	1.5	7	380	3.97	
185	Umgala	Alfred	Utrecht	101	9	6	3.8	1.17	1972	1995	23	2.4	110	2.37	
186	Umgala	Alfred	Utrecht	100	8.5	6.5	3.3	1.13	1974	1981	7	2.2	130	2.58	
187	Umgala	Alfred	Utrecht	97	9	6.6	3.7	1.14	1973	1994	21	7	300	2.43	
188	Umgala	Alfred	Utrecht	51.5	6	6	3.9	1.30	1973	1991	18	1	80	1.54	
194	Sigma	OFS 2A	Vaal Basin	96	12	6	6	1.28		1991		75	115	2.00	
195	Sigma	OFS 3	Vaal Basin	82	12	6	3	2.37		1991		75	190	4.00	
196	Sigma	OFS 2A	Vaal Basin	104	12	6	3	1.87	1977			27.5	100	4.00	
192	Sigma	OFS 2B	Vaal Basin	41	13.090909	6	5.5	3.500	1989	1995	5.5	0.2	9	multiseam mining not	
193	Sigma	OFS 3	Vaal Basin	35	9	6	2.7	4.226	1987	1995	8	0.2	12	included in the analyses	

Table 1-1 Collapse database; Salamon and Munro, 1967, Madden, 1991, New data,

Case No.		Seam	Coalfiled	Depth (m)	Pillar Width (m)	Bord Width (m)	Mining Height (m)	Safety Factor	Date of Working	Date of subsidence	Time Interval (years)	Surface Area Affected (hectares)	No of Pillars	w/h	
152	Cornelia	OFS No 2	Vaal Basin	45	6	6	3.5	1.60		1969	2			1.71	
153	Cornelia	OFS No 3	Vaal Basin	46	5.78	6.22	3.29	1.48		1981				1.76	
154	Cornelia	OFS No 3	Vaal Basin	51	5.76	6.24	3.41	1.30	1978	1980	2			1.69	
155	Cornelia	OFS No 3	Vaal Basin	113.7	12	6	2.75	1.81		1979	8			4.36	
171	Cornelia	OFS No 3	Vaal Basin	103.5	11.66	6.34	2.94	1.77	1978	1982	5	1.3		3.97	
172	Cornelia	OFS No 3	Vaal Basin	47	5.9	6.1	3.21	1.55	1978	1982	4	1.37		1.84	
173	Cornelia	OFS No 3	Vaal Basin	90	9.1	5.9	2.53	1.76	1974	1983	7	5.25		3.60	
174	Cornelia	OFS No 3	Vaal Basin	98	10	6	3	1.60	1979	1984	4.5	6.18		3.33	**DATA NOT**
175	Cornelia	OFS No 3	Vaal Basin	59.6	8.9	6.1	3.57	2.01	1980	1984	3.5	1.84		2.49	**USED**
176	Cornelia	OFS No 3	Vaal Basin	40	5.7	6.3	3.15	1.70	1979	1987	8	3.46		1.81	**BY**
177 a	Cornelia	OFS No 3	Vaal Basin	103.7	11.13	6.37	3.05	1.63	1982	1985	3	35.14		3.65	**MADDEN**
177 b	Cornelia	OFS No 3	Vaal Basin	99.6	11.44	6.06	3.07	1.81		1985				3.73	
177 c	Cornelia	OFS No 3	Vaal Basin	105.9	11.5	6	3.04	1.73		1985				3.78	
177 d	Cornelia	OFS No 3	Vaal Basin	106.4	11.5	6	3.11	1.70		1985				3.70	
177 e	Cornelia	OFS No 3	Vaal Basin	106.5	11.56	5.94	3.05	1.74		1985				3.79	
177 f	Cornelia	OFS No 3	Vaal Basin	103	14.02	5.98	3.38	2.07		1985				4.15	
177 g	Cornelia	OFS No 3	Vaal Basin	105.5	14.15	5.85	3.06	2.21		1985				4.62	
178 a	Cornelia	OFS No 3	Vaal Basin	99	14.24	5.76	3.34	2.26	1984	1986	2	10.25		4.26	
178 b	Cornelia	OFS No 3	Vaal Basin	99	14.65	5.35	3.3	2.44	1984		2			4.44	
146	Brakfontein	W4	Witbank	13.5	3.9	5.5	6	2.10		1965		0.03	3	0.65	
147	Coronation	W2	Witbank	24	6.2	5.8	2.4	4.16		1966		0.16	11	2.58	
94	Klipfontein	?		21.3	5.49	6.71	3.05	2.87	?	1944		1.21	1.03	1.80	
95	SACE (Navigation)	W2	Witbank	21.3	6.1	6.1	2.44	4.31	1918	1948	30	1.34	112	2.50	
96	Vierfontein	Main	Free State	87.8	7.62	6.1	1.68	1.83	1958	1959	0.67		32	4.54	
97	Coronation	W1	Witbank	21.3	6.1	6.1	4.27	2.98	?	1959		1.01	88	1.43	
98	Klipfontein	?		21.3	5.49	6.71	3.05	2.87	?	1944		0.81	72	1.80	
99	Old Largo	Springs Top	Springs-Witbank	33.53	5.49	6.71	2.13	2.31	1942	1946	4	2.23	196	2.58	
		Springs Mlddle	Springs-Witbank	45.72								2.23	214		
		Springs Bottom	Springs-Witbank	51.82								2.23	224		
100	Old Schoonezicht	W2	Witbank	43.59	6.1	6.1	2.12	2.31	?	1957		2.63	243	2.88	
		W1	Witbank	51.82				1.94				2.63	257		
101	Kroonstad	?	?	27.4	4.57x10.7	4.57	2.13-2.44	4.88	1913	1921	8	1.7	182	2.80	
102	Klipfontein	?	?	21.3	5.49	6.71	3.05	2.88	?	1944		0.61	56	1.80	**DATA NOT**
103	Old Largo	Springs Top	Springs-Witbank	33.53	6.1	5.49	2.13	3.32	1922			1.86	186	2.86	**USED**
		Springs Mlddle	Springs-Witbank	45.72	7.62	6.1	2.44	2.75	1914				146	3.12	**BY**
104	Vierfontein	Main	Free State	17.07	4.57	4.57x10.7	2.13-2.44	3.42	?			1.21	122	2.00	**SALAMON**
105	Old Largo	Springs Top	Springs-Witbank	33.53	5.49	6.71	2.13	2.31				1.42	133	2.58	
		Springs Mlddle	Springs-Witbank	45.72											
		Springs Bottom	Springs-Witbank	54.86											
106	Heilelberg	Springs	Springs-Witbank	23.1	5.49	6.1	1.83	4.12	?	1958		0.61	64	3.00	
107	Old Largo	Springs Top	Springs-Witbank	42.67	5.49	6.71	2.13	1.82	?	1946		4.45	382	2.58	
		Springs Mlddle	Springs-Witbank	51.82				1.50					401		
		Springs Bottom	Springs-Witbank	60.92				1.27					421		
108	Vierfontein	Main	Free State	27.4	4.57x10.7	4.57	2.13-2.44	4.88	1913	1916	3	1.42	155	2.80	
109	Coronation	W1	Witbank	22.86	6.1	6.1	3.05	3.47	1944			0.4	41	2.00	
110	Old Largo	Springs Top	Springs-Witbank	33.53	6.1	5.49	2.13	3.32	?	1922		2.63	251	2.86	
		Springs Mlddle	Springs-Witbank	54.86	7.62	6.1	2.44	2.29				2.63	207	3.12	
111	Old Largo	Springs Top	Springs-Witbank	42.67	6.71	5.49	1.83	3.29	1946	1946	Current	4.05	351	3.67	
		Springs Mlddle	Springs-Witbank	51.82			2.13	2.45				4.05	370	0.00	
		Springs Bottom	Springs-Witbank	60.96			1.83	2.31				4.05	389	0.00	
114	Consolidation	?	?	76.2	7.62	6.1	1.37	2.41	1944	1944	Current	41.68	2564	5.56	
121	Springfield	Main	South Rand	173.74	15.85	5.49	2.29	1.89	1951/53	1954	1	18.21	637	6.92	
				181.36	18.29	6.1	2.44	1.89	1914	1954		18.21	497	7.50	
123	Old Vierfontein	Main	Free State	27.4	4.57x9.75	4.57	2.13-2.44	4.68	1913	1922	9	1.38	157	5.45	
124	Vierfontein	Main	Free State	12.8	4.57	6.1	1.83	5.57	1957	1958	0.12	1.21	123	2.50	
125	Old Vierfontein	Main	Free State	29.6	4.57x10.7	4.57	2.13-2.44	4.51	1914	1959	45	1.01	119	2.80	

	Salamon Data	Madden Data	New Data	Data Not used by Madden	Data Not used by Salamon
Average Depth (m)	75.85	81.66	74.64	85.39	47.21
Pillar Width (m)	7.13	7.88	8.99	10.26	6.97
Bord Width (m)	6.71	6.16	5.75	6.03	5.92
Mining Height (m)	3.84	3.69	3.50	3.14	2.33
Width to height ratio	1.89	2.12	2.93	3.30	2.98
Average SF	1.05	1.24	1.90	1.80	2.99
Average Time Interval	5.41	19.20	14.21	4.25	9.16

1996 (continued)

1.6 References

Beukes, J. S., 1990. Stooping Practices in South Africa. Part 4 : Guidelines for Pillar and Rib Pillar Extraction. Research Report No. 43/90, Chamber of Mines of South Africa.

Beukes, J.S., 1992. Design Guidelines for Pillar and Rib Pillar Extraction in South African Collieries. Master Thesis University of the Witwatersrand. Johannesburg.

Bieniawski, Z.T. and Mulligan, D., 1968. In Situ Large Scale Tests on Square Coal Specimens Measuring 5ft in Width and up to 5ft in Height. CSIR Report MEG 567, Pretoria, South Africa, July.

Bieniawski, Z.T. and Van Heerden W.L. The Significance of In Situ Tests on Large Rock Specimens. Int. J. Rock Mech. Min. Sci. & Geomech. Abstr.Vol. 12, pp. 101-103.

Cook, N.G.W., Hodgson, K and Hojem, J.P.M., 1971. A 100-MN Jacking System For Testing Coal Pillars Underground. Journal of South Africa Inst. Min & Metall. pp. 215-224.

Esterhuizen, G.S., 1992. Theoretical Investigations into the Strength and Loading of Barrier Pillars. University of Pretoria, Project No 286/89.

Hoek, E., 1966. First Report on the Testing of Large Scale Coal Specimens in Situ. CSIR Report MEG 452. June.

Hill, R.W., 1989. Multiseam Mining in South Africa. SANGORM Symposium: Advances in Rock Mechanics in Underground Coal Mining. Witbank, September.

Madden. B.J., 1987. The Effect of Mining method on Coal Pillar Strength. Chamber of Mines Research Report 15/87.

Madden, B.J., 1991. A Re-assessment of Coal-Pillar Design. J. S. Afr. Inst. Min. Metall., vol. 91, no. 1. January. pp. 27 - 37.

Madden, B.J. and Hardman, D.R., 1992. Long Term Stability of Bord and Pillar Workings. COMA : Symposium on Construction Over Mined Areas, Pretoria, May.

Madden, B.J., Canbulat, I., Jack, B.W., Prohaska, G.D., 1995. A reassessment of coal pillar design procedures, SIMRAC Final Project Report - COL021, CSIR Division of Mining Technology.

Madden, B. J. and Canbulat, I., 1995. Review of South African Coal Pillar Research: 1965-1995. SAIMM Symposium, SIMRAC Safety in Mines Research Advisory Committee, 1 September, Mintek, Randburg.

Madden B.J. and Canbulat I., 1997. Practical Design Considerations for Pillar Layouts in Coal Mines. SARES 97, 1st Southern African Rock Engineering Symposium. 15 – 17 September, Johannesburg, South Africa.

Oravecz, K.I., 1973. Loading of Coal Pillars in Bord and Pillar Workings. COMRO Contract Report No 40/73. Johannesburg.

Özbay, M.U., 1994. Strength of Laboratory-Sized Coal Samples from Delmas and Sigma Collieries. Submitted reported to CSIR-Miningtek, January.

Salamon, M.D.G., 1967. A Method of Designing Bord and Pillar Workings. J. South African Inst. Min. Metall, Vol. 68, no.2. pp. 68-78.

Salamon, M.D.G., 1982. Unpublished Report to Wankie Colliery.

Salamon, M.D.G and Munro, A.H., 1967. A Study of the Strength of Coal Pillars. J.South African Inst.Min.Metall. September.

Salamon, M.D.G. and Oravecz, K.I., 1966. Displacement of Strains Induced by Bord and Pillar Mining in South African Collieries. Proceedings of the 1st Congress of ISRM, Lisbon, 25 September-10 October.

Salamon, M.D.G. and Oravecz, K.I., 1976. Rock Mechanics in Coal Mining. Chamber of Mines of South Africa.

Salamon, M.D.G. and Wagner, H., 1985. Practical Experience in the Design of Coal Pillars. Safety in Mines Research Proceedings of the 21st International Conference. Sydney, October.

van der Merwe, N., 1993. Revised Strength Factor for Coal in the Vaal Basin. J. South African Inst. Min. Metall, Vol. 93, no 3. pp. 71-77. March.

Wagner, H., 1974. Determination of the Complete Load-Deformation Characteristics of Coal Pillars. Proceedings of the 3 rd. ISRM Congress. December. pp 1076-1081.

Wagner, H., 1980. Pillar Design in Coal Mines. Journal of South African Institute of Mining and Metallurgy. January. pp. 37-45.

Wagner, H., and Madden, B.J., 1984. Fifteen Years Experience with the Design if Coal Pillars in Shallow South African Collieries: An Evaluation of the Performance of the Design Procedures and Recent Improvements. Design and Performance of Underground Excavations. ISRM/BGS, Cambridge. pp 391 - 399.

Wiid, 1963. Tests to determine Various Mechanical Properties of Rock and Coal from Wolvekrans Section, Witbank Colliery. Part1: The Uniaxial Compressive Strength and Elastic Constants of Coal Measure Rock Specimens. _CSIR Contract Report No C/MEG 548, Pretoria, South Africa, July.

2 Methodology to estimate the effect of discontinuities on the strength of coal pillars

2.1 Introduction

This chapter addresses Enabling Output 2 in the project proposal. Coal, like most rock types, contains natural discontinuities which have an effect on its strength. In general, the greater the intensity of discontinuities, the weaker the rock mass becomes. The strength of coal pillars should therefore also be affected by the intensity of discontinuities in the coal. The pillar design procedures used in South African collieries do not explicitly account for the effect of discontinuities. Instead, a suitable factor of safety is used when designing pillars to account for local variations in pillar strength. In spite of this factor of safety, a number of collapses of coal pillars have taken place (Madden, 1996). Intense jointing and other discontinuities in the coal were identified as one of the major causes of failure in some of the collapsed cases.

Initial studies of the effects of discontinuities on coal pillar strength was carried out under the SIMRAC project COL005A . That project characterised the discontinuities in coal seams and determined their potential effect on the strength of coal pillars. The objective of the research reported here was to develop a methodology which will allow rock engineers to estimate the effect of discontinuities on coal pillar strength.

2.1.1 Types of discontinuities in coal

Discontinuities in coal may be classified according to their persistence. For the purpose of this research, discontinuities were classified as follows (Esterhuizen, 1995):

- Cleats: minor discontinuities having trace lengths less than 1.0 m and occurring at frequencies of 5 per metre to 20 per metre. Cleats are considered to be part of the coal material structure. Cleats are usually vertical and strike in two nearly orthogonal directions.

- Joints : similar to joints in rock, having trace lengths of more than 1.0 m and typically extending from the roof to the floor of the coal seam, but seldom extending into the surrounding strata.

- Slips : joints which are extensive in the strike direction; being up to several tens of metres long, they often extend into the surrounding strata and may have minor displacements along them.

In all the work which follows the cleats were not considered in the evaluation of the strength of coal. It was assumed that the effect of cleats (features less than 1.0 m in length) would be incorporated in the determination of the coal material strength.

2.2 Discontinuities and pillar strength

In South Africa the Salamon and Munro (1967) equation is used as a basis for pillar design. This equation provides the strength value of a "typical" pillar, and a factor of safety of 1.6 is used to allow for local variations in pillar strength. One of the causes of variations in the strength of pillars may be a variation in the amount of jointing in the coal. It is possible to carry out geotechnical mapping to determine whether particular pillars have more or less joints than the “typical” pillars (“typical” based on the Salamon and Munro database). This knowledge may be used to adjust the pillar strength upwards or downwards. The question that needs to be resolved is: by how much should the strength be adjusted?

The appropriate adjustment in strength may be estimated by classifying the coal mass using one of the accepted rock mass classification techniques (Bieniawski, 1976 or Barton, Lien & Lunde, 1974) and using the resulting classification as input into the Hoek-Brown failure criterion (Hoek & Brown, 1988) to obtain the large scale strength of the coal. However, the Hoek-Brown criterion does not address the problem of anisotropy of the coal - it assumes that the material being evaluated is uniformly jointed in all directions. South African coal typically contains one or two steeply dipping joint sets, which would result in anisotropic strength. The Hoek and Brown approach may result in unacceptably low coal mass strength values.

2.3 Objectives and scope

An alternative approach may be to use the classification results in numerical models to evaluate the pillar strength. This technique was used by Duncan-Fama (1995) to develop a numerical model which was used to determine the strength of rib pillars in highwall mining. However, in the day to day design of pillars in a coal mine, it is not desirable to have to develop a numerical model of the pillars for the purpose of designing the pillars. Obtaining input parameters and setting up numerical models are specialised tasks. A method is required in which a rock engineer can identify the critical factors and apply adjustments to a standard pillar strength equation.

The overall objective of the research presented in this chapter was to develop a simple methodology which practising rock engineers may use to estimate the effect of jointing on the

strength of coal pillars. Once a method had been developed, a secondary objective was to calibrate it against actual pillar performance and carry out case studies to test the method.

Since this research is only concerned with the discontinuity aspects of pillar strength, the effect of the contact surfaces of the coal with the surrounding strata, the effect of weak roof and floor strata and the effect of weak coal material were not evaluated.

The important characteristics of discontinuities which should be included when assessing the strength of jointed pillars were first determined by considering different rock classification methods and methods of estimating rock mass strength. Discontinuity data collected as part of project COL005 was used in the analysis. A published equation for the strength of jointed rock samples was modified so that it would be suitable for the calculation of pillar strength. The equation was calibrated against jointing information and pillar performance at a number of mines. The result was a set of equations which may be used to modify the strength of pillars to account for jointing. Two case studies are presented.

2.4 Development of a methodology to estimate the effect of discontinuities on the strength of coal pillars

2.4.1 Background

The primary objective during the development of the methodology was that it should be simple to use and should be based on standard discontinuity data. The following paragraphs describe the steps in the development of the methodology. A full description of each of the stages in the development of the methodology are presented in Appendices A-C.

2.4.2 Important jointing characteristics

The importance of discontinuities in the strength of a rock mass is evident from inspection of established classification methods. The most widely used rock classification methods are the rock mass rating (RMR) method of Bieniawski, (1976) and the Q-system of Barton, Lien and Lunde (1974). These two methods were examined to establish which jointing parameters are considered important and what their relative importance is in the rating systems, see Appendix A. The study showed that joint frequency and joint frictional resistance were the two common factors in the classification systems.

In the RMR method the joint frequency is taken into account in the rock quality designation (RQD) and in the joint spacing ratings. The frictional resistance of the joints is taken into

account in the “condition of joints” rating. The joint orientation relative to excavations is taken into account as an adjustment to the final rating. Other factors in the rating system, not directly related to joints, are the intact rock strength and the groundwater conditions.

The Q-system accounts for joint frequency in the RQD parameter and the “Joint set number” parameter. It accounts for joint frictional strength in both the “Joint alteration” and the “Joint roughness” numbers. Factors in the rating system not directly related to joints are the groundwater and stress factors.

It was clear from the study that joint frequency and joint shear resistance were the two parameters which should be considered in any system which attempts to quantify the effect of jointing on coal pillars.

2.4.3 Jointing and pillar strength

The effect of jointing on the strength of pillars is not directly addressed in the literature. Numerous results exist, however, from laboratory tests on rock samples containing joints. These results provide insight into the effect that joints would have on coal pillars. One of the reasons that the laboratory results are not applicable to pillars is that most of the tests were conducted on samples with width to height ratios which are well below those commonly found in coal pillars.

A useful set of laboratory results were obtained by Arora (1987), who found that the important parameters affecting the strength and modulus of jointed rock samples are the joint frequency, joint inclination with respect to the major principal stress and the joint frictional strength. Since pillars may be seen as large rock samples, these parameters are also expected to affect the strength of pillars. Rock mass classification methods also contain joint frequency and joint strength as the main input parameters, confirming their importance in determining rock mass strength. It is the orientation that is not adequately accounted for in classification methods for the purpose of pillar design. The work of Arora (1987) was further expanded upon by Ramamurthy et al (1988), where a set of equations were developed for estimating the jointing effect on the strength of rock samples. These results were identified for further evaluation in the development of a methodology for coal pillars.

Numerical model analyses, carried out in SIMRAC project COL005A, showed that the effect of discontinuities on pillar strength varies according to the geometry of the pillar being considered and the orientation of the discontinuities (Esterhuizen, 1995). These results showed that when designing pillars, it is not sufficient to only calculate the coal mass strength and apply it equally to the strength of all pillars regardless of the width to height ratio. The strength should be

adjusted by varying amounts, depending on the width to height ratio of the pillar and the orientation of the discontinuities.

2.4.4 Selection and modification of a suitable method

Since rock mass classification methods were found to be unsuitable to estimate the effect of jointing on pillar strength, an alternative method was sought. The method of Ramamurthy *et al* (1988), which is based on laboratory strength tests, was considered to be the most amenable to modification so that it may be used to calculate the jointing effect on pillar strength. It makes use of three easily determined jointing parameters: the joint frequency, joint orientation and joint strength. These parameters were also found to be the important parameters which affect rock mass strength. The equations are as follows:

$$\frac{\sigma_{cj}}{\sigma_{ci}} = e^{-0.017F} \qquad \textit{Equation 2-1}$$

$$F = \frac{J_f}{n_r} \qquad \textit{Equation 2-2}$$

where J_f is the joint frequency, n is an orientation parameter, σ_{ci} is the intact rock strength, σ_{cj} is the jointed rock strength, and r is a joint strength parameter.

The equations were first modified to calculate the strength of cubes of coal, rather than cylindrical specimens, which Ramamurthy and co-workers used as a basis for developing their equation. It required that the method of calculating the joint frequency and the exponent in Equation 2-1 be changed. This modification was necessary, since the strength of a cube of coal is used as the basis for pillar strength calculations. Details of the method of determining the modifications and verification are presented in Appendix A.

A second modification was necessary to correctly predict the effect of inclined joints on the strength of pillars. This required the modification of the orientation parameter *n* in Equation 2-2. Pillar behaviour is different from the behaviour of slender laboratory specimens, since inclined joints often daylight on opposite sides of a laboratory specimens, but not in pillars which have larger width to height ratios. The results of extensive numerical modelling, carried out as part of project COL005 (Esterhuizen, 1995) was used as a basis for determining the appropriate values of *n.*

A new parameter, W_p, was added to the equations, to account for the width to height ratio of a pillar. An initial value for W_p was obtained from the aforementioned numerical modelling results.

Details of the reasoning behind the modifications and the method of analysis are presented in Appendix A.

2.4.5 Calibration of the modified equations against pillar performance

Final values of the parameters in the modified equations were obtained by calibrating the equations against jointing information and pillar performance at a number of collieries so that they predicted the actual stability and instability of pillars. An iterative procedure was used in which the W_p parameter was modified successively using a spreadsheet program. The final values for W_p were obtained by satisfying the following two requirements:

- The Salamon and Munro equation predicts the strength of typical pillars; pillars with less than average jointing should be stronger than predicted by this equation and pillars with more than average jointing should be weaker. The jointed pillar strength should therefore be split equally above and below the strength predicted by the Salamon and Munro equation.
- Since a large variety of workings were mapped, some of the sites should have a jointed factor of safety of just greater than 1.0, owing to the variations in the coal mass strength. None of the factors of safety should however be below 1.0, since all the areas visited were stable.

The resulting equations take the following form:

$$e^{-0,017F} = \frac{\sigma_{pj}}{\sigma_{pi}} \qquad \textit{Equation 2-3}$$

where σ_{pj} is the strength of a pillar containing joints, σ_{pi} is the strength of the pillar without any joints and *F* is a joint factor.

The value of *F* is determined as follows:

$$F = \frac{10(1 - e^{-0.23hJ_f})}{\sqrt{Rn}\tan\phi} \qquad \textit{Equation 2-4}$$

where R is the width to height ratio of the pillar, J_f is the joint frequency per metre, h is the pillar height in metres, *n* is the joint orientation parameter, which depends on the inclination of the joints and may be obtained from Table 2-1, and ϕ is the peak friction angle of the joints. The methodology to obtain ϕ is shown in Appendix A.

Table 2-1 Joint orientation factor* n *for pillars with width to height ratios of 2.0 to 6.0.

Joint dip	**20°**	**30°**	**40°**	**50°**	**60°**	**70°**	**80°**	**90°**
n	0.51	0.30	0.21	0.20	0.21	0.30	0.54	0.82

The factor of safety of pillars calculated using the above equations is compared to the factor of safety calculated by the Salamon and Munro equation in Figure 2-1. The results for 62 different locations in South African mines are shown in the figure. The details of the mine sites, locations, pillar dimensions, discontinuities and depth below surface are presented in Appendix A.

Referring to Figure 2-1, it can be seen that the factors of safety, after accounting for jointing, are split equally above and below the line representing equality between the two methods. No jointed strength values plot below the line representing a factor of safety of 1.0, which satisfies the requirements set out above.

The line representing equality between the two methods indicates that jointing may reduce the strength of a pillar considerably below the Salamon and Munro predicted strength, but the absence of jointing does not result in significantly increased strength. This observation led to the conclusion that the strength of a pillar without any joints (σ_{pj}) is approximately 1.1 times the strength predicted by the equation of Salamon & Munro (1967).

The effect of joint frequency and orientation on the strength of pillars with a width to height ratio of 2.0 is shown in Figure 2-2. The graph was calculated assuming a joint friction angle of 20° and a pillar which was 1 m high and 2 m wide. The graph illustrates that as the joint orientation approaches 45°, the weakening effect on the pillar reaches a maximum. Steep joints do not affect the pillar as severely as the oblique joints. The joint frequency is shown to have a significant effect on the pillar strength. Note that the equations are sensitive to the volume of the pillar being evaluated; the graph is therefore only valid for pillars which are 1 m high and 2 m wide.

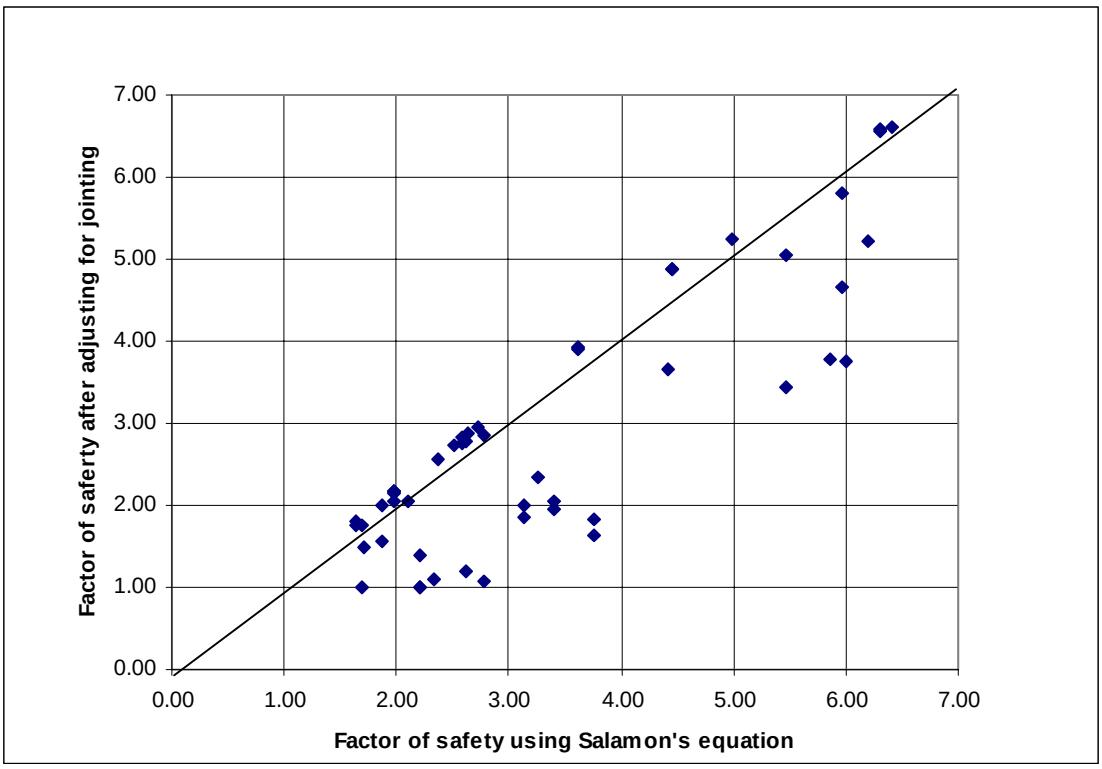

Figure 2-1 Relationship between factors of safety of pillars calculated using the Salamon & Munro equation and after adjusting for the effect of jointing.

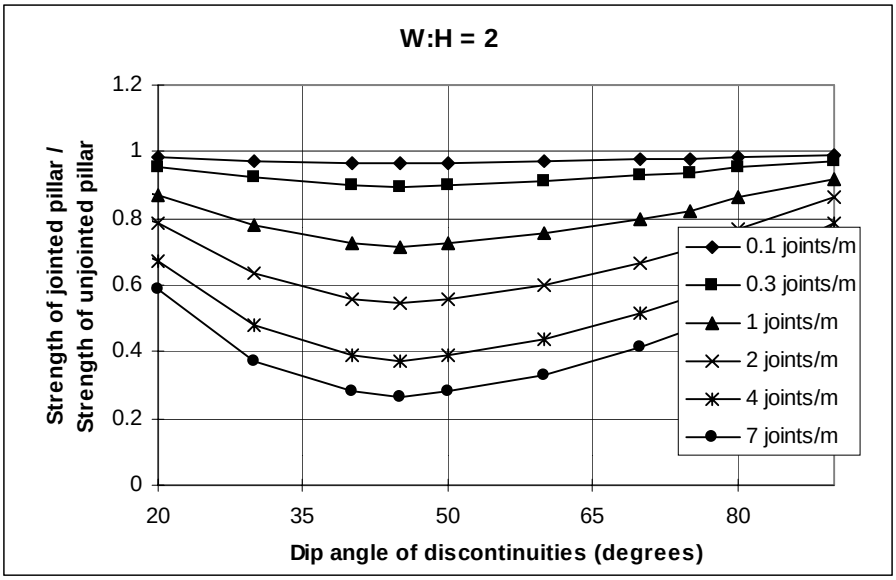

Figure 2-2 Graph showing the effect of discontinuity orientation and frequency on the strength of pillars with a width to height ratio of 2.0.

The results of the study showed that as the width to height ratio of pillars increases, their sensitivity to the presence of discontinuities decreases. This is illustrated in Figure 2-3 where

the effect of 2 joints per metre at different inclinations is plotted for pillars with width to height ratios of 2.0 to 6.0. The results show that a pillar with a width to height ratio of 6 would maintain about 70 per cent of its unjointed strength if it contains 2 joints per metre dipping at 45°, while the strength of a pillar with a width to height ratio of 2.0 would drop to 54 per cent of its unjointed strength. The sensitivity to the presence of jointing has an important bearing on the failure probability of pillars. The strength of pillars with smaller width to height ratios will be more variable than wider pillars, owing to their sensitivity to variations in jointing. Their failure probability will therefore be higher than that of wider pillars with a similar factor of safety.

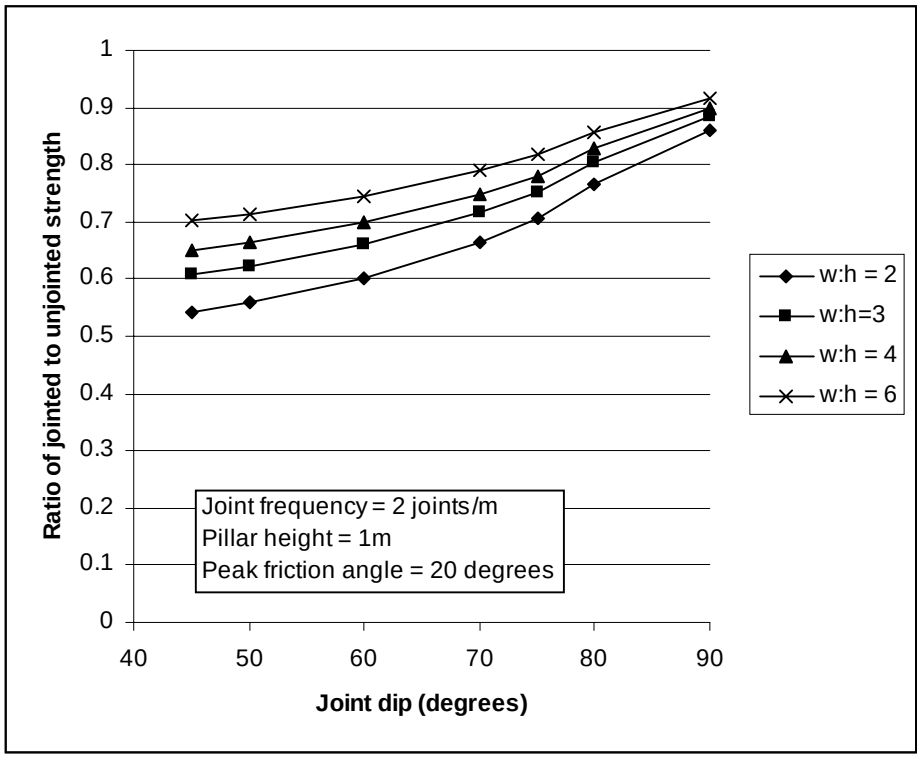

Figure 2-3 Graph showing the effect of joints at the indicated dips on the strength of pillars with different width to height ratios, joint frequency is 2 joints per metre.

2.4.6 Discontinuity data collection

The geotechnical data required to calculate the strength of jointed pillars are the joint frequency, joint dip and the peak friction angle. The joint frequency and dip may be readily measured in the field using a tape and clino-rule or geological compass. It is suggested that the peak friction angle be determined using the equation of Barton and Choubey (1977) which takes the following form:

$$\tau = \sigma_n \tan\left[\phi + \text{JRC}\log_{10}\left(\frac{\text{JCS}}{\sigma_n}\right)\right] \qquad \textit{Equation 2-5}$$

Where JRC is a joint roughness coefficient varying between 1 for the smoothest joints and 20 for the roughest joints, JCS is the joint wall compressive strength in MPa and ϕ_r is the base friction angle of the coal material in degrees. The term between the square brackets represents the peak friction angle in degrees.

In the course of this research the JRC values were either determined by using a carpenters profiler to trace the joint surface profiles and comparing them to the published roughness profiles of Barton & Choubey, or by use of Table 2-2.

Table 2-2 Estimation of joint roughness coefficient

Stepped			Undulating			Planar		
Rough	Smooth	Slicken sided	Rough	Smooth	Slicken sided	Rough	Smooth	Slicken sided
20	14	11	14	11	7	2.5	1.5	1.0

The joint wall compressive strength may be determined in the field by the use of a Schmidt hammer. Alternatively, a simple index test may be carried out with a geological pick and a pen knife as indicated in Table 2-3.

The base friction angle of the joints may be determined by a sliding test. The inclination at which sliding occurs along a smooth, diamond saw cut coal surface is simply measured.

Table 2-3 Estimation of joint wall compressive strength

Weaker than coal				Unaltered coal	Stronger than coal
Soft clayey	Crumbles when struck with geological pick	Shows 3 mm indentation when struck with geological pick	Cannot be scraped off with a pen knife	No infilling or alteration	Hard infill materials
< 0.1 MPa	3 MPa	7 MPa	20 MPa	30 MPa	> 30 MPa

The frequency of joints and slips in the coal should be measured separately, where possible. When measuring the joint frequency, the scan line should be at least 10 m long and the average joints per metre determined. When measuring the slip frequency it is suggested that 100 m scan

lines should be used, and the slip frequency per metre determined from the results. This is to ensure that widely spaced joints or slips are not omitted. Where possible two orthogonal scan lines should be mapped, this is usually not a problem in coal mine workings. When data from two orthogonal scan lines are available, the highest joint frequency should be used in the calculation of the effect of jointing.

A sample data logging sheet is presented in Appendix B.

2.4.7 Calculation of jointing effects

Once the geotechnical data has been collected, the calculation of the jointing effects on pillar strength is done by calculating the effect of joints and slips separately using Equation 2-4. This will result in two values for the joint factor *F* called F_s and F_j for slips and joints, respectively. The combined strength reduction may then be calculated as shown in Equation 2-6.

$$\sigma_{pj} = \sigma_{pi} \times e^{-0.017(F_j+F_i)} \qquad \textit{Equation 2-6}$$

This method ensures that similar results are obtained whether the slips are counted as joints or counted separately.

2.5 Case studies

2.5.1 Collapse of pillars in the Klip River coal field

The techniques developed to predict the effect of jointing on the strength of coal pillars were applied to a case study where pillars had collapsed at a mine in the Klip River coal field. The mine makes use of drill and blast, bord and pillar methods to extract the main seam at depths which vary between 25 m and 70 m below surface. The mining height is approximately 2.0 m. The initial intention was to develop the pillars for later extraction. As a result the pillars were mined to a calculated factor of safety well in excess of 1.6, based on the Salamon equation. However, before the pillars could be extracted, collapses started to occur in some of the panels which had been developed. In one of the panels, the collapse occurred whilst mining was taking place. The collapse was not violent, and it was possible to remove most of the mining equipment before access became too dangerous. Subsequent to the collapses, the mine was visited and the author was able to collect jointing information adjacent to one of the collapsed panels and in a number of the stable panels. The details are presented below.

The pillars were rectangular in plan, 7 m by 5 m, mined to a height of 1.9 m. The immediate roof and floor are weak laminated shales, about 1.2 m thick, which collapsed in many of the

intersections. Owing to the poor roof conditions, the bords were mined to a width of approximately 5 m. It is reported that roof collapse was not prevalent in the area where the pillars collapsed. This is confirmed by the fact that it was possible for the mine personnel to retrieve the equipment after the pillars had started failing. The pillars contained many through going discontinuities, an example of which is shown in Figure 2-4.

The factor of safety of the pillars was calculated using the Salamon equation. Since the pillars are rectangular the equivalent width of the pillars was determined, using the method suggested by Wagner (1980). The equivalent width of the pillars was calculated to be 6.25 m mined to a height of 1.9 m. The width to height ratio was therefore 3.29. The calculated pillar strength, using the Salamon equation, is 10.91 MPa. The depth to the floor was 61m, which results in an average pillar stress of 4.94 MPa, for a bord width of 5 m. The resulting factor of safety is 2.2. This should ensure stable pillars under typical coal mass strength conditions.

Figure 2-4 Through-going joint in a pillar at the Klip River case study

The fact that the panel collapsed indicates that the strength of the system of pillars was well below the predicted strength. Inspection of the workings indicated that the coal was highly jointed and that the roof and floor were weak. The collapse could also have been initiated by weaker burnt coal where the panel approached a dyke. No signs of floor heave were observed and, as mentioned above, extensive roof failure, which may have increased the height of the pillars, did not occur. The jointing in the coal was therefore likely to have been a major contributing factor in the collapses which took place.

Joint data was collected at two locations, called sites A and B, adjacent to the collapsed area. The jointing at site A was assumed to be typical of the jointing in the collapsed panel since it was measured directly opposite the collapsed panel in the main development. The jointing in site B was representative of the jointing near a dyke which intersects the collapsed panel. Jointing data was collected at seven other sites in the mine which showed that the intensity of jointing at site A was not particularly high. However, near the dyke at site B, the intensity was the highest of all the sites. The details are summarised in Table 2-4.

Table 2-4 Frequency of joints and slips at Klip River case study

	Site								
	A	B	1	2	3	4	5	6	7
Joint & slip frequency / metre	1.5	3.3	1.01	0.31	0.71	0.83	2.1	1.5	1.8

In general, the jointing in the mine may be described as being spaced 1 to 2 m apart, dipping at 45 degrees, with thin calcite infilling of less than 2 mm. The joints were continuous from the roof to the floor of the coal seam and may have extended into the over lying strata. Major slips also occurred, which had similar characteristics to the joints, and were spaced about 3 m apart in poor ground areas, but they may have been as much as 50 m apart in better ground.

Table 2-5 Calculation of jointing parameter* F *for the pillars at Site A and Site B of the Klip River case study

Site	Joint frequency (joints/m)	Joint friction angle	Joint inclination	Width to height ratio of pillar	*F*	Ratio of jointed to unjointed strength of pillar
A	1.8	22°	45°	3.29	37.16	0.532
B	3.3	22°	45°	3.29	52.34	0.411

The effect of jointing on the pillar strength was calculated using the equations developed in this section. Table 2-5 summarises the data and results of the calculations. The results show that the jointing reduced the strength of the pillars which are remote from the dyke by a factor of 0.53, whilst the strength of the pillars near the dyke was reduced by a factor of 0.41. The strength of these pillars according to the Salamon equation was 10.95 MPa. Assuming that unjointed pillars are 10 per cent stronger than predicted by the Salamon equation, the jointed strength of the pillars at site A was:

$$\sigma_{pj} = 10.95 \times 1.1 \times 0.532$$
$$= 6.41\,\text{MPa}$$

and pillars adjacent to the dyke at site B:

$$\sigma_{pj} = 10.95 \times 1.1 \times 0.41$$
$$= 4.94\ \text{MPa}$$

Table 2-6 Calculation of factor of safety of pillars at collapsed sites in Klip River coal field

Site	Jointed pillar strength (MPa)	Depth (m)	Pillar dimensions (m)	Bord width (m)	Pillar stress (MPa)	Factor of safety
A	6.41	61	5 x 7	5	4.94	1.30
B	4.94	61	5 x 7	5	4.94	1.00

Assuming tributary loading on the pillars, the factors of safety in the panel were calculated as shown in Table 2-6. The above factors of safety were calculated assuming that the strength of the coal, excluding the effects of jointing, was "typical" of South African coal. Any reduction in the coal strength caused by devolitisation of the coal near the dyke, or increase in loading, or any other influence may have initiated the collapse near the dyke. The fact that the other pillars remote from the dyke had a factor of safety of only 1.3 appears to have been an insufficient safety margin to accommodate the additional loading when failure commenced near the dyke. The entire panel eventually collapsed. The collapse did not take place in a violent manner, possibly owing to the width to height ratio of 3.0, and the fact that jointing appears to soften the post peak performance of a pillar.

2.5.2 Jointed pillars in the Piet Retief coal field

The pillars in this case study occur in the Lower Dundas seam at a depth of between 160 m and 210 m, owing to variations in the surface topography. The pillar centres were initially 40 m with 5.0 m bords and a mining height of 3.0 m. The 35 m pillars were split and quartered leaving pillars which were 15x15 m in plan. Three rows of smaller pillars were present in the panel; two of the rows of pillars were 15 x 10 m in plan and one row was 15 x 7.5 m. The management of the mine was interested in extracting the remaining pillars in the panel. There was some concern about the stability of the smaller pillars and whether they could be extracted. It is the stability of these smaller pillars which were investigated as a case study. The small pillars were bounded by 35x35 m pillars on one side and 15x15 m pillars on the other.

The immediate roof of the panel consists of competent sandstone some 4.25 to 8.5 m thick. The sandstone is overlain by the upper Dundas seam which is about 1 m thick, followed by sandstone. A dolerite sill, about 100 m thick, overlies the mining area. Inspection of the underground workings showed that major discontinuities intersected the coal, and it was decided to evaluate the stability of these pillars using the techniques developed in this section.

Jointing data were collected at three sites within the panel. It was found that the coal was intersected by between two and six joints per 10 m distance. The joints were steeply dipping and did not contain any infilling. Major slips were observed, between 40 and 70 slips per 100 m dipping at between 50° and 70°. An example of the slips in the coal seam is shown in Figure 2-5.

Owing to the variable pillar dimensions, the great depth and the small mined out span, it was not possible to calculate the loading on the pillars using the tributary area method. An analysis using the BEPIL program (Ryder & Özbay, 1990) was carried out which was able to model the various pillar dimensions. The BEPIL model assumed a depth of 190m, the modulus of elasticity of the seam and surrounding strata were 3 GPa and 40 GPa respectively. A 175 m long section through the panel was modelled. The results showed that the stress in the smaller pillars were 8.1 MPa for the 10 m wide pillars and 8.5 MPa for the 7.5 m wide pillars.

Figure 2-5 Major discontinuities in a pillar at the Piet Retief case study

The geotechnical properties of the coal seam in the panel were collected at three sites in the panel. The average properties of the joints and slips at the sites are summarised in Table 2-1. The base friction angle of the coal was measured to be 23° by a sliding test. These data were

used to determine the peak friction angles. In the calculation of the peak friction angle, the normal stress was set at 8 MPa, which approximates the pillar stress.

Table 2-7 Summary of average discontinuity properties at Piet Retief case study

Feature	Frequency	Dip	JRC	JCS	Peak friction angle
Joints	4.2 per 10 m	85°	14	30 MPa	31°
Slips	51.7 per 100 m	59°	8	12 MPa	24°

The strength of the pillars was first calculated using the Salamon and Munro equation. Since the pillars are rectangular, the equivalent width of the pillars was determined, using the method suggested by Wagner (1980). The equivalent width of the pillars was calculated to be 10 m for the 7.5 x 15 m pillars and 12 m for the 10 x 15 m pillars. The mining height was 3.0 m. The calculated pillar strength, using the Salamon equation, is 10.06 MPa and 10.94 MPa for the 7.5 m and 10 m wide pillars respectively.

The effect of jointing on the pillar strength was calculated using the procedures presented in this report. The results for the 7.5 m wide pillars are summarised Table 2-8.

Table 2-8 Calculation of jointing parameter F for the 7.5 m wide pillars at Site A and Site B of the Piet Retief case study

Feature	Frequency (per m)	Friction angle	Inclination	Width to height ratio of pillar	*F*
Joints	0.42	31°	85°	3.33	3.585
Slips	0.52	24°	59°	3.33	15.462

The resulting reduction in pillar strength may be calculated from Equation 2-6 as:

$$e^{-0.017(F_j+F_s)} = e^{-0.017(3.585+15.462)}$$
$$= 0.723$$

The jointed pillar strength of these 7.5 m wide pillars may then be calculated as :

$$\sigma_{pj} = 10.06 \times 1.1 \times 0.723$$
$$= 7.99 \text{ MPa}$$

Similarly, the strength of the 10 m wide pillars was calculated as 8.94 MPa. The factors of safety against failure of the pillars are presented in Table 2-9, which shows that the 7.5 m wide pillars are below a safety factor of unity while the 10 m wide pillars are just above. This indicated that the three rows of narrow pillars were unstable and could fail at any stage. The fact that the narrow pillars had not failed may be explained by the fact that they were surrounded by large, stiff pillars and the immediate roof was competent. It was decided that no attempt should be made to extract the narrower pillars in the panel owing to their marginal stability condition.

Table 2-9 Factors of safety of pillars in Piet Retief case study

Pillar dimensions	Pillar stress (MPa)	Jointed pillar strength (MPa)	Factor of safety
7.5 x 15 m	8.5 MPa	7.99	0.94
10 x 15 m	8.1 MPa	8.94	1.10

2.6 Discussion and conclusions

The results presented in this report show that joint frequency, joint condition and joint orientation have an important effect on the strength of coal pillars. Published equations which take into consideration the effect of jointing on rock strength were modified so that they are suitable for predicting the strength of coal pillars. The parameters used in the equations were determined by calibration against numerical model results and the results of field data. An evaluation of the field data showed that pillars without any joint structures are likely to be only about 10 per cent stronger than predicted by the empirical Salamon and Munro equation. Jointing observed in South African coal mines can, however, reduce the strength of a cubic metre pillar by more than 50 per cent. Some of the mines which were visited had consistently low jointed coal strengths, and the mine operators tended to leave larger pillars owing to their local experience with instability in the mine.

Information gathered adjacent to a collapsed panel of pillars, in the Klip River Coalfield, indicated that the jointed strength of the coal was such that, in spite of the large width to height ratios of pillars in this mine, the pillar collapse could have been predicted using the modified strength of the pillars.

A second case study in the Piet Retief coal field indicated that jointing is likely to have weakened pillars in a panel where pillar extraction was planned. The pillars were shown to be marginally stable and it was decided not to proceed with the extraction of the pillars.

It is concluded that the methodology presented in this report may be used to determine the effect of jointing on the strength of coal pillars. The equations will be useful to identify areas

which are likely to be under designed when using the Salamon and Munro equation. The result is that site specific coal pillar design can be done to accommodate the effect of jointing.

It must be borne in mind that the equations only consider the effect of jointing, and other effects such as weak roof or floor and weak contacts between the coal and the surrounding strata are not accounted for.

Further verification of these equations should be done before they are widely used for pillar design. A trial period is suggested in which rock engineers make use of the equations in different areas and compare results so that confidence is built up in their applicability in different geological settings.

2.7 References

Arora, V.K. 1987. Strength and deformational behaviour of jointed rocks. *Ph.D. Thesis,* Indian Institute of Technology, Delhi.

Barton, N. & Choubey, V. 1977. The shear strength of rock joints in theory and practice. *Rock Mechanics* no. 10.

Barton N., Lien, R. & Lunde J. 1974. Engineering classification of rock masses for the design of rock support. *Rock Mechanics 6,* pp 189-263.

Bieniawski, Z.T. 1976. Rock mass classification in rock engineering. In *Exploration for rock engineering* ed. Z.T. Bieniawski, AA Balkema. Rotterdam. pp 97-106.

Duncan Fama, M.E., Trueman, R. & Craig, M.S. 1995.Two- and three-dimensional elasto-plastic analysis for coal pillar design and its application to highwall mining*. Int. J. Rock Mech. Min. Sci. & Geom. Abstr.*, Vol. 32: pp 215 - 225.

Esterhuizen, G.S. 1995. Progress report, *Safety in mines research controlling committee*, Project COL005A, January 1995.

Hoek, E. & Brown, E.T. 1988. The Hoek and Brown failure criterion - a 1988 update. *Proc 15th Canadian Rock Mech Symposium.* Toronto, pp 31 - 38.

Madden, B.J. 1996. Coal pillar design procedures. *Safety in mines research controlling committee*, Report project COL337, Johannesburg.

Ramamurthy, T., Rao, G.V. & Singh J.A. 1988. A strength criterion for anisotropic rocks. *Proc. 5th Australia-New Zealand Conf. on geomechanics,* Sydney, Vol 1. pp 253 - 257.

Ryder, J.A. & Özbay, M.U. 1990. A methodology for designing pillar layouts for shallow mining, *Proc. Static and dynamic considerations in rock engineering.* Balkema, Rotterdam. pp.273 - 286.

Salamon, M.D.G. & Munro, A.H. 1967. A study of the strength of coal pillars. *Jnl South African Inst Min. & Metall.* Vol. 67. pp. 56-67.

Wagner, H. 1980. Pillar design in coal mines*, Jnl. S. Afr. Inst. Min. Metall*. Vol. 80. pp. 37-45.

by pillar scaling

3.1 Introduction

This section forms part of Enabling Output 2.

Most South African bord and pillar workings are planned using a pillar design methodology developed more than 30 years ago. During the intervening years this approach to design has proved to be successful in most instances (Salamon and Wagner, 1985; Madden, 1991). However, during the last few years an increasing number of reports has been published which indicate that the behaviour of pillars does not always accord with the expectations arising from the original work of Salamon and Munro (1967). In the already mentioned paper Madden shows that two of the failures he reported had particularly large safety factors. Van der Merwe (1993) goes considerably further and indicates that the "…Vaal Basin has long been recognised as a difficult area for coal mining in South Africa." A number of pillar collapses have occurred in collieries situated in this Basin. For example, he goes on to say, "Sigma colliery experienced three unrelated pillar failures in 1991. In one of these cases neighbouring seams were mined and floor lifting was also practised. In the other two cases no unusual circumstance was known to exist, nevertheless the panels collapsed." The safety factors of the pillars in these panels had been 1.7 and 2.8, respectively. According to the work of Salamon and Munro the probability of failure at a safety factor of 1.7 is about 0.0004. This is a very remote possibility. The probability of failure at 2.8 is just short of impossible. Not surprisingly, van der Merwe concluded that the traditional design procedure should be modified for the Vaal Basin.

There can be many reasons for this anomalous pillar behaviour. Perhaps the most obvious potential cause for such abnormal behaviour is a reduction in coal strength. For example, it has often been suggested that the strengths of coals encountered in different seams or in different coalfields are likely to differ from each other. Some recent publications appear to raise doubt concerning the practical significance of this observation. Mark and Barton (1996) stated that the *in situ* coal strength remains remarkably constant in a wide variety of conditions. Salamon *et al* (1996) have analysed both South African and Australian data concerning coal pillar behaviour and found that a *single pillar strength formula* can describe pillar behaviour remarkably well in *both* countries. Obviously these papers do not rule out the possibility of variation in coal strength

strength can be approximated well by a single formula. However, there are cases where this formula fails to yield an acceptable pillar strength, and of course a factor of safety of 1.6 is used in the design procedure, indicating the degree of uncertainty in the distribution and influence of factors that degrade pillar strength.

The search for the explanation of abnormal behaviour must not stop at anomalously low coal strength. Pillars may be debilitated by some weakness in the floor or roof (i.e., foundation failure) or in the seam itself. Problems may also arise because of some anomaly at the contact surfaces between the seam and the surrounding strata. Madden and Canbulat (1996) in a recent survey of South African collieries have identified a number of pillar collapses that may be attributed to these somewhat abnormal conditions. Van der Merwe (1993) called attention to another scaling as a mode of failure. Both of these phenomena can lead to the deterioration or even the collapse of pillars.

Van der Merwe argues that a given depth of scaling has a greater detrimental effect than the equivalent height of roof fall. He reports that according to his observations "…scaling is much more common than roof falls. In most areas of the Vaal Basin, virtually all pillars scale, while roof falls tend to be restricted in extent and in occurrence." In view of van der Merwe's experience and because of the importance of designing safe and economical pillars even in areas where scaling is prevalent, it has been decided to explore the influence of pillar side scaling on coal pillar design. The intention here is to present the results as a preliminary study.

The work described here focuses on situations where scaling represents the primary threat to the pillars. In this process coal strength remains unaltered and the weakening of the pillars is due merely to a reduction in pillar width induced by spalling.

The investigation combines the statistical pillar strength model developed by Salamon and Munro (1967) with a simple set of hypotheses concerning the mechanism of scaling. First, a brief review of the relevant background is presented and then an attempt is made to review the basic concepts of coal pillar mechanics in conditions where side wall scaling occurs. Here concepts such as *pillar life* and the *probability of survival* for a given period of time are introduced. An initial attempt is also made to estimate possible *rate of scaling* by back-calculation from data collated for the Vaal Basin and the Witbank area. Finally, a tentative method of *pillar layout design* is proposed. The method is not deterministic but recognises the

stress (or load) acting on the pillar could be determined, failure would occur when these two quantities become equal. Unfortunately, it is not possible to quantify these "true" values and consequently the true safety factor of pillars cannot be calculated. This problem arises because no accurate method exists to compute the strength of coal pillars (or any other rock pillars for that matter). Pillar strength is estimated from empirical formulae which, at best, can be regarded only as approximate. Even the tributary area method of pillar stress calculation is imprecise.

The ratio of the approximate pillar strength and approximate pillar load can only yield an approximate value for the safety factor. These ratios may be referred to as *apparent* or nominal safety factors. It follows, therefore, that the factors obtained for instances of pillar collapse, are either larger or smaller than unity. Salamon and Munro postulated that the apparent safety factor arising from pillar collapses, that is SF, is a random variable and that the log-normal distribution is an acceptable approximation of its frequency distribution. Thus,

$$f(SF) = \frac{1}{\sqrt{2\pi}\sigma SF} \exp\left[-\tfrac{1}{2}\left(\frac{\ln SF}{\sigma} \right)^2 \right] \qquad \textbf{Equation 3-1}$$

This distribution has its median at $SF = 1$ and σ is its standard deviation in the logarithmic scale. (For the sake of simplicity, natural logarithm is used here, as opposed to the base 10 version employed in the original paper.) The probability that failure will *not* occur, or the *probability of survival*, at a given apparent safety factor is given by the cumulative distribution function:

$$p(S_c) = \int_0^{S_c} f(x)dx = \int_{-\infty}^{\ln S_c/\sigma} Z(\varphi)d\varphi = P\left(\frac{\ln SF}{\sigma} \right) \qquad \textbf{Equation 3-2}$$

The definitions employed here are as follows:

$$Z(x) = \frac{1}{\sqrt{2\pi}} e^{-\frac{x^2}{2}} \qquad P(x) = \int_{-\infty}^{x} Z(\varphi)d\varphi \qquad \textbf{Equation 3-3}$$

where $Z(.)$ is the standard normal distribution function and $P(.)$ is the standard cumulative normal probability distribution.

Note that w and h are the width and height of a pillar of a square cross-section. Parameters α and β are dimensionless constants. The multiplier k is the compressive strength of a reference block of coal of height h_0 and width w_0. In the SI system h_0 and width w_0 are taken to be 1.0 m. It should be noted that k is not a property of the material (i.e., of the coal), but the property of the involved system. The system referred to here consists of the union of the block and the loading conditions prevailing underground. The metric version of the constants found by Salamon and Munro (1967) are:

$$k = 7.2\ \text{MPa} \qquad \alpha = 0.46 \qquad \beta = -0.66 \qquad \sigma = 0.159 \qquad \textbf{Equation 3-5}$$

Subsequently, it became apparent that for squat pillars an alternative expression may give a better estimate of the pillar strength. This squat pillar strength formula can be put in the following form (Salamon, 1985):

$$\sigma_{Squ} = K(w^2 h)^a R_o^b \left\{ \frac{b}{\varepsilon} \left[\left(\frac{w}{hR_o} \right)^{\varepsilon} - 1 \right] + 1 \right\} \qquad \textbf{Equation 3-6}$$

The following definitions apply in this expression:

$$a = \tfrac{1}{3}(\alpha + \beta) \qquad b = \tfrac{1}{3}(\alpha - 2\beta) \qquad R_o = 5 \qquad \varepsilon = 2.5 \qquad \textbf{Equation 3-7}$$

The original formula in Equation 3-4 is used when $w/h \leq R_0$. The squat formula in Equation 3-6 is applied in the alternative case of $w/h > R_0$. For the sake of brevity rectangular pillars are not dealt with. For the same reason the alternative linear pillar strength formula (where strength is a linear function of the width to height ratio) is omitted also. Both of these refinements can be incorporated without difficulty.

3.3 A model of pillar side scaling

3.3.1 Basic Properties of the Model

exposed coal skin in the presence of a humid environment. The pillar skin would swell in the direction perpendicular to the pillar side. The resulting tensile strain may cause the affected skin to peel off, exposing fresh coal and starting the process anew. Such a "weathering" mechanism is the basic premise of the model to be introduced next. Thus, in the sequel it is assumed that (i) the time dependent pillar deterioration is solely due to pillar side scaling or spalling and (ii) that this scaling is not due to excess stress, but to environmental conditions.

This or some similar process would result in a time dependent reduction of the widths of pillars. It will be assumed here that the scaling is uniform over the sides of the pillars and the pillar width at time t can be expressed in the following form:

$$w(t) = w_i - 2d(t) \qquad \textbf{Equation 3-8}$$

where w_i is the *initial* pillar width, that is the width at time zero and function $d(t)$ represents the thickness of coal peeled off one of the pillar sides between time zero and *t*. Obviously, the decrease in pillar width is accompanied by a corresponding increase in bord widths, as the pillar centre distances remain unaltered. Function $d(t)$ can be expressed as an integral of the scaling rate $r(t)$:

$$d(t) = \int_0^t r(\xi) d\xi \qquad \textbf{Equation 3-9}$$

Since no information is available concerning the nature of the scaling function, the simplest assumption is used in this paper. It is postulated that the scaling rate is constant, thus

$$d(t) = rt \qquad \textbf{Equation 3-10}$$

where parameter *r* represents the uniform rate of scaling.

It follows from this development that in the presence of scaling the apparent safety factor of a pillar also becomes a function of time. If $w(t)/h \le R_o$, the safety factor can be put in the following form:

$$SF_{Squ}(t) = \frac{\ldots}{q_m(t)} \left[w(t) \ldots h \ldots \right] R_o \ldots \left\{ \varepsilon \left[\left(\frac{\ldots}{hR_o} \right) \ldots - 1 \right] + 1 \right\}$$ ***Equation 3-12***

In these expressions $q_m(t)$ represents the tributary load (mean pillar stress) adapted for the present purpose:

$$q_m(t) = \gamma \quad H \left[\frac{C}{w(t)} \right]^2$$ ***Equation 3-13***

Here, the pillar centre distance $C = w_i + B = w(t) + 2d(t) + B$ remains unaffected. As usual, *B* is the original bord width in this relationship.

In the presence of scaling both the true and the apparent safety factors of pillars diminish with time. The apparent safety factor can be computed from Equation 3-11 or Equation 3-12 if the magnitude of scaling is known. The true factor must remain unknown right up to the moment of failure (if failure is to occur at all) when, by definition, it is equal to unity. In the absence of any contrary indication, it seems reasonable to postulate that the apparent safety factor at failure, or the *critical safety factor,* continues to be distributed in accordance with the original log-normal distribution defined in Equation 3-1.

3.3.2 Maximum Depth of Scaling

According to the simple version of the proposed model, scaling proceeds at a steady rate. This seems to imply that in all cases where such deterioration occurs the pillars will eventually collapse. Simple considerations reveal, however, that failure is not inevitable. The piles of coal that have peeled off the pillar sides will gradually restrain the scaling process. As the piles grow in height this restriction becomes more significant. For simplicity, it is postulated here that scaling of the sides will proceed unimpeded, as illustrated in Figure 3-1, until the height of the peeled off coal piles reaches the roof. At this stage scaling is arrested and*, as long as this crumbled coal is left in place*, the pillar will remain unchanged. This is a conservative assumption. In reality, pillar scaling will slow down and will even stop before the rubble reaches the roof. Of course, in contrast it will be realised that some pillars may never reach this condition, simply because they collapse before the scaling is choked in this manner.

The maximum depth to which scaling may penetrate before choking takes place, d_m, can be estimated by equating two volumes. The volume of loose coal lying around a pillar must be equal to the bulked volume of the solid coal that has peeled off the pillar.

In the first case, that is when the piles of coal corresponding to each pillar are independent of each other, this criterion leads to a quadratic equation for d_m (see Appendix D). If the bulking factor and the angle of repose are denoted by δ and ρ, respectively, then the solution of this equation results in the following maximum scaling depth (see Equation D-9 in the Appendix D):

$$d_m = \frac{h}{2\delta\mu}\left[1+\delta\mu R_i - \sqrt{1+(\delta\mu \quad R_i)^2 - \tfrac{4}{3}\delta}\right] \qquad \textbf{Equation 3-14}$$

where

$$\mu = \tan\rho \qquad R_i = w_i/h \qquad \textbf{Equation 3-15}$$

Here R_i represents the initial width to height ratio of the pillar.

The result in Equation 3-14 is valid as long as the piles do not come into contact at the bord centre. This requirement is fulfilled if the following inequality is satisfied (see Equation D-12 in the Appendix D):

$$B \geq B_{co} = \frac{h}{\mu}\left\{2 - \frac{1}{\delta}\left[1+\delta\mu R_i - \sqrt{1+(\delta\mu R_i)^2 - \tfrac{4}{3}\delta}\right]\right\} \qquad \textbf{Equation 3-16}$$

where B_{co} is that particular bord width at which the toes of the coal piles corresponding to neighbouring pillars first come into contact. If, however, $B < B_{co}$ then the coal piles coalesce and the maximum scaling can no longer be calculated from Equation 3-14, but an alternative value must be found. This is achieved by equating again the volume of the fragmented coal around a pillar with the bulked volume of the material that had scaled off the same pillar. This approach, when using the appropriate expressions for the volumes, leads to a cubic equation. This equation is given in the Appendix D (Equation D-19) and can be solved for d_m by, for example, iteration.

more useful form by defining a critical width to height ratio, R_{cr}. All pillars with an initial width to height ratio smaller than or equal to R_{cr} will fail, if scaling occurs. (Obviously the converse is not necessarily true. Pillars with width to height ratios greater than R_{cr} may or may not collapse.) This critical width - height ratio is defined by:

$$R_{cr} = \frac{2}{\sqrt{3\delta\mu}} \qquad \textbf{\textit{Equation 3-17}}$$

If reasonably typical values for the bulking factor ($\delta = 1.35$) and the angle of repose ($\rho = 35^{\circ}$) are used, the value of this critical width - height ratio is 1.42.

3.3.3 Life of Pillars

Perhaps the most important information concerning a panel supported by coal pillars, which are affected by scaling, is the period that elapses between the formation and collapse of the pillars. This period will be referred to as *pillar life* in the sequel. The expressions in Equation 3-11 and Equation 3-12 define safety factors that decrease with the passage of time. These results do not imply, however, that the life of a particular panel can be pre-calculated from the dimensions of the initial mining layout and the rate of scaling. This is understandable since the apparent safety factor corresponding to a specific failure is not known in advance. It was found (Salamon and Munro, 1967), however, that the frequency of the apparent safety factor at failure could be represented by a log-normal distribution, where the variance σ had been determined earlier as given in Equation 3-5.

To illustrate the problem, postulate that ten geometrically identical panels exist and the pillars in them are all subject to scaling at the same rate. In spite of these similarities, the panels cannot be expected to fail at the same time. This is because the apparent safety factor at failure is a random variable. This can be illustrated using the Monte Carlo method to draw a random sample of ten critical safety factors from the log-normal distribution. These values are tabulated in the first row of Table 3-1.

The layout parameters used to construct the second and third rows of Table 3-1 are as follows:

are not squat ($R_i = 4.67$), it is obvious that the scaled pillars will not be squat either. In this case, following the approach proposed by van der Merwe (1993), the expression in Equation 3-11 can be solved for d_c , that is, for the scaling at the time of failure. The result is:

$$d_c(SF) = \frac{1}{2}\left[w_i - \left(\frac{\gamma H S F C^2}{k h^{\beta}} \right)^{\frac{1}{2+\alpha}} \right] \qquad \textbf{Equation 3-19}$$

This formula, when the already specified parameters and the tabulated critical safety factors are utilised, yields the second row of Table 3-1. The third row of the same table is obtained from

$$t_c(SF) = d_c(SF)/r \qquad \textbf{Equation 3-20}$$

which yields the time elapsed to failure, or the *pillar life*, in years. Next, for control purposes, the values of maximum scaling and the corresponding minimum bord width are calculated:

$$d_m = 1.73 \text{ m} \qquad B_{co} = 5.10 \text{ m} \qquad \textbf{Equation 3-21}$$

Since the bord width in Equation 3-18 is 5.5 m, the requirement that $B \geq B_{co}$ is satisfied and the coal piles from adjacent pillars will not come into contact.

Table 3-1 A random sample (of size ten) of critical safety factors with corresponding depths of scaling and pillar lives.

SF	0.93	0.90	0.93	0.86	0.76	1.01	0.98	1.09	1.42	1.14
d_c	1.40	1.48	1.40	1.58	1.85	1.21	1.28	1.03	0.35	0.92
t_c	3.51	3.70	3.51	3.95	4.61	3.03	3.21	2.58	0.89	2.31

Note: In this table d_c and t_c are measured in metres and years, respectively.

It is important to note the variations, *for ostensibly identical pillars*, in the values of the parameters presented in Table 3-1. In this particular sample of ten randomly selected cases, the apparent safety factors at failure range from 0.76 to 1.42, the depth of scaling from 0.35 m to 1.85 m and most importantly, the pillar life from 0.89 years to 4.58 years. Moreover, it will be

and pillar life. In Figure 3-4 an updated version of Madden's (1991) plot of apparent safety factors as a function of pillar life is shown. This illustration, which was prepared on the basis of field data, reinforces the conclusion that any relationship between design safety factor and pillar life is masked by the stochastic nature of the problem. Of course, there is an underlying trend, but this is blurred by the random behaviour of the apparent safety factors. This problem is especially serious when the sample is small.

3.4 Pillar life expectancy and probability of survival

It is not possible, due to the probabilistic definition of pillar strength, to determine unequivocally whether a pillar will or will not fail. All we have is an estimated probability that failure will, or will not occur. If the composition of coal results in pillar side spalling, the situation becomes even more complex. As was illustrated in the previous section, the effect of spalling reduces the pillar width and, therefore, may cause the failure of a pillar at some later time. The Monte Carlo technique can be employed to gain a greater insight into this phenomenon.

Postulate that m panels have been constructed in accordance with an identical set of mining dimensions. Using the dimensions employed in the previous section, the layout of the panels is defined by:

$$H = 150\ m \qquad w = 14\ m \qquad B = 5.5\ m \qquad h = 3.0\ m \qquad \textbf{\textit{Equation 3-22}}$$

In addition, the constants in Equation 3-5, together with the following parameters are taken to represent the behaviour of scaling pillars:

$$\delta = 1.35 \qquad \rho = 35^{\circ} \qquad r = 0.2\ \text{m / year} \qquad \textbf{\textit{Equation 3-23}}$$

The initial safety factor computed from the dimensions in Equation 3-22 and using Equation 3-11 has a value of $SF_i = 1.61$. In view of this safety factor, it can be said that these mining dimensions represent a conventionally designed layout. The probability that failure will not occur at a given initial safety factor is given in Equation 3-2. Since logically, the probability of failure is $p^*(SF_i) = 1 - p(SF_i)$, it is simple to compute that $p^* = 0.0014$. As before, the maximum scaling or the choking depth of scaling is $d_{\infty} = 1.73$ m and the limiting bord width is $B_{\infty} = 5.10$ m. Since

values were non positive. This number approximates fairly closely the value of 14 that would arise from the probability of failure. These are the instances where the pillars will fail during their formation. Furthermore, there were 807 cases where the computed d_c value did reach or exceeded the choking depth of scaling. These instances represent the case where scaling is stopped by the surrounding rubble and the pillars are stabilised permanently.

The data resulting from the simulation is presented in two illustrations. In Figure 3-5 the histogram of the frequency of collapses is plotted as a function of time. This histogram gives a good indication of the distribution of pillar life. It is apparent that during the first year or so after the formation of the panels only a few collapses, but later the rate of failure increases significantly. The most frequently occurring life is about five to six years. From this time onwards, the rate of failure begins to diminish as fewer and fewer panels are left standing.

There are two apparently anomalous bars on this graph. The first at zero life is hardly noticeable and corresponds to the eleven cases where the failure is instantaneous. At the other end of the life scale, that is at $t_{max} = 8.66\,\text{years}$, there is a conspicuous bar representing the 807 cases that remain standing permanently.

In Figure 3-6 the estimate of the survival probability is depicted. Here the ordinate $p(t)$ approximates the probability that the pillars in this panel will survive without collapse to time t. Clearly the probability of survival is very nearly unity initially, but it begins to diminish, first slowly and later quite rapidly. Finally, at 8.66 years the probability drops to $807/10000 = 0.0807$. Since the remaining 807 panels remain standing permanently, this probability remains constant from then onwards.

It is worthwhile to examine the probability of survival curves for two more cases. The first example involves a panel where the design safety factor of the pillars is low. The other case relates to the situation where the pillars have an unusually high safety factor. In both cases the properties of the coal are assumed to be the same as specified earlier in Equation 3-5 and Equation 3-23. Starting with the case of low safety factor and keeping all mining dimensions, with the exception of the pillar width, the same as those given in Equation 3-22. The new pillar width and the corresponding design safety factor are:

$w = 10\,\text{m} \qquad SF = 1.12$ ***Equation 3-24***

with the passage of time. At five years the survival probability is negligible.

A very different situation prevails if the pillars are over-designed. In this case the pillar width and the safety factor are significantly higher than before:

$$w = 18\,\mathrm{m} \qquad SF_i = 2.06 \qquad \textbf{Equation 3-25}$$

The survival probability distribution corresponding to this case is illustrated in Figure 3-8. In this instance the probability remains virtually unity up to almost six years and then reduces only to $9065/10000 = 0.9065$. After 8.50 years the probability remains unaltered indefinitely. Figure 3-8 appears to suggest that it is possible to design layouts, even in seriously spalling seams, where the probability that the pillars will remain unfailed is high.

As this discussion reveals, if exposed walls of a coal seam suffer from scaling induced by weathering, the mechanics of coal pillar behaviour becomes considerably more complex. An interesting insight into the deterioration of such pillars and their probability of survival can be gained by a close study of Figure 3-6, Figure 3-7 and Figure 3-8.

3.5 Back-calculation of scaling rates

No direct evidence appears to exist to substantiate the proposed model of pillar scaling. Thus, it is not possible to prove convincingly the validity or otherwise of the approach. However, some evidence can be marshalled which can be used to establish at least the plausibility of the assumptions put forward in the previous sections of the paper. This evidence consists of 13 documented cases of collapse that have occurred in collieries mining the No. 3 Seam in the Vaal Basin. No direct observation exists to prove that these failures were caused by scaling. However, in view of the earlier mentioned observations of van der Merwe (1993) concerning this geological region, it is not unreasonable to accept this supposition. This data contains sufficient information to perform some back-calculation. The aim of such analysis is to estimate the rate of scaling which prevailed in the recorded cases and seemingly caused the collapse of the pillars.

If the *depths* of scaling, d_c, were known for the 13 cases, the *rate of scaling* could be calculated from $r = d_c/t_c$ (see Equation 3-20). Unfortunately, the scaling depths were not observed in these cases, therefore, this formula cannot be used in this simple manner. An alternative

As mentioned earlier, non-positive depth of scaling values represent instantaneous failure, thus no scaling can be associated with them. At the other end of the scale, in other words at high values, scaling is restricted sometimes by choking, which occurs when $d_c > d_m$. The cases satisfying this restriction correspond to that part of the distribution where the pillars do not fail. Hence, these instances again do not yield useful information concerning scaling that terminates in pillar collapse. Thus, using this approach and rejecting, if and when appropriate, the abnormal values at either ends, the remaining elements of the vector can be used to calculate a series of scaling rates. This procedure was followed for all of the 13 cases.

Using all the usable values of scaling depth, scaling rates were computed with the aid of the earlier mentioned simple formula. An example of the scaling rate distribution obtained in this manner is illustrated in Figure 3-9. Once the distributions of scaling rates were obtained for all 13 cases, a corresponding number of *mean scaling rates* were calculated. The mean rates are summarised in Table 3-2, together with the other relevant data concerning the 13 case histories.

It is apparent that the data in this table can be subdivided into two groups. The first eleven cases seem to belong to a geologically consistent region which can be represented by one set of parameters. The difference between this group and the group represented by the last two cases is so large that they must be treated separately. The second group consists of the last two cases, that is, 178a and 178b. In view of the small number of cases here, this group had been excluded from further analysis. The average of the eleven mean rates in the firsts group is 0.197 m/year. This value gives a good indication of the magnitude of scaling rates in mines where scaling appears to be a serious problem.

The correlation coefficients between rate of scaling and the other variables included in Table 3-2 were investigated next. The appropriate calculations show that the correlation coefficients between the mean rate of scaling and the pillar life, the design safety factor, the pillar height and the width to height ratio are -0.586, 0.369, 0.198 and 0.184, respectively. These figures indicate that there appear to be no significant correlations between the safety factor and the rate of scaling, the pillar height and the rate of scaling, or the width to height ratio and the rate of scaling. There is, however, a weak negative correlation between the rate of scaling and the pillar life. This correlation is explored in Figure 3-10 where the computed mean rates are plotted as a function of pillar life. Two further curves are shown in the same illustration. These curves

functions on the basis of the illustration. Similarly, the correlation coefficients corresponding to the two expressions are almost identical and only slightly higher than the earlier mentioned coefficient. Perhaps on physical grounds the exponential form is to be preferred. However, in the light of the large scatter around the curves, no firm conclusion can be inferred.

Table 3-2 Scaling rates and related data from case histories in the Vaal Basin, No. 3 Seam.

Case No.	Pillar life [years]	Mining depth [m]	Design Safety Factor	Pillar height [m]	Width to height ratio	Rate of scaling* [m/year]
180	4.0	82.0	2.28	2.80	3.6	0.339
181	11.0	96.0	2.07	2.90	4.1	0.126
154	2.0	51.0	1.30	3.41	1.7	0.150
155	8.0	113.7	1.81	2.75	4.4	0.150
171	5.0	103.5	1.77	2.94	4.0	0.237
172	4.0	47.0	1.55	3.21	1.8	0.121
173	7.0	90.0	1.76	2.53	3.6	0.132
174	4.5	98.0	1.60	3.00	3.3	0.193
175	3.5	59.6	2.01	3.57	2.5	0.313
176	8.0	40.0	1.70	3.15	1.8	0.068
177a	3.0	103.7	1.63	3.05	3.6	0.332
178a	2.0	99.0	2.26	3.34	4.3	0.845
178b	2.0	99.0	2.44	3.30	4.4	0.862

*Mean rates estimated through Monte Carlo simulation.

It is important to put the results in Table 3-2 into proper perspective. It would appear that the simple model proposed in this paper provides an acceptable explanation of the first eleven cases in the table. The obtained scaling rates are of reasonable magnitudes and tolerably

whether the failures in the table are, in fact, the result of pillar side spalling.

In addition to the information back-calculated from the records obtained in the Vaal Basin, a few pieces of additional data concerning pillar scaling have come to light. These data were obtained by direct measurements in two collieries operating in the Witbank area and they relate to unfailed pillars. While the observations cannot claim to be of high precision, they do provide the opportunity of estimating scaling rates in regions where pillar side spalling has not proved to be a serious problem in the past. The pillars in these cases have not collapsed, therefore, the rates relate to pillar scaling in progress. The basic data, together with the derived rates, are presented in Table 3-3. Collieries A and B were mining in the No. 2 and No. 4 Seams, respectively.

Table 3-3 Mining dimensions and scaling rates.

Case	Pillar life year	Mining depth [m]	Safety factor	Pillar height [m]	Width to height ratio	Rate of scaling* [m/year]
Col. A						
(a)	22	88	1.0	3.5	2.2	0.019
(b)	25	88	1.1	3.5	2.2	0.021
(c)	22	84	1.4	3.5	2.7	0.016
Col. B						
(a)	19	60	2.0	3.8	2.5	0.076
(b)	19	76	1.9	3.8	2.5	0.021
(c)	14	56	1.9	3.8	2.3	0.041

* Rates calculated from field observations.

The observed lives of the pillars in these examples are long and the scaling rates are much lower than those tabulated in Table 3-2. The tentative estimate of the mean scaling rates in the Nos. 2 and 4 seams in the Witbank area are 0.019 m/year and 0.046 m/ year, respectively.

cannot be ignored. Two design problems come to mind. The *first* of these entails the determination of the pillar width which guarantees that the probability of survival does not drop below p even after the elapse of t_p years. The *second problem* involves the computation of that width which ensures that the survival probability of the pillars does not fall below p for an *unlimited period*. Clearly, the solution of the second of these problems represents the more cautious design and leads to larger pillars.

To solve either of the problems it is necessary first to determine the critical safety factor SF corresponding to the probability of survival p. This can be achieved with the aid of the definition in Equation 3-2. In the *first problem* the pillar centre distance is given by $C = w(t_p) + 2rt_p + B$, because $d(t_p) = rt_p$ and $w(t_p)$ is the residual pillar width at time t_p. The next step is to solve the following equations for the residual pillar width:

$$SF_{Pwr}(w(t_p)) = SF \quad \text{(a)} \qquad SF_{Squ}(w(t_p)) = SF \quad \text{(b)} \qquad \textbf{Equation 3-27}$$

where the safety factor functions on the left hand sides are defined in Equation 3-11, Equation 3-12 and Equation 3-13. These equations represent the requirement that the safety factor of the residual pillars should be SF. Two equations are specified because it is not known in advance whether or not the obtained pillar will be squat. Let the solutions of equations (a) and (b) be w_{Pwr} and w_{Squ}, respectively. If the pillar width calculated from (a) corresponds to a squat pillar, that is, if $R_o < w_{Pwr}/h$, then the solution of Equation 3-27 is w_{Squ}. If the pillar is not squat, the solution is clearly w_{Pwr}. Denote the actual solution of Equation 3-27 simply by w. This is the residual pillar width that accords with the probability p. The initial or the design pillar width is $w_i = w + 2rt_p$. Using this width, the design safety factor of the pillar can be computed from either Equation 3-11 or Equation 3-12, depending on whether or not the pillar is squat.

The solution obtained here is valid only if $d_m \geq rt_p$ and $B \geq B_{co}$, where d_m and B_{co} are given in Equation 3-14 and Equation 3-16, respectively. Violation of the first inequality reveals that a solution was found where the scaling reached a depth which is greater than the maximum possible value, that is, d_m. This is an unacceptable result and the valid solution can be obtained by following the route prescribed for the second problem. Breaching of the second inequality

The relevant form of the formula is (see Equation D-7 in Appendix D):

$$d_m = d(w) = \frac{h}{2\delta\mu}\left[\sqrt{\left(\delta\mu\frac{w}{h}\right)^2 + 2\delta\mu\frac{w}{h} + \frac{4}{3}\delta} - \delta\mu\frac{w}{h}\right] \qquad \textbf{Equation 3-28}$$

On this occasion the distance between pillar centres can be expressed as $C(w) = w + 2d(w) + B$, where the dependence of the depth of scaling on w must be taken into account. Again two solutions are obtained from the following equations:

$$SF_{Pwr}(w) = SF \quad \text{(a)} \qquad SF_{Squ}(w) = SF \quad \text{(b)} \qquad \textbf{Equation 3-29}$$

One of the solutions corresponds to a non-squat (equation (a)) and the other to a squat (equation (b)) pillar. As before, the appropriate choice picked from these values is the solution of the problem. The applicability of this solution is limited only by the inequality $B \geq B_{co}$. If this limitation is violated then the piles of fragmented coal are merged and the solution relevant to that case should be sought.

To illustrate the capability of the design method a few examples are discussed next. Assume that the mining site in question is in the Vaal Basin, therefore, let the rate of scaling be 0.2 m/year. The relevant mining dimensions are as follows:

$$H = 100\,\text{m} \qquad B = 5.5\,\text{m} \qquad h = 3.0\,\text{m} \qquad \textbf{Equation 3-30}$$

Assume that the colliery is remote from populated areas and the long term survival of the pillars is not of great concern. In these conditions it may suffice to require that the probability of survival of the pillars for five years ($t_p = 5$ years) should not be less than $p = 0.99$. This requirement yields $SF = 1.4476$. Scaling, during the specified period of five years, reduces the pillar width by 2.0 m ($d(t_p) = 1.0$ m). The solution of the problem posed in Equation 3-27 is a residual pillar width of 10.78 m. Hence, the initial pillar width that can accommodate 2.0 m of spalling is $w_i = 12.78$ m. The design safety factor would have to be $SF_i = 2.20$ to obtain this pillar width using the conventional methodology. This layout would yield 51.1 per cent extraction.

3.7 Summary and recommendations

The results presented in this chapter establish reasonably convincingly the *plausibility* of the proposed model. No attempt is made to claim a stronger descriptor to characterise the current status of the research, because the field evidence to support the formulation is meagre. The object of the model is to describe the deterioration of pillars due to one and only one particular cause, namely pillar side scaling or spalling. The model deals with a time dependent deterioration which can be described loosely as weathering.

The attractiveness of the model lies in its simplicity and versatility. It can readily explain the reason for the failure to discern, on the basis of a small field sample, sensible relationships between pillar life and other parameters such as safety factor. If an estimate of the *rate* of scaling is known, it is possible to quantify, using a Monte Carlo technique, the expected life or the survival probability (up to a specified age) of coal pillars. Moreover, the model permits the design of scaling pillars. Two approaches have been discussed. Pillars may be designed by specifying a probability of survival for a *given number of years*. Alternatively, it might be required that the probability of survival for an *indefinite period* should not be less than a specific value.

The model can be used for purposes of back-calculation as well. For example, if the initial mining dimensions and the life of the pillars are known, it is possible to estimate the rate of scaling that prevailed to cause the eventual failure of the pillar. Such back-calculations have suggested that the rate of spalling in the Vaal Basin, No. 3 Seam is usually in the order of 0.2 m/year (eleven case histories). However, two further cases in the same area have yielded significantly higher rates (0.85 m/year). Some underground observations in the Witbank area have provided considerably lower rates, in the order of 0.02 - 0.04 m/year.

The model is a straightforward extension of the ideas put forward by Salamon and Munro (1967). It is postulated that the underlying strength of pillars remains unaltered, changes come about merely as a result of time dependent reduction in pillar width. Moreover, the apparent safety factors at failure are distributed according to the same log-normal distribution obtained in the original derivation. For simplicity, it is taken that faces of pillars scale uniformly and, therefore, the changes in dimensions can be expressed merely as a reduction in pillar width. Furthermore, it is assumed that the span of the panel in question is sufficiently large to ensure that the full weight of the prism attributable to a particular pillar continues to load that pillar. In

the light of further studies. First, the rate of scaling is taken to be constant. Second, the rubble heap must reach the roof before scaling ceases and finally, the restraint provided by this pile of coal acts as an 'off' or 'on' brake on scaling.

It is important that the cause of abnormal collapses is investigated and explained as soon as possible. Such study is likely to find that anomalous behaviour is due to more than one cause. Van der Merwe's (1993) observations imply that pillar scaling could be a reason for some of the premature failures. This deduction and the promising performance of the model proposed here provide a powerful basis for recommending that further study should be initiated to clarify the role of scaling or spalling in pillar mechanics. Three possible areas for additional research come to mind.

Study of scaling. Attempts should be made to establish the prevalence of scaling in South African collieries. Such investigations should cover mines that are suspected of being prone to spalling and those which hitherto were presumed to be free of time dependent deterioration. This research would involve the study of old workings to determine the presence and the extent of scaling. Depending on the outcome of these investigations, the pillar strength formula, which is central, may have to be revisited.

The existence of scaled rubble at the foot of pillars is a good qualitative indication of pillar scaling. To estimate the magnitude and rate of spalling, an attempt should be made to compare old surveyor's and current pillar offset data. This approach seems to have yielded reasonable data in the past.

Composition of coal. An attempt should be made to correlate the pervasiveness of scaling with the chemical composition of the coal. The analysis of the presence and composition of clay minerals may prove to be a fruitful direction of research in this respect.

Model studies. It must not be lost sight of that during the last three decades the original pillar design approach, which does not explicitly recognise scaling as a factor of significance, has proved to be effective in most applications. Future approach to design must account for this past observation and, at the same time, cater properly for scaling where it is necessary. It may be necessary to recognise that in certain situations scaling is an insignificant factor. In terms of an alternative option, the differences in behaviour may be accounted for by large contrasts

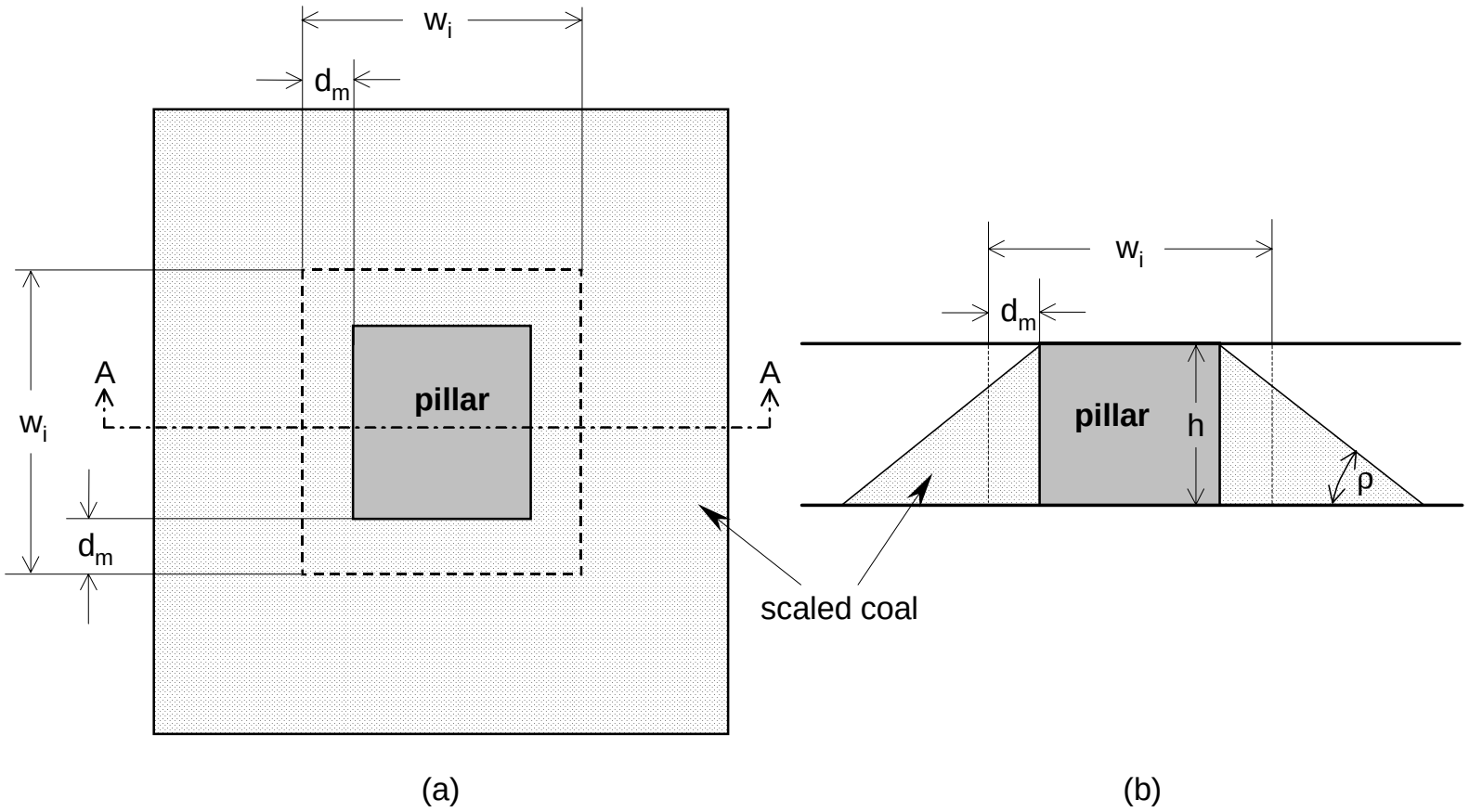

Figure 3-1 Plan (a) and section (b) illustrate maximum scaling that can be experienced by an isolated pillar(maximum scaling depth, d_m; initial pillar width, w_i, pillar height, h; angle of repose of scaled coal, ρ).

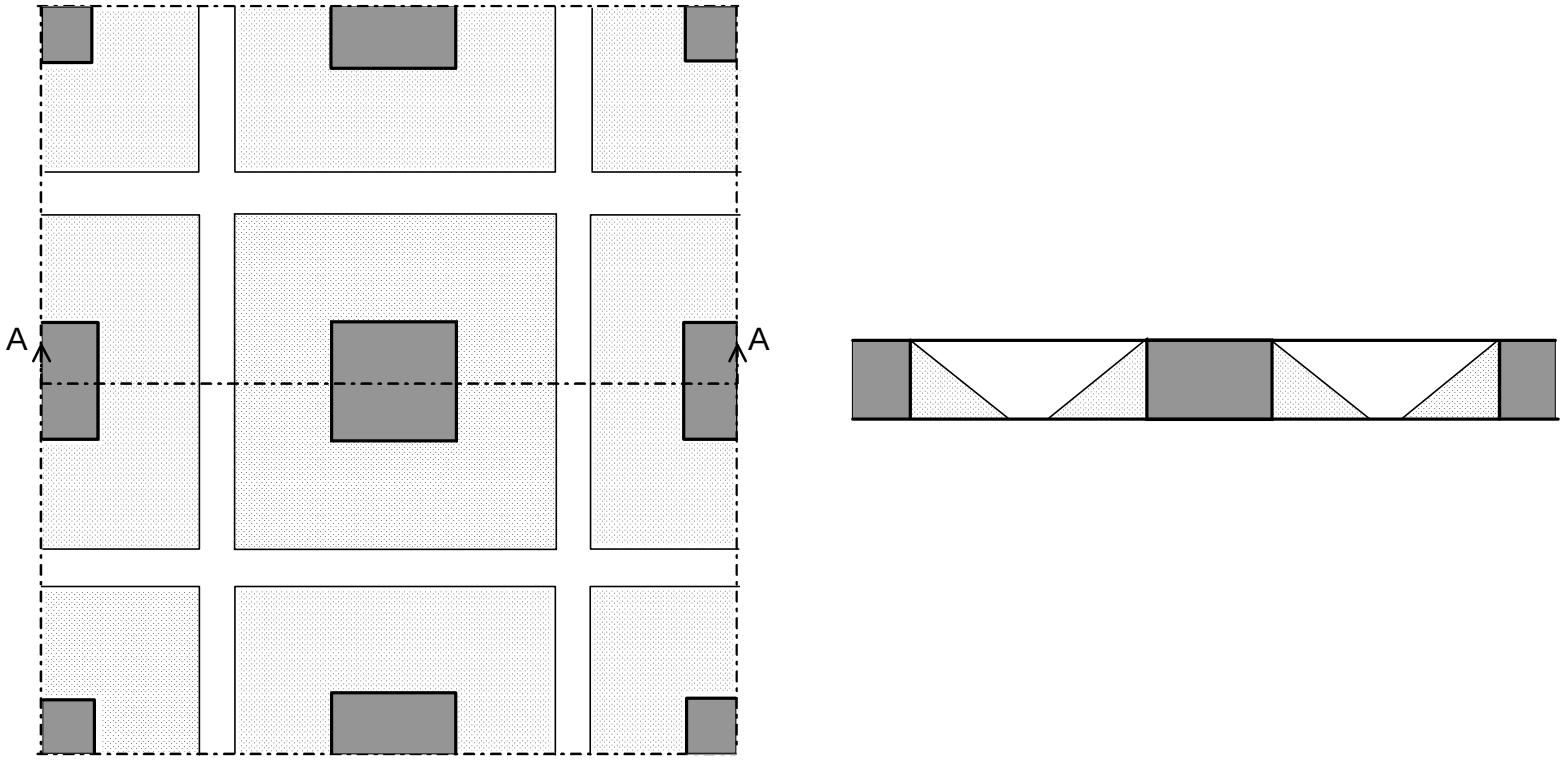

Figure 3-2 Plan (a) and section (b) depict pillar scaling when the scaled coal piles from neighbouring pillars do not come into contact at the bord centres.

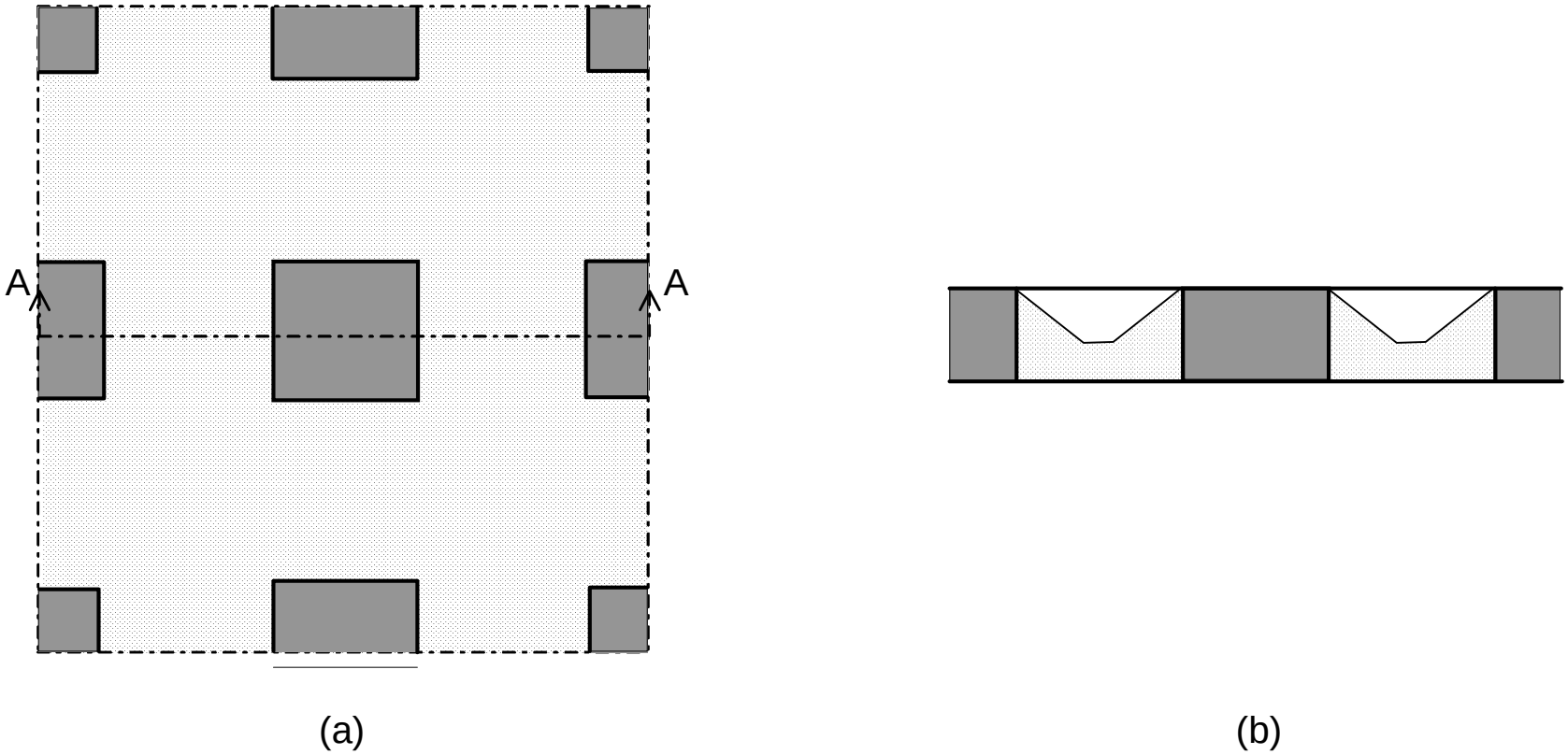

Figure 3-3 Plan (a) and section (b) show maximum pillar scaling when the scaled coal coalesces and forms a continuous pile in the bords.

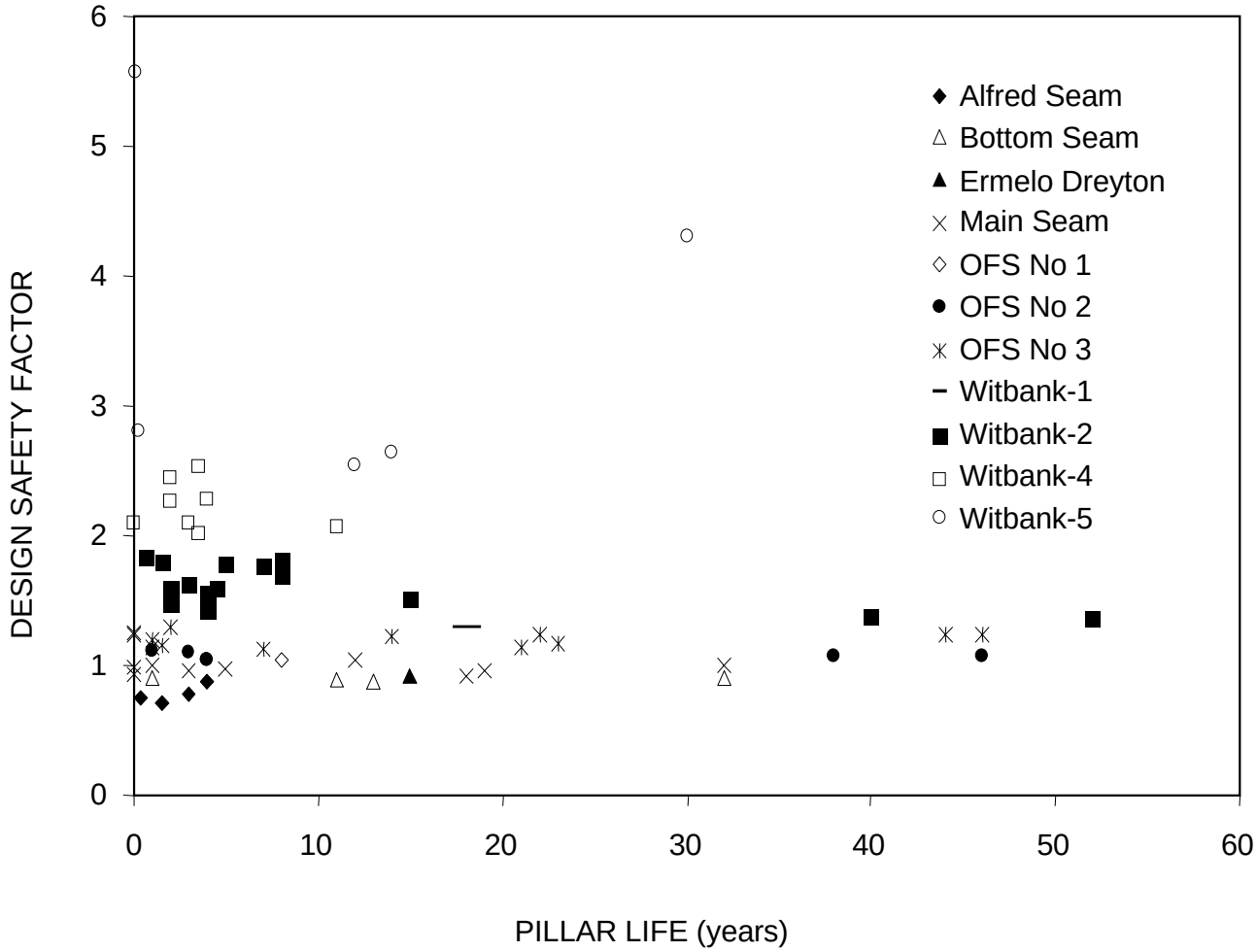

Figure 3-4 Plot of pillar life versus design safety factor for 65 pillar collapses occurred in 11 different seams. An updated version of the illustration presented by Madden (1991).

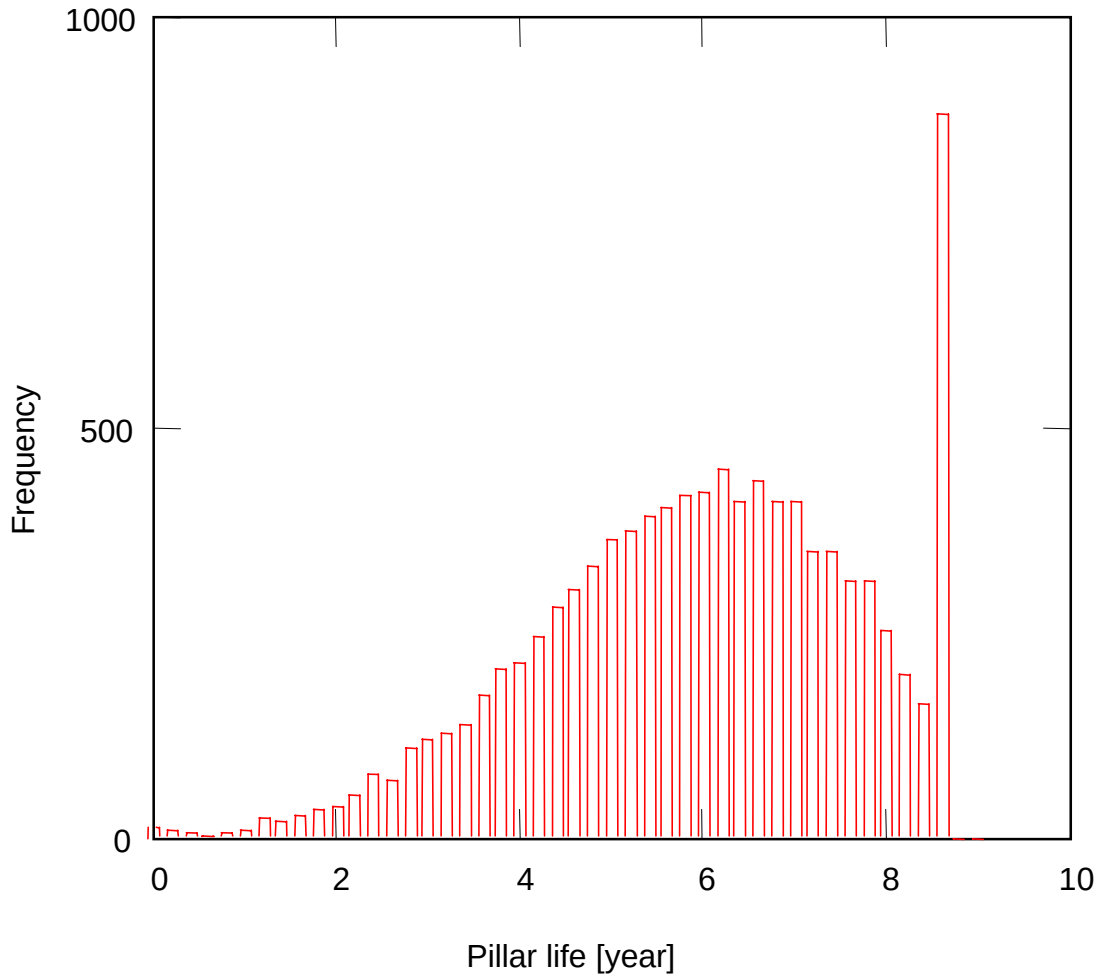

Figure 3-5 Histogram of pillar life. The first bar on the left and last bar on the right represent zero and infinite life, respectively.

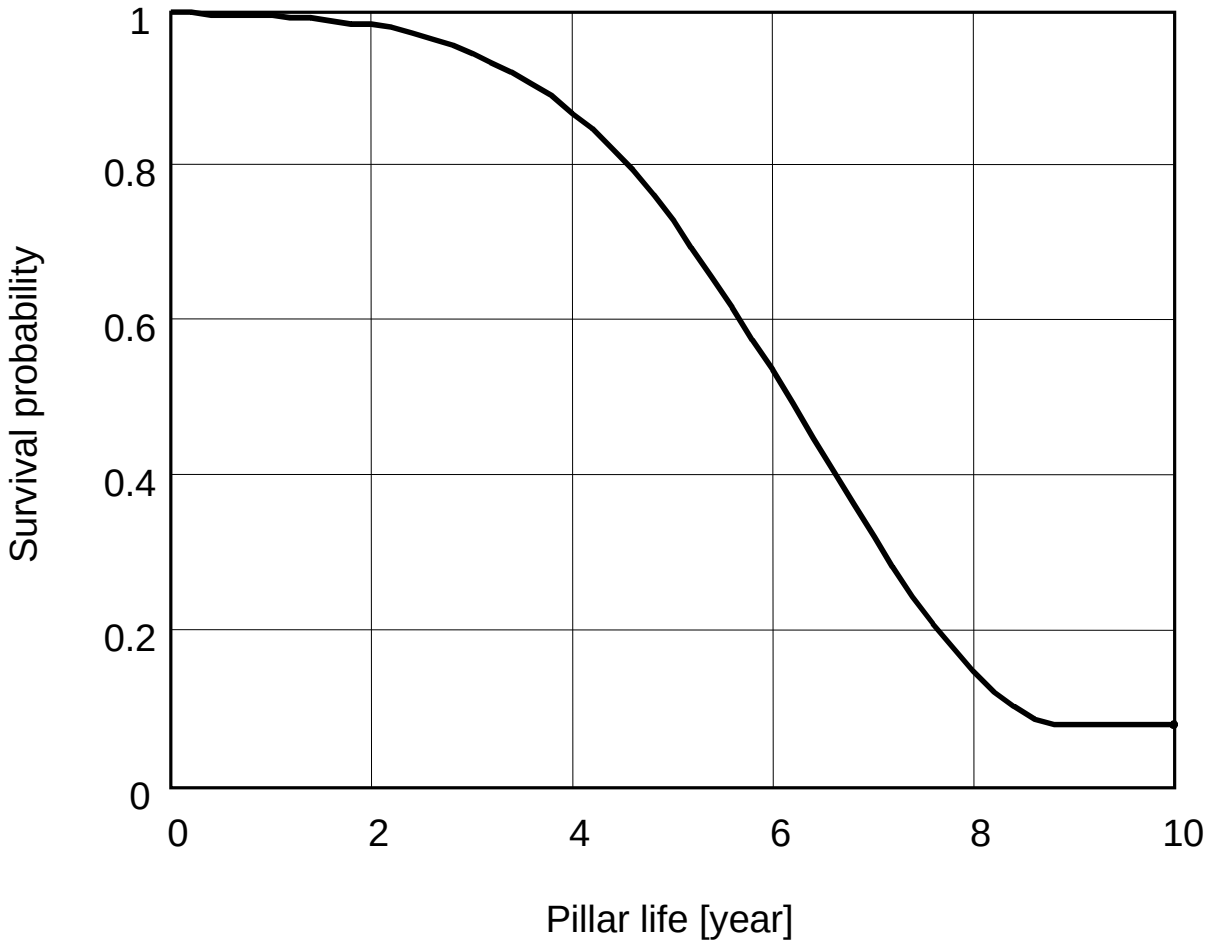

Figure 3-6 Survival probability versus pillar life relationship for conventionally designed pillars. ***The initial pillar width and the design safety factor are 14 m and 1.61, respectively.***

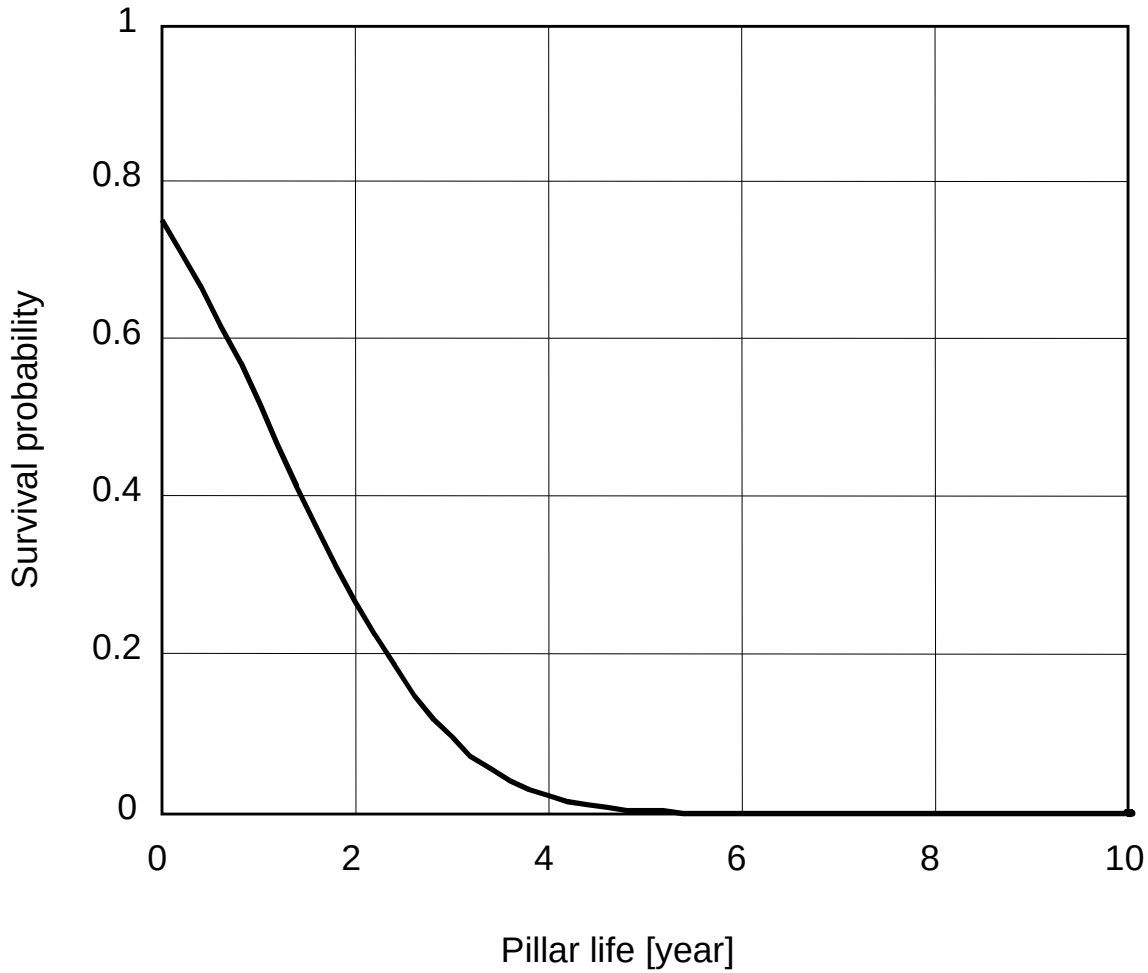

Figure 3-7 Survival probability versus pillar life relationship for under-designed pillars. The pillar width and the design safety factor are 10 m and 1.12, respectively.

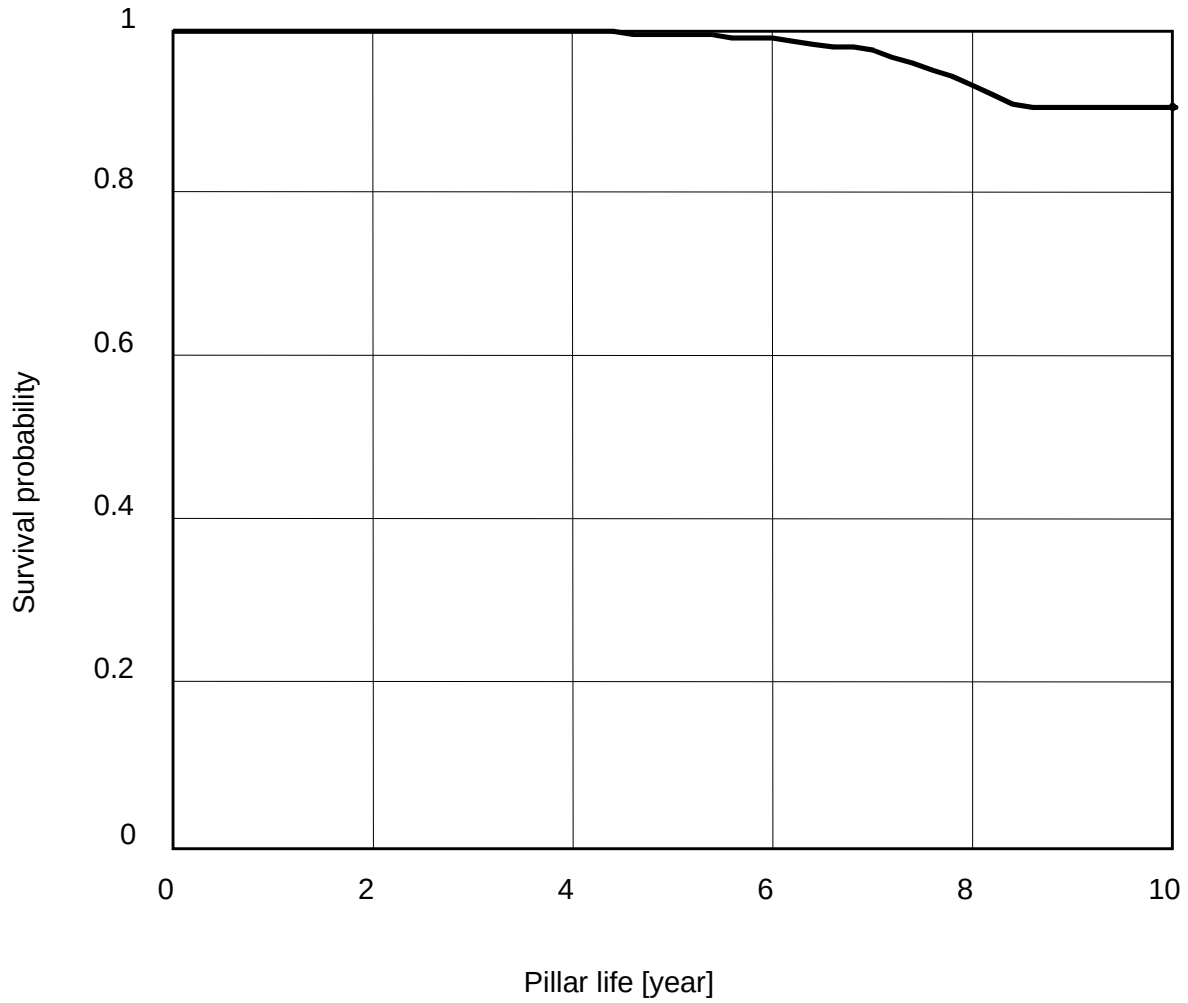

Figure 3-8 Survival probability versus pillar life relationship for over-designed pillars. The pillar width and the design safety factor are 18 m and 2.06, respectively.

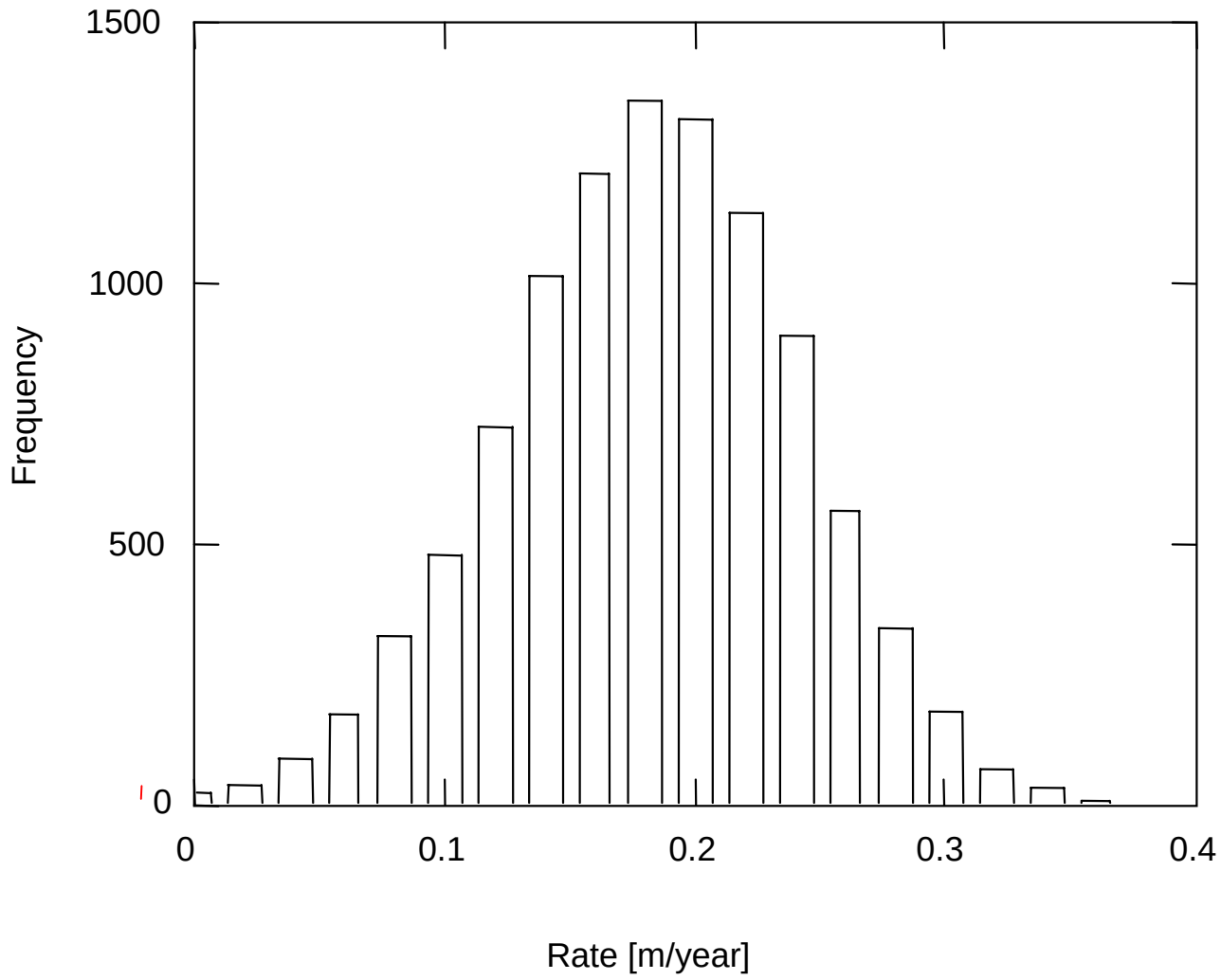

Figure 3-9 Histogram of rate of scaling. The mean rate is 0.193 m/year.

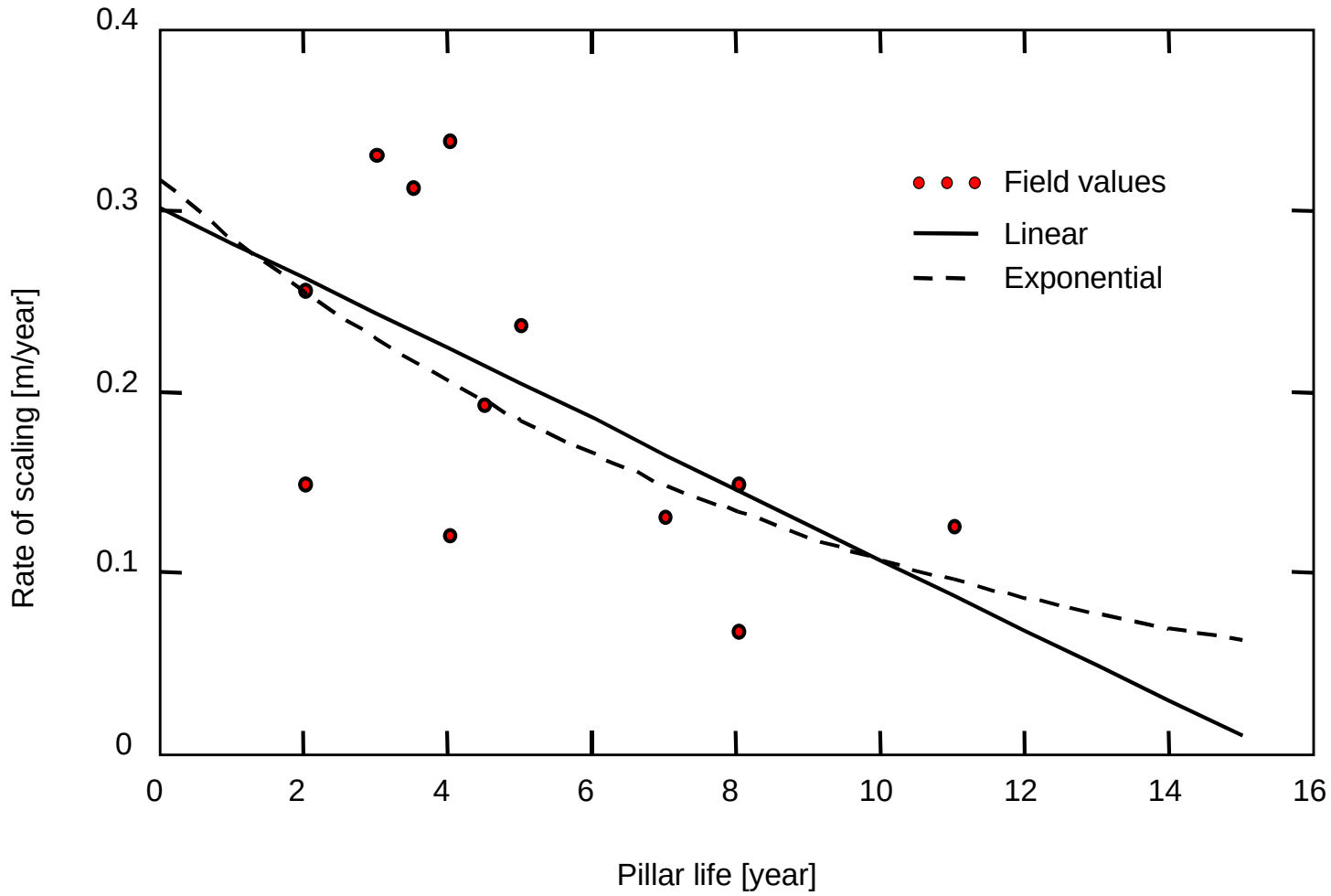

Figure 3-10 Plot of mean rates of scaling for eleven cases. The illustration also depicts the linear and exponential regression curves.

Madden, B. J. (1991) *A re-assessment of coal pillar design*. J. S. Afr. Inst. Min. Metall., v.91, no 1. pp. 27-37.

Madden, B. J. and Canbulat, I. (1996) *Re-assessment of coal pillar design procedures*. SAIMM Symposium on Safety in Mines Research Advisory Committee, 5 Sept., Mintek, Randburg.

Mark, C. and Barton, T (1996) *The uniaxial compressive strength of coal: Should it be used to design pillars?* Proc. 15th International Conf. On Ground Control in Mining. Golden, Colorado.

Salamon, M.D.G. and Munro, A.H. (1967) *A study of the strength of coal pillars*. J. S. Afr. Inst. Min. Metall., v.68, pp. 55-67

Salamon, M.D.G. and Wagner, H. (1985) *Practical experiences in the design of coal pillars*. Proc. 21st International Conference of Safety in Mines research institutes, 21-25 Oct. Sydney, Australia, pp 3-9.

Salamon, M.D.G., Galvin, J.M., Hocking, G. and Anderson, I. (1996) *Coal pillar strength from back-calculation*. Strata Control for Coal Mine Design. Progress Report No. 1/96. The Department of Mining Engineering, The University of New South Wales. 60 p.

Van Der Merwe, J.N. (1993) *Revised strength factor for coal in the Vaal Basin*. J. S. Afr. Inst. Min. Metall., v.93, pp. 71-77.

4 Current pillar design methodology

4.1 Introduction

It is well known that Salamon and Munro's pillar formula has successfully been used since 1967 in South African collieries. Their back analysis of collapsed pillar cases between competent roof and floor strata inherently contained many different combinations of factors, which could degrade pillar strength, which remains valid within its empirical range or where similar conditions are found. Pillar instability may result should some of these parameters be dominant and outside of the empirical range, as seen in the analysis of new pillar collapses. Thus cognisance of the local conditions must be taken into account.

An idealised pillar system design methodology based on current rock engineering knowledge has been developed to take into account all factors affecting pillar stability. It should be emphasised that this methodology considers that the pillars are not one element in an integrated mining layout. The methodology therefore includes the design of all the elements in the layout and their interactions. A system design approach has thus been taken.

This methodology also establishes where the gaps in the knowledge exist.

4.2 Pillar system design

Coal pillar system design is a function of many parameters including geology, discontinuities, seam strength, time, weathering, loading rate and the surrounding strata properties. Where one of these parameters becomes dominant, or new factors which were not present in the original area of study are encountered, the stability of the pillar system may not be predicted by the current pillar design methodology.

These parameters may vary from mine to mine, even section to section, and can be localised. Therefore, to improve and extend the design methodology it is necessary that these parameters and their effect on pillar stability should be investigated individually.

Figure 4-1 shows a conceptual generalized pillar system design methodology, which takes into account all relevant parameters. The rock engineering system design components given in Figure 4-1 are further described from Figure 4-2 to Figure 4-11.

It should be noted that this design model is not a methodology to be followed, but rather forms the basis and framework for the research and identifies parameters which must be taken into

account when designing coal pillars. Also, it establishes the gaps in knowledge in the current pillar design process and areas where further research is required.

To explain the rationale of the methodology, selected blocks in the rock engineering design in the flowchart (Figure 4-1) are discussed in detail.

Controls: These parameters cannot be altered in rock engineering design. These parameters include seam characteristics, rock mass properties, surface restrictions, multiseam mining, previous mining in the area, time and the management philosophy. The details of the control parameters are given in Figure 4-2

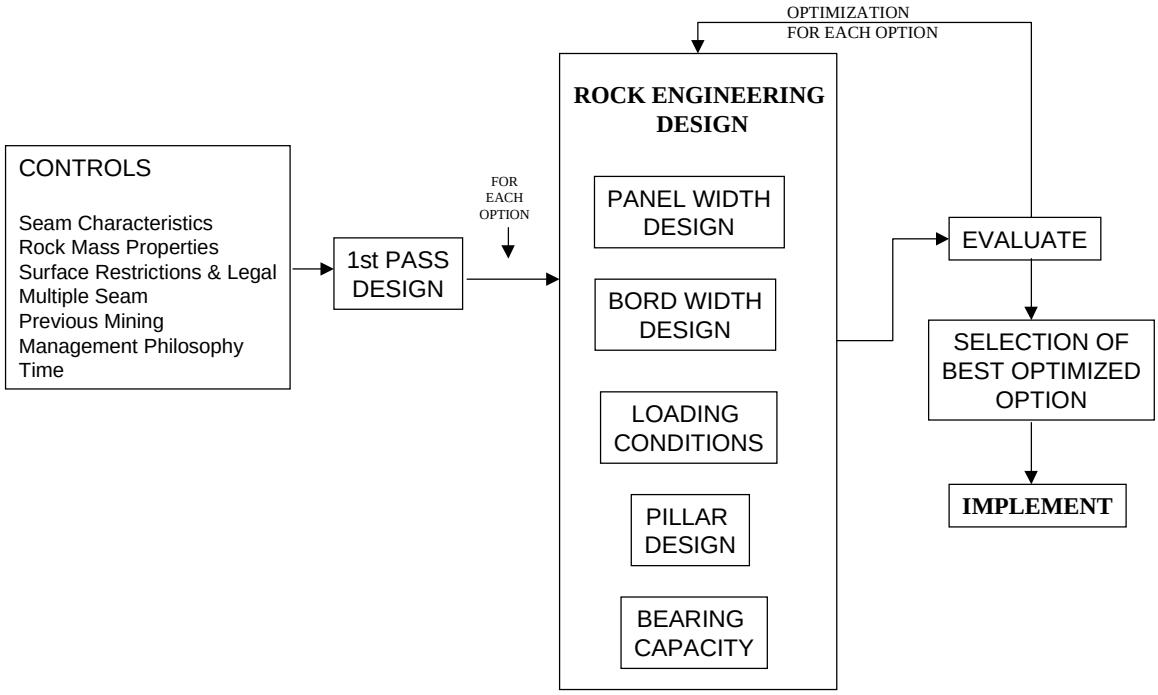

Figure 4-1 Pillar system design flowchart

1st pass design: Control parameters can result in various mining options. All of the more feasible of these options then may be investigated using the rock engineering criteria to be able to determine the most economical and practical methods.

R.E. design: As given in Figure 4-1 the components of the pillar system are panel width, bord width, loading environment, the pillar itself and bearing capacity.

1) Panel width: The first critical issue which needs to be dealt with is the design of the panel width, which determines the number of roadways in a panel and influences the loading environment. In laboratory testing, the platens on the testing machine continue to apply load or displacement to a specimen as it compresses. In the

mining environment, the situation is not so simple. The roof strata is not necessarily able to move down and continue to fully load a pillar as it compresses. This can arise when stiffer pillars (barrier pillars) surround the pillar of interest. These barrier pillars can be stiffer because they have a high width to height ratio. They provide greater resistance to the weight of the overburden and prevent the roof strata from displacing downwards and continuing to fully load the softer in-panel pillars. Some of the load that would otherwise act on the softer pillar is transferred onto the stiffer surrounding pillars.

The main function of barrier pillars are to divide the mine workings into discrete compartments for the following purposes :

i) Ventilation control

ii) Regional instability control

iii) Water control

iv) Pressure outburst control

v) Fire control

Panel width is a function of geotechnical parameters, stress environment, intact material strength, dip of the seam and mining method such as future pillar extraction or longwalling, Figure 4-3. Discontinuity properties, such as orientation, spacing, cohesion, friction angle and dilation are also relevant. Once these parameters are determined, the internal outputs which comprise the rock mass modulus deformation limits and beam thickness can be obtained, to determine the stable panel dimensions (Figure 4-3). However, in order to obtain stable panel dimensions from the above determined parameters, further comprehensive research is required

2) Bord width: The second critical component of pillar system design is bord width design. The effect of mining is to remove support to the surrounding rock mass. To achieve a state of equilibrium or stability, forces have to be redistributed around the excavation. This means that if caving does not occur, the rock (or pillars) which remains after mining has to support a greater proportion of the overburden load. In order to remove the compressive stresses that used to act around the perimeter of the roadway, equal and opposite tensile stresses have to be introduced. These exert a downward pull on the roof, an inward pull on the ribsides and an upwards pull on the floor. Hence, roof deflection, rib

displacement and floor lift always occur to some degree when a roadway is driven.

The effect of increasing bord width is to increase the magnitude of induced vertical load (stress) in the roadway sides. The compressive stresses in the ribsides increase in order to balance the effects of the additional tensile stresses induced in the roof and floor. The effect of increasing roadway height is to increase the magnitude of induced horizontal load (stress) in the roof and floor strata.

In an idealised bord width design, detailed borehole information, laboratory testing and rock mass classifications are required, Figure 4-4. This information will determine the rock mass characteristics and intact rock mass strength. If the rock mass characteristics and intact rock mass strength are determined, then the back analysis can be conducted to determine the failure mechanism. However, in order to determine the failure mechanism, comprehensive research is required. Once the failure mechanism is identified, then the unsupported stable span limits can be determined, which requires again extensive research. The support system then can be designed for determined failure mechanisms, unsupported stable span limits and mining width requirements.

3) Loading: The third component of the pillar system design is loading environment or conditions. The effect of mining is to remove support to the surrounding rock mass. To achieve a state of equilibrium again, forces have to be redistributed around the excavation. This means that if caving does not occur, the rock pillars which remain after mining have to support a greater proportion of the overburden load. Pillar load depends on the stiffness of both the surrounding strata and the pillars themselves. There are many layouts where average pillar load can be determined in a simple manner. These occur when a large area is mined with a reasonably uniform pattern of pillars. The large area reduces the stiffness of the roof strata and causes most of the pillars to be subjected to dead-weight loading. The uniform pattern of pillars results in pillars of similar stiffness so that load is shared equally between pillars. In these regular bord and pillar layouts, pillar load can be calculated by considering the load acting on just one pillar. Because the layouts is regular, it can be assumed that each pillar will support the full load of the overburden within its area of influence. This concept is referred to as the Tributary Area Theory. Consistent with most other pillar design techniques and with the principles of empirical research, the

procedure deals only with a calculated average pillar stress. Load is not distributed uniformly across a pillar. Load transfer is more concentrated nearer to the pillar sides. Roof sag also induces load near to pillar sides. Because the edges of the pillars are the least confined, they tend to yield at low values of load, causing load to be transferred further into the pillar.

The loading of pillars is a function of mining induced stresses, the load transfer mechanism, mining history and surface loading (Figure 4-5). From these parameters, loading profile and average pillar stress can be obtained. These parameters should be used in a sequence as given in a loading environment design methodology, Figure 4-6.

4) Pillar design: The fourth component of the pillar system design is the pillar design itself. Almost all metalliferous and coal mining systems involve developing at least two or more parallel or near excavations in the same horizontal or vertical plane in the rock mass. The effect of these operations is, in the simplest case, the formations of a pillar.

When the excavations are separated by a very wide pillar, the abutment stress profiles do not interact. The pillar therefore functions as if it were an abutment. This situation is typical for a barrier pillar. As pillar width decreases, the abutment stress profiles generated by the adjacent excavations increasingly overlap. These profiles are additive and result in an increase in pillar stress. This situation is typical for panel pillars in bord and pillar workings. Another effect of reducing pillar width is to reduce the width to height ratio (w/h) of the pillar. The w/h ratio governs the stiffness of the pillar and the strength of the coal pillar. Pillar strength decreases with decrease in pillar w/h ratio. Therefore, with further reductions in pillar width, the maximum load carrying capacity of the pillar may be exceeded, resulting in pillar failure. The failure mode of a pillar, i.e. gradual and controlled or sudden and uncontrolled, is a function of the ratio of the stiffness of the surrounding strata to the stiffness of the coal pillars.

The functions of pillars are to :

i) Restrict surface movement (locally or regionally).

ii) Protect critical service corridors from the effects of high load and abutment stress, e.g. conveyor/transport/ventilation roads.

iii) Prevent hydraulic connections to overlying water bodies and water bearing strata by preventing fracturing of the super incumbent strata.

iv) Provide temporary roof support in thick seam primary workings, thereby enabling a higher percentage extraction to be obtained from top or bottom coal operations than from pillar extraction (NOTE: unless carefully planned, these operations have a high potential for sudden collapse with no warning)

v) Act as ventilation partitions

The strength of any material or structure is defined as the maximum load it can support per unit area. Since “load per unit area” is defined as stress, strength can also be defined as the greatest magnitude of stress which a material or structure can support.

No unique value of strength can be given for rock. The strength of a rock sample is a function of its size, its shape, the amount of confinement provided to its sides and the direction of the applied stress.

Uniaxial Compressive Strength (UCS) refers to the strength of rock in compression when it is not confined. Triaxial Compressive Strength refers to the strength of rock in compression when it is subjected to a specific confining pressure. The compressive strength of rock increases significantly with increase in confining stress. Conversely, rock is typically 10 times weaker in tension than in uniaxial compression. The strength of fissured rocks, such as coal, is volume (size) and shape dependent. For a given shape, the strength of coal decreases as the volume of the specimen or pillar increases. For example, the strength of a cube of coal at the *in situ* scale is about one ninth that of a 25 mm cube of coal (see Section 6.6.3). This means that laboratory testing grossly over-estimates the field strength of coal.

The strength of coal increases as the width to height ratio of a specimen or pillar increases. One of the reasons for this behaviour is that as the height is held constant and the width is increased, the strength of the core of the pillar increases due to the increased amount of confinement provided by the outer coal to the core.

The load-bearing capabilities of the pillar corners and, to a lesser extent, pillar sides, are small compared with those at the centre of the pillar. This highlights the influence of confinement on the strength of a pillar. The corners and sides

are the least confined portion of the pillar, whereas the central portion is subjected to the greatest confinement. The central portion of a coal pillar is capable of withstanding extremely high stresses even if the circumferential portions of the pillar have already failed.

The parameters which affect the ultimate pillar design are: coal strength, geotechnical parameters, roof and floor loading profile, geometry, dip of seam, time, extraction techniques, reinforcement, contact conditions, horizontal stresses, the weak layers and bands in a pillar (layers, bands), and the size of the pillars, Figure 4-7. Once all these parameters are known then the modulus, stiffness, ultimate pillar strength, post failure characteristics, recompaction, residual strength and strains can be determined. These parameters should be used in a sequence as given in the ultimate pillar capacity design methodology, Figure 4-8. This diagram is discussed further in Section 6.10.

5) Bearing capacity: The fifth critical factor in the rock engineering design is bearing capacity. The coal pillar element does not always comprise the weakest link in the pillar system. Empirical pillar strength formulae can result in pillars of adequate strength but the pillar system may become unstable because the roof of floor strata cannot support the load. Foundation failure or bearing capacity failure can take a number of forms, depending on the strength, thickness and location of a weak stratum within the roof or floor horizons. A convenient means for conceptualising bearing capacity failures is to deal with extremes. If the floor material has only marginally lower in situ strength properties than the pillar, high loads can be generated in the pillar prior to the onset of failure. Bearing capacity failure develops around the edges of the pillar because:

i) Peak pillar loads occur close to the pillar edges

ii) The floor strata is weaker in these regions due to the removal of the vertical confinement.

iii) As a result of removing the vertical confinement, the floor strata near the pillar edges is both loaded in shear and free to fail in shear. Since the shear strength of coal measure rocks is typically only half that of their compressive strength, the floor strata may fail, resulting in floor heave in this manner in the vicinity of pillar edges. This can cause blocks of floor strata to rotate out from under the pillar edges into the roadway.

Loss of bearing capacity around the edges of a pillar has two effects:

i) Load previously supported by the failed foundation is transferred further into the pillar.

ii) Pillar strength is reduced due to a reduction in the surface area of the end constraints.

Three factors interact to determine whether stability can be re-established. The questions to be answered are:

i) Is the confinement that builds up as failure progress under (or over) the pillar sufficient to arrest the foundation failure?

ii) Is the increase in pillar load and the reduction in pillar strength that results from foundation failure sufficient to indirectly induce pillar failure?

iii) What effect does the resulting increase in effective bord width have on roadway stability and, if roof control is lost, what effect does the increase in pillar height have on pillar strength.

A feature of bearing capacity failure in strata of moderate or higher shear strength is that it tends to progress gradually rather than suddenly. Resistance to the process can build up as it progresses. Energy (load) has to be continuously added to the pillar system to overcome resistance and drive the process. Unless the situation is one of pure deadweight loading (load controlled system) and the load can "chase" displacement, this energy is not immediately available. In mining situations, one is usually dealing with a displacement controlled system where load input is governed by displacement of the roof strata. The stiffness of the roof strata controls the rate of loading into the pillar system. Hence, failure usually develops over time. As pillar width increases, greater confinement is provided to the failing foundation and there is increased probability of arresting foundation failure and maintaining pillar stability. However, whilst the pillar may function as an effective regional support element, roadways may become unserviceable due to very poor local conditions.

The bearing capacity of strata is a function of geometry, parting planes, layers, dip, stress environment, pillar stress profile, fracturing, time, mining method, acceptable limitations and rock mass characteristics, Figure 4-9. These parameters need to be known to be able to determine the bearing capacity. The design methodology for bearing capacity is given in Figure 4-10.

These five critical parameters should be determined for each option obtained from the first pass design.

Evaluation: The design obtained from the rock engineering criteria must be economical, practical and acceptable for ventilation, Figure 4-11. Referring to Figure 4-1, each pillar system design option may be optimised. The best optimised option will then be selected and implemented.

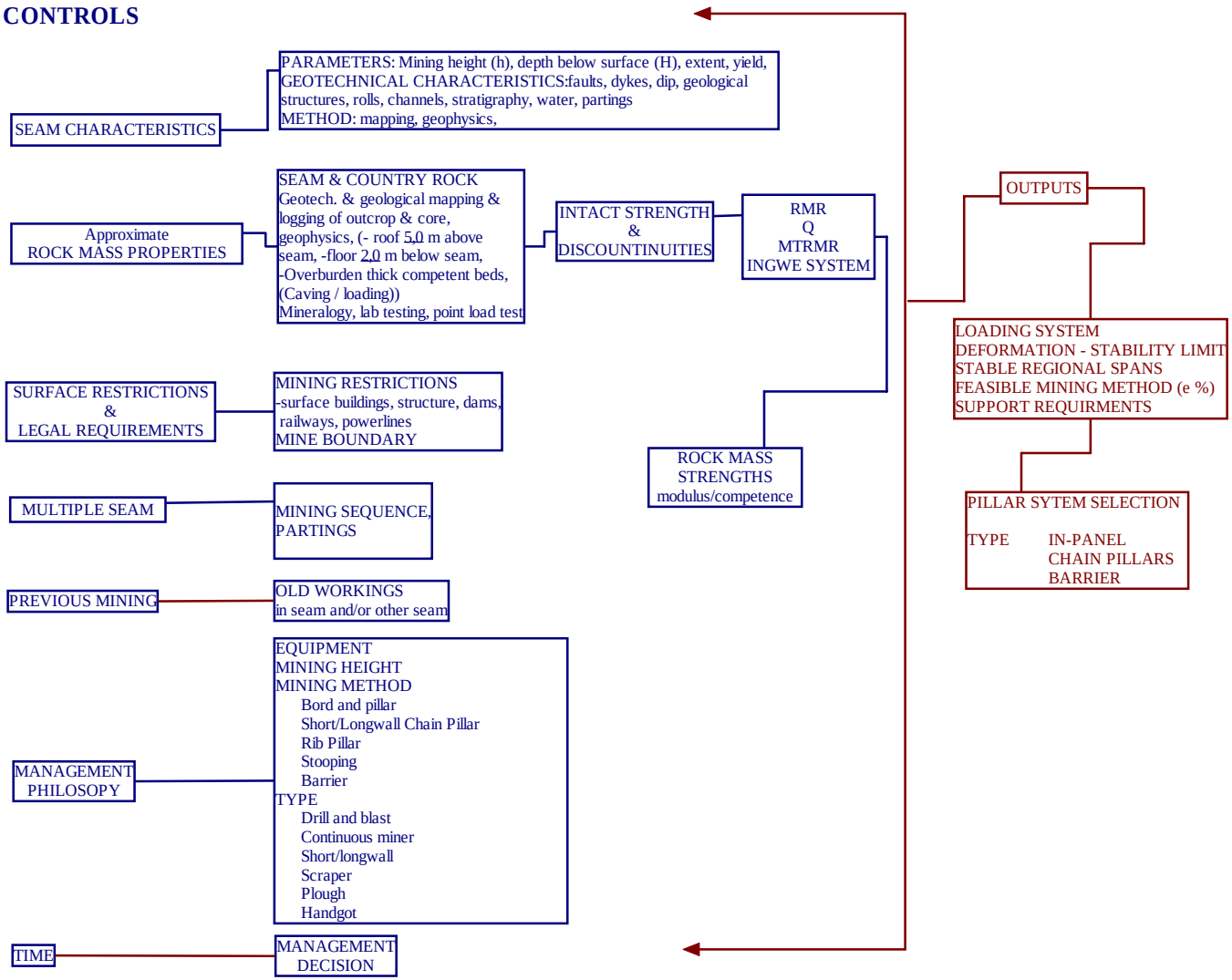

Figure 4-2 Analysis of control parameters.

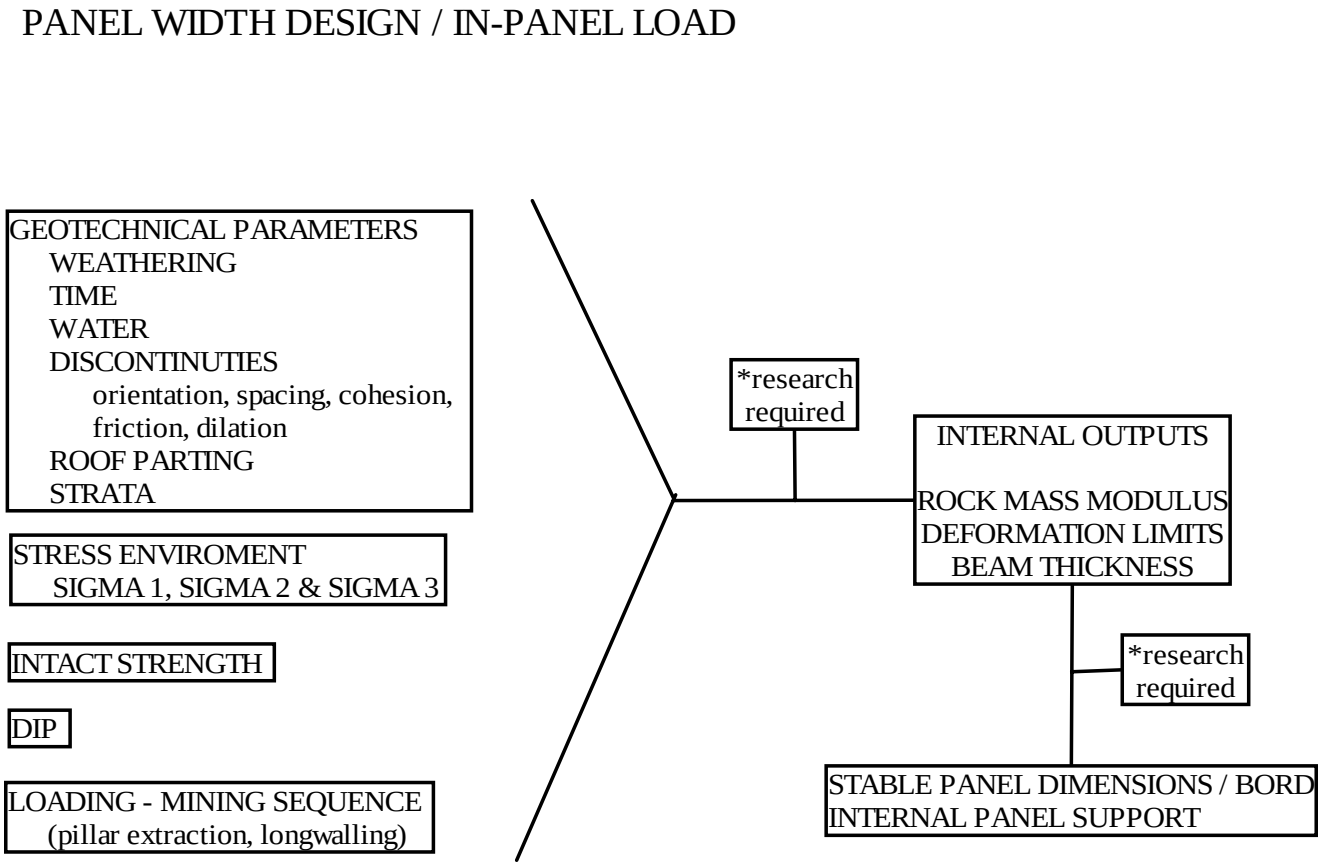

Figure 4-3 Panel width design parameters and methodology.

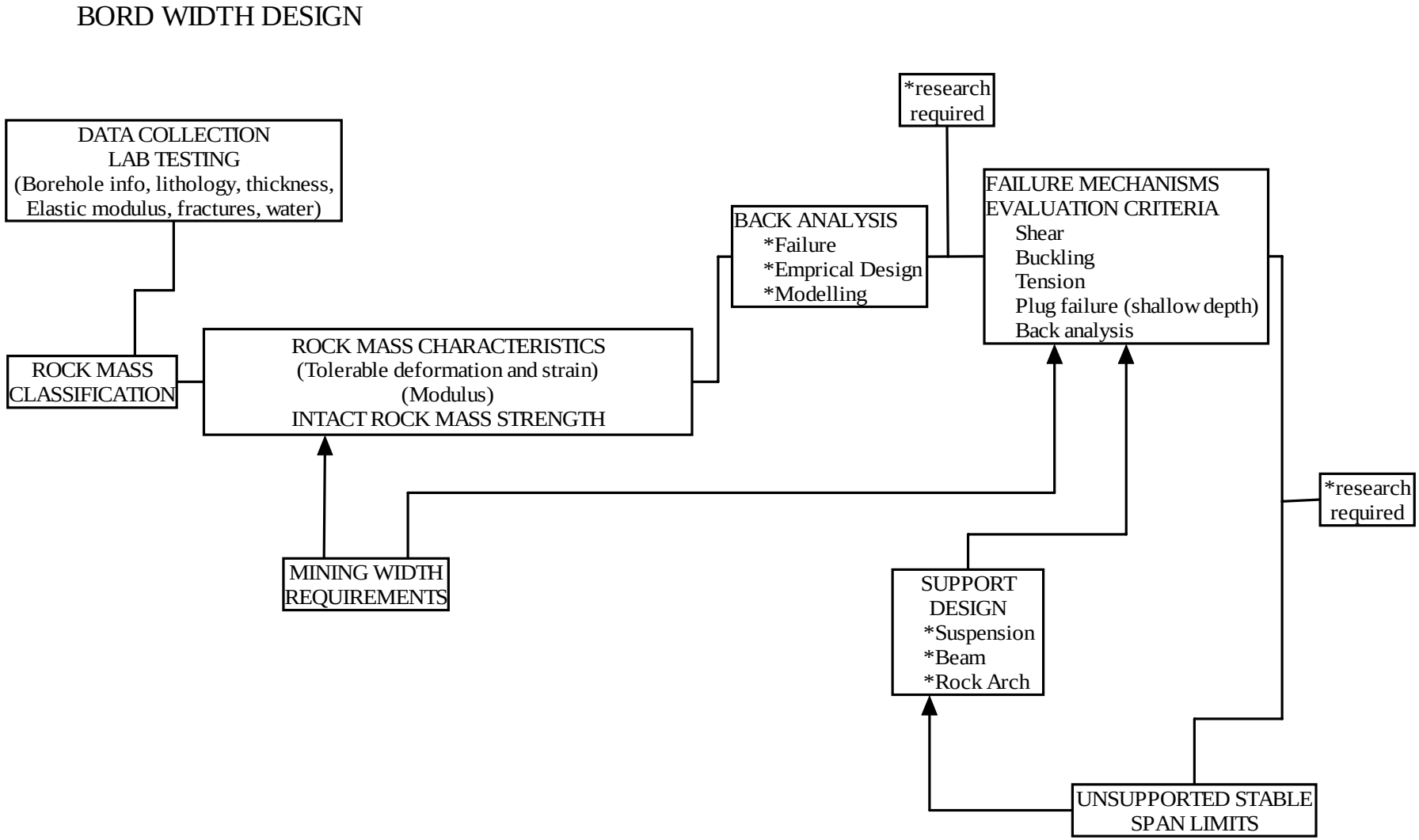

Figure 4-4 Bord width design parameters and methodology.

LOADING ENVIRONMENT

PARAMETERS :

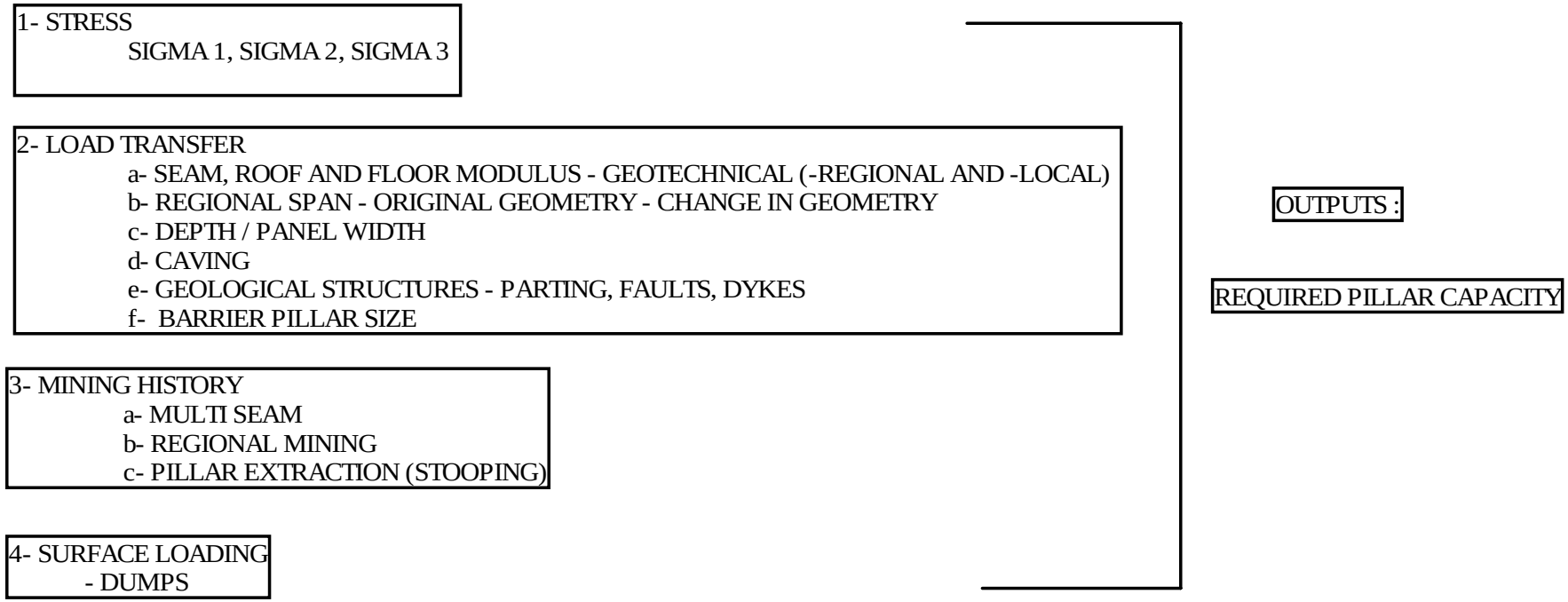

Figure 4-5 Loading environment design parameters.

LOADING ENVIRONMENT

DESIGN METHODOLGY :

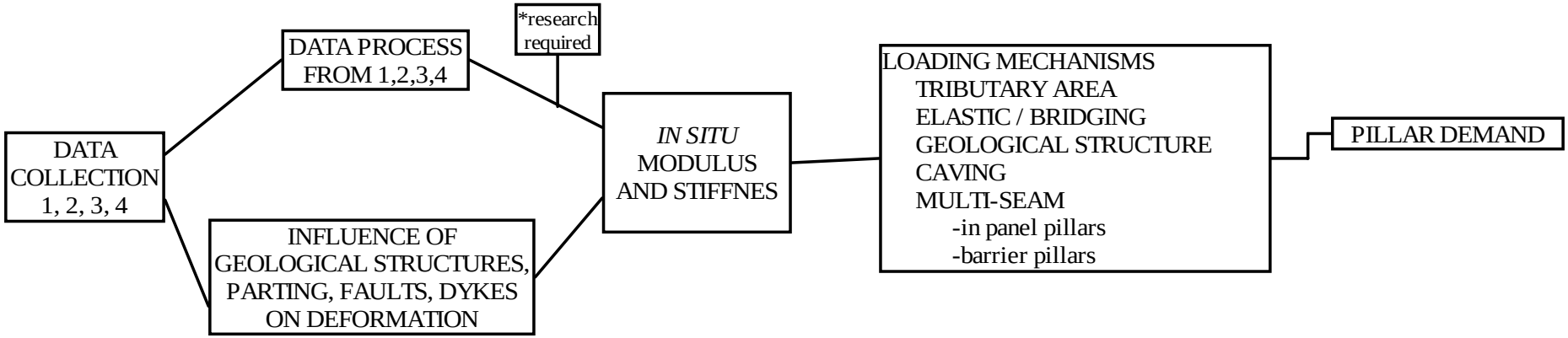

Figure 4-6 Loading environment design methodology.

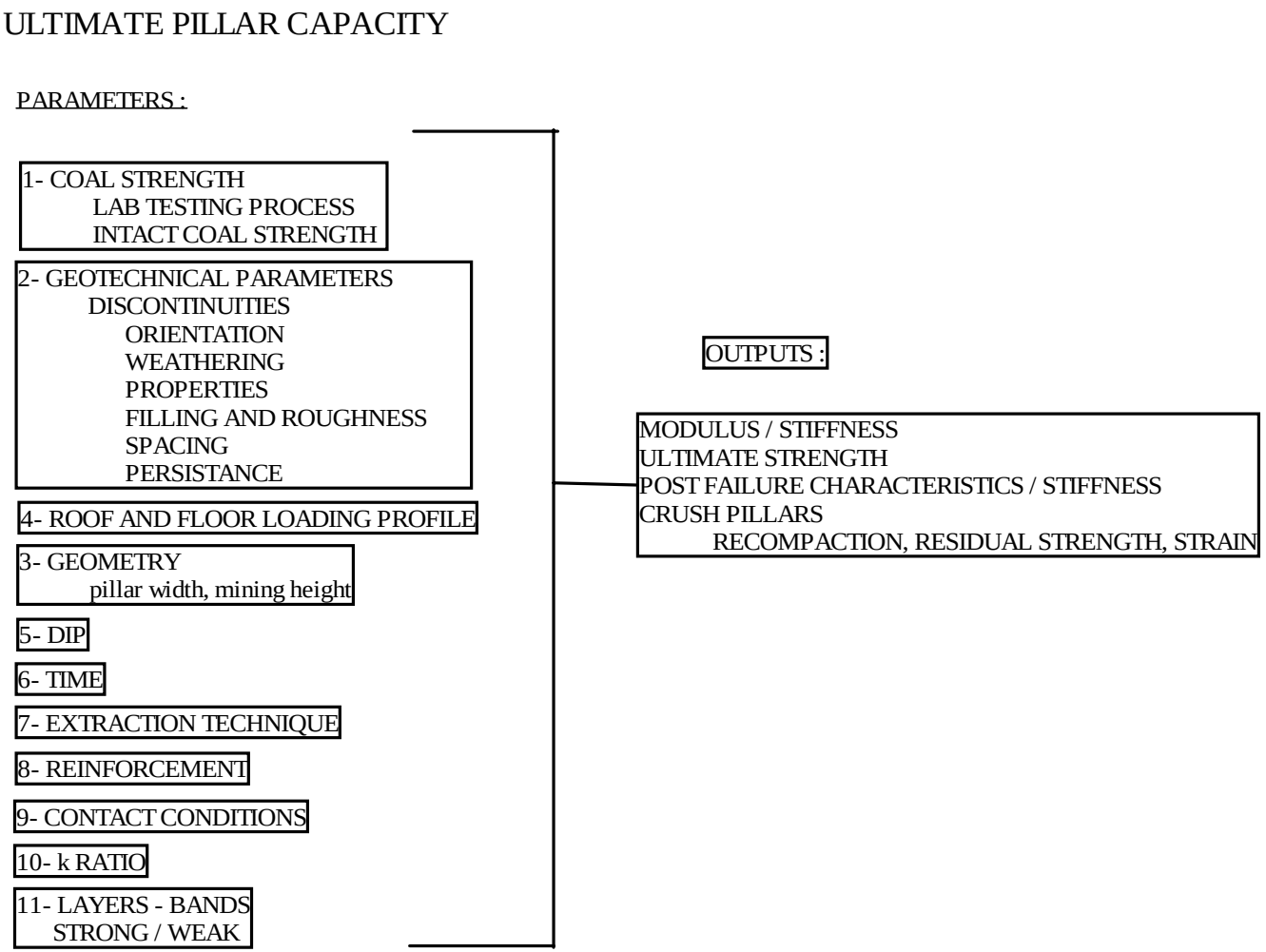

Figure 4-7 Ultimate pillar capacity design parameters.

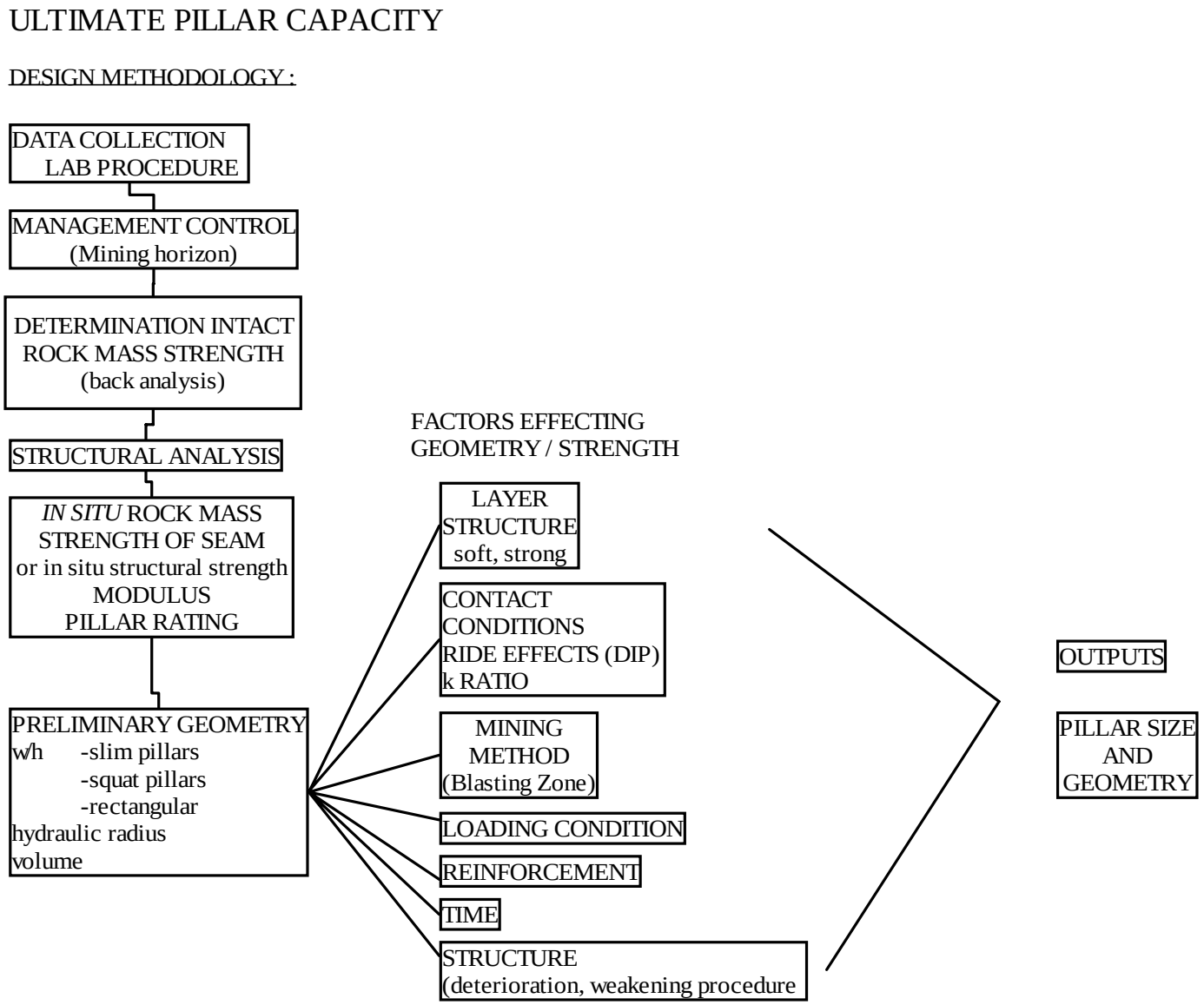

Figure 4-8 Ultimate pillar capacity methodology.

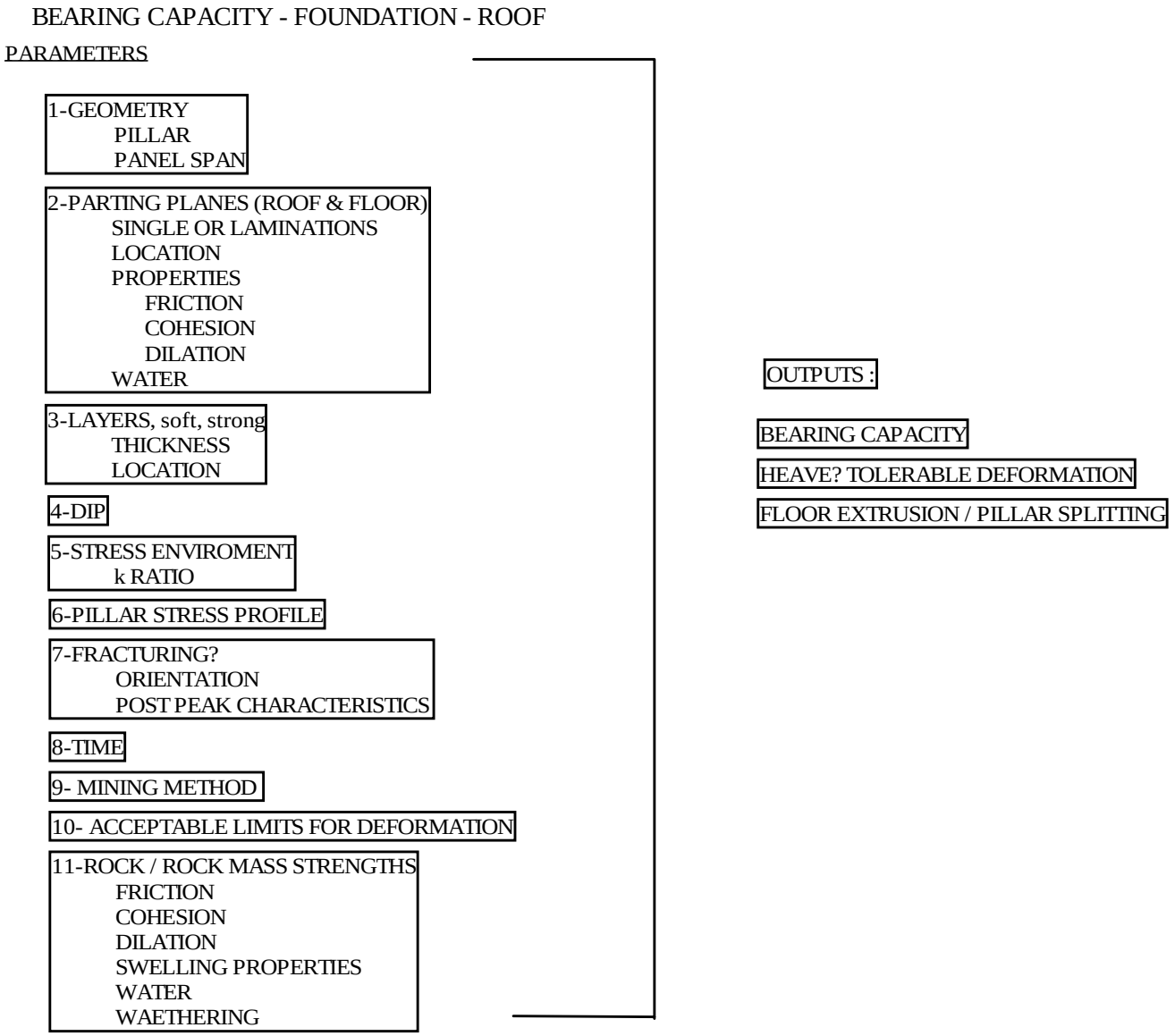

Figure 4-9 Bearing capacity design parameters.

BEARING CAPACITY - FOUNDATION - ROOF

DESIGN METHODOLOGY :

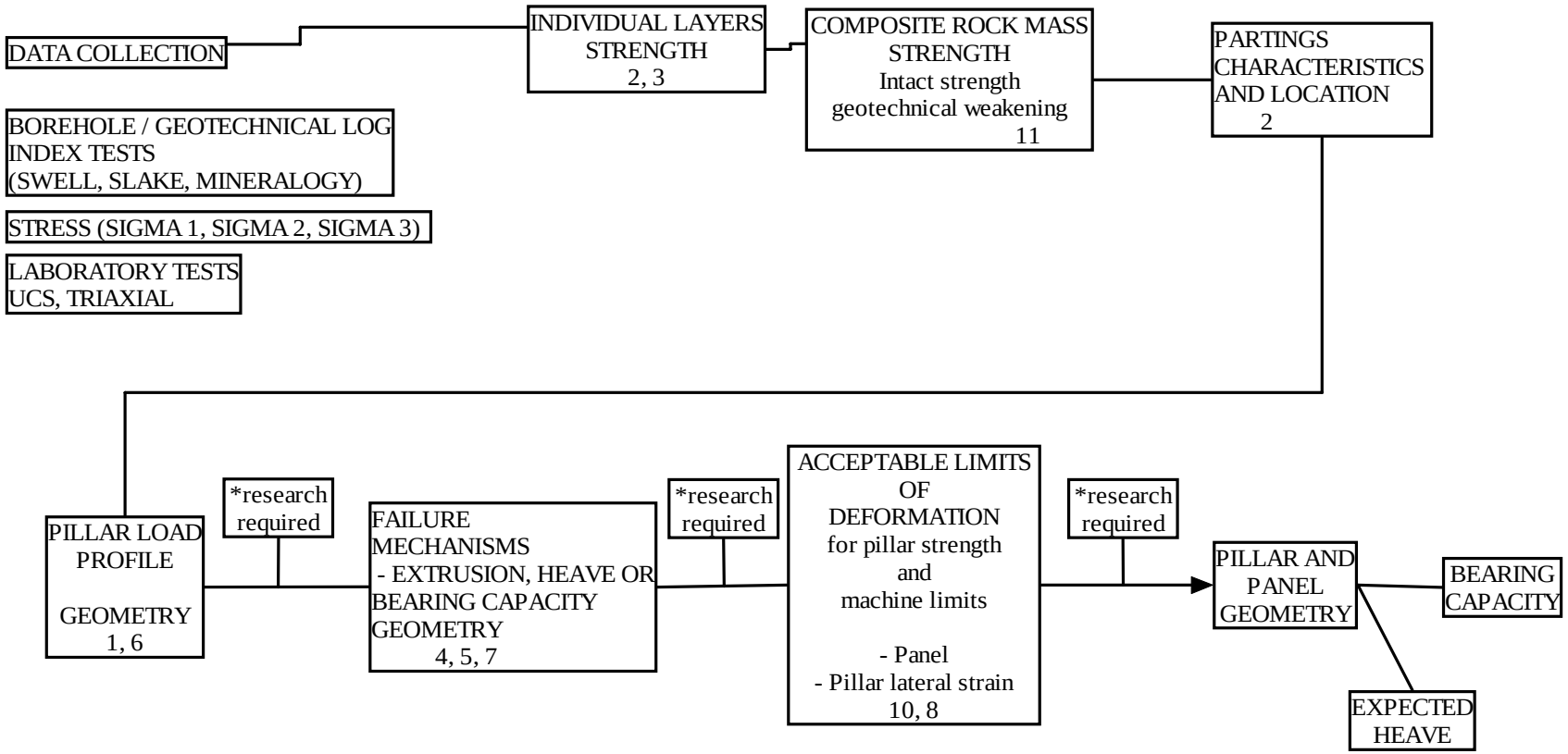

Figure 4-10 Bearing capacity design methodology.

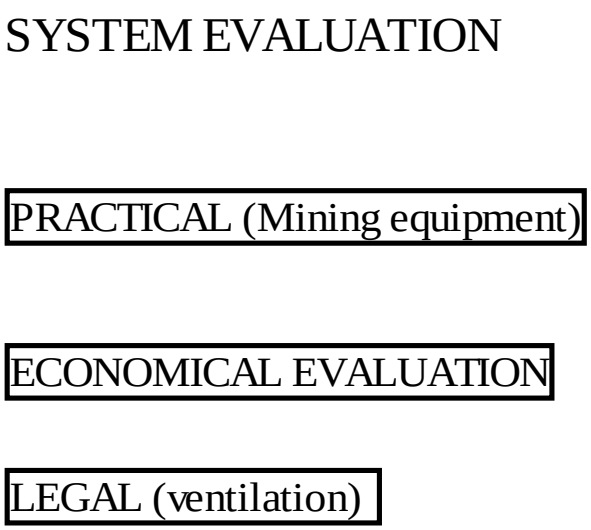

Figure 4-11 System evaluation design methodology.

5 Knowledge gaps in the current pillar system design methodology

Investigation into the pillar system design established the knowledge gaps in the current methodology of pillar design.

The current pillar design methodology and the additional knowledge required are presented in Table 5-1 to Table 5-6. Due to the number of publications involved in this study, the references are not included in the final report, however, all references were collated and can be obtained from CSIR Mining Technology.

As seen from these tables there is a need for a comprehensive study to cover all aspects of a proper pillar design methodology. On the other hand many authors have investigated pillar design aspects over the years. In fact all these investigation highlighted the gaps in the pillar design methodologies.

The knowledge gaps in the conceptual design methodology, which are detailed in the following tables, can be summarized as follows;

- Proper evaluation with regard to geotechnical parameters such as weathering, time, water, discontinuities, dip and partings.
- Interpretation of comprehensive laboratory testing to identify the material properties of both coal and surrounding strata (including the scale effect)
- A rock mass classification system which takes into account all critical parameters of both pillar and surrounding strata including roof and floor.
- A detailed investigation of stress environment and its components in both barrier pillars and in-panel pillars is required.
- The effect of pillar and bord widths on system stiffness and stress distribution.

Table 5-1 Current and additional knowledge required for control parameters.

Parameter	Current	Knowledge gaps	Reference
Seam Characteristics	Obtained by geologist & geophysicist Lab testing	Evaluate information with regard to Geotechnical design	Geophysics – ACIRL, 1985 Bieniawski (S-wave), 1980
Seam & Country Rock Rock Mass Properties	Geological logging Geotechnical logging Testing UCS, Elastic modulus, Poisson's ratio, shear strength, point load, slake durability, swell-index, tensile strength Mineralogy	Field stress	
Rating	RMR/Q/Laubscher/GSI Madden (pillar rating)	MTRMR requires further development to incorporate discontinuities, orientation, stress. Investigation of Modulus Applicability of current systems to coal mining	Baron, 1974 CSIR - Bieniawski 1970 Laubscher, 1990 Oldroyd & Buddery, 1983
Rock Mass Strengths	Classification of rock mass to give modulus/competence based on case histories	Requires further development	
Surface Restriction & Legal			
Multiple Seams	Multiseam guidelines Salamon and Oravecz Bradbury & Hill		Salamon & Oravecz, 1976 Bradbury & Hill, 1989 R. Hill, 1994

Table 5-2 Current and additional knowledge required for bord width design.

Parameter	Current	Knowledge gaps	Reference
Laboratory Testing	UCS, tensile strength Discontinuities - shear tests, dilation angle, cohesion, friction angle	Index tests to obtain tensile strength	
Data Collection (Borehole info)			
Rock Mass Classification			
Rock Mass Characteristics			
Failure Mechanisms Evaluation Criteria Unsupported & Supported	Shear, buckling, tension, back analysis, models, analytical, cantilever, empirical, Stacey & Page, beam theories, Wagner, shallow sinkhole guidelines Numerical modelling (UDEC, Phase2, FLAC, Elfen)		Beam Theory (Wagner), 1985 Stacey & Page, R Hill, 1996 Vd Merwe, 1995 Spann and Napier,1983
Mining Environment	Machine limits		
Stable Span Limits Unsupported			
Influence of Internal Support	Support interaction, props, temporary support, roofbolts	Cost evaluation, structural stable span then comparison between internal support and cost of support	Hattingh, 1989 A Haile, 1999

Table 5-3 Current and additional knowledge required for panel width design.

Parameter	Current	Knowledge gaps	Reference
Machine Limits	Cable (± 200 m) and machine limits		
Strata	Borehole, geological/geotechnical logging, determine the competent layer		
Span	Galvin's dolerite formula Vd Merwe's dolerite formula Beukes & Wagner incompetent layer formula		Galvin, 1981 Vd Merwe, 1995 Beukes & Wagner, 1990
Determine critical, sub-critical panel width	Galvin's dolerite formula Vd Merwe's dolerite formula Beukes & Wagner incompetent layer formula	Loading of sub-critical pillars in panels	Galvin, 1981 Vd Merwe, 1995 Beukes & Wagner, 1990
Numerical modelling	Load determination Bepil 2D FLAC 2D UDEC 3D Map3D 3D Minlay 3D		
Bord and Pillar	Every production section should be isolated. Barrier pillar width should be at least same as in-panel pillar width (Esterhuizen).	Geotechnical Parameters Weathering	Esterhuizen, ?

		Time Water Discontinuities Roof parting Stress Environment Sigma1, Sigma2 & Sigma3 Intact strength Dip Loading – Mining sequence	

Table 5-4 Current and additional knowledge required for loading environment.

Parameter	Current	Knowledge gaps	Reference
Load	Elastic Models Layering? MINLAY UDEC/Map3D/Bepil Tributary Area Pillars, rigid, abutment, dip Stiffness of layers Elastic Bepil, (Ryder & Özbay, stability studies) if complex, UDEC Multiseam rigid Coal Limiting Distance Salamon Guidelines Geologic structures NZ stress-meter Surface stress measurements (N. Gay)	*In situ* Modulus? Need *in situ* measurements Back analysis Empsi/Ermelo with neg pillar slope, FLAC Multi crush pillar requires further study Back analysis Horizontal stress	Salamon & Ryder, (Tributary area, stiffness) R. Hill, 1994 Salamon, Bradbury & Hill, 1989 Ryder & Özbay, 1990
	Limits of rock mass stability Dependent on geology, deferential movement	Strain criteria, regional span control by regional pillars	Wagner & Madden, 1984
Pillar Demand Loading Profile	Lab Testing Increased Height decreased stiffness $E_{pillar}=(E_{seam/1-v})$	Stiff & soft stress profile	Salamon (stiffness),

Table 5-5 Current and additional knowledge required for ultimate pillar strength.

Parameter	Current	Knowledge gaps	Reference
Intact Rock Mass Strength	Visual observation coal in combination with stress profile. Pillar rating (Madden)	Investigation of number of samples to be tested. Vertical variability within coal seam	SIMRAC 95 Coal pillar project Final Report Wagner & Madden, 1984
Geotechnical Parameters Weakening Procedures (Salamon, Özbay & Madden, Deterioration) Structural Analysis	Joint orientation and geometry	MTRE not measuring geot. data correctly and not using information Define structure and continuum analysis Define when continuum becomes structural	Salamon, Özbay & Madden, 1997 Effect of discontinuities (COL337), 1999
Layers in Pillar primary and secondary effects	Brummer, Özbay & Spencer	Lab testing & modelling Young's Modulus, Poisson's Ratio, contact properties, strength	Brummer (COMRO),… Özbay & Spencer,….
Contact Conditions	Galvin's notes		Galvin, 1995
k-ratio	Lab. Models show horizontal stress has effect on pillar strength Babcock (1969), Stress measurements database (SRK)	Numerical models of lab tests to examine the influence of horizontal stress Field stress	Babcock, 1969 GAP027, 1998 Galvin, 1995

Dip	Stress field in relation to pillars, influence of gravity, Galvin, w_{eff}	If numerical models show significant effect require more information in situ	SRK, 1998
Mining Method	Madden blasting effects coal 0.25-0.3 m		Galvin, 1995 Wagner & Madden, 1984
Geometry Rectangular Squat Slim	w/h ratio, 40% strength increase, Wagner 2w overestimate, Salamon & Galvin min w with low w/h, w_{eff} with increase w/h, Cook's results, Evans & Pomery, Ultimate Pillar Strength	Triaxial results sigma1 vs sigma2 & Madden w/h tests done on same sandstone. Comparison b/t both lab results field deformation/convergence measurements required geometry-confinement relationship, Fundamentally explain in terms of material properties, length to width ratio, volume effect.	Galvin / Salamon,1997 Wagner & Madden, 1984 Salamon, 1982 Salamon, 1967
Loading Conditions	Stiffness		Salamon (stiffness)
Time	Deterioration		COL337, 1999
Reinforcement			Johnson & Madden, 1998
Shallow Bord & Pillar Guidelines	Shallow bord and pillar guidelines		Madden & Hardman, 1992

Table 5-6 Current and additional knowledge required for bearing capacity.

Parameter	Current	Knowledge gaps	Reference
Data Collection	Geotechnical, geological logging, water, parting planes, soft layer (location), seam dip	Rating	
Laboratory testing	Slake durability, swell index, geoduribility, friction, cohesion, dilatation		
Stress environment		k ratio	
Pillar stress profile	Modelling of pillar geometry		
Time	?		
Acceptable limits	Back analysis – limits Galvin's chart		Galvin, 1995 Oldroyd, 1998

6 Formulation of a new pillar system design methodology

6.1 Introduction

The Salamon and Munro pillar design formula has been used successfully in South Africa. There have been a number of pillar collapses, despite the use of the formula. This has been mainly due to the application of the formula in design problems out of the range of the empirical database used by Salamon and Munro. An important implicit aspect of the database was the geotechnical conditions. As seen in Figure 1-4, pillar design in geotechnical conditions unlike those of the pillar collapses in the database, resulted in less successful design using the Salamon and Munro formula.

It is therefore important to take different geotechnical conditions into account when designing pillars. This is obvious to practicing rock engineers in the coal industry. Much of the modifications to the standard Salamon and Munro design formula take the form of an adjustment to the Safety Factor (SF).

The factors that influence the strength of pillars are varied. The rationale introduced in this chapter is to explicitly determine the quantitative influence of these various factors, as part of a pillar system design methodology. If this is achieved, then mining area specific changes to pillar design can be affected with confidence, allowing a rational basis for changes in SF.

The power-type formula has the ability to handle large variations in volume. It is suggested in this chapter that the w/h effect is adequately explained by the simple linear function, in the absence of a volume effect. Given that almost all underground pillars are larger than 1.5 m in width, it is suggested that there is no volume effect underground. This will be demonstrated in this chapter. Further modifications to pillar strength are then dependent on explicit quantifiable factors, as part of the pillar design process. The influence of these factors are used to adjust the basic strength obtained as a function of the inherent strength of the material and the w/h effect.

Unexpected results were encountered while performing the numerical modelling. Fundamental problems were encountered when comparing results obtained for Merensky Reef and coal pillars. A large amount of effort has been expended to solve this problem. However, the problem has not yet been resolved on a fundamental level. A semi-empirical method of back analysis has been used to circumvent the problem.

Due to the time spent on trying to resolve the fundamental numerical modelling problem, the initial underground verification could not be performed.

6.2 The critical rock mass strength

In general, it is accepted that the strength of material decreases with increasing scale (size), as shown in Figure 6-1. As used in this report, the scale effect is applied to rock specimens with no visible joints, other than cleating found in coal. Many of the early workers in coal material testing, in an effort to obtain pillar design strengths from laboratory testing, noted this effect. Hustrulid (1976), in his comprehensive survey of pillar formulae, reports that Gaddy, in a study on cubes ranging from about 5 cm (2 inches) to about 23 cm (9 inches), from five different coal beds, found that formulae of the form $S = kw^d$ fitted the data from the various coal beds well. K is a numerical constant depending on the coal bed, w is the width of a cube, and d is the power. The values of d were found to group fairly closely around –½.

Greenwald *et al* (1941) showed that a relation of the form $S = k\frac{w^{1/2}}{h^{5/6}}$, where w is the sample pillar width and h is the sample pillar height, provided an excellent correlation with *in situ* test data (Figure 6-2). The data is shown in Table 6-1. Significantly, the data points that do not lie on the straight line were not included in the derivation of the formula (the labels in Figure 6-2 correspond to “pillar no.” in Table 6-1). These specimens had significantly smaller widths than the other test specimens. These points all lie above the curve in Figure 6-2. This shows a clear scale effect, with smaller samples being stronger. If the equation is used for a cube (w = h), then the equation reduces to the form used by Gaddy, $S = kw^d$, with $d = -\frac{1}{3}$.

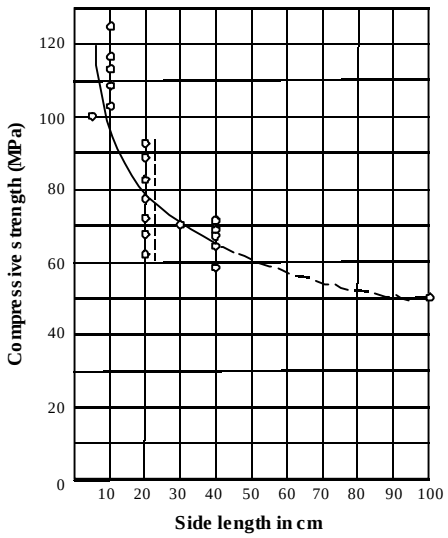

iron ore (Jahns, 1966)

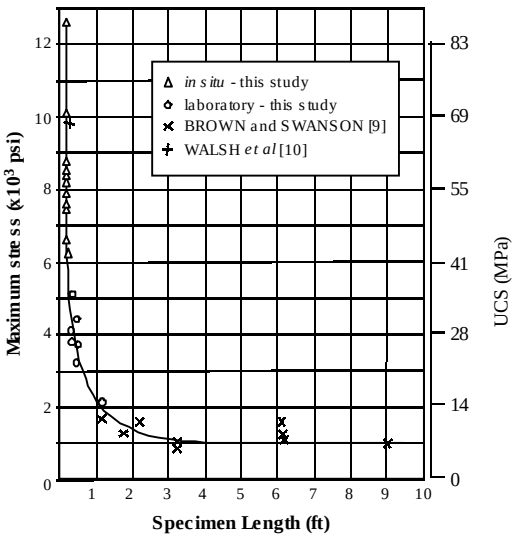

quartzitic diorite (Pratt *et al* (1972)

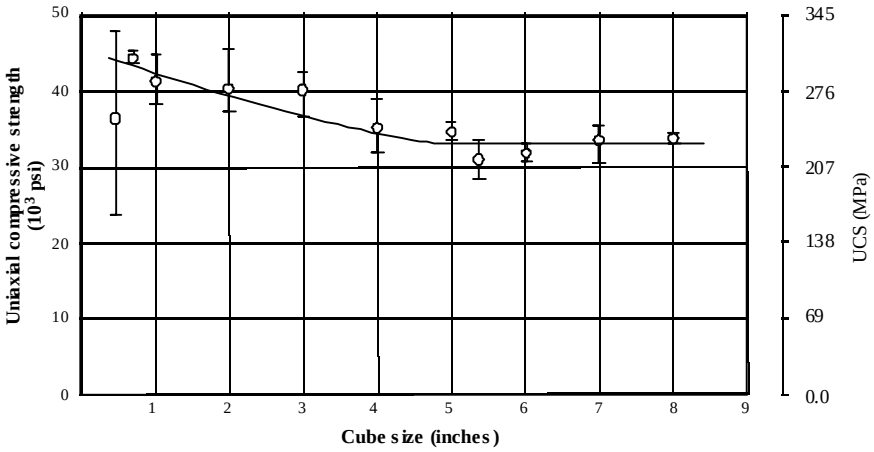

norite (Bieniawski, 1968)

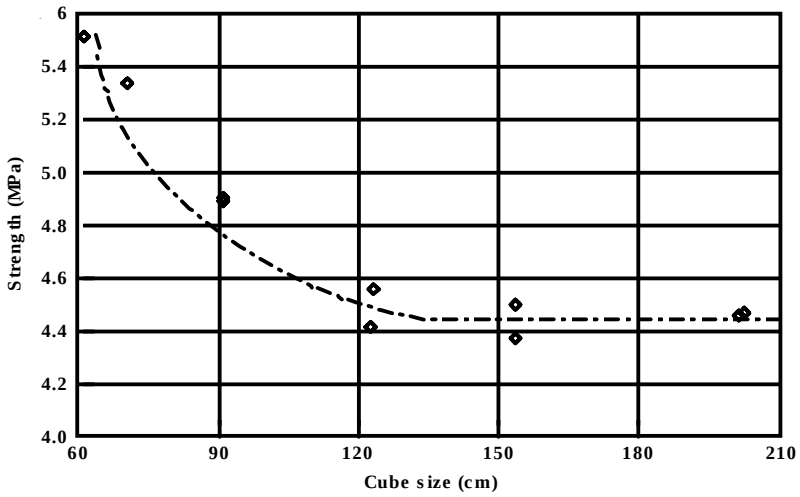

coal (Bieniawski, 1968a)

Figure 6-1 The strength – size effect for various rock types.

Table 6-1 Results of* in situ *tests on pillars performed by Greenwald* et al*, 1941 (units converted from inches and psi).

Pillar no.	w (mm)	h (mm)	w/h	strength (MPa)
2	800	1600	0.50	3.49
4	1205	1607	0.75	4.19
7	1615	1615	1.00	4.85
5	808	785	1.03	6.43
6	818	810	1.01	6.18
8	1070	770	1.39	7.33
9	521	754	0.69	6.29
10	522	757	0.69	6.64
11	1297	772	1.68	8.38
12	303	739	0.41	5.59

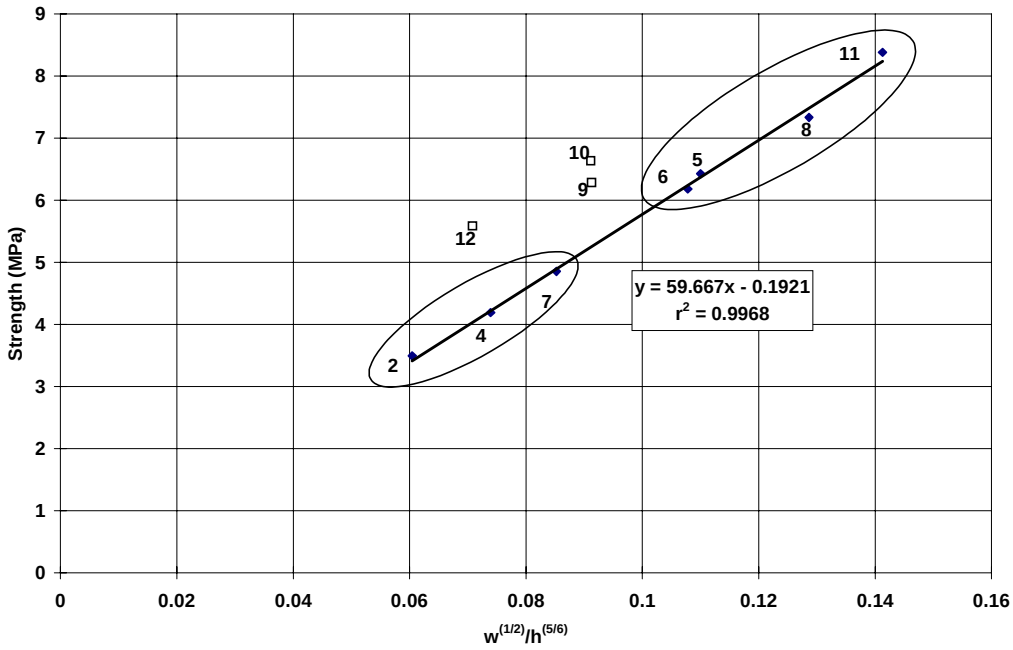

Figure 6-2 Results of* in situ *tests on coal performed by Greenwald* et al *(1941). The marked groupings are discussed in Section 6.5.

Steart (1954), postulated that the effect of cube size on the strength would be inversely proportional to the square root of the side dimension. No experimental evidence was presented to

support this. Evans *et al* (1961), after tests on Barnsley Hards coal, found values of d of -0.17 and -0.25 for two separate consignments, in cubes up to 5 cm in dimension.

Salamon and Munro (1967), in a rigorous statistical analysis of actual *in situ* failed and intact coal pillars, provided a formula:

$$S = 7.17h^{-0.66}w^{0.46} \qquad \textbf{\textit{Equation 6-1}}$$

where S = the expected pillar strength (in MPa)

h = pillar height (m)

w = pillar width (m).

Salamon and Munro's data were from the South African coal fields that produced the majority of the coal in the country. If the equation is used for a cube, the formula again reduces to the form used by Gaddy, $S = kw^d$, with d = -0.2.

The preceding investigations were with reference to laboratory or *in situ* tests, performed on small coal pillars, other than the survey of *in situ* pillars performed by Salamon and Munro (1967). The investigators mentioned, and many others involved in coal pillar research, have tried to use such tests to predict the strength of full scale *in situ* pillars. The common feature is that the strength decays with size to a negative power. The result is that a sample of very large size would be predicted to have a negligible strength.

However, the results shown in Figure 6-1 demonstrate a levelling off of strength with increasing size, for coal, iron ore, norite and altered quartz diorite. The evidence seems quite convincing that, for some rocks at least, there is a certain size beyond which no further decrease in strength is apparent. This phenomenon was defined by Bieniawski and van Heerden (1975). Denkhaus (1962) pointed out that large steel structures are designed according to the strength of cylinders approximately 2.5 x 50 cm in size.

According to the evidence presented, it is suggested that, for engineering purposes, it would be reasonable to assume a constant material strength beyond a certain size. Bieniawski and van Heerden (1975) termed the size at which no further strength reduction occurs, the *critical size*. The critical strength defined at the critical size was defined by Bieniawski as the strength of the *in situ* rock mass. In this report the strength of this size (for cubed shaped geometry) will be termed the *critical rock mass strength*.

If the *in situ* pillar has no geological jointing, and minimal blast induced fracturing, the rock may be called intact. In this case, the critical rock mass strength may be taken as the *in situ* rock mass strength. The critical rock mass strength cannot be used as the *in situ* rock mass strength if the *in*

situ pillar exhibits geological jointing, weak bedding and/or significant blast induced fracturing. In this case, pillar strength should be modified for the effects of the discontinuities.

This discussion excludes the effects of different testing conditions in the laboratory and *in situ*, including humidity, loading rate, end conditions, blast induced damage and temperature. The difference in the loading systems is also excluded.

6.3 The factors affecting pillar strength

The concept of the critical rock mass strength as an input parameter in the determination of the *in situ* rock mass strength has been discussed. Once the in situ rock mass strength has been determined, the other factors that determine the pillar strength need to be taken into account. Some are :

1) the pillar dimensions, including mining height (these lead to the w/h ratio)
2) the effect of jointing
3) loading system, “geological” and “local”
4) contact conditions
5) k ratio (the ratio of virgin horizontal to vertical stresses)
6) the stability of the roof and floor
7) the length : width ratio
8) dip
9) creep and other time effects.

Some of these factors are material properties, others are a function of the loading system, others a function of the stratigraphy, and so on. These factors, which need to be taken into account in a pillar system design, will be termed pillar system factors.

In the rest of this section, the effect of each of the above pillar system factors on the pillar system will be briefly discussed. The purpose of this discussion is to review present knowledge, put forward some new notions, and highlight areas of inadequacy.

The pillar dimensions are usually used to form a w/h ratio. For increasing w/h beyond 1, a strength increase is generated due to increasing confinement in the pillar core, with respect to the critical rock mass strength. It is generally these dimensions alone that are used in design, to determine the strength of a pillar. Consistent with the previous discussions, it is proposed that it is incorrect to build a volume effect into a pillar design formula for the *in situ* scale, for pillars of w/h < 5. This will be discussed in more detail in Section 6.5.

A pillar strength so obtained, however, will be modified by the other pillar system factors mentioned. The effect of jointing would need to be accounted for. Two possible alternatives may apply to the particular rock mass :

- the rock mass may be approximated as a weakened continuum, in the case of a highly jointed rock mass
- the rock mass may not be approximated as a continuum - the discontinuities are such that a structural stability analysis needs to be performed.

A structural stability analysis would explicitly model major discontinuity patterns, and their effect on pillar strength. This would be applicable to most coal pillar applications. The effect of jointing has been addressed in Chapter 2, where graphs showing the influence of joint orientation on pillar strength are presented.

A *"geological" loading system* refers to the influence that major geological structures such as sills, dykes or faults have on load transfer to pillars and abutments. The overall stiffness of the loading system affects the load transfer to pillars. The load transferred to a set of pillars in a particular area may be increased or decreased due to the geological environment. Large displacements may be localised adjacent to a fault. A false picture of *in situ* pillar strength is obtained if the geologically driven loading is not understood. The massive Coalbrook disaster of 1960 is an excellent example of overestimation of the coal pillar strength due to a lack of understanding of the geological loading system.

Assuming an intact frictional or integral interface between the sample/pillar and loading platen/roof and floor, any given loading condition falls somewhere between stress and displacement controlled loading. These two conditions form the extremes of a continuous spectrum. To the extent that a test is stress controlled, a test sample is likely to fail at lower stress levels than a displacement controlled test due to higher edge stresses developed. Note that, for the purposes of this discussion, the boundary condition is applied at the top of the platen, not directly to the sample.

Locally, a *softer loading system* can lead to apparently weaker pillars due to the bending affect. To illustrate this, a block of elastic material was loaded in these two ways in a simple computer model. The friction angle on the interface between the sample and the platen was taken as 30°. The computer code used was FLAC (Cundall, 1993). In Figure 6-4, it can be seen that the edge stresses are lower in the case of displacement controlled loading, which is explained by the greater displacement of the corner of the sample in the case of stress controlled loading (Figure 6-4). This is due to the bending effect of the platen that is exacerbated by a stress boundary. A platen wider than the sample increases the stress concentrations at the edge of the sample. There is little difference between a displacement and stress boundary if a platen is thick enough and not much wider than the sample. The bending effect is also affected by the relative Young's moduli and

Poisson's ratios of the platen and sample, such that a lower platen modulus leads to higher stress concentrations at the edge of the sample.

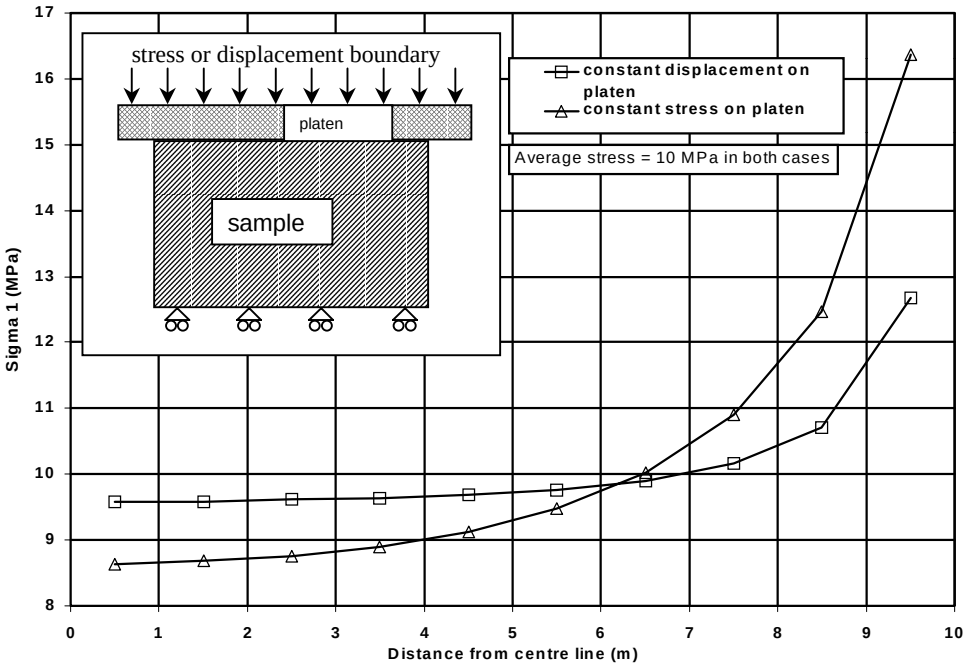

Figure 6-3 The effect of different boundary conditions on the stress distribution in a sample at the interface between the loading platen and the sample.

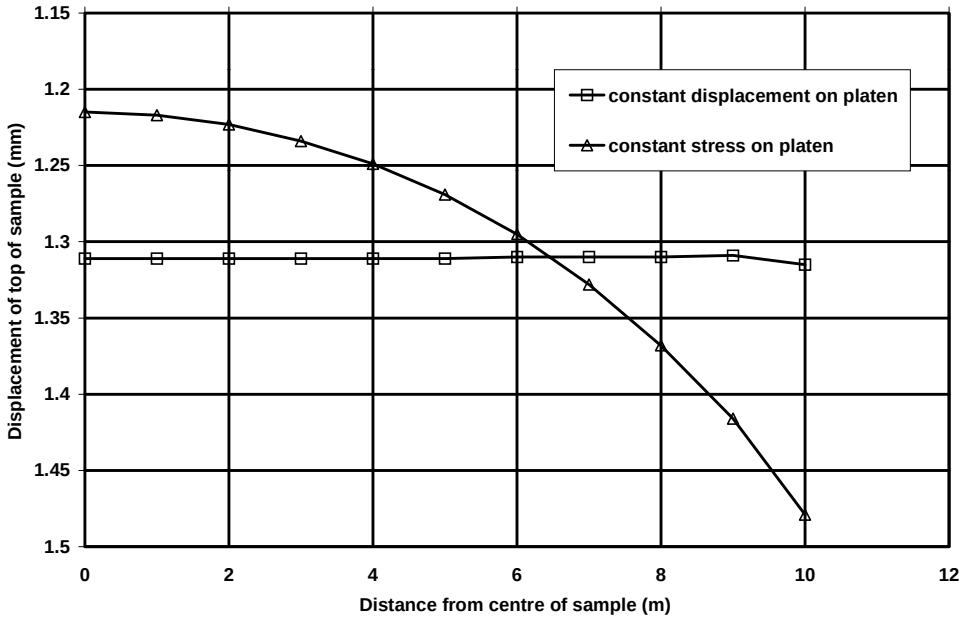

Figure 6-4 The effect of different boundary conditions on the displacement profile in a sample at the interface between the loading platen and the sample. The geometry is the same as shown in Figure 6-3.

Contact conditions, with respect to *friction*, can strengthen or weaken a pillar or sample. The effect of the platen/sample contact angle of friction on the clamping shear stress was modelled using the computer program DIGS (Napier, 1990). The results are shown in Figure 6-5a. As long as the value of excess shear stress (ESS) remains negative, the platen acts to clamp the sample, and confining stresses in the sample will be generated. For the particular set of loading conditions modelled (platen and sample geometry and respective elastic constants), the ESS at the edge of the sample increases to zero for a friction angle of 15°.

At lower levels of friction angle, slip occurs at the sample/platen interface. Under these conditions, tensile stresses are induced in the sample due to the bending of the platen. The minor principal stresses at the top of the sample are shown for the extreme cases of no friction and almost no friction (friction angle = 5°) in Figure 6-5b. It can be seen that tensile stresses (positive) are induced down to 15 per cent of the sample height. The average vertical stress is 100 MPa. The level of tensile stress induced is higher than the tensile strength of most rocks. This phenomenon has been observed in laboratory testing on samples of Merensky Reef, pyroxenite and anorthosite. All these rock types are found in the Bushveld Complex. The strengths of Merensky Reef, pyroxenite and anorthosite were reduced by 57, 58 and 49 per cent respectively when a friction reducer was used in laboratory tests (1995). The friction reducer was stearic acid. Samples failed due to vertical tensile cracks that split the circular sample radially in most cases in four, or in some cases in three or five segments. The cracks initiated at the edge of the sample and propagated to the centre. This is predicted by the modelling, which shows the peak tensile strength at the edge of the sample (Figure 6-5b). The model thus predicts the initiation of failure at the edge of the sample.

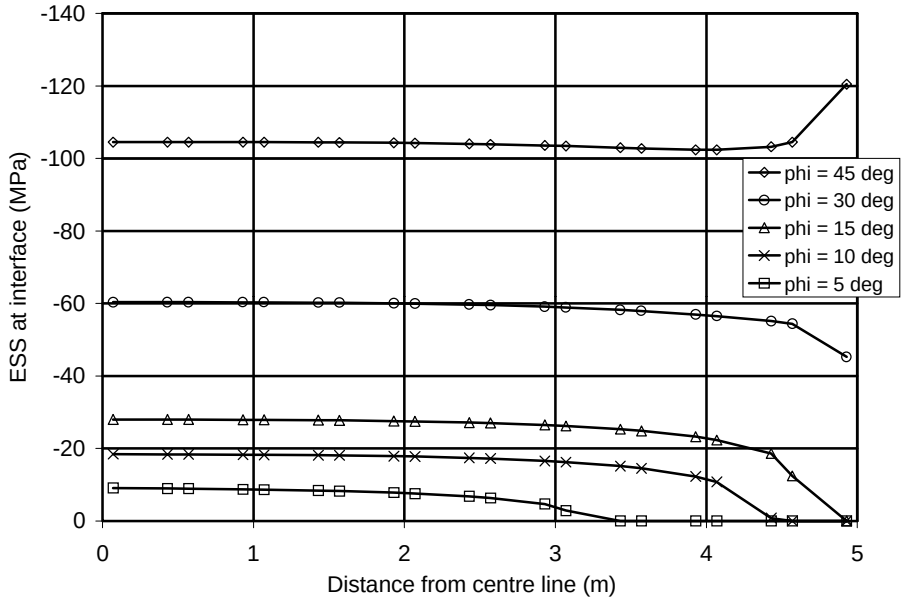

Figure 6-5a The effect of the friction angle at the interface between a model pillar and the loading platen on the excess shear stress along the interface.

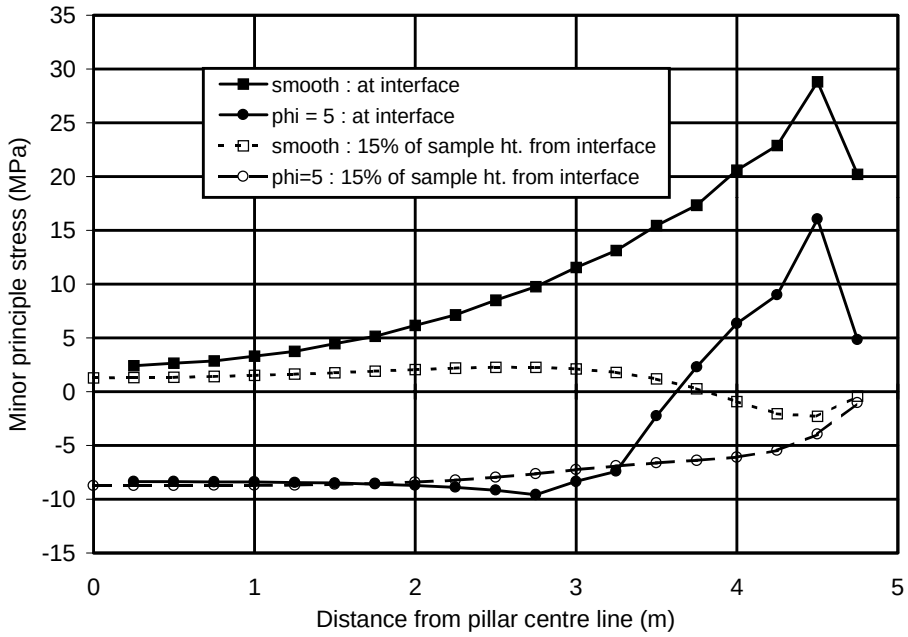

Figure 6-5b The effect of the friction angle at the interface between a model pillar and the loading platen on the minor principal stress in the sample at two sections.

A large *k ratio* that leads to higher compressive stresses in the roof can increase the strength of pillars. Babcock (1969), in an extensive test programme, tested samples of four rock types (limestone, marble, sandstone and granite) with the aim of determining the effect of end constraint on sample strength. The two variables tested were the w/h ratio and the radial confining stress at the top and bottom ends of the sample. The confining stresses at the ends were applied by means of clamping rings. The results showed roughly the same trends for all four rock types tested. Table 6-2 shows the results for the granite specimens. The effect of the confining stresses at the ends is evident from Table 6-2b, while the effect of the confining stresses and w/h ratio combined are seen in Table 6-2c. While these results are not directly applicable to underground pillars, these results imply a strengthening effect on in situ pillars in a high horizontal stress environment.

Table 6-2 The effect of end constraint due to w/h ratio and radial stress applied at the ends of granite samples (after Babcock, 1969).

Table 6-2a The actual strength values (averaged).

w/h ratio	**3.5**	**2**	**1**	**½**	**⅓**
DETAILS	Strength (averaged) (MPa)				
no radial stress	337	262	220	203	196
21 MPa radial stress	476	330	261	210	194
34 MPa radial stress	532	351	256	205	202

Table 6-2b The strength values normalised to the "no radial stress" value for each w/h ratio.

no radial stress	1.00	1.00	1.00	1.00	1.00
21 MPa radial stress	1.41	1.26	1.19	1.04	0.99
34 MPa radial stress	1.58	1.34	1.17	1.01	1.03

Table 6-2c: The strength values normalised to the strength value at w/h=1 and no radial stress.

no radial stress	1.53	1.19	1.00	0.92	0.89
21 MPa radial stress	2.17	1.50	1.19	0.96	0.88
34 MPa radial stress	2.42	1.60	1.17	0.93	0.92

A *parting in the foundation* that slides significantly may lead to a limit in the load that a pillar/floor system accepts, or may result in tensile splitting of the pillar. The Matla pillar collapses are a classic case of this phenomenon.

The *length to width ratio* (l/w) of rectangular pillars, as reported in the literature, does not have a uniform effect for all rock types. Bieniawski (1968a) noted no effect for norite specimens of w/h=2 and l/w ratio ranging from 1 to 2.75 (maximum sample size was approximately 5 x 10 x 28 cm). Cook *et al* (1970), in their *in situ* tests, noted that the four jacks in the corners of a rectangular pillar had similar load - displacement curves as the four jacks in a square pillar, especially in the post peak portion (jacks A in Figure 6-6). Jacks B indicated peak and residual strengths roughly double those of jacks A. Cook *et al* noted that not taking this phenomenon into account would lead to conservative design practice. Wagner (1974) noted this effect and proposed an effective width as $W_{eff} = 4A/C$, where A = area in plan, C = circumference in plan. No evidence was provided to substantiate this. Strong laboratory experimental evidence was provided by Stavropoulou (1982) for sandstone. She showed a strength in plane strain 49 per cent higher than the UCS (uniaxial compressive strength) value. Stavropoulou noted that frictional conditions at the loading platen/sample interfaces changed the strength. Stavropoulou stated that false conclusions would result if this were not catered for by means of friction reducers. As a result of a survey, Ryder and Özbay (1990) suggested strength increase factors of 1.1,1.2 and 1.3 for l/w ratios of 2, 4 and plane strain conditions respectively. It would seem that there is no universal or common effect. The effect of the l/w ratio needs to be evaluated for each rock type.

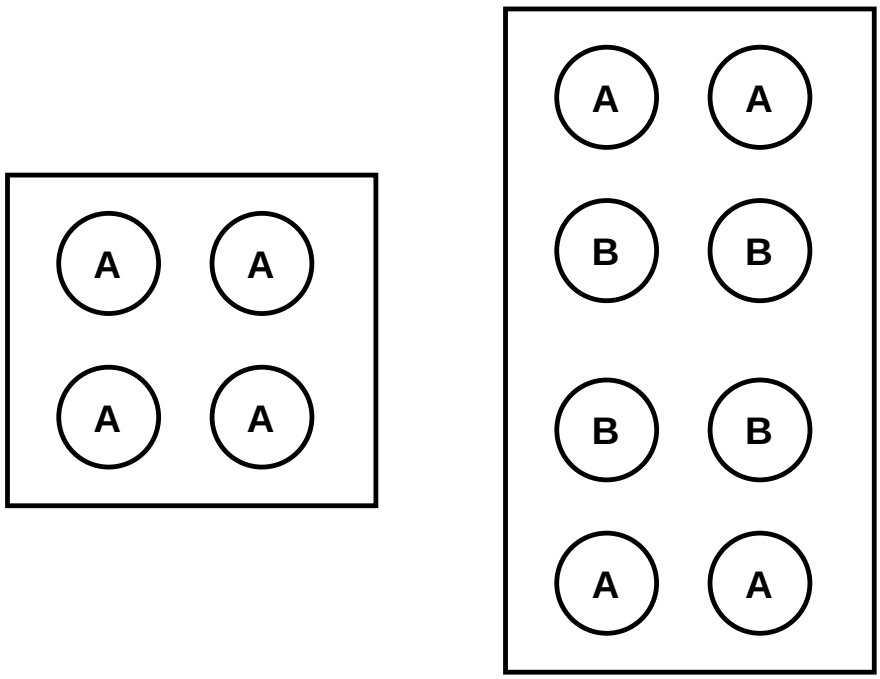

Figure 6-6 Cook et al (1970) showed that jacks A had quantitatively similar post peak strengths and moduli for pillars square and rectangular in plan, while jacks B showed peak and residual strengths double those of jacks A.

The *effect of time* on the change in pillar safety factor in coal mines due to scaling of the pillar edges has been investigated in the scope of this project, and has been reported in Chapter 3.

6.4 Accounting for the factors that affect pillar strength explicitly

Empirical formulae, such as those of Salamon and Munro (1967), Bieniawski (1968), have the limitation that they must be used with caution for design values that fall outside the empirical range. There is another limitation that is not as often appreciated.

The pillar formula that is most strongly based on *in situ* data is that of Salamon and Munro (1967). Their database was built as a result of replies to questionnaires sent to the industry. Cases of pillar collapses that could not be clearly attributed to the pillars themselves failing as the weakest element, were rejected. For both collapsed and intact pillars, little information was collected regarding the above mentioned pillar system factors. The actual data that was used in their statistical analysis were the dimensions of the pillar, the mining height and the depth. Other data collected included rock type, surface effects, comments on mining activities at the time of failure

and whether there were any early warning signs. The pillar system factors mentioned above were not explicitly catered for in the analysis.

Therefore, Salamon and Munro's database contained an unknown combination of the above mentioned, and probably other, pillar system factors. The combination is unknown in two senses: it is not known which factors were present in each case, and what the relative importance and interdependence of the various factors were.

The power formula, involving two geometric variables, w and h, cannot explicitly cater for this unknown combination of factors. In addition, the values of k, α and β obtained are the maximum likelihood parameters for the particular data set, that is, for the particular combination of pillar system factors taken as a whole. The values obtained are thus unique to that data set and only applicable to situations of like conditions. Also, k, α and β are obtained as a result of one statistical process, and form an indivisible set of parameters that best fits the data set. K cannot be separated from α and/or β. *K is therefore not a material strength parameter as is commonly assumed*, but is merely a point on the strength-size curve, depending on whether Imperial or SI units are used; and α and β are not material constants that define the strength decay with volume. If the value of 1322 psi is converted to units of MPa, the value of k obtained is 9.1 MPa (see Figure 6-7). Yet, a k of 7.2 MPa is widely quoted as the Salamon and Munro value. The discrepancy lies in the fact that the value of 9.1 MPa represents the strength of a foot cubed, i.e. approximately 0.028 m^3. To obtain the “representative” strength for SI units (i.e. one metre cubed), one needs to use Salamon and Munro’s original equation for a cube of side 1 m, but in units of feet. The strength in units of psi is obtained, which can be converted to units of MPa. The value so obtained is 7.2 MPa. Whether k is 1322 psi for a cubic foot, or 7.2 MPa for a cubic metre, these are two separate points on the same strength-volume curve. Aside from the scale effect arguments presented in Section 6.6, on the basis of Figure 6-7, k should not be considered a material property, but an arbitrary point on the curve, depending on the units of length chosen.

The strength decay with volume is empirically true (weakly, the volume exponent p = -0.067, see Equation 6-4); however, in the light of the evidence of a constant strength beyond a critical size, as well as consideration of the pillar system factors mentioned (especially the “geometrical” effect), it is postulated that Salamon and Munro's empirically observed volume strength decay is a function of the pillar system factors, rather than a pillar material property. It is clear that Salamon and Munro's formula implicitly lumps together the particular set of pillar system factors that were present in their data set. These pillar system factors are expressed, or captured, in the derived coefficients, k, α and β. Taking this concept further, any particular pillar strength formula, whether derived from in situ tests, as Bieniawski did, or based on laboratory tests, will have the same

essential feature: the prevailing pillar system factors are expressed in the derived coefficients or constants of the particular formula.

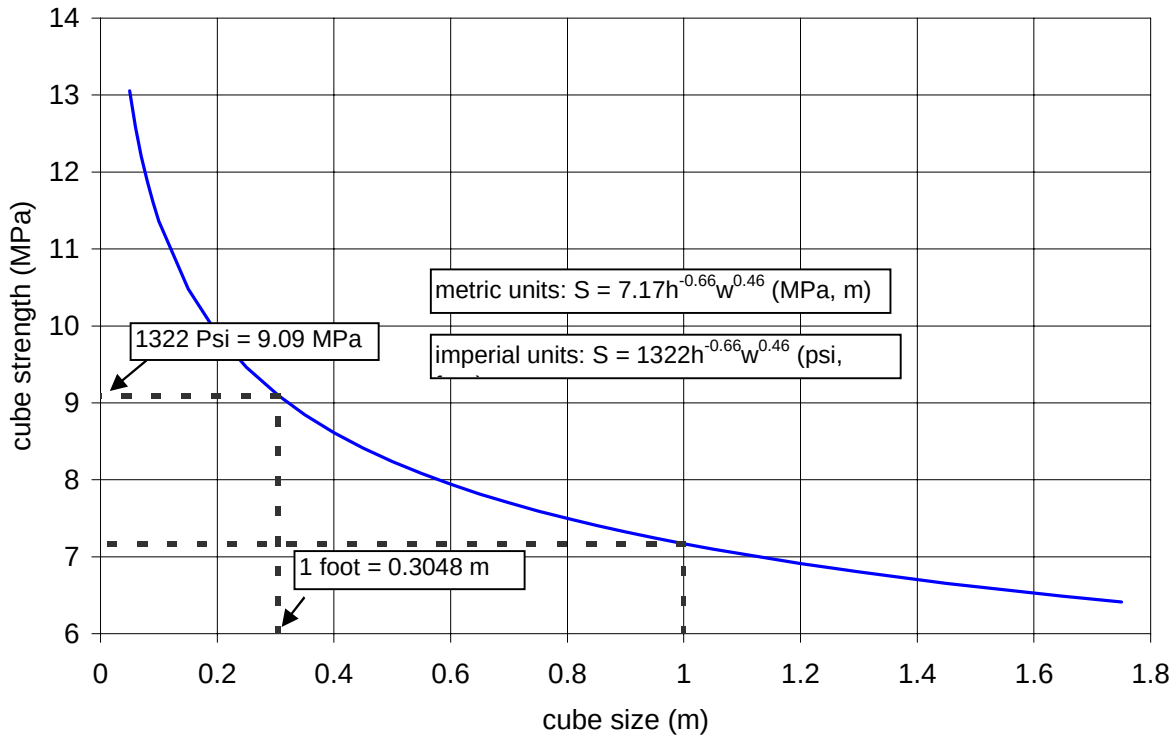

Figure 6-7 An illustration of the change in the value of k, depending on which system of units are used.

It is clear from the above considerations of pillar system factors, that a pillar cannot be designed as a stand alone structure. There is an interaction between the behaviours of the pillar, the roof, the floor and the loading system. A holistic design procedure that explicitly takes this interactive pillar system behaviour into account is required. The pillar system design will produce a pillar system strength (as opposed to a pillar strength), or pillar system load bearing capacity, which will depend on the weakest element, or perhaps the dominant influence of, say, the contact conditions.

It is also clear that seam strength alone is not a basis for design, because seam strength is just one of several factors that determine the overall pillar system strength. Mark and Barton (1996), in back analysis of a large database, found the factor of safety for *in situ* pillars to be almost meaningless when individual seam strengths were used. The factor of safety was a substantially more reliable indicator when a uniform, or average, seam strength was assumed. This shows that the other pillar system factors had a large influence on the strengths of the pillars, perhaps so much so as to overwhelm the effect of the different seam strengths. Equally, this shows that the particular pillar system factors present in laboratory testing on model pillars are different to those

found underground, so as to actually make the laboratory-based seam specific strengths almost valueless, if considered as a primary design parameter.

Some of these factors are additive, such as the frictional restraint generated by increasing w/h ratios (assuming a frictional contact) and a high k ratio. Conversely, exactly how a progressively softer loading system (weakening effect) interacts with a highly frictional contact condition (strengthening effect) is not known. A high k ratio would in any case have no effect if there is a low friction roof contact.

In view of the above considerations, the requirement for enhanced pillar design is to explicitly quantify the most influential factors that affect pillar strength. Such a quantification should be built into a pillar design procedure. The advantage of such an approach would be the ability to design on a site or region specific basis, both for increased and decreased strength, as required in specific circumstances. Such a pillar design methodology is proposed in Section 6.10.

6.4.1 The meaning of rock strength

The following aspects of rock strength have already been discussed in this report and will be briefly mentioned here for clarity in the argument that follows. The different loading conditions for the series of in situ tests conducted by Wagner, Bieniawski and van Heerden have been postulated to influence the strength results. This was supported by simple modelling (Figure 6-3 and Figure 6-4). The laboratory strength of hard rock in the Bushveld Complex has been shown to be reduced by 50 per cent when no friction is allowed between the loading platen and the sample (Haile, 1995). This was also supported by modelling results (Figure 6-5b). It is also accepted that the strengthening effect of increasing w/h ratio is due to the increased influence of the end frictional restraint on the stress field in the sample.

It is therefore clear that the strength of a rock is a function of the end, or boundary, conditions, both with respect to frictional conditions and the relative material properties and geometry of the loading platen / end piece / hangingwall (assuming other conditions such as loading rate, temperature and moisture content are unchanged). Strength is therefore not a stand alone value, but is a value for a given set of boundary conditions. It is suggested that, especially for model pillar studies, previous results have been presented with ill defined boundary conditions.

6.5 A review of *in situ* tests and Salamon and Munro's pillar collapse database

The two main forms of pillar design formulae in use are the "power" and the "linear" formulae. The power formula has the form:

$$S = kh^{\alpha}w^{\beta} \qquad \textit{Equation 6-2}$$

where S = the expected pillar strength

h = pillar height

w = pillar width

k, α and β are empirical constants (Salamon and Munro: 7.17 MPa, -0.66, 0.46 respectively – see Equation 1-2).

The linear formula has the form:

$$S = m(w/h) + d \qquad \textit{Equation 6-3}$$

where w/h = the ratio of pillar width to height

m and d are empirical constants.

The power formula is able to explain changes in strength over a large range of volume. Equation 6-2 may be written as:

$$S = kV^{p}(w/h)^{q} \qquad \textit{Equation 6-4}$$

where V = volume (assuming a pillar square in plan).

In this case, for pillars square in plan:

$$p = 1/3(\alpha + \beta)$$

$$q = 1/3(\beta - 2\alpha) \qquad \textit{Equation 6-5}$$

The linear formula, in the form stated above, cannot take volume into account, because w/h is a dimensionless parameter. The linear function records the geometric effect of increasing the w/h ratio.

Greenwald *et al's* data can be divided into three subsets. Data points 2, 4 and 7 in Table 6-1 were "full height" pillars. Data points 5, 6, 8 and 11 were "half height" pillars. Data points 9, 10 and 12 were "half height" pillars, but with the smallest dimensions significantly smaller than the other half height pillars, therefore showing the scale effect mentioned earlier. A linear function was fitted firstly to all the data, then to each of the three subsets. Let the term "volume ratio", as applied to a set of data, be defined as the ratio of the largest volume to the smallest volume in that set. The

volume ratios and r^2 values for each category are shown in Table 6-3. The r^2 values indicate the proportion of the total variation in strength which is accounted for by the variation of the independent variable/s in the fitted functions. The volume ratio is defined as the ratio of the maximum to the minimum volumes in the data set. As seen, the volume ratio of 62 corresponds to a low r^2 value, while the lower volume ratios correspond to much higher r^2 values that are comparable to the r^2 value shown in Figure 6-2. As can be seen by the grouped data points in Figure 6-2, the full height and half height data form separate groupings.

Table 6-3 Analysis of the effect of the volume ratio on fitted straight line strength functions, to Greenwald* et al's *data divided into volume ranges.

Details	data points (see Table 6-1)	Volumetric ratio	r^2
all data points	all	62	0.53
full height	2,4,7	4.1	1.00
½ height	5,6,8,11	2.5	0.99
full ht and ½ ht	2,4,7 and 5,6,8,11	8	0.92

The data used by Salamon and Munro (1967) in the derivation of their formula has been analysed. Only the collapsed cases are dealt with, of which there are 27. Salamon and Munro only considered collapsed cases if the following two conditions were met:

1) the collapse had to be only due to failure of the pillar

2) the extent of mining had to be such that tributary area loading was assumed to apply.

The collapse load used by Salamon and Munro was therefore the tributary area load.

If the logarithmic form of the power formula is applied, the r^2 value is 0.59 for Salamon and Munro's collapsed cases. If the linear function is applied, the r^2 value drops to 0.40. However the ratio of smallest to largest volume is 81. The pillar collapse loads are plotted as a function of w/h in Figure 6-8. The pillar with the smallest volume appears to be anomalously high. The load is 32 per cent higher than the next closest load, and more than 50 per cent above the trend line. The dimensions of this pillar were width = 3.35 m and height = 1.52 m. The width is therefore well above the critical size (1.5 m) as defined by Bieniawski and van Heerden (1975). This implies that volume is not a contributing factor in the higher pillar load (or pillar strength). Other pillar system factors, such as unusual geology, or unusual geotechnical characteristics of the seam, may have applied in this particular case.

If the pillar with the smallest volume is removed, the volume ratio is 48. In this case, the r^2 value increases to 0.53, a value that is almost as good as that of the power formula.

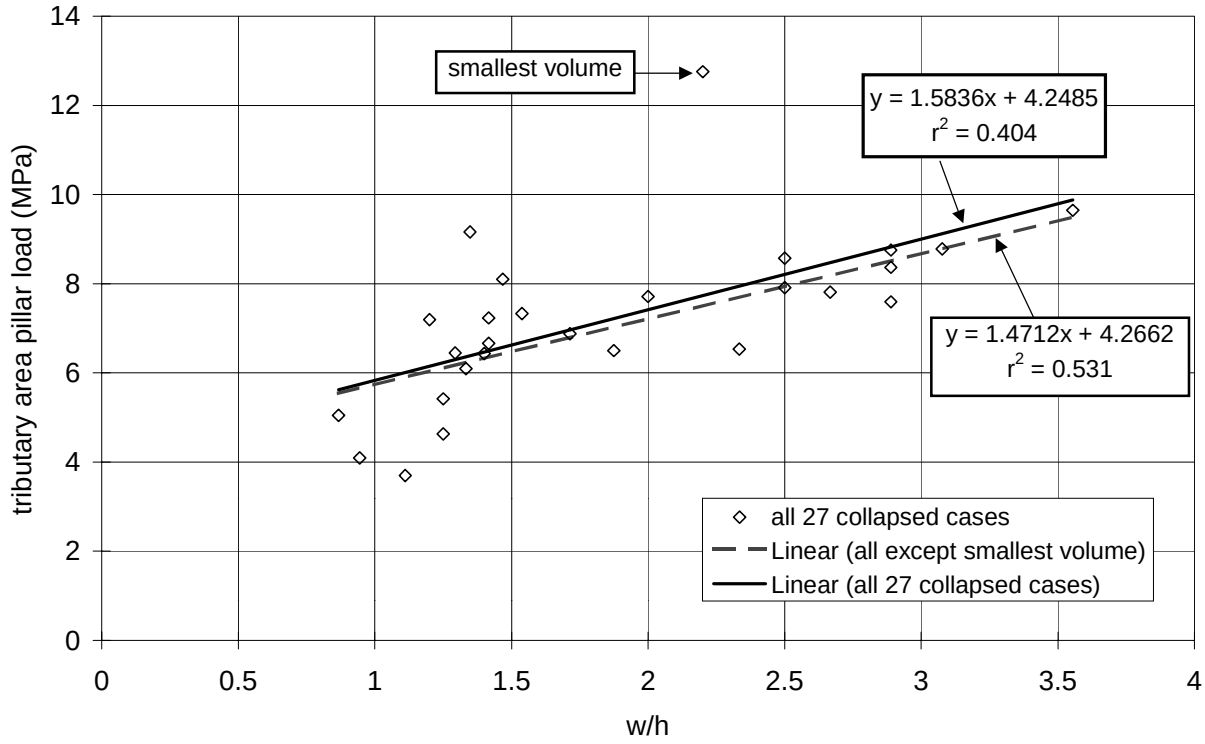

Figure 6-8 Salamon and Munro's (1967) collapsed cases data, plotted against w/h.

If the power formula fitted to the 26 collapsed cases (i.e. without the minimum volume) is written according to the form in Equation 6-4, the following is obtained:

$$S = kV^{-0.045}\left(\frac{w}{h}\right)^{0.506} \qquad \textit{Equation 6-6}$$

The exponent of volume is small. The calculated pillar loads (which are equivalent to strengths on the assumption of tributary area loading) for the Salamon and Munro collapse cases are shown as a function of volume in Figure 6-9. The near-horizontal best fit lines show that the strength is independent of volume at the *in situ* scale. This has two corollaries:

1) the critical size is less than the practical *in situ* pillar dimensions

2) the variation of strength about the best fit lines indicates that other factors affect pillar strength.

This also explains why the r^2 values for the power and linear formulae are similar (and low).

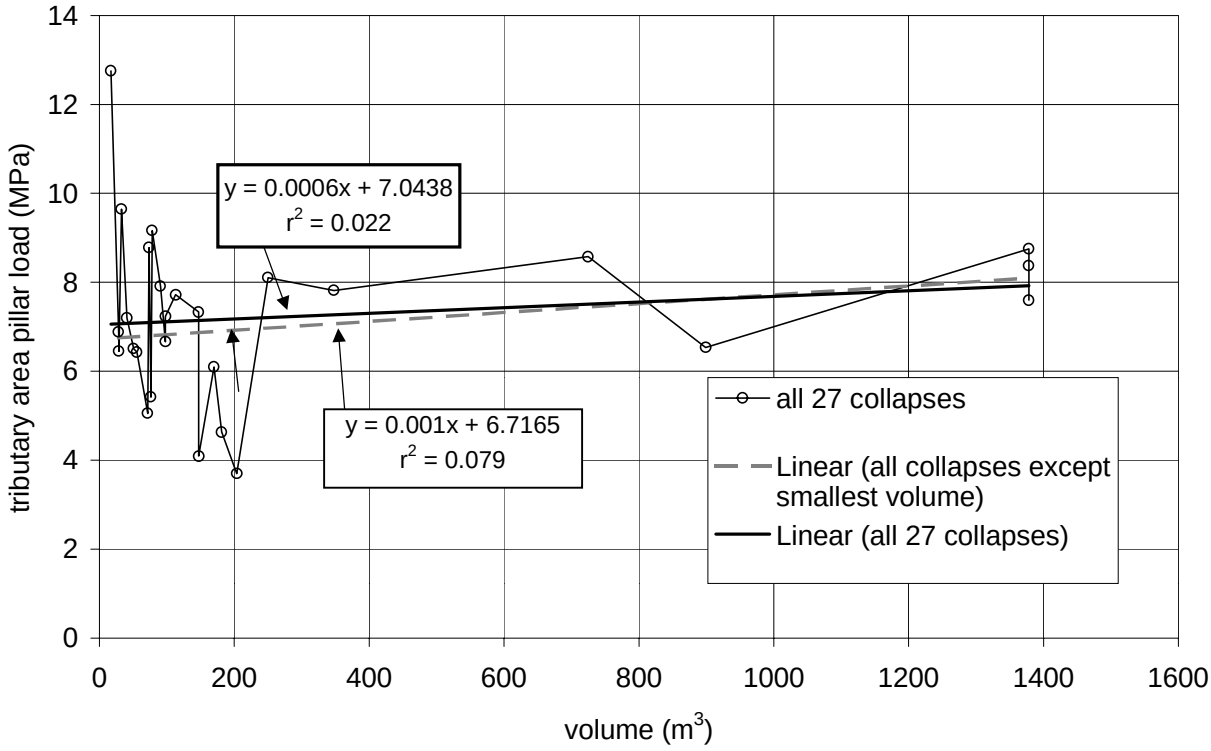

Figure 6-9 The calculated pillar loads assuming tributary area loading for the Salamon and Munro collapses cases as a function of volume.

A reworking of original published data has been performed on three sets of *in situ* large scale compression tests on coal. The results are shown in Figure 6-10, as a function of w/h. Salamon and Munro's original data set of collapsed cases is also plotted. The three sets of *in situ* compression tests are as follows:

- van Heerden (1974) obtained a cube strength value of 14.6 MPa on 1.4 m cubes at New Largo Colliery
- the results from Usutu Colliery (Wagner, 1974) showed the strength of 1.8 m cubes to be 11.3 MPa
- a straight line fit through Bieniawski's large scale tests (1.5 and 2 m square in plan) results in a cube strength of 4.3 MPa. Bieniawski's (1968) critical strength value of 4.5 MPa was based on cubes of side dimensions up to 2 m.

Two observations may be made regarding the Salamon and Munro data plotted in Figure 6-10:

- Salamon and Munro's k value was 7.2 MPa; assuming that the true critical size for coal is 1.5 m (as suggested by Bieniawski), the value provided by Salamon and Munro's empirical formula (see Equation 1-2) for a 1.5 m cube is 6.6 MPa

- a straight line fit through Salamon and Munro's collapse cases (with the smallest volume removed as described in the preceding paragraph) results in a cube strength of 5.7 MPa (Figure 6-10).

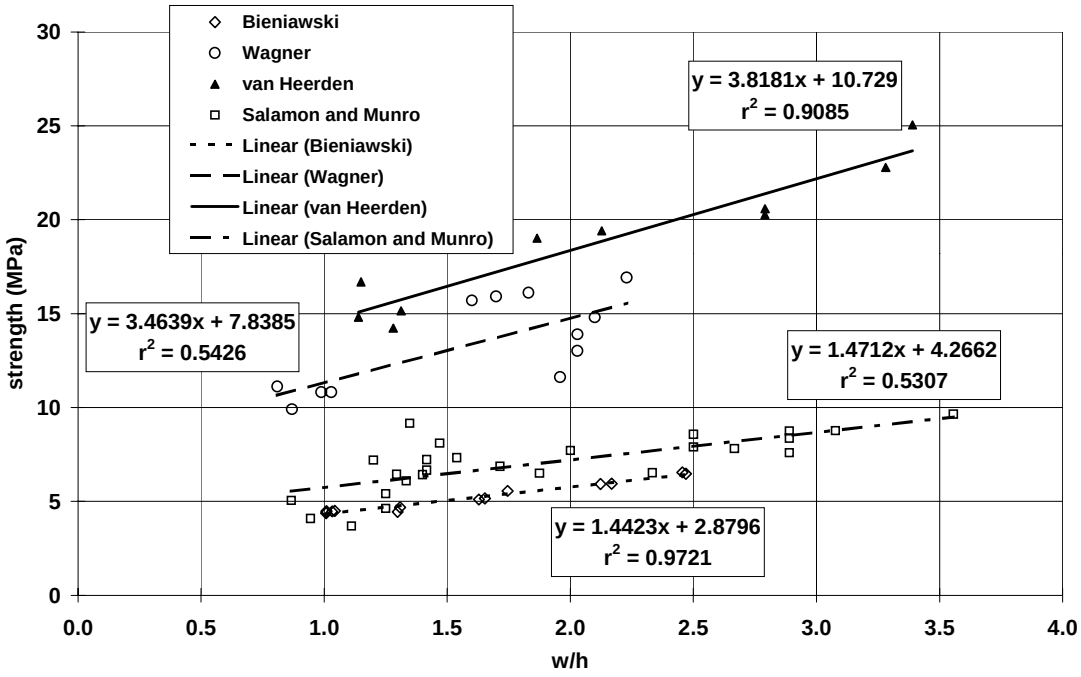

Figure 6-10 Results of South African* in situ *compressive strength tests on coal.

Bieniawski's, van Heerden's and Wagner's strength values are site specific. Salamon and Munro's data was from most of the coal fields in South Africa. Their results can be considered representative of most South African coals.

The methods of loading of the *in situ* tests reviewed are illustrated in Figure 6-11. It will be argued that these test methods (Bieniawski, Cook and van Heerden), the *in situ* loading conditions, and the laboratory loading conditions fall into three categories of loading conditions.

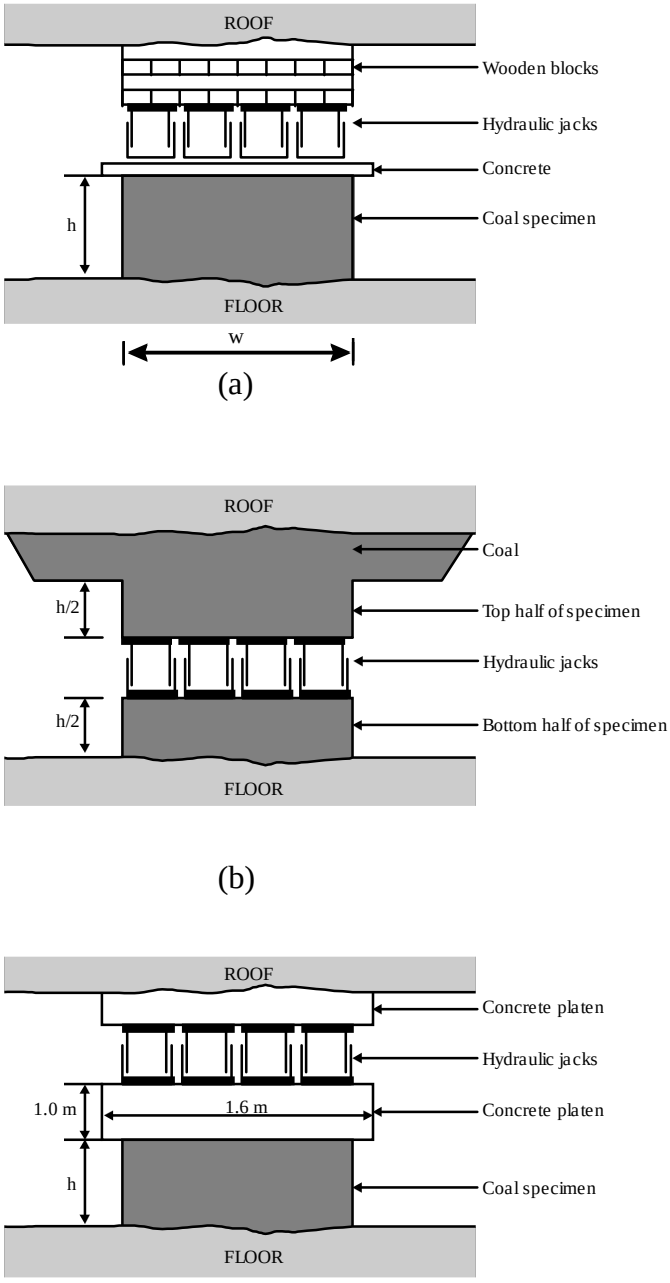

Figure 6-11 The different loading conditions as applied by (a) Bieniawski (1968(a)), (b) Cook* et al *(1970) and Wagner (1974) and (c) van Heerden (1974).

Salamon and Munro's *in situ* collapse cases represent the loading system that is closest to a stress load, in that the “loading platens” are the relatively low stiffness roof and floor. Also, the roof and floor are very “wide” platens which exacerbates the stress concentration (see Figure 6-3). The loading rate of true *in situ* pillars is much lower than any of the testing rates, which would lead to lower strengths due to creep, weathering, stress corrosion and other time effects.

Bieniawski transmitted a constant stress through a concrete cap at the top of the sample, but the bottom of the sample was maintained in the floor (Figure 6-11(a)). The concrete cap was approximately 7.5 cm thick, with an overhang of approximately 23 cm. Steel channels were used between the jacks and the concrete. Wooden blocks were used as spacers between the top of the jacks and the roof. This system therefore also tends towards a stress loading condition.

The loading arrangement as suggested by Cook (1970), shown in Figure 6-11(b), consisted of maintained contacts in the roof and floor, with a displacement controlled loading condition across the centre of the pillar pushing vertically towards the roof and floor. This loading system was suggested by Cook as a means of most accurately maintaining the actual *in situ* pillar loading condition when performing *in situ* tests. The displacement is applied along the pillar horizontal line of symmetry along which, theoretically, no vertical movement occurs in a real pillar (if there is no dip). There should also be no horizontal constraint across the mid-line. This system was implemented by Wagner (1974). However, only the bottom half consisted of coal (Salamon, 1997). The jacks were servo controlled to maintain constant displacement conditions at the loading surface. Although the jacks are free to move relative to each other, thereby maintaining the overall symmetry condition, friction is present between the jack contacts and the coal. Thus the requirement that there be no horizontal constraint along the line of symmetry is violated, and true symmetry may not be maintained. Unfortunately, both Wagner (1974) and Cook *et al* (1970) fail to comment in detail on the failure mechanisms produced in these tests.

Van Heerden (1974) applied a constant displacement to the sample through a 1.0 m thick concrete block (Figure 6-11(c)). In addition, a concrete block was cast above the jacks in contact with the roof. The thickness of the block in contact with the sample probably ensured uniform displacement at the boundary. It can be accepted that this system imparted a fairly rigid boundary to the top of the specimen (i.e. tending towards a displacement boundary).

In the following paragraphs, a comparative assessment of the loading conditions is made. The true collapse cases (Salamon and Munro's collapse cases) were founded in the natural roof and floor end conditions. This implies a “loading platen”, and a significant draping effect. The modelling (Figure 6-4) has shown that this can lead to significant stress concentrations at the edges of the sample. This explains why the *in situ* data set results in a comparatively low cube strength (see Figure 6-10).

In the *in situ* tests (Bieniawski, van Heerden, Wagner), one side of the specimen was founded in the natural end conditions. Bieniawski's tests were stress controlled. Van Heerden (1974) stated that tilting of the loaded surface was difficult to control. Although the uniform stress was not applied through the concrete overhang, the slight rotations that may have occurred, together with the thinness of the concrete platen, leads to the conclusion that undue stress concentrations may have

been present in the series of tests performed by Bieniawski. This may explain why Bieniawski's results were the lowest. These high stress concentrations may be the link between Bieniawski's tests and the *in situ* collapse cases. Bieniawski's results and the *in situ* collapse cases are thus possibly paired, according to the loading system.

Van Heerden, similarly to Bieniawski, replaced the natural top contact by an artificial loading mechanism. In contrast to Bieniawski, van Heerden applied a rigid (displacement controlled) boundary condition. This explains the difference between the two sets of results.

If one ignores possible minor imperfections discussed above, the method of Cook should most accurately replicate the real end conditions of *in situ* pillars. The method also correctly accounts for the boundary conditions in the middle of the pillar. Accordingly, this method should also be very close to the *in situ* collapse cases. The large difference could be ascribed to geology, as Wagner's results are site specific. Loading rate could also be a factor which increased the strength of Wagner's samples. The rate of pillar loading in tests is significantly higher than the rate resulting from mining.

Laboratory specimens of model pillars are tested under conditions that tend to a displacement controlled loading condition on both sides of the specimen to a greater degree than any of the *in situ* test methods mentioned. On the basis of this boundary condition alone, laboratory tests can be expected to result in higher strengths than *in situ* tests. In addition, the loading rate of the laboratory tests was much higher, and the samples were probably drier than the *in situ* tests and collapse cases. These are both factors that tend to increase measured strength.

Taking all the above arguments into account, the different test methods and boundary conditions can be divided into three overall categories:

- a stress boundary ("soft") loading system: Bieniawski, *in situ* collapse cases and Cook's method
- a displacement boundary ("stiff") platen at one end: van Heerden
- "stiff" platens at both ends: laboratory.

The *in situ* test conditions that are closest to the laboratory conditions are those of van Heerden.

6.6 Some considerations regarding the linear and power pillar design formulae

6.6.1 Introduction

The linear function has been compared to the power formula, with respect to performance and other rock mechanics considerations. The scale effect and w/h effect are examined, followed by a discussion of the implications of the findings.

6.6.2 Laboratory data

An analysis was performed on the extensive database of laboratory tests established in SIMRAC project COL021. Eleven large blocks of material were obtained from ten collieries in South Africa. Weathering was minimised for all but two of the 13 blocks used, by painting the approximately 1.5 m cube coal samples with bituminous paint and then encasing each block in a plastic bag. Each block was painted the same day that the block was bought to surface. In addition, new blocks were not obtained before the current block had been sampled. This minimised the time between the removal of any particular block from underground and the testing of material from that block.

The number of tests was 924, with nominal diameters 25, 50, 100, 200 and 300 mm. The w/h ranged from 1 to 6 for all diameters, while the first three sizes were also tested at w/h=0.5. The 50 and 100 mm sizes were also tested up to w/h=8. The estimates of k, α and β were obtained by non-linear regression analysis performed on the full set of COL021 laboratory data. A new linear function was fitted for each diameter, while the power formula parameters were derived from a statistical analysis on the whole data set (all diameters). The comparative results are shown in Table 6-4.

The last column in Table 6-4 shows the ratio between the smallest and largest volume for each diameter. The volume ratio between the smallest and largest volume is over 10 000. The r^2 of the power formula fit is similar to the average r^2 of the linear fits. This demonstrates the ability of the power formula to handle volume. The average of the linear function r^2 values is almost the same as the overall r^2 value for the power fit. The linear function is as effective (using r^2 as the measure) as the power formula if the volume ratio is comparatively small – in this case 31.

Table 6-4 A comparison between the performance of the power formula and the linear function.

Diameter (mm)	No. of samples	power formula r^2	linear function r^2	Volume ratio
250-298	91	0.86	0.84	7
180-193	75	0.78	0.82	8
90-101	242	0.61	0.59	25
50-62	290	0.62	0.63	31
24-26	226	0.63	0.63	16
Overall r^2 – power		0.71		
Average r^2 – linear			0.70	

6.6.3 Scale effect and w/h effect

An alternative form of the linear function (Equation 6-3) may be written as:

$$S = \Theta[(1-a)(w/h) + a] \qquad \textit{Equation 6-7}$$

where S = the expected pillar strength

Θ = the strength at w/h=1

= m + d (from Equation 6-3)

$a = d / \Theta$, and

$$1-a = m / \Theta \qquad \textit{Equation 6-8}$$

In this form of the equation, the value of m in Equation 6-3 is normalised to Θ. The linear fits and normalisation to the cube strengths of the COL021 and South African *in situ* results are shown in Table 6-5.

The values of 1-a from Table 6-5 are shown in Figure 6-12. As can be seen, the values of 1-a are fairly constant for all the sizes and different loading conditions, as noted by Sorenson and Pariseau (1978) for their more limited database. The first five points in Figure 6-12 are from the same suite of laboratory testing (COL021). It can therefore be presumed that the loading conditions of these tests are more similar to each other than the other data points. Yet the variation in these points encompasses the whole variation in the value of 1-a. It is suggested that the small variation in the value of 1-a is a reflection of a small variation in interface friction angles of the different tests, including the *in situ* tests. The value of 1-a is taken as constant, equal to 0.28 (see Figure 6-12).

Table 6-5 Parameters of fits of linear functions to the COL021 and South African* in situ *results.

Source	Size (mm)	no. of samples	Fitted function		Normalised		r^2
			m	d	Θ	1-a	
Lab : COL021	25	226	12.95	37.86	50.81	0.25	0.63
Lab : COL021	50	290	8.64	37.96	46.59	0.19	0.63
Lab : COL021	100	242	7.51	26.71	34.22	0.22	0.59
Lab : COL021	200	75	7.56	21.04	28.60	0.26	0.82
Lab : COL021	300	91	8.02	12.82	20.84	0.38	0.84
Bieniawski 0.9 and 1.2 m	1050[1]	11	1.83	3.03	4.86	0.38	0.72
van Heerden	1400	10	3.82	10.73	14.55	0.26	0.91
Bieniawski 1.5 and 2.0 m	1500[2]	13	1.44	2.88	4.32	0.33	0.97
Wagner	1800	12	3.46	7.84	11.30	0.31	0.54
Salamon and Munro	7128[1]	26	1.47	4.27	5.74	0.26	0.53

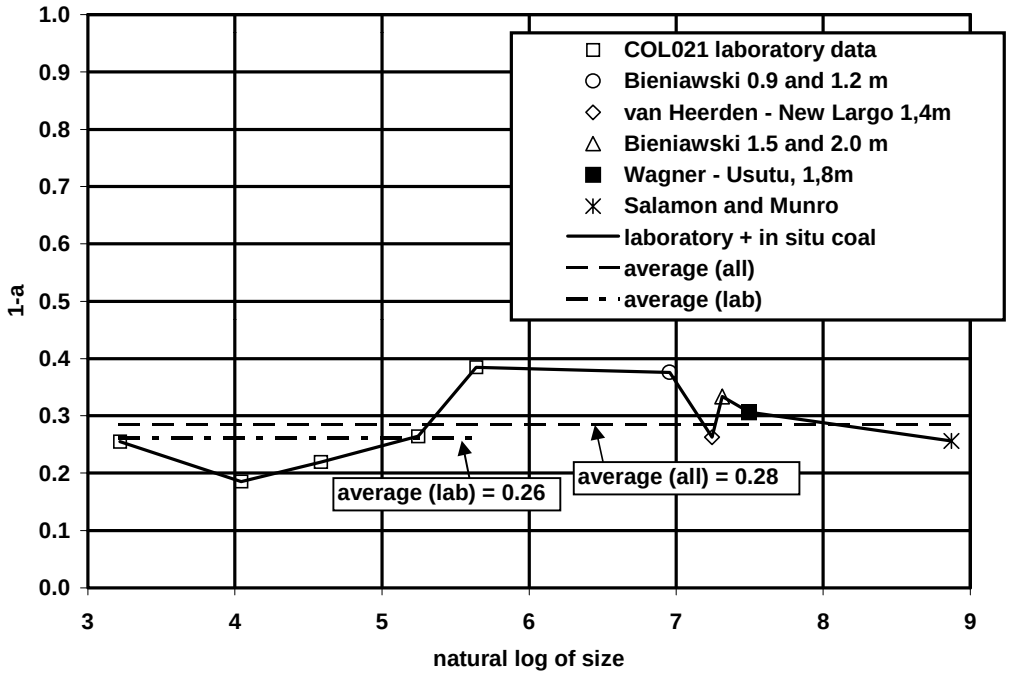

Figure 6-12 The w/h effect normalised to the cube strength for the COL021 laboratory tests and various* in situ *results.

[1] Average size in data set.
[2] Bieniawski's critical size is defined as 1500 mm.

The values of Θ for the data in Table 6-5 are shown as a function of size in Figure 6-13. The grey dashed trend line was drawn by hand. However, the trend of strength – size is strikingly similar to the strength – size relation found by Bieniawski (1968a) shown in Figure 6-1, in terms of the size at which the curve shows signs of flattening. Therefore, the value of Θ can be regarded as a function of size for the series of linear fits to w/h tests on coal of various sizes. The parameter Θ appears to capture a scale effect.

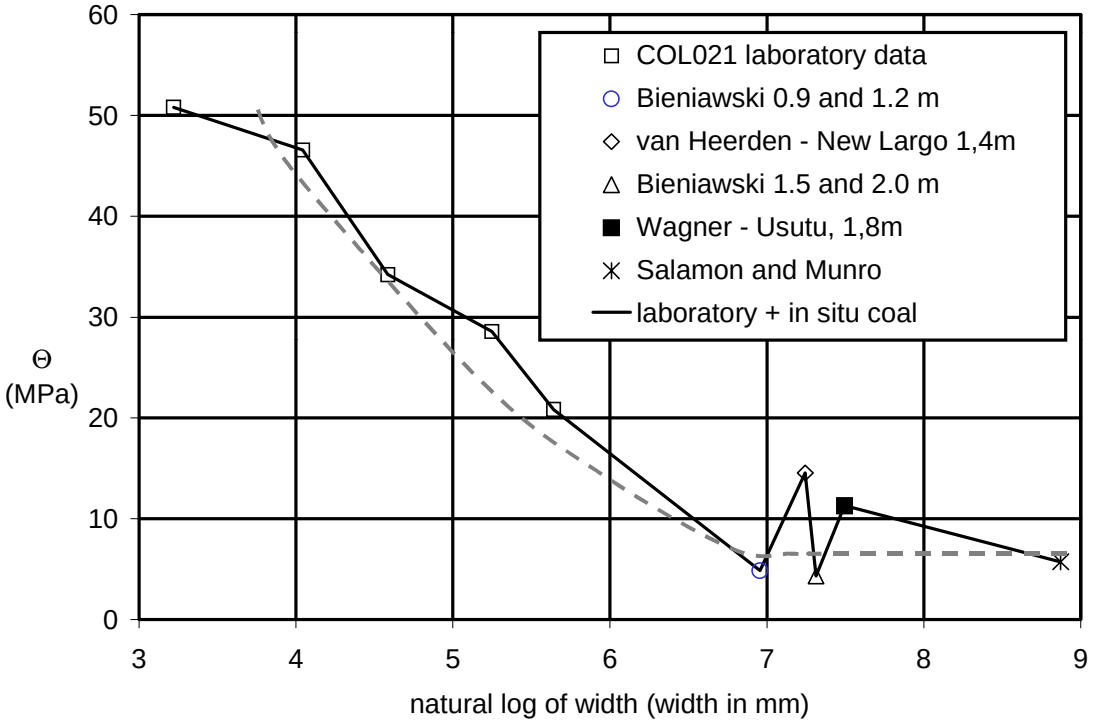

Figure 6-13 The cube strengths plotted as a function of the natural logarithm of size, for the COL021 laboratory tests and various* in situ *results.

In any one test series (corresponding to any one data point in Figure 6-13), a cube strength may be considered to be a function of:

1) the cohesion (c)
2) the angle of internal friction (ϕ)
3) the contact friction angle, i.e. the friction angle between the pillar and the roof or platen (ϕ_c)
4) the ratio of yield stress to peak stress.

Regarding the last point, the yield stress is defined in Figure 6-14. The ratio of yield to peak stress is a convenient, but simplified, way to encapsulate the strain hardening behaviour of the material, in the context of a cube being crushed.

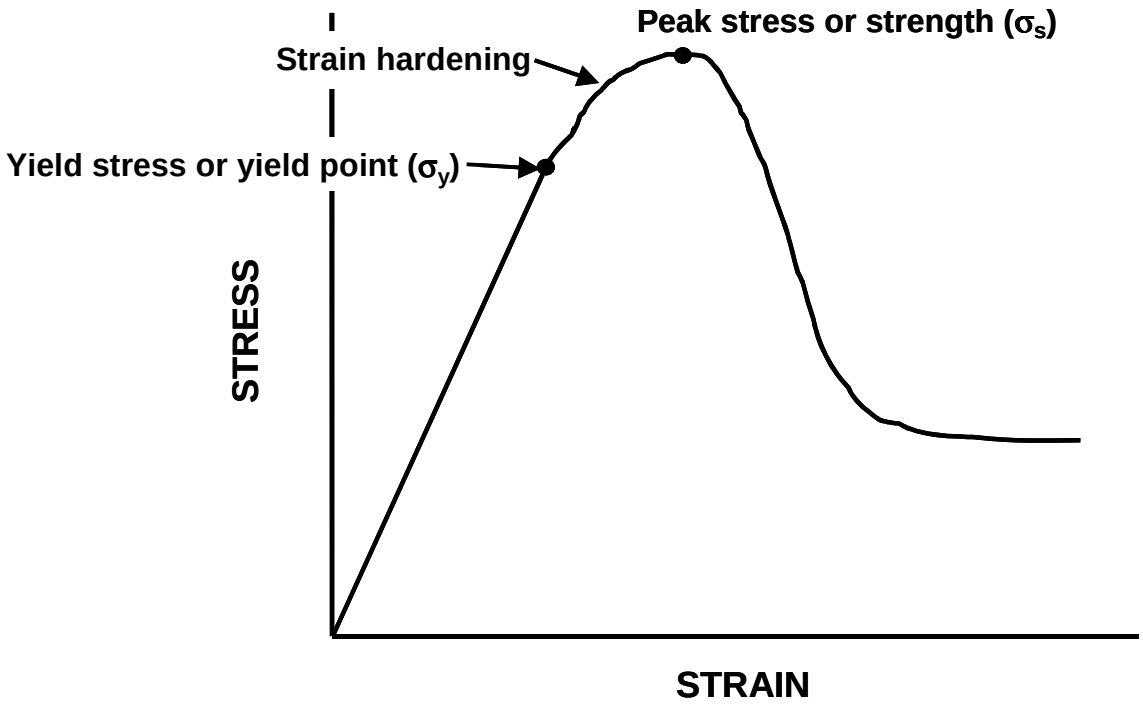

Figure 6-14 Definition of yield stress and peak stress.

In the laboratory test series especially, other factors such as loading rate and loading conditions may be considered to be identical for the different test series. In addition, when comparing different test series in the following discussion, the following assumptions are made:

1) a change in size does not of itself lead to a change in loading conditions

2) the ratio of yield stress to peak stress is constant with size

3) a change in size does not of itself lead to a change in the frictional end restraint condition due to geometry (including the effect of the relative Poisson's ratio).

In Equation 6-7, the parameter "1-a" can be interpreted as a reflection of the confining effect due to the w/h ratio, normalised to the cube strength. This confining effect is due to the friction between the sample and the platen (see Figure 6-15).

For a series of w/h tests of a given size (width or diameter), the cohesion and friction angles can be taken as constant. The increase in strength as the w/h increases is due to the change in the induced stress field as samples are loaded. More specifically, as the w/h increases, the lobes of confined material get closer and eventually overlap (see Figure 6-15). An increase in confining pressure increases the strength. The magnitude of confining pressure in the sample is a function of the contact friction angle (ϕ_c). The Mohr-Coulomb parameter that accounts for and controls the degree of strength increase for a given increase in confining pressure is the angle of internal

friction (ϕ). There are probably other effects, such as the relative Poisson's ratio between the platen and the sample, or roof and pillar. However, because these are assumed to be scale independent (as stated above), they can be neglected for this discussion.

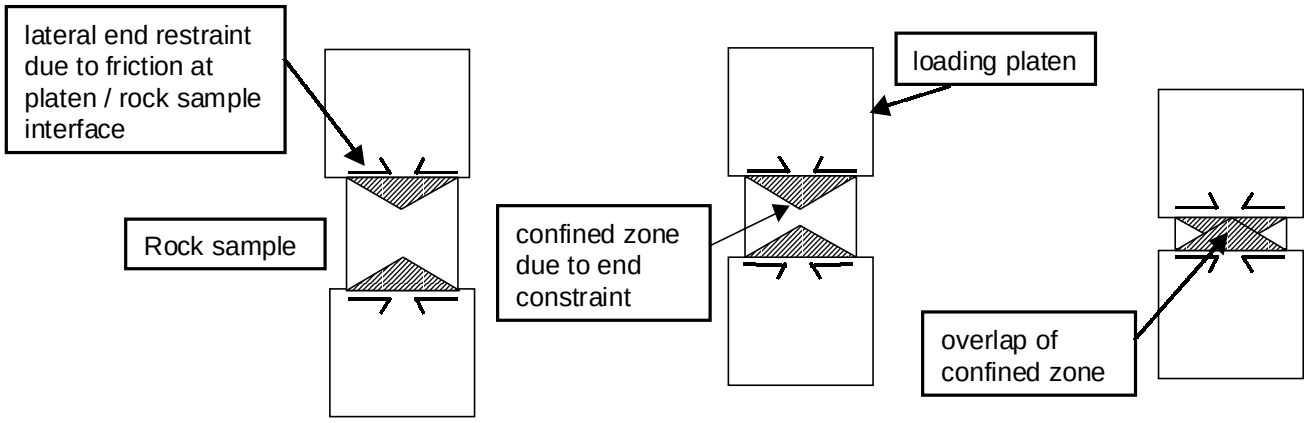

Figure 6-15 A conceptual diagram of the effect of frictional end restraint on the confinement of a sample, depending on its w/h.

The strength of a standard uniaxial strength sample (i.e. w/h ≈ 0.4) is related to cohesion and the friction angle by the following relationship:

$$UCS = 2cN_{\phi} \qquad \textit{Equation 6-9}$$

where UCS = uniaxial compressive strength

c = cohesion

$$N_{\phi} = \sqrt{\frac{1+\sin\phi}{1-\sin\phi}} \qquad \textit{Equation 6-10}$$

ϕ = angle of internal friction

In terms of Mohr Coulomb parameters, cohesion (c) can be defined as the intrinsic shear strength of a material. The angle of internal friction (ϕ) can be described as the parameter that accounts for the increase in strength as a result of confining stress.

A sample of w/h = 1 is stronger than a UCS sample because of the mechanism illustrated in Figure 6-15. By substituting S = UCS and w/h = 0.4 into Equation 6-7 and rearranging, Θ may be expressed as:

$$\Theta_x = \frac{UCS_x}{0.4 + 0.6a} \qquad \textit{Equation 6-11}$$

where the subscript x denotes that the value may vary with size. Although UCS is usually taken to mean a test on a rock sample of 50 mm diameter and height approximately 125 mm, in principle, a

test of the same w/h can be performed for different diameters. As seen in Figure 6-12, the value of a is constant with size. Therefore, the denominator in Equation 6-11 is constant. If we let

$$D = \frac{1}{0.2 + 0.3a} \qquad \textit{Equation 6-12},$$

then by combining Equation 6-9 and Equation 6-11, Θ_x is seen to depend on cohesion and friction angle only:

$$\Theta_x = D c_x N_\phi \qquad \textit{Equation 6-13}$$

Thus, the cube strength with size is linearly related to cohesion and N_ϕ. Therefore, the parameter 1-a (see Equation 6-7) is a normalisation of the parameter m (Equation 6-3) to cohesion and N_ϕ.

The slope of each series is plotted as a function of Θ in Figure 6-16. The data point markings are the same as in Figure 6-13. If m_x/Θ_x = 1-a is truly constant, then a best fit straight line should go through the origin, with a slope equal to the average 1-a shown in Figure 6-12.

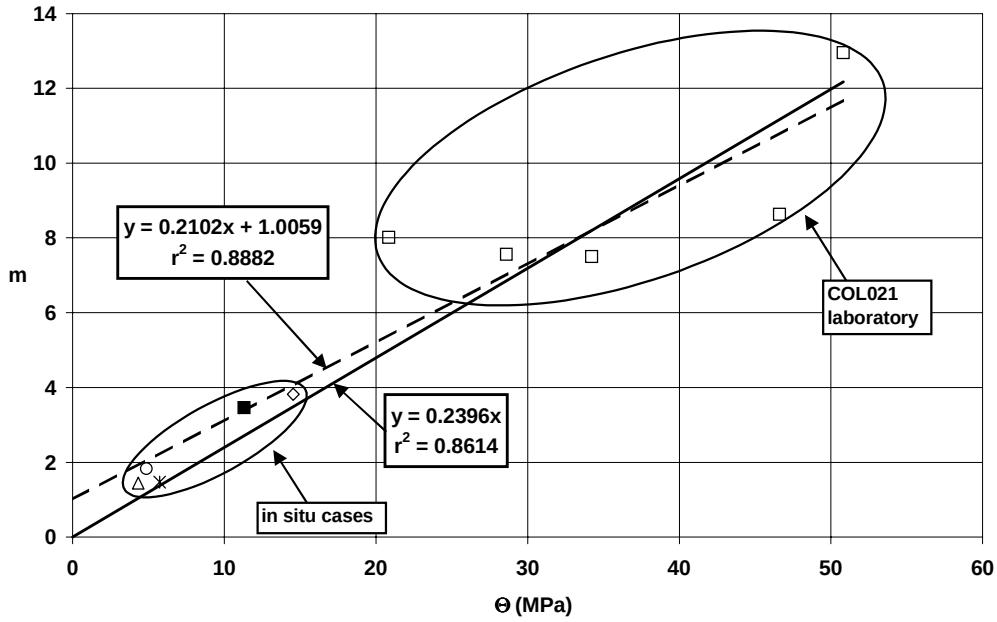

Figure 6-16 The relation between the slopes of the straight lines and the cube strengths for each data series.

Two straight lines have been fitted to the data plotted in Figure 6-16: one in which the y-intercept was set to zero, and the other in which the slope and y-intercept were both determined by linear regression. As can be seen, the difference between the two fits is small, with a similarly high r^2 value for both fits. The high r^2 value confirms that the ratio m_x/Θ_x is constant. The slope of the line

going through the origin = 0.24, which is fairly close to the average value of 0.28 (see Figure 6-12). The values of m and Θ also have an experimental error associated with them.

It is remarkable that such a consistent relation can be drawn for such a wide scale range. Separate fits are shown for the laboratory and *in situ* data in Figure 6-17. While the fit is poor for the laboratory data, the trend is similar to the other trends.

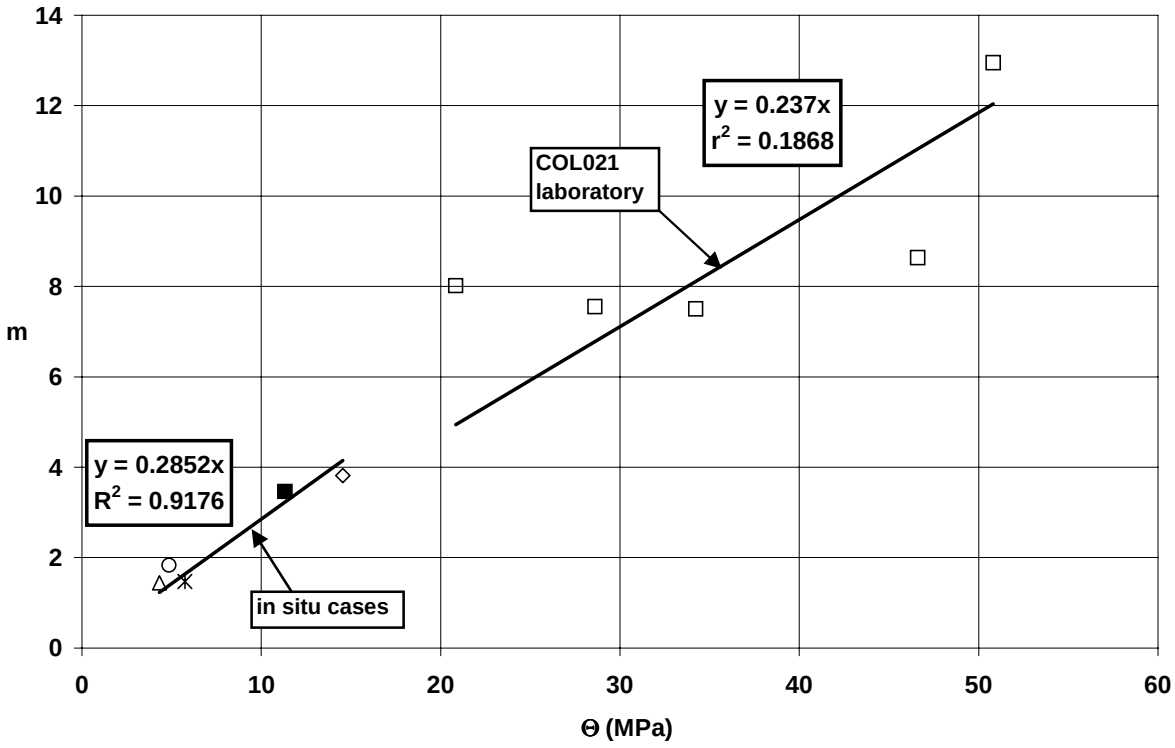

Figure 6-17 The relations between the slopes of the straight lines and the cube strengths for the* in situ *and laboratory data separately.

If 1-a is constant, and Θ_x relates linearly to c_x and N_ϕ, then the slope of a given test series (m_x) must also be linearly related to c_x and N_ϕ. By substituting Equation 6-8 and Equation 6-12 into Equation 6-13, the following relation is found:

$$m_x = \frac{1-a}{0.2+0.3a} c_x N_{\phi x} \qquad \textit{Equation 6-14}$$

The relation between ϕ and N_ϕ (Equation 6-10) is shown graphically in Figure 6-18. From the literature, it appears that a reasonable range for ϕ for coal for all scales is probably in the range 30° to 45°. The corresponding values of N_ϕ are 1.73 and 2.41 (Equation 6-10). The reduction in N_ϕ in the range from 45° to 30° is a factor of 0.72. This is probably the maximum reduction in N_ϕ. Referring to Table 6-5, the strength of the 25 mm samples of w/h = 1, is Θ_{25} = 50 MPa. This value

is based on samples from 10 collieries in South Africa, and can be considered fairly representative of South African coal, with a few exceptions. The Θ for the most representative of the *in situ* data bases (that of Salamon and Munro) is 5.74 MPa. The reduction factor is 0.11 (from 25 mm to *in situ*). Therefore the minimum reduction factor for cohesion is 0.15, that is, a minimum six-fold reduction. Thus the scale effect is mostly explained by a change in cohesion. If, as is likely, variations in ϕ are not a function of scale, but rather due to natural variability, then the scale effect would be only explained by the change in c.

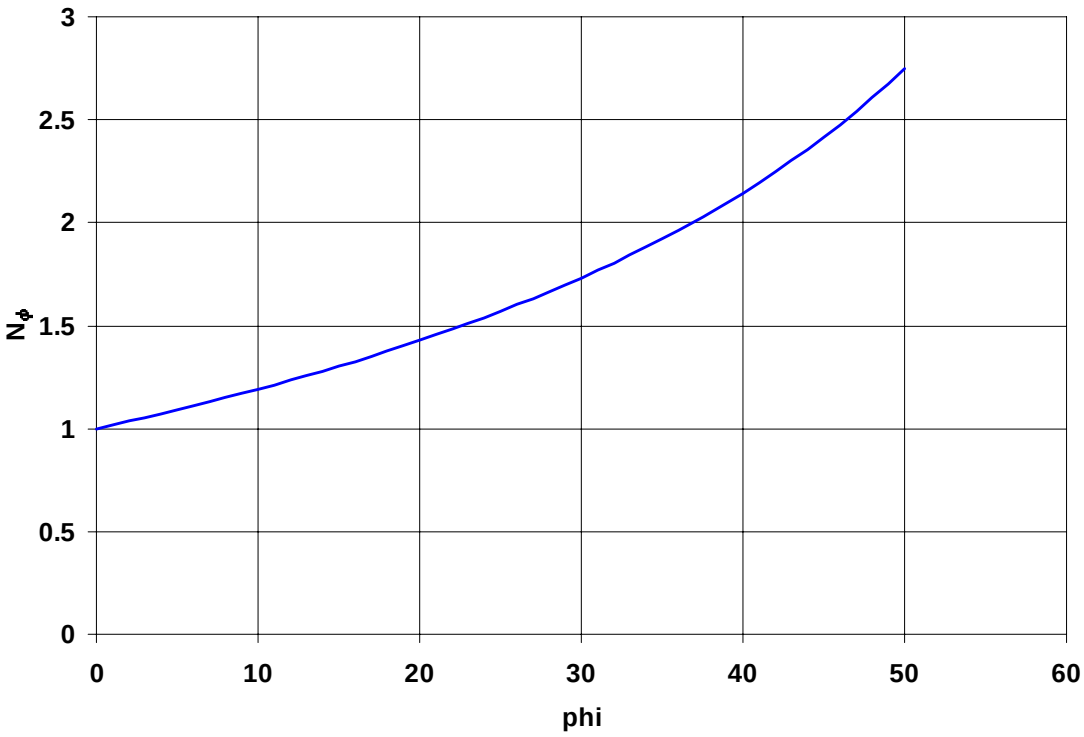

Figure 6-18 The relation between phi (ϕ) and N_ϕ.

The scale effect is a complex phenomenon, and not well understood. In the context of this report, the Mohr Coulomb parameter cohesion implicitly encapsulates the complexities of the scale effect in one parameter.

The value of Θ implicitly captures the effects of the loading condition, stress or displacement (see Figure 6-4). Included in this would be the effects of loading rate, temperature, etc. However, it is surmised that the loading condition is the primary influence. Hence, the measured strength is also influenced by the particular pillar system factors present in each data set, as well as scale. This explains the different cube strengths measured in the *in situ* tests discussed.

6.6.4 Discussion

In the rather extensive data reviewed, it was found that the linear formula performs as well as the power formula. The data sources and the respective r^2 values are summarised in Table 6-6. For the laboratory data the volume ratio for the different sets of data has a maximum of 31. In these cases the performance of the linear function is as good as the power formula (with the understanding that a separate linear function was fitted to each laboratory data set, while one set of power formula parameters was determined for all five sets of laboratory data). When the smallest volume is removed from Salamon and Munro's *in situ* collapsed pillars data set, the linear function performs reasonably well compared to the power formula. The volume ratio is reduced from 80 to 48. Galvin *et al* (1996), in a statistical comparison between the power formula and the linear function on a set of Australian coal pillar collapse cases, state that the difference between the two formulae is not statistically significant. It is suggested that this is precisely because the *in situ* volume range is small.

From this table, it can be seen that if the volume ratio is kept reasonably small, then the linear function performs reasonably well compared to the power formula. A suggested upper range for the volume ratio may be between 50 and 60.

Table 6-6 A summary of the comparative assessments of the performance of the linear formula compared to the power formula.

Source	Average width (mm)	Volume ratio	power formula r^2		linear function r^2
laboratory : COL021	250-298	7	0.86	OVERALL of POWER FIT to COL021: • $r^2 = 0.71$ • volume ratio > 10 000	0.84
laboratory : COL021	180-193	8	0.78		0.82
laboratory : COL021	90-101	25	0.61		0.59
laboratory : COL021	50-62	31	0.62		0.63
laboratory : COL021	24-26	16	0.63		0.63
Salamon and Munro: include smallest volume	6988	80	0.59		0.40
Salamon and Munro: exclude smallest volume	7128	48	0.58		0.53
Greenwald *et al*	896	62	0.96		0.53

In the case of linear fits to small volume ranges, the linear formula provides a good fit to strength-w/h relations, as shown in Table 6-7. The r^2 values reported in Table 6-6 and Table 6-7 are plotted as a function of the volume ratio in Figure 6-19. As seen, a trend is established.

Table 6-7 A summary of the performance of linear fits to other data.

Source	Volume ratio	linear function r^2
Greenwald: full height	4.1	1.00
Greenwald: ½ height	2.5	0.99
Greenwald: full ht and ½ ht	8.2	0.92
Bieniawski 0.9 and 1.2 m	4.3	0.72
van Heerden	3.1	0.91
Bieniawski 1.5 and 2.0 m	5.5	0.97
Wagner	2.8	0.54

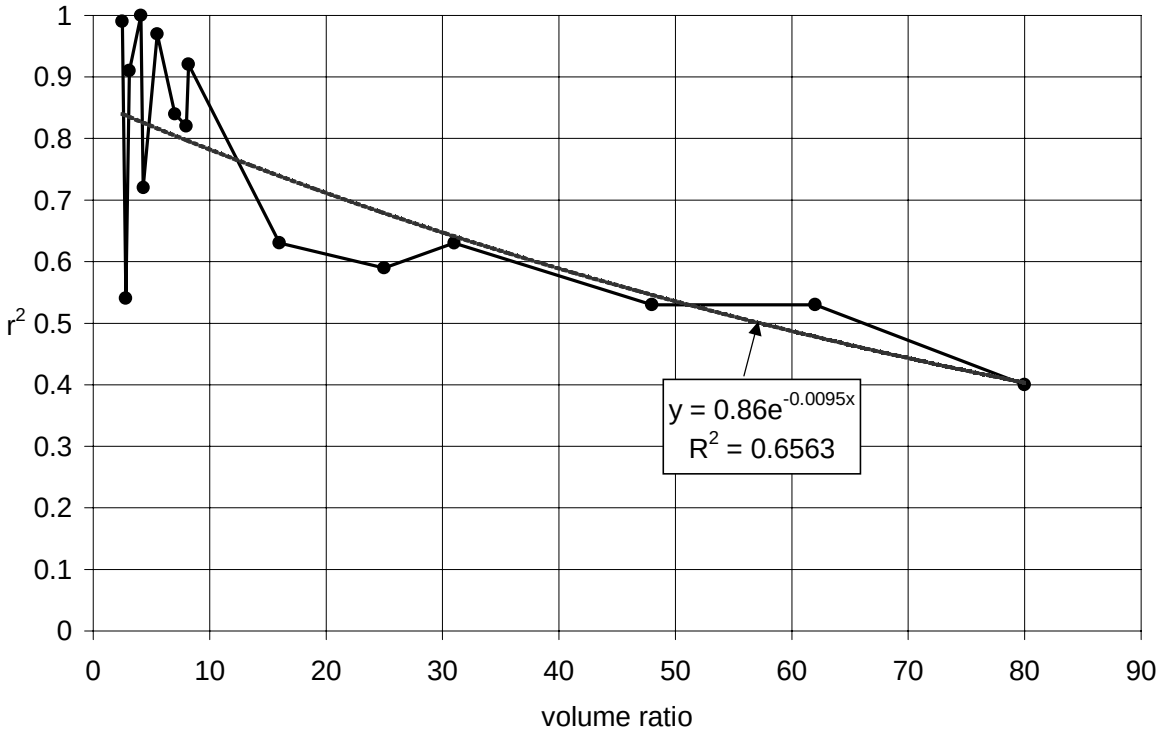

Figure 6-19 The performance of linear fits to the data reported in Table 6-6 and Table 6-7, as a function of the volume ratio.

The acceptance of the notion of a critical size and an associated critical rock mass strength implies that no additional volume effect is expected above a certain volume. The lack of a volume effect in Salamon and Munro's *in situ* collapsed cases data has been demonstrated. Strength (in terms of a design formula for pillars square in plan) can then only be a function of some base strength value and the confining effect due to changes in the shape of the pillar. The logically consistent form

(excluding the “squat pillar” effect) for an *in situ* pillar design formula is therefore the linear function, in the form in Equation 6-5, repeated here for convenience:

$$S = \Theta[(1-a)(w/h) + a] \qquad \textbf{\textit{Equation 6-7}}$$

In this form, Θ expresses the strength component, which is a material property. This is the critical rock mass strength (see Section 6.2). The strength of the pillar increases as the w/h increases, i.e. as the shape changes: and is controlled by the dimensionless parameter 1-a. This equation is dimensionally correct.

Equation 6-7 does not explicitly account for many of the pillar system factors mentioned in Section 6.3. In the case of the *in situ* and laboratory tests reviewed, jointing was absent, while the loading system characteristics have been implicitly captured in the values of Θ and 1-a. In the case of the *in situ* collapse data, the pillar system factors discussed in Section 6.3 are implicitly lumped in the parameters Θ and 1-a. A methodology to cater explicitly for some of the pillar system characteristics is addressed in Section 6.10.

6.7 Friction angle tests on *in situ* roof / pillar contacts

A number of borehole samples were obtained with the purpose of testing the contact friction angle between the various types of roof and coal using shear box tests. As shown in Table 6-8, the contact types varied quite widely.

Despite the variation in contact types, the standard deviation of the peak friction angle is relatively low: 15 % of the average. The 99 per cent confidence interval for the peak ϕ_c is 21.7° to 26.5° (see Appendix E for the calculation method). The residual friction angle is, on average, 90 per cent of the peak friction angle, again with a low standard deviation. The 99 per cent confidence interval for the residual ϕ_c is 21.0° to 24.8° (again, refer to Appendix E for the calculation method).

It is suggested that the residual friction angle be used in pillar design. In this case, in the absence of a methodology to accommodate the variability of the input parameters, the lower 99 per cent level is used on the residual friction angle. This is 21°.

The samples as tested may have been influenced by the drilling process. The influence of this has not been determined.

Table 6-8 Results of shear box tests on various contacts typically found in coal mines.

Number	Contact details	Contact condition	Peak ϕ_c	Residual ϕ_c	Residual ϕ_c / peak ϕ_c (%)
1	coal/sandstone	open	23.6	20.1	85
2	shale/sandstone	Intact	24.3	20.5	84
3	coal/shale	intact	24.8	24.4	98
4	shale/sandstone	open	21.7	21.9	101
5	shale/sandstone	intact	24.7	22.6	91
6	shale/sandstone	intact	29.8	25	84
7	coal/shale	intact		17.9	
8	coal/sandstone	open	25.8	23.5	91
9	coal/sandstone	open	25.8	23.5	91
10	sandstone/carbonaceous sandstone	intact	24.3	21.8	90
11	coal/shale	intact	22.9	19.9	87
12	sandstone/granite	intact		34.2	
13	sandstone/carbonaceous shale	intact	25.1	23.2	92
14	mudstone/carbonaceous shale	open		27.7	
15	coal/carbonaceous shale	intact	23	20.7	90
16	sandstone/carbonaceous shale	intact	20.2	19	94
17	coal/coal	open	27.8	24.3	87
18	coal/calcite	open	26.8	19.9	74
19	mudstone/carbonaceous shale	open	11.4		
20	sandstone/carbonaceous shale	intact	22.7	22.1	97
21	coal/sandstone	intact	27.7	25.6	92
22	coal/carbonaceous shale	intact		22.1	
23	coal/sandstone	intact	25.1	24.5	98
24	coal/laminated sandstone	intact	25.2	21.9	87
25	coal/laminated sandstone	intact		23.4	
Average			**24.1**	**22.9**	**90**
Standard deviation			**3.7**	**3.3**	**6**
Standard deviation as a percentage of average			**15.4**	**14.4**	**7**

6.8 Numerical modelling

6.8.1 Introduction

The purpose of the numerical modelling was to determine the w/h effect as a function of the contact friction angle between the sample pillar and the platens in the laboratory, with all other factors remaining constant. This is used as a building block in the formulation of a new pillar design methodology.

The laboratory results referred to in Section 6.6 form a substantial database, which provides excellent information for numerical back analysis. This was done to ensure that the numerical model was based on reality. The laboratory tests represent the w/h effect at a particular contact friction angle. Once the w/h effect in the laboratory had been back analysed, the effect of different contact friction angles was investigated. The aim of this was to produce a design chart relating the w/h effect to the contact friction angle. The effect of scale and jointing on *in situ* pillar strengths are catered for in Section 6.10, in which the new pillar design methodology is described.

In the numerical modelling of laboratory model pillar simulations, the parameters that are considered relevant are the following:

1) cohesion

2) friction angle

3) contact friction angle between the steel platen and the coal sample

4) rate of cohesion loss of the coal (as a function of plastic strain).

The effect of the latter parameter on the macro load-deformation behaviour of the modelled specimen is mesh dependent. The effect of the same modelling parameters can result in different behaviours simply by changing the mesh. Therefore, the approach used was to regard this parameter as empirical.

The scale effect on intact samples, as shown in Figure 6-1, cannot be directly addressed with current numerical modelling technology. As was discussed in Section 6.6.3, the scale effect may be catered for by varying the cohesion.

6.8.2 Geometry of the FLAC model

The geometry of the FLAC model is shown in Figure 6-20. This geometry is very similar to the laboratory test geometry.

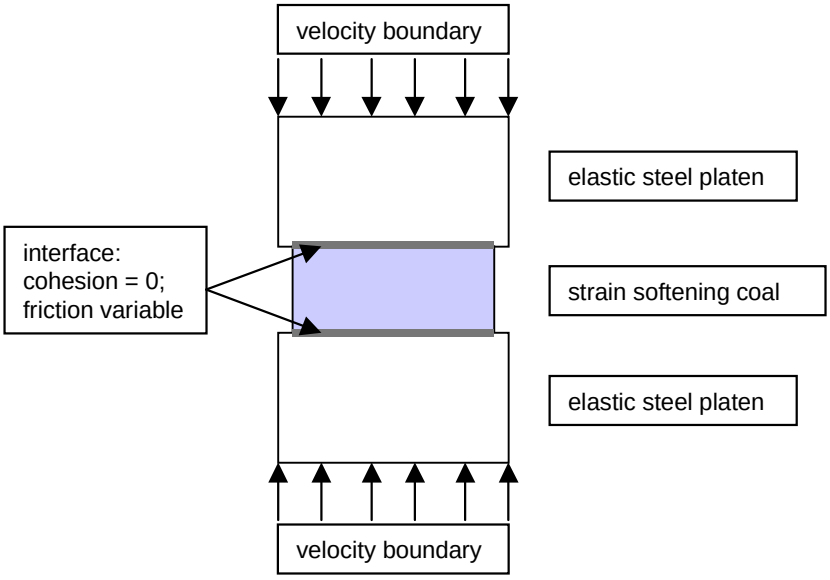

Figure 6-20 The geometry of the FLAC model.

Quarter symmetry was used. The top right quarter of the diagram in Figure 6-20 was modelled. The FLAC mesh for a sample of w/h = 1 is shown in Figure 6-21. The elements are square, thus avoiding inaccuracies due to changes in element size in different parts of the model. The vertical dimension of the steel platen is equal to the height of the sample. Samples of w/h greater than one were created by decreasing the number of elements in the vertical direction. Thus the quarter symmetry sample of w/h = 1 consisted of 72 elements in the lateral and vertical dimension, while a sample of w/h = 6 consisted of 72 elements in the lateral direction and 12 elements in the vertical dimension. Sample models were done with full symmetry for comparison, but very small differences were found.

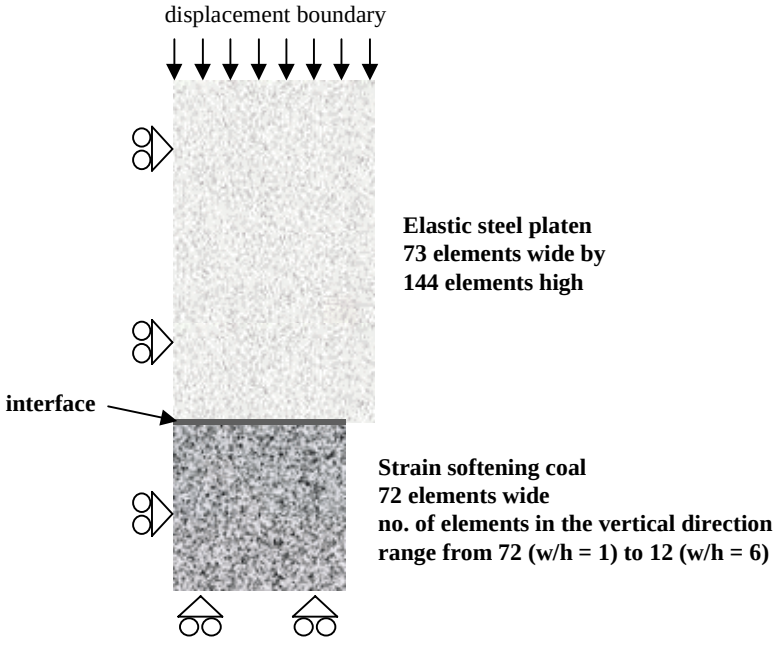

Figure 6-21 The FLAC mesh for a simulation of a laboratory test.

6.8.3 Material constitutive model and properties

The basis for soil mechanics and rock mechanics plasticity is provided by the equation suggested by Coulomb in 1773 (Chen, 1975):

$$\tau = c + \sigma \tan \phi \qquad \textit{Equation 6-15}$$

where: τ = maximum shear stress

c = cohesion

σ = normal stress

ϕ = angle of internal friction.

This can be re-written as the following linear function:

$$\sigma_1 = C_0 + m\sigma_3 \qquad \textit{Equation 6-16}$$

where: σ_1 = major principal stress

C_0 = y – intercept of the fitted linear function, which is equivalent to the UCS (not always the case if the data is not linear, or if there is a poor fit to the data)

σ_3 = normal stress

ϕ = angle of internal friction.

This is the Mohr Coulomb yield criterion, and is illustrated in Figure 6-22 with real data. Any (σ_1, σ_3) pair falling below the envelope is an allowable stress state. If the material is loaded such that the major principal stress equals the value provided in Equation 6-16, the material will undergo plastic deformation so as to maintain the value of the major principal stress inside the envelope. The Mohr-Coulomb yield criterion implies “perfect plasticity”, that is, continued plastic deformation at constant stress, as shown by the dashed line in Figure 6-23. This is an idealisation, and stress strain curves of real materials exhibit strain hardening prior to the peak load, and post peak strain softening (see Figure 6-23).

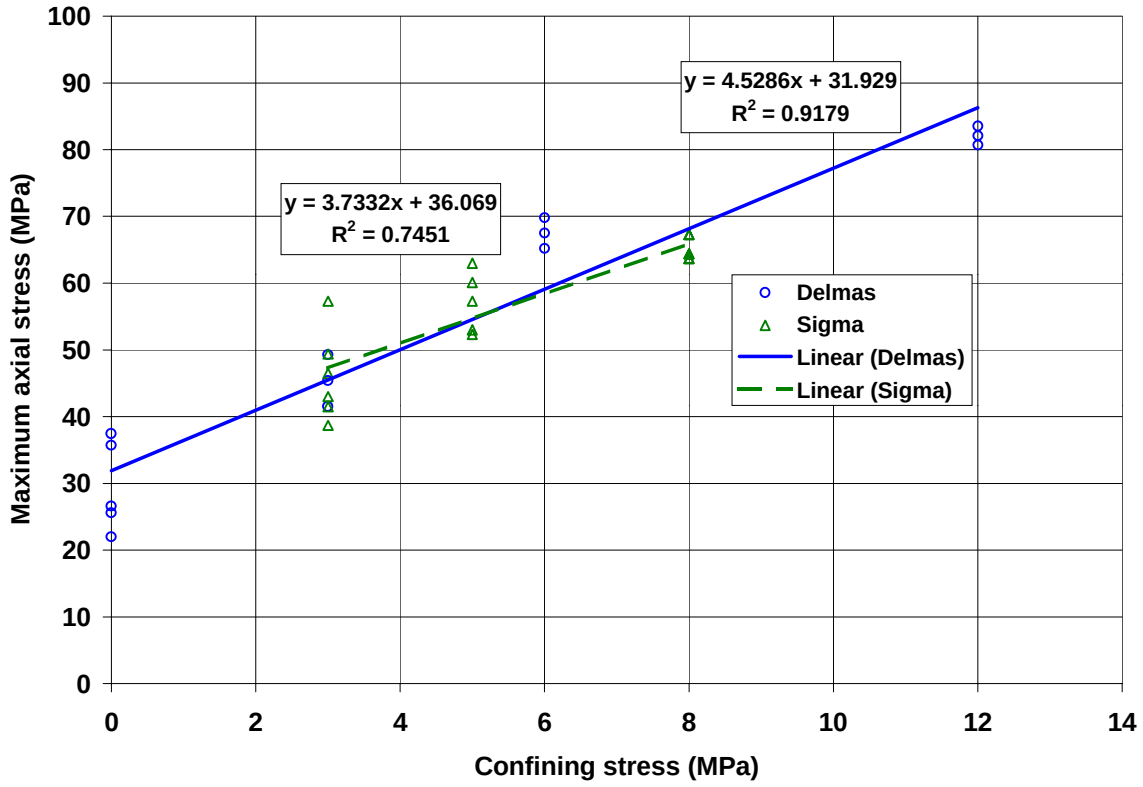

Figure 6-22 The peak strength of Delmas and Sigma coal as a function of confining stress.

The Mohr-Coulomb material properties used for the numerical modelling in this report were based on the series of triaxial cell tests performed on coal samples from Delmas mine, in the SIMCOL021 project (one of the 11 coal seams samples for the test data discussed in Section 6.6). The results are shown in Figure 6-22. Also shown is a best fit linear function, with slope m = 4.53 and y-intercept = 31.93. The y-intercept is equivalent to the average UCS of the samples (see Equation 6-16). There will be a slight error due to the imperfect linear fit to the data. The values of Mohr-Coulomb angle of internal friction (ϕ) and cohesion (c) are given by:

$$\phi = \sin^{-1}\left(\frac{m-1}{m+1}\right) \qquad \textit{Equation 6-17}$$

and

$$c = \frac{UCS}{2\sqrt{m}} \qquad \textit{Equation 6-18}$$

Substituting m = 4.53 and UCS = 31.93, the following values are obtained: ϕ = 40°, and c = 7.5 MPa. The analysis of seam specific strengths of the 11 coal seams that were tested in COL021 showed no statistical difference between the seams. Thus, the Mohr-Coulomb values

derived, although from one test suite of one of the 11 coal materials tested in COL021 (as discussed in Section 6.6), are deemed to be reasonably representative of the overall test series. The cohesion is 7.5 MPa, but this is only valid for a particular size. In this case, the diameter of the triaxial test samples was 53 mm. For a given friction angle, the strength can be adjusted by changing the value of cohesion.

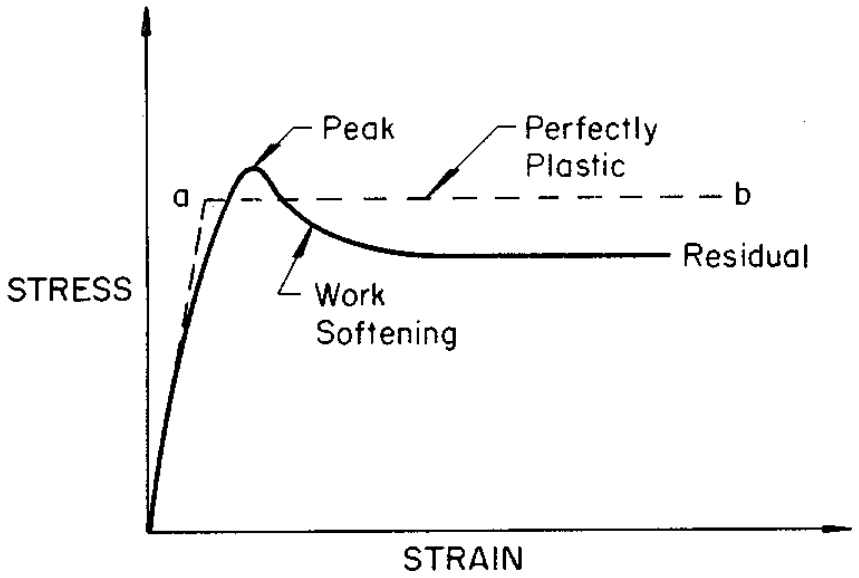

Figure 6-23 The perfectly plastic Mohr Coulomb idealisation (dashed line) compared to a more realistic test curve showing pre-peak strength work hardening, and post peak softening (after Chen, 1975).

It is well known that the edges of a pillar, or laboratory model pillar, fail prior to the attainment of peak strength, especially as the w/h increases. At large w/h ratios, the degree of failure prior to the attainment of peak strength may be great. This can be thought of conceptually as the edges of the pillar losing cohesion, even though the pillar is bearing increasing load. This implies that the interior of the pillar is able to accept more load, and is in fact doing so. This was excellently demonstrated by Wagner (1974) (see Figure 1-3).

In this case, the Mohr-Coulomb model is not adequate to model the failure of pillars. This is because the Mohr-Coulomb model assumes that there is no cohesion loss. Therefore Mohr-Coulomb models over-estimate the strength of pillars. The alternative model is a strain softening model. Such a model allows the value of any of the Mohr-Coulomb parameters to be specified as a function of plastic strain.

Cassie and Mills (1992) show a set of peak and residual strengths of a set of triaxial tests on coal (Figure 6-24). The dashed trend lines have been drawn by hand by the author of this report. The trend of the residual strength appears to cross the y-axis close to the origin (albeit an

extrapolation). This implies that the cohesion of the samples at the residual strength stage is zero or close to zero, as is intuitively obvious.

In addition, the trend lines are roughly parallel. Parallelism implies that the friction angle is the same for the samples at both the peak and residual stages (see Equation 6-17). This is a highly significant result. It therefore seems reasonable to assume that the friction angle is constant between the peak strength and the residual strength.

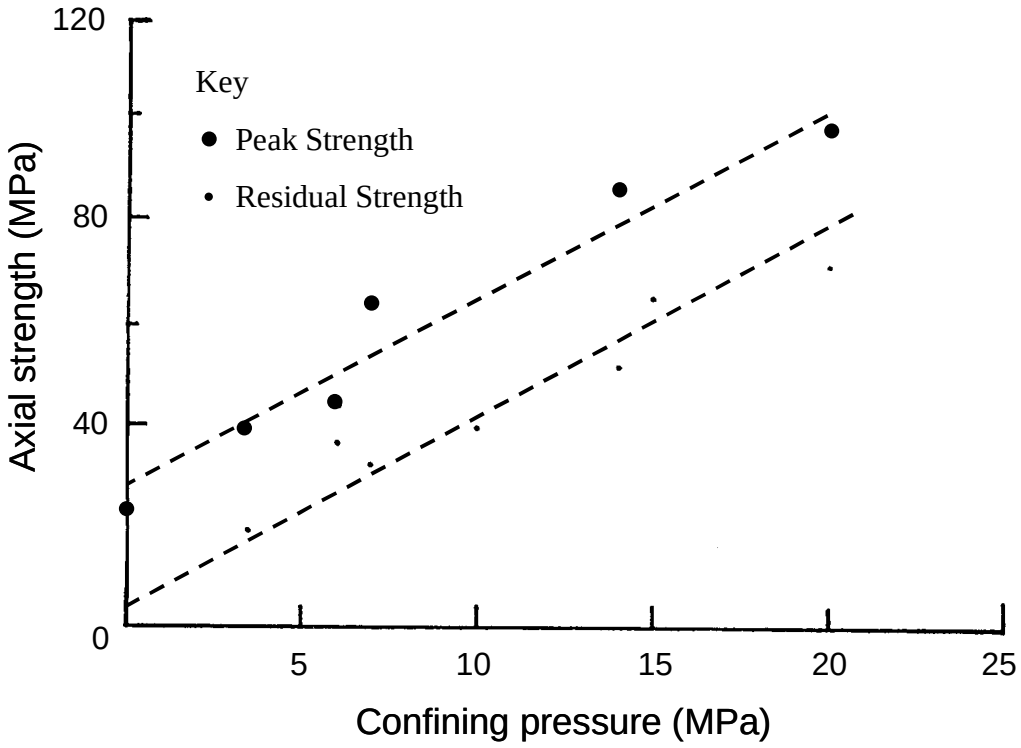

Figure 6-24 Triaxial tests for the Parkgate Seam, showing peak and residual strengths, after Cassie and Mills (1992). The dashed lines were added by the author of this report.

The assumption in the numerical modelling is that the cohesion loss is linearly proportional to the plastic strain, according to the schematic relation shown in Figure 6-25. Plastic strain is defined as (Vermeer and de Borst, 1984):

$$\varepsilon^p = \varepsilon_1^p - 2\varepsilon_2^p \qquad \textit{Equation 6-19}$$

where ε^p = plastic strain

ε_1^p = plastic strain in the major principal stress direction

ε_2^p = plastic strain in the minor principal stress direction.

This equation has been implemented in FLAC in the strain softening model. In Figure 6-25, the cohesion at zero plastic strain is the Mohr-Coulomb cohesion: 7.5 MPa. The value of the plastic strain at which the cohesion is set to zero, termed ε^{p}_{max}, was determined empirically by comparing the numerical modelling results to the laboratory data. In the two curves shown in Figure 6-25, ε^{p}_{max} is 0.2 and 0.4.

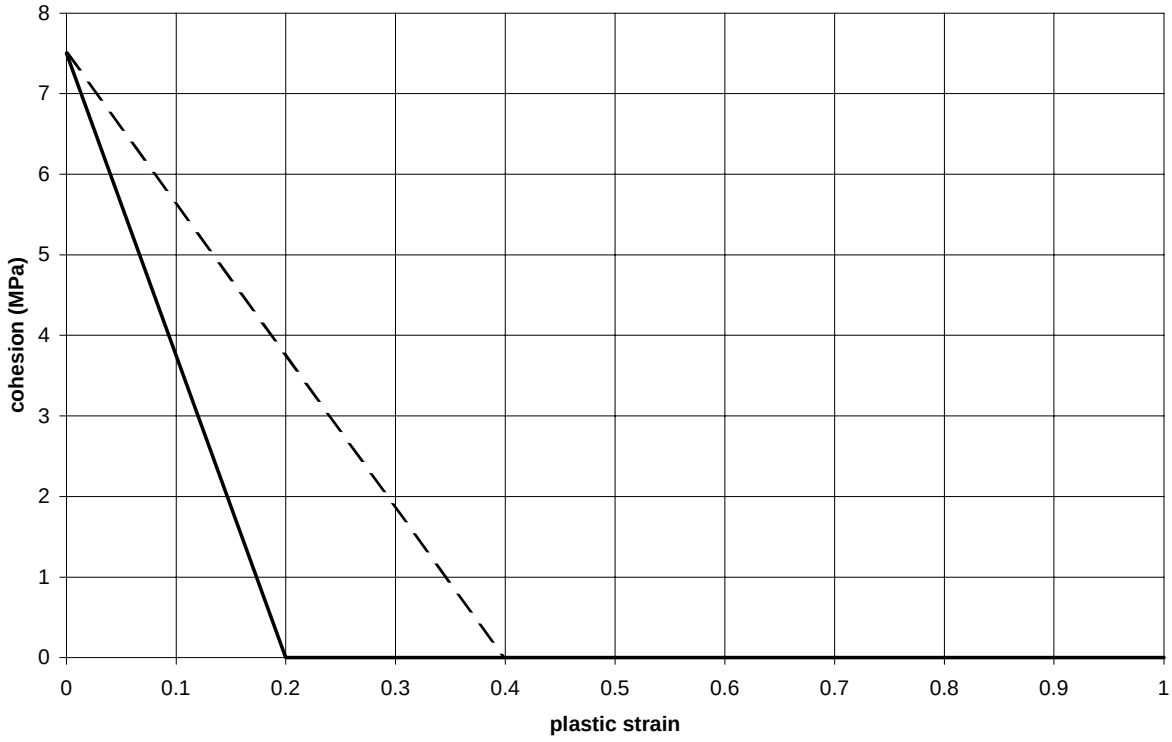

Figure 6-25 A schematic of the assumed linear relation between cohesion and plastic strain.

6.8.4 Contact friction angle between coal samples and steel platen

The contact friction angle was measured between coal samples and steel platens by using a shear box. The coal samples and steel platens were prepared to the same finish as for normal tests. A typical result is as shown in Figure 6-26. The contact friction angle (ϕ_c) is given by:

$$\sigma_n = \tau.\tan(\phi_c) \qquad \textit{Equation 6-20}$$

where: σ_n = normal stress (MPa)

τ = shear stress (MPa)

ϕ_c = contact friction angle.

From Figure 6-26, $\tan(\phi_c) = 0.2263$. This implies that that $\phi_c = 12.8°$. Two other tests were performed, with the average of the three tests being 15.0°.

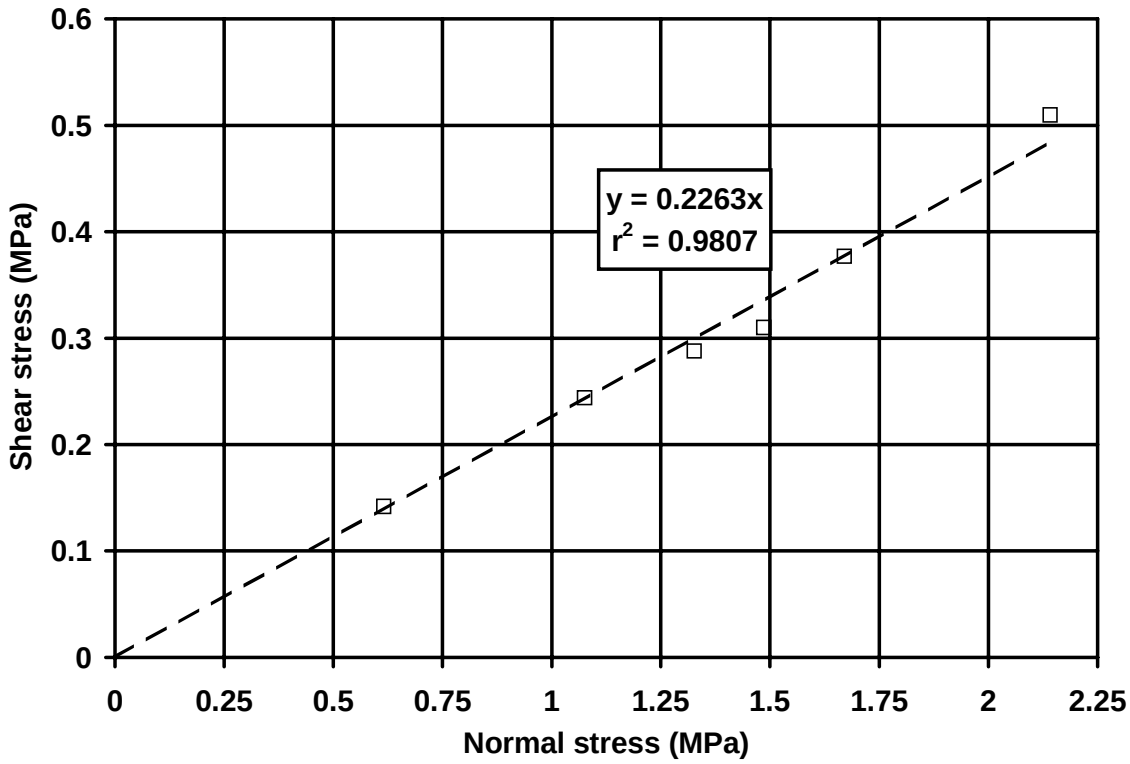

Figure 6-26 The shear stress resistance of a steel platen / coal interface as a function of normal stress.

6.8.5 Back analysis to laboratory model pillar behaviour

The average UCS of the samples, according to the straight line fit in Figure 6-22, was 31.93 MPa. The numerical model of a UCS test resulted in very small errors in strength. The size effect can be catered for by changing the value of cohesion. However, as shown in Section 6.6.3, the w/h effect is scale independent. This allows the w/h ratio effect to be studied numerically, without needing to take scale effects into account. The average value of 1-a for the laboratory tests was 0.26 (see Figure 6-12).

Of the parameters controlling the behaviour of model pillars mentioned in Section 6.8.1, cohesion, friction angle and the contact friction angle were kept constant. The value of ε^p_{max} was varied to determine the value that would best fit the value of 1-a derived from the laboratory behaviour. This is, in effect, an empirical determination of the best value of ε^p_{max}. The relations of w/h and peak strength for various values of ε^p_{max} are shown in Figure 6-28.

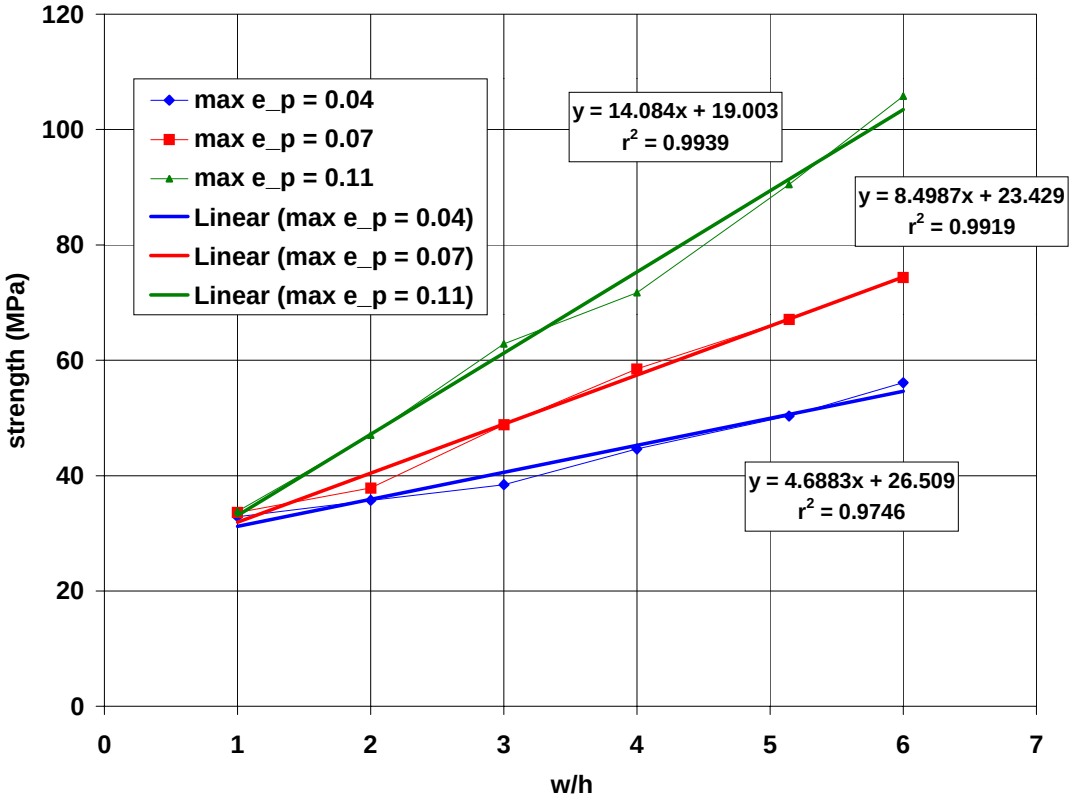

Figure 6-27 Peak strength as a function of w/h for various values of ε^p_{max}. ϕ_c was 15°.

The results of Figure 6-26 are summarised in Table 6-9. The values of 1-a and Θ are also shown in Table 6-9. 1-a is shown as a function of ε^p_{max} in Figure 6-28.

Table 6-9 The linear function and derived values of 1-a and Θ from the relations shown in Figure 6-26.

ε^p_{max}	m	c (MPa)	r^2	1-a	Θ (MPa)
0.04	4.69	26.51	0.97	0.15	31.20
0.07	8.50	23.43	0.99	0.27	31.93
0.11	14.08	19.00	0.99	0.43	33.08

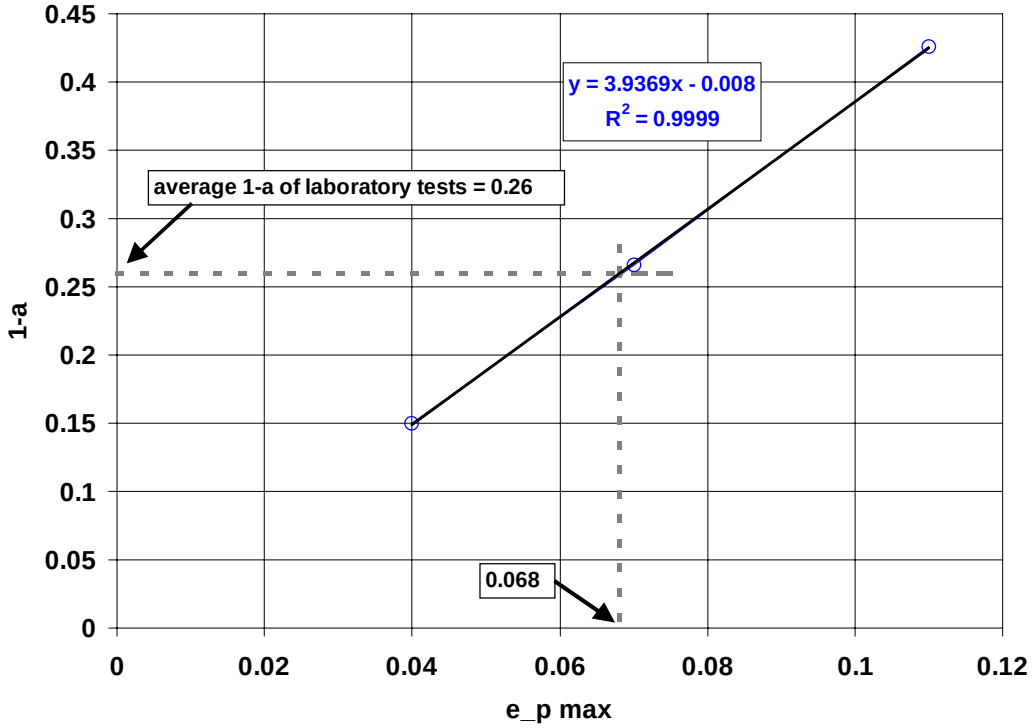

Figure 6-28 The value of 1-a determined by numerical modelling as a function of ε^{p}_{max}. Setting ε^{p}_{max} to 0.068 will result in replication of the laboratory w/h - peak strength relationship.

As shown in Figure 6-28, the value of ε^{p}_{max} which results in the laboratory derived value of 1-a is 0.068. This value was used in subsequent runs to investigate the effect of w/h and the contact friction angle.

6.8.6 The effect of w/h and the contact friction angle

The value of ε^{p}_{max} = 0.068 was used in a series of numerical models, with the contact friction angle between the steel platen and coal platen modelled successively as 0°, 10°, 20° and 30°. The resultant w/h – strength curves are shown in Figure 6-29. The curves seem to have three distinct phases:

1) The first phase seems linear in the region from w/h = 0.4 (the standard UCS geometry) to w/h = 2.

2) The second phase is linear, starting from w/h = 2, but with an increased slope compared to the first phase. This linear portion ends when the “squat pillar” effect occurs (Madden, 1991). For ϕ_c = 10°, this does not occur, even up to w/h = 8. The squat pillar effect occurs between w/h =

5.14 and w/h = 6 for $\phi_c = 20°$. For $\phi_c = 30°$, the squat pillar effect occurs between w/h = 3.4 and w/h = 4.

3) the third phase is the squat pillar phase.

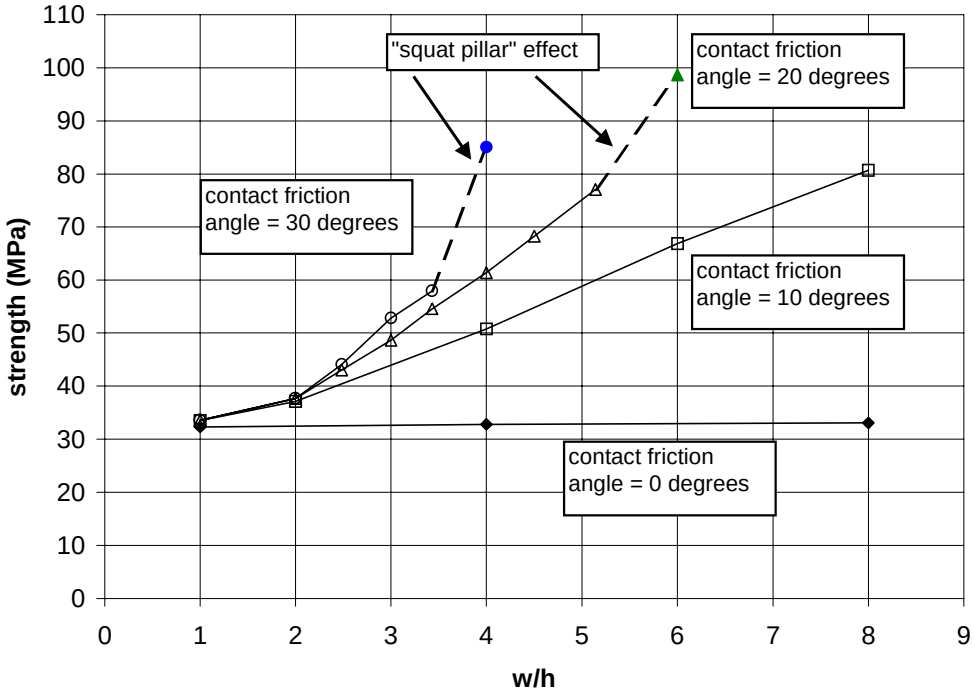

Figure 6-29 The w/h – peak strength relationship for various values of contact friction angle.

There are some unexpected features to these curves. The strength is the same (or very similar) in the first linear phase from w/h = 0.4 to w/h = 2, regardless of ϕ_c, (except $\phi_c = 0°$). There is a difference in the slope of the curves after w/h = 2, as a function of ϕ_c. The curves are expected to be linear from w/h = 1 until the squat pillar effect occurs. The difference between the slope of the $\phi_c = 20°$ and the $\phi_c = 30°$ curve is relatively small. Despite this, the w/h at which the squat pillar effect occurs for $\phi_c = 30°$ is substantially less than for $\phi_c = 20°$.

A straight line was fitted through each of the curves in Figure 6-29 for values of w/h from one until the squat pillar effect begins. The parameters are shown in Table 6-10. The parameters Θ and 1-a are also shown in Table 6-10. The relation between 1-a and ϕ_c is plotted in Figure 6-30.

Table 6-10 The parameters of the fitted straight lines to the curves shown in Figure 6-29. The normalised parameters are also shown.

ϕ_c	m	d	Θ	1-a	r^2
0°	0.12	32.21	32.33	0.04	0.94
10°	6.61	26.63	33.24	0.20	0.99
20°	9.77	22.55	32.32	0.30	0.95
30°	10.34	20.45	30.85	0.34	0.93

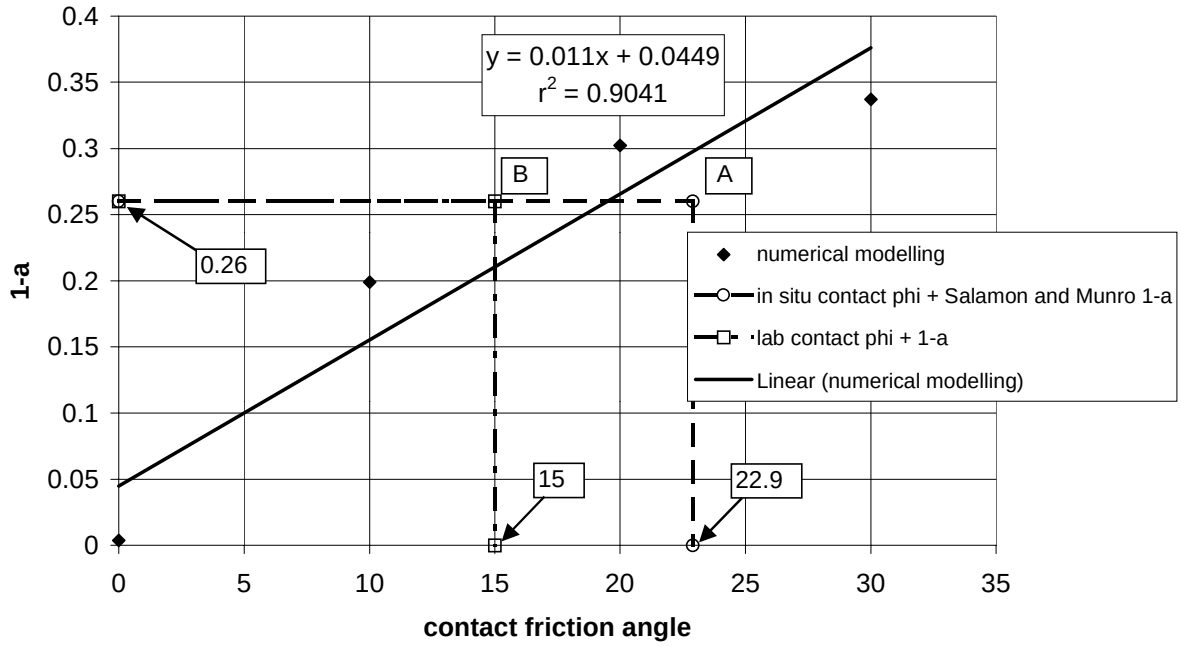

Figure 6-30 1-a as a function of ϕ_c derived from numerical modelling.

It was shown in Table 6-5 that the value of 1-a derived from Salamon and Munro's database was 0.26. This value, labelled point A, is plotted against the average value of the residual *in situ* friction angle (see Table 6-8) in Figure 6-30. In this context, it should be remembered that 1-a is scale independent. Point A is below the fitted curve. This is explained by the difference in the two data sets: in the numerical model, increases in strength were a function only of w/h and the contact friction angle. As discussed in Section 6.4, the empirical nature of 1-a as determined from Salamon and Munro's *in situ* database implicitly includes the pillar system factors mentioned in Section 6.3. The fact that point A is below the line indicates the weakening influence of the additional pillar system factors. Of these, the main influence was probably jointing. This influence has been fully discussed in Chapter 2.

The value of 1-a derived from the laboratory testing was also 0.26. This is plotted against the laboratory determined ϕ_c as point B. Point B plots to the left of point A. This also indicates the weakening influence of the *in situ* pillar system factors.

The curve in Figure 6-30 can be used as a design chart to determine the effect of the contact friction angle on the w/h strengthening ratio, in a pillar design procedure. This will be demonstrated in Section 6.10.

6.9 A methodology to estimate the critical rock mass strength based on laboratory samples

The value of Θ for the Salamon and Munro *in situ* collapsed cases is 5.74 MPa (see Table 6-5). This is the best available basis for an Θ_c because it is fairly representative of South African coal, whereas other *in situ* tests were site specific. It also implicitly includes the pillar system factors.

It was shown in Section 2.4.5 that the strength of a pillar without any joints is approximately 1.1 times the strength predicted by the equation of Salamon and Munro (1967). Therefore, Θ_c may be taken as 5.74 x 1.1 = 6.3 MPa.

However, as has been shown in Section 6.6, Θ is directly proportional to the intrinsic coal strength. That is, for the same pillar system conditions, an increase in the basic strength of coal by 10 per cent would result in a 10 per cent increase in Θ, as is intuitively obvious.

The strengths for the w/h=1 samples in the COL021 database of laboratory tests are plotted in Figure 6-31. As may be seen, the material gets weaker with increasing size. The scatter also decreases with size.

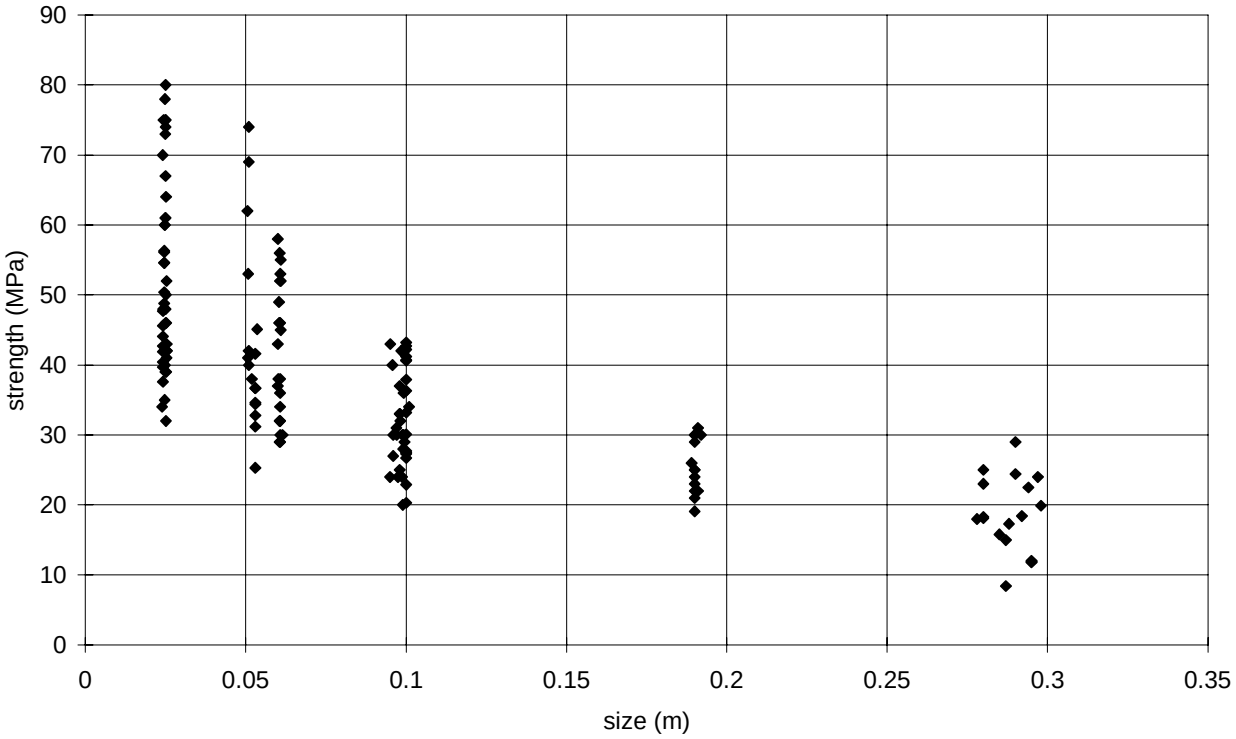

Figure 6-31 Strength as a function of size for the samples of w/h=1 in the COL021 laboratory test database.

The mean size and strength of each group of data in Figure 6-31 were determined. The standard deviation of the strength for each group was also determined. This was then expressed as a percentage of the mean strength, termed s_m. The results are tabulated in Table 6-11.

Table 6-11 The standard deviation as a percentage of the sample means of the strength of w/h = 1 samples of each size in the COL021 database.

mean of sample size (mm)	Mean of sample strength (MPa)	standard deviation - *s* (MPa)	s_m
24.76	52.1	13.4	25.7
56.98	42.6	11.3	26.5
98.76	32.1	6.8	21.0
190.2	25.5	3.9	15.3
288.4	18.5	5.5	29.6
		Average	**23.6**

The average standard deviation as a proportion of the mean of the strength is 23.6 per cent. Column 4 of Table 6-11 is plotted as a function of column 1 in Figure 6-32. The fitted straight line is virtually horizontal, with the y-intercept almost the same as the average shown in Table 6-11, showing that s_m is independent of size.

The value of Θ_{25} is, on average 52.1 MPa, and Θ_{288} is, on average, 18.5 MPa. The value of Θ of Salamon and Munro is 5.7 MPa. The average Θ of the *in situ* tests and that of Salamon and Munro is 8.15 MPa. Therefore the strength reduction from 25 to 288 mm accounts for about $\frac{2}{3}$ of the strength reduction from 25 mm to *in situ*. It therefore seems reasonable to assume that s_m remains constant to the *in situ* scale.

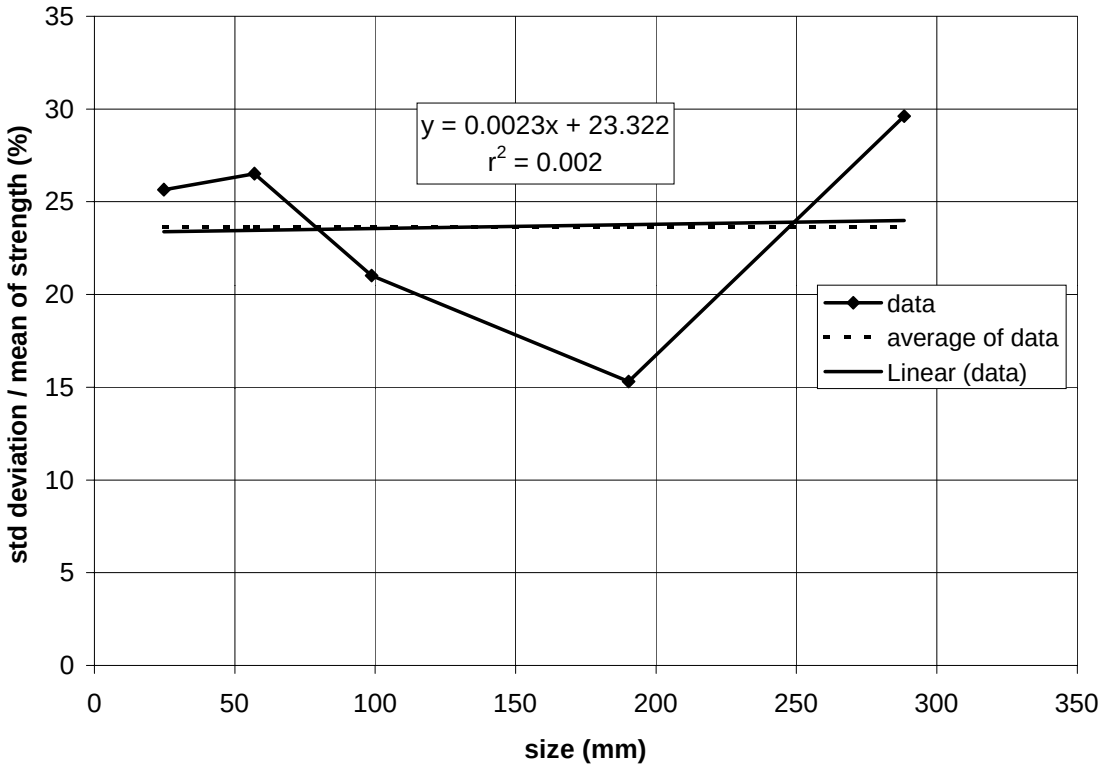

Figure 6-32 The parameter s_m is shown to be independent of size from 25 mm to 300 mm.

The distribution of strengths for each size was tested to determine whether they were normally distributed. The statistical method involved the use of the χ^2 distribution. The calculation methodology is shown in Appendix F. The distribution of the 25 mm strengths proved to be non-normal. The distribution of strengths of the 57 mm and 99 mm sizes proved to be normal. The 190 mm and 288 mm sizes did not have enough data points to be able to determine whether the strengths in these sizes were normally distributed. However, in Figure 6-33 it can be seen that the actual distribution of strengths is qualitatively close to the normal distribution, for the 288 mm

samples. The normal distribution is plotted assuming the sample mean and standard deviation for the 288 mm data in Table 6-11.

The strength values are therefore deemed to be normally distributed, in general. In this case, if a batch of tests on say, 100 mm samples, from a particular mining section results in a sample mean *significantly* higher than that found in the COL021 database (for the same size), then the variance from the population mean (that of the COL021 database) can be assumed to be "real". (Statistical *significance* implies that the difference is very unlikely to have occurred by chance; this can be determined by statistical techniques.) This variance can then also be assumed to apply at the *in situ* scale. Therefore, Salamon and Munro's Θ_c can be adjusted. If, for example, a 30 per cent increase in the strength is verified as "real", then Θ_c can be increased by 30 per cent.

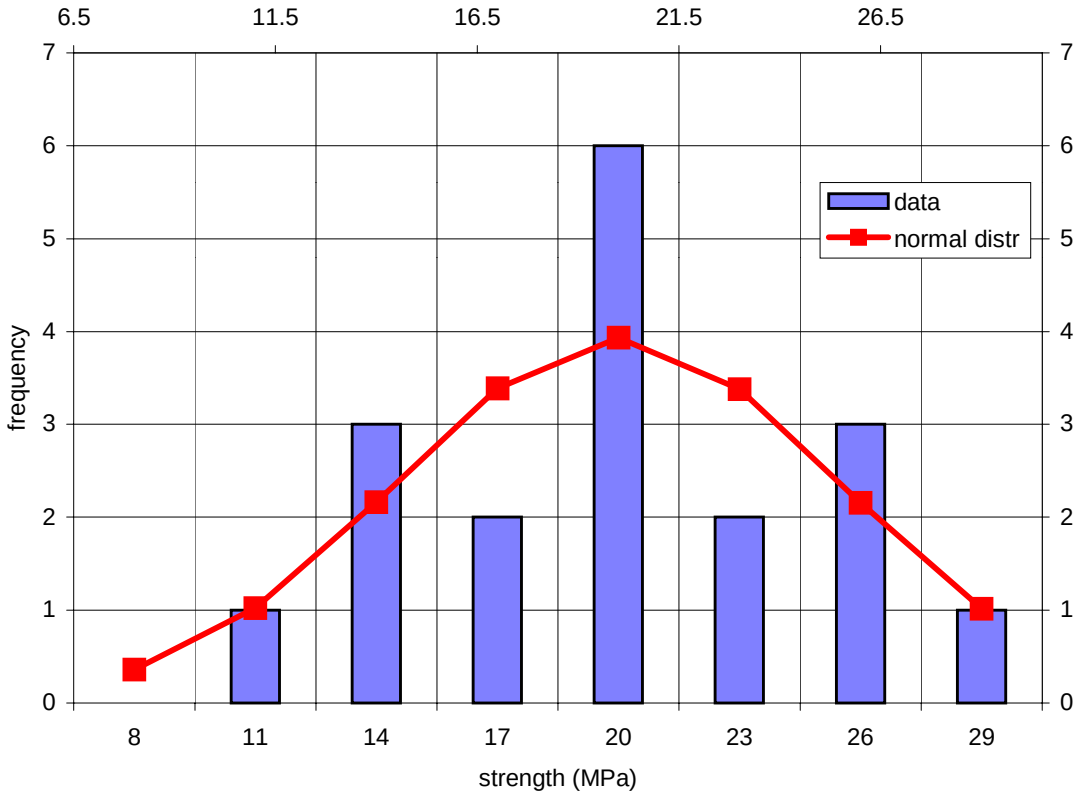

Figure 6-33 The distribution of the actual strength data for the 288 mm diameter samples, compared to the normal distribution.

The 95 per cent confidence interval for s_m is from 16.7 to 30.6 per cent. This was calculated in the same way as the 99 per cent confidence intervals were calculated for the peak and residual ϕ_c in Section 6.7.

6.10 A new pillar design methodology

The pillar design methodology shown in Figure 4-8 contains many factors. Of the factors presented, Θ_c, w/h and jointing are probably the most influential. These factors have been discussed in Section 6.9, Section 6.8.6, Chapter 2, and Section 6.8.6 respectively. A methodology with the new understandings developed in the scope of this report is shown in Figure 6-34.

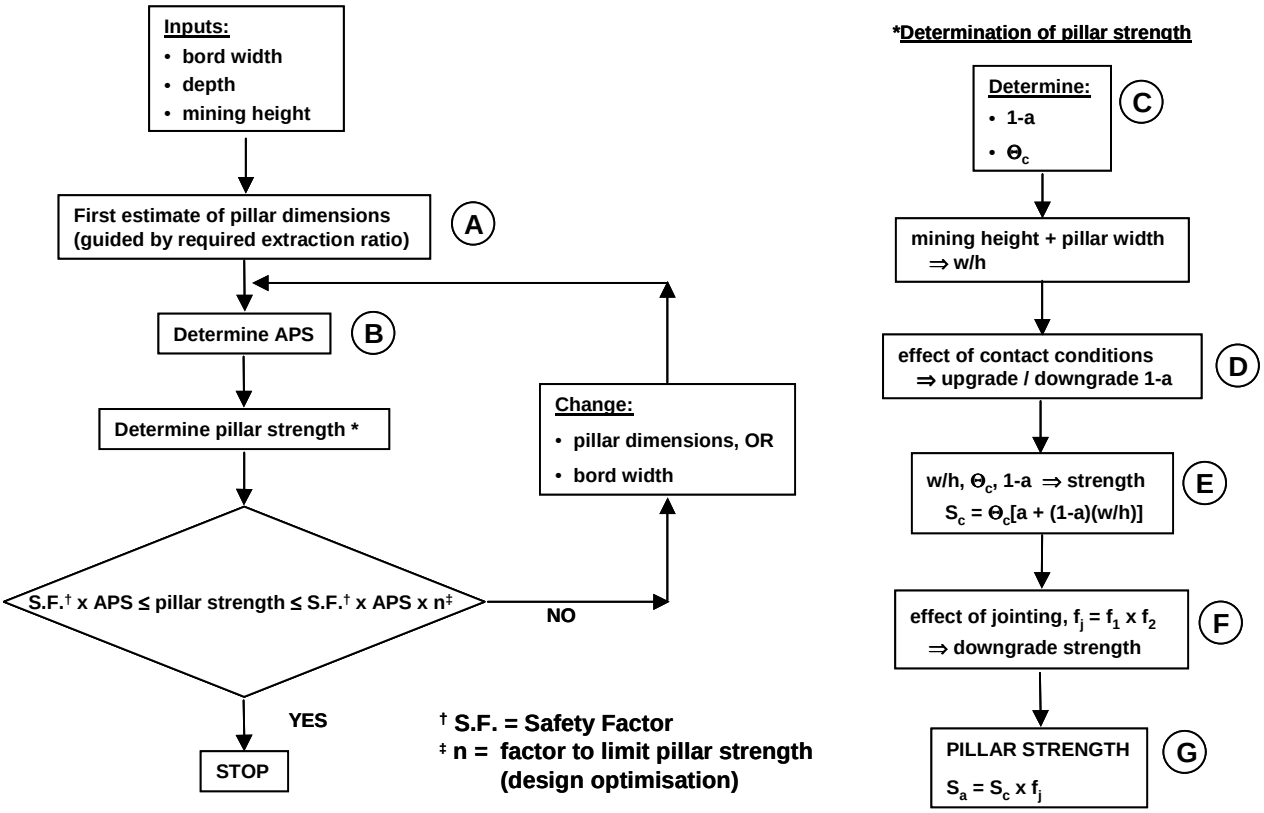

Figure 6-34 A pillar design methodology based on the new knowledge developed in the scope of this report.

Block A: The required extraction ratio and probable bord width will guide the first estimate of the pillar width.

Block B: The average pillar stress (APS) can be determined by tributary area theory, or by numerical modeling.

Block C: From the linear analysis of Salamon and Munro's *in situ* data, Θ_c may be taken as 5.74 MPa (see Table 6-5). However, it was shown in Section 2.4.5 that the strength of a pillar without any joints is approximately 1.1 times the strength predicted by the equation of Salamon and Munro (1967). Therefore, Θ_c may be taken as 5.74 x 1.1 = 6.3 MPa.

The value of 1-a (also from Table 6-5) is 0.26. However, 1-a has been shown to be scale independent, therefore laboratory derived values of 1-a are applicable to *in situ* pillar

design. Laboratory w/h tests could be performed on a convenient diameter, such as 50 mm. Site, mine or area specific values of 1-a may then be derived. Some areas may have a higher w/h effect, while others have a lower w/h effect.

Block D: ϕ_c between coal and steel platens is of the order of 15°. The value of the w/h strengthening parameter 1-a is proportional to the contact friction angle. From the best fit straight line in Figure 6-30, 1-a is 0.21. However, the *in situ* ϕ_c is 23°. In this case, the predicted 1-a is 0.30.

If the *in situ* contact conditions in a particular area are deemed to be higher than 23°, it is suggested that 1-a be increased, according to the relationship shown in Figure 6-30.

The effect of contact friction has not yet been back analysed to *in situ* pillars. This is an area that requires future work. Due to this, if the value of 1-a is upgraded, it is suggested that the upgrade is limited to a value corresponding to a contact friction angle of approximately 30°, which according to the best fit line in Figure 6-30 is 0.37. If the value of 1-a derived from laboratory testing is greater than 0.37, then such a value should be used.

The effect of topcoaling on pillar strength has not been explicitly investigated. However, it is thought that this is likely to increase the strength of pillars, because the angle of internal friction of coal is most often greater than 22°. Similarly to the preceding paragraph, it is suggested that the maximum value of 1-a in this case should also be 0.37, due to the lack of further *in situ* knowledge.

Block E: Once a trial value of w/h has been selected, and suitable values of Θ_c and 1-a have been derived, Equation 6-7 may be used to determine the pillar strength (S_c) taking contact conditions and the critical rock mass strength into account.

Block F: If a face is intersected by more than one joint set, the most persistent, or dominant, joint set should be selected. Slips should also be catered for. The pillar strength reduction factor for each direction is obtained as a function of the dip and frequency of the joint set (see Chapter 2). The strength reduction factor for each direction is termed f_1 and f_2.

To account for the effect of joint sets intersecting each of the orthogonal faces, the factors for each direction are multiplied, i.e. $f_j = f_1 \times f_2$. The method to determine the effect of jointing in any one direction is given in full detail in Chapter 2.

Block G: The pillar strength (S_a) taking all the quantified pillar system factors into account is expressed as follows:

$$S_a = S_c \times f_j \qquad \textit{Equation 6-21}$$

A comparison of the Salamon and Munro formula and the new methodology is shown in Figure 6-35. For this illustrative purpose, the effect of joints were not taken into account. Whereas the Salamon and Munro formula is fixed, the new methodology allows for the parameters to be changed.

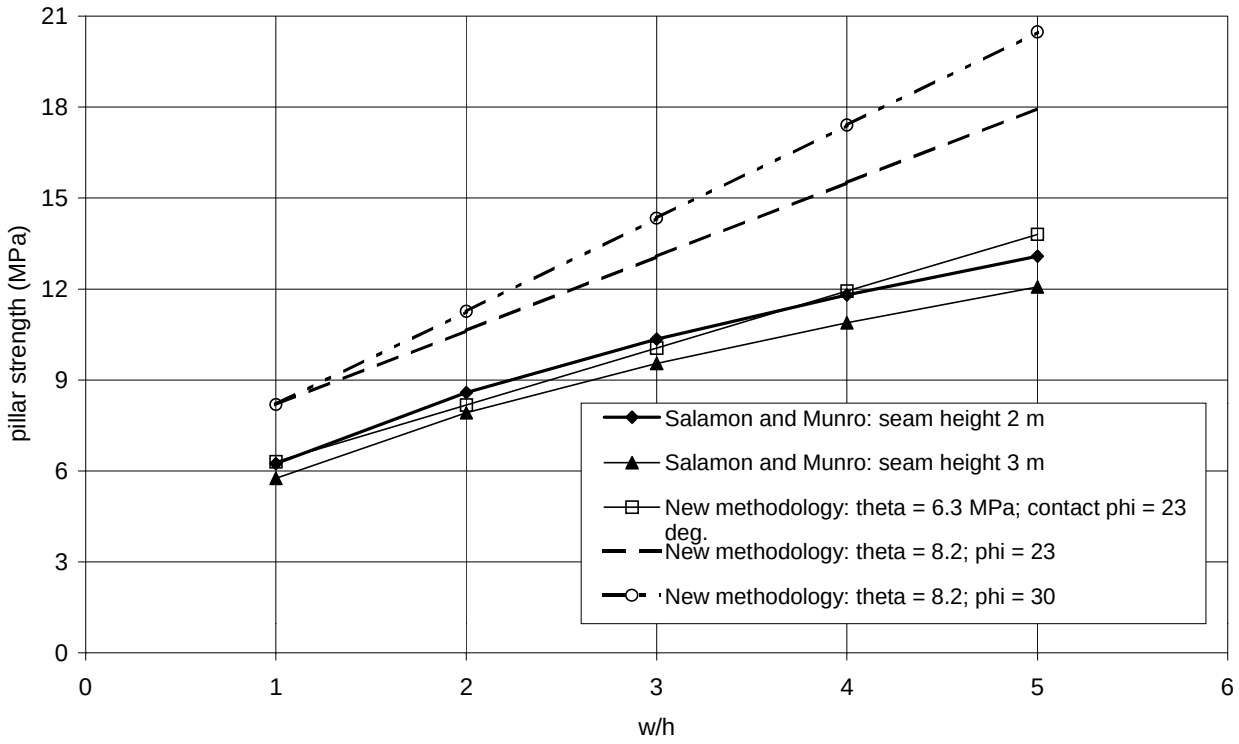

Figure 6-35 A comparison between the formula of Salamon and Munro, and the new methodology with different values of Θ_c and ϕ_c.

6.11 Worked examples

Worked Example 1:

Design a stable pillar system, given the following data:

mining depth	85 m
rock mass density	2500 kg /m^3
bord width	6 m
mining height	2.5 m
joint density in direction 1	0.5 joints/m
direction 1, joints dipping	75°
joint density in direction 2	0.3 joints/m

direction 2, joints dipping	60°
based on RMR, joint friction angle	20°

Solution:

Block A: A w/h of four should suffice, so try pillar width w = 10 m.

Block B: The extraction ratio is given by $e = 1 - \frac{bw}{BW}$, therefore $1 - e = \frac{bw}{BW}$.

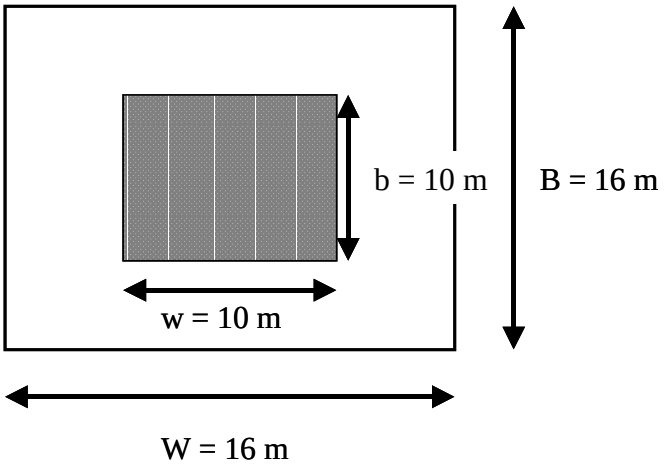

With a pillar 10 m square, bords 6 m wide, 1-e = $10^2/16^2$ = 0.39 = 39 %.

APS = ρgH / 1-e = 2500.10.85/0.39/1e6 = 5.45 MPa.

Block C: In the absence of any other information, take 1-a based on the average *in situ* ϕ_c = 23°. From Figure 6-30, 1-a = 0.30.

In the absence of any other information, take Θ_c as 6.3 MPa.

Block D: No information on underground contact conditions, so assume 1-a = 0.30

Block E: Substitute w/h = 10/2.5 = 4, Θ_c = 6.3 MPa, 1-a = 0.30:

$S_c = \Theta_c[(1\text{-}a)(w/h) + a]$

$= 6.3[(0.3)(4) + 0.7]$

$= 11.97$ MPa.

Block F: Joints in direction 1:

For joints dipping at 75°, from Table 2-1, n = 0.42 by interpolation.

Substitute h = 2.5, J_f = 0.5 jts/m, R = w/h = 4, ϕ = 20° into

$$F = \frac{10(1 - e^{-0.23hJ_f})}{\sqrt{R}n\tan\phi} \text{ (Equation 2-4)}$$

$$F = \frac{10(1 - e^{-(0.23)(2.5)(0.5)})}{\sqrt{4}(0.42)(\tan 20)}$$
$$= 8.17$$

From Equation 2-3, the strength reduction factor for direction 1:

$$f_1 = e^{-0.017F}$$
$$= e^{-(0.017)(8.17)}$$
$$= 0.87$$

Joints in direction 2:

For joints dipping at 60°, from Table 2-1, n = 0.21

Substitute h = 2.5, J_f = 0.3 jts/m, R = w/h = 4, ϕ = 20°:

$$F = \frac{10(1 - e^{-(0.23)(2.5)(0.3)})}{\sqrt{4}(0.21)(\tan 20)}$$
$$= 10.36$$

The strength reduction factor for direction 2:

$$f_2 = e^{-(0.017)(10.36)}$$
$$= 0.84$$

Total reduction factor for both directions: $f_j = f_1 \times f_2 = 0.87 \times 0.84 = 0.73$

Block G: Pillar strength taking jointing into account:

Sa = Sc x f_j
= 11.97 x 0.73
= 8.73 MPa

Safety Factor = 8.73 / 5.45 = 1.60 ⇒ pillar design is acceptable.

Worked Example 2:

The Rock Engineering department now has further information at its disposal: the contact friction angle in the specific mining area is 30°. Also, laboratory tests on 100 mm diameter samples have shown that the strengths are 30 per cent greater, to a statistically significant degree, than assumed in Worked Example 1. All other information is the same as Worked Example 1.

Solution:

Block A: Try a reduction of the pillar dimensions to 8 m; w/h = 3.20.

Block B: With a pillar 8 m square, bords 6 m wide, 1-e = $8^2/14^2$ = 0.33 = 33 %.

APS = ρgH / 1-e = 2500.10.85/0.33/1e6 = 6.44 MPa.

Block C: A 30 per cent increase in strength $\Rightarrow \Theta_c$ = 6.3 x 1.3 = 8.19 MPa

Block D: given *in situ* $\phi_c = 30°$, from Figure 6-30, 1-a = 0.37

Block E: Substitute w/h = 8/2.5 = 3.2, Θ_c = 8.19 MPa, 1-a = 0.37:

$S_c = \Theta_c[(1\text{-}a)(w/h) + a]$

$= 8.19[(0.37)(3.2) + 0.63]$

$= 14.86$ MPa.

Block F: Joints in direction 1:

Substitute n = 0.42, h = 2.5, J_f = 0.5 jts/m, R = w/h = 3.2, $\phi = 20°$ into

$$F = \frac{10(1-e^{-0.23hJ_f})}{\sqrt{Rn}\tan\phi}$$ (Equation 2-4)

$$F = \frac{10(1-e^{-(0.23)(2.5)(0.5)})}{\sqrt{3.2}(0.42)(\tan 20)}$$

$$= 9.14$$

From Equation 2-3, the strength reduction factor for direction 1:

$$f_1 = e^{-0.017F}$$

$$= e^{-(0.017)(9.14)}$$

$$= 0.86$$

Joints in direction 2:

Substitute n = 0.21, h = 2.5, J_f = 0.3 jts/m, R = w/h = 3.2, $\phi = 20°$:

$$F = \frac{10(1-e^{-(0.23)(2.5)(0.3)})}{\sqrt{3.2}(0.21)(\tan 20)}$$

$$= 11.59$$

The strength reduction factor for direction 2:

$$f_2 = e^{-(0.017)(11.59)}$$
$$= 0.82$$

Total reduction factor for both directions: $f_j = f_1 \times f_2 = 0.86 \times 0.82 = 0.71$

Block G: Pillar strength taking jointing into account:

$$Sa = Sc \times f_j$$
$$= 14.86 \times 0.71$$
$$= 10.56 \text{ MPa}$$

Safety Factor = 10.56 / 6.44 = 1.64 $\Rightarrow$ pillar design is acceptable.

6.12 Discussion and conclusions

It has been shown that the volume effect in Salamon and Munro's database of collapsed cases is negligible. In connection with this, Bieniawski and others have demonstrated the existence of the critical rock mass strength. In either case, the practical conclusion is that if there is a size effect at the *in situ* scale, it is negligible.

There are a number of factors that affect pillar strength. Any empirical curve fit to a set of data that does not include all the variables as explicit inputs to design, results in a lumping of the effect of the undefined variables in the statistical parameters that emerge. That is, with reference to the Salamon and Munro formula, k, α and β contain the influence of all the pillar system factors mentioned, and possibly other factors. The influence of each pillar system factor is implicit and undefined.

The statistical parameters k, α and β are an indivisible set that provides the best fit to the data set, given the nature of the formula, and the statistical method employed by Salamon and Munro. In view of this and the preceding paragraph, k cannot be regarded as a material property. The representative volume that k refers to is dependent on the units of length employed.

The effect of the critical rock mass strength, w/h and ϕ_c have been investigated in detail. The effect of jointing is discussed in Chapter 2. The results of these investigations have been put together to form the basis of a new methodology for pillar design. A pillar design flowchart has been produced.

A qualitative indication of the degree to which the *in situ* pillar system factors reduce pillar strength is the degree to which point A is below the fitted curve and to the right of point B in Figure 6-30.

A representative value of Θ_c based on a linear fit to Salamon and Munro's *in situ* data is 5.7 MPa. This value implicitly includes factors such as jointing and other pillar system factors. It was shown in Chapter 2 that unjointed pillars are, on average, 1.1 times stronger than jointed pillars. Therefore, 5.7 x 1.1 = 6.3 MPa may be used as Θ_c.

It has been shown that the ratio of standard deviation to mean strength of w/h = 1 samples is constant for sizes from 25 to 288 mm. Given that this particular size range covers about $^2/_3$ of the reduction in strength of the 25 mm samples to the *in situ* scale, it is assumed that this ratio is valid *in situ*. *In this case, significant (in the statistical sense) differences in coal material strength detected in the laboratory can lead to a modification of Θ_c.*

The small variation in the *in situ* ϕ_c implies that the average value of 23° can be used with confidence. Due to the use of the SF in pillar design, it is not suggested that the 90 per cent value be used, as this together with a SF would be unnecessarily conservative. If the *in situ* contacts are measured with a friction angle of greater than 23°, then the design chart in Figure 6-30 may be used to increase 1-a.

The modular approach to pillar design, with explicit quantification of the influence of jointing, w/h and ϕ_c, allows scope for site or geotechnical area specific pillar design. This requires measurement of ϕ_c and joint set parameters.

Other results of significance are:

1) The scale effect can be simulated in numerical modelling by a reduction in the macro-Mohr-Coulomb cohesion. The friction angle is assumed to remain constant for pre- and post-peak strength.

2) While the power formula has the ability to handle large volume ratios, an empirical guide is that the linear function performs as well as the power formula as long as the volume ratio is below 50. In any case, *in situ* strength is at the critical rock mass strength.

3) The 99 per cent confidence interval for the peak ϕ_c is 21.7° to 26.5°. The residual contact friction angle is, on average, 90 per cent of the peak friction angle. The 99 per cent confidence interval for the residual ϕ_c is 21.0° to 24.8°.

There are a number of issues not yet resolved. Among them are:

1) an underground verification is required to verify the proposed new design methodology

2) the effect of coaltopping has not been determined

3) the factors that form part of the pillar design methodology have been assumed to act in series; this is not necessarily the case.

6.13 References

Hustrulid, W.A. 1976. A review of coal pillar strength formulas. *Rock Mechanics* 8, 115-145.

Babcock, C.O. 1969. Effect of end constraint on the compressive strength of model rock pillars. *Transactions, Society of Mining Engineers,* AIME, Vol. 244, Dec.

Bieniawski, Z.T. 1968. *In situ* large scale tests on square coal specimens measuring 2 meters in width. *CSIR report MEG 694.*

Bieniawski, Z.T. 1968a. The compressive strength of hard rock. *Tydskrif vir Natuurwetenskappe,* vol. 8, no 3/4, Sept./Dec., pp 163-182.

Bieniawski, Z.T. and Van Heerden, W.L. 1975. The significance of *in situ* tests on large rock specimens. *Int. J. Rock Mech. Min. Sci. & Geomech. Abstr*. Vol. 12, pp. 101-113

Cassie, J. W. and Mills, K. W. 1992. Study of pillar behaviour in the Parkgate Seam at Asfordby Colliery. *Proceedings of the workshop on Coal pillar mechanics and design.* USBM, Sante Fe.

Chen W.F. 1975. Limit Analysis and soil plasticity. Elsevier Scientfic Publishing Company, Amsterdam.

Cook, N.G.W., Hodgson, K. and Hojem, J.P.M. 1970. A 100 MN jacking system for testing coal pillar underground. *C.O.M. Ref. Rep. 48/70*.

Cundall, P.A. 1993. FLAC User's Manual, version 3.22.

Denkhaus, H.G. 1962. A critical review of the present state of scientific knowledge related to the strength of mine pillars, *J. South Afr. Inst. Min. Metall.,* Sept.

Evans, I., Pomeroy, C.D., Berenbaum R. 1961. The compressive strength of coal, *Colliery Eng.*, March.

Galvin, J.M. Hebblewhite, B.K. Salamon, M.D.G. 1996. Australian coal pillar performance. *International Society of Rock Mechanics News Journal,* Vol. 4 No. 1 Fall.

Greenwald, H.P., Howarth, H.C., Hartmann, I. 1941. Progress Report : Experiments on strength of small pillars of coal in the Pittsburgh bed. *USBM, R.I. 3575,* June, 1941

Haile, A.T. 1995. Develop guidelines for the design of pillar systems for shallow and intermediate depth, tabular, hard rock mines and provide a methodology for assessing hangingwall stability and support requirements for the panels between pillars. *SIMRAC Final Project Report - GAP024/OTH002*, CSIR Division of Mining Technology, Dec.

Hoek, E. and Brown, E.T. 1980. Empirical strength criterion for rock masses. *J: Geotech. Engng Div., ASCE*, 106 (GT9), pp 1012-1035.

Jahns, H. 1966. Measuring the strength of rock *in situ* at an increasing scale. *Proc. 1st ISRM Congress,* Lisbon , 477-482.

Madden, B.J., 1991. A Re-assessment of Coal-Pillar Design. *J. S. Afr. Inst. Min. Metall.,* vol. 91, no. 1. January. pp. 27 - 37.

Mark, C. and Barton, T. 1996. The uniaxial strength of coal : should it be used to design pillars? *15'th Int. Conf. On Ground Control in Mining,* Ozdemar *et al* (eds.), Golden, Colorado, Aug.

Napier, J.A.L. 1990. Modelling of fracturing near deep level gold mine excavations using a displacement discontinuity approach. *Mechanics of Jointed and Fractured Rock,* Rassmanith (ed.), Rotterdam.

Pratt, H.R., Black, A.D., Brown, W.S. and Brace W.F. 1972. The effect of specimen size on the mechanical properties of unjointed diorite. *Int. J. Rock Mech. Min. Sci.* Vol. 9, pp. 513-529.

Ryder, J.A. and Özbay, M.U. 1990. A methodology for designing pillar layouts for shallow mining. *ISRM Symp. : Static and Dynamic Considerations in Rock Engineering,* Swaziland, Sept.

Salamon, M.D.G. 1997. Pers. comm., 1997

Salamon, M.D.G. and Munro, A.H. 1967. A study of the strength of coal pillars. *J. South Afr. Inst. Min. Metall.* September.

Sorenson, W.K. and Pariseau, W.G. 1978. Statistical analysis of laboratory compressive strength and Young's modulus data for the design of production pillars in coal mines, *19'th US Symp. on Rock Mechanics,* Mackay School of Mines, May.

Steart, F.A. 1954. Strength and stability of pillars in coal mines. *J. Chem, Metal., and Min. Soc. of South Africa,* March.

Stavropoulou, V.G. 1982. Behaviour of a brittle sandstone in plane-strain loading conditions. *Proc. 23'rd Symp. on Rock Mechanics,* University of California, AIMMPE, pp 351-358.

van Heerden, W.L. 1974. *In situ* determination of complete stress-strain characteristics for 1.4m square coal specimens with width to height ratio of up to 3.4. *CSIR report ME 1265*, Pretoria, South Africa, January.

Vermeer P.A. and de Borst R. 1984. Non-associated plasticity for soils, concrete and rock. *Heron*, vol. 29, no. 3, pp 1-64.

Wagner, H. 1974. Determination of the complete load deformation characteristics of coal pillars. Proceedings of the 3rd ISRM congress, pp 1076-1081, December.

7 Underground experiment

7.1 Introduction

The main aim of this aspect of the project recorded here is to obtain load/deformation characteristics of pillars designed to ultimately crush. In these *in situ* pillar strength experiments the super incumbent strata is used as the loading mechanism, to fail a pillar underground, while at the same time monitoring the load deformation characteristics.

Previously two sites had become available but both contained pillars that were too large to fail, having width to height ratios of 8.8. Some useful information was however gained from comparisons made between the monitored pillar compression and the modelling predictions.

A third site was identified where a pillar was reduced in size to a width to height ratio of 2.0 and the remainder of the pillars in the section stooped. Attempts at monitoring the load increase in the pillar and convergence adjacent to it ended prematurely when the goaf severed the monitoring cables. At the same time the goaf ran up against two sides of the pillar affecting the longer-term pillar strength by applying lateral confinement, thus increasing the strength of the pillar.

As a result of these experiences it became apparent that unless the integrity of the immediate roof around the pillar could be maintained and the goaf prevented from running up to and applying confinement to the pillar, even a successful monitoring programme would produce inconclusive results. With this in mind the emphasis shifted from extensive monitoring, to attempting to control the immediate roof and the area around the pillar. The installation of packs and/or sticks close to and around the test pillar was suggested to try and support the immediate roof and keep goaf material away from the pillar sides.

In the experiment described in this report a pillar in the centre of a section was reduced in size and the surrounding pillars extracted in a stooping operation. The general layout of the area is shown in Figure 7-1. The panel layout with pillars numbered according to the extraction sequence is presented in Figure 7-2. The overall panel width after extraction was 67 m. The average bord and pillar dimensions were 7 m and 13 m x 13 m respectively. The depth below surface was 103 m with a mining height of 3.5 m giving an initial safety factor of 1.7. The pillars were extracted using a Voest Alpine road header. The test pillar was reduced in size to approximately 4 m x 5 m giving it a width to height ratio of about 1.2, which if loaded sufficient would be expected to crush.

7.2 Numerical Modelling

In the early planning stages of the experiment, numerical modelling of various mining steps was carried out using MINLAY, an elastic displacement - discontinuity program. Working from this purely elastic interpretation, if it were possible to extract all eight pillars surrounding the small test pillar completely, the maximum compression of the pillar would be about 10 to 15 mm. On a pillar height of 3.5 m this equates to 3 to 4 millistrains which was considered as insufficient to fail the pillar. Nevertheless it was decided to continue with the experiment at this site.

For comparison purposes a series of runs using MAP3D as the numerical model were carried out. In the elastic format these results confirmed those of MINLAY giving a value of 11 mm using an overburden modulus of 10 GPa.

During 1991 Miningtek [then COMRO] field tested a modified extensometer system. A borehole was drilled from surface, ahead of the underground mining face, to intersect the centre of a pillar that was to be developed in a bord and pillar section. Part of this exercise was to measure the seam / pillar compression as the pillar was being formed and as the face advanced away from it. All the pillars were then systematically reduced in size as the mining operation retreated from the section.

Having these results in the database provided an ideal opportunity for carrying out a numerical simulation of this particular exercise to compare the predicted values against those that had been measured. MAP3D, again in the elastic format, was used and produced a final result of 4.6 mm, some 15 per cent higher than the 4 mm measured. This boosted confidence in the MINLAY and MAP3D elastic predictions for the experimental pillar area and the accuracy of the extensometer.

7.3 Instrumentation

In order to have some idea of if, and when, the pillar failed, it was necessary to install some form of instrumentation that would function for as long as possible after any goafing occurred within the panel. The most appropriate form of instrumentation was extensometers installed in a borehole drilled from surface to intersect the test pillar as close as possible to its centre. This was the same type of instrumentation as had been used in the 1991 pillar compression monitoring programme.

The borehole was surveyed using a down hole instrument, in order to ascertain that it had intersected the seam horizon within the original pillar in an acceptable position. The reduction in size of the test pillar was then planned around the position of the borehole to ensure that it was as close as possible to the centre of the final pillar position.

Ingwe Rock Engineering carried out geotechnical tests on the core from the borehole and produced the geotechnical borehole log presented in Figure 7-3. The positions of the five anchors installed in the borehole as part of the extensometer system are also indicated in the figure.

With the micrometer reading procedure of the extensometer system, it is possible to determine if each wire is free to move in the hole all the way to its particular anchor. It is also possible to detect any restriction or dislocation in the hole and the approximate elevation at which this occurs. This system has been used successfully at depths of 167 m. The overall accuracy is estimated to be of the order of 0.5 mm.

A collar pipe is erected on surface at the mouth of the borehole, a diagram of which is presented in Figure 7-4. Each individual monitoring wire comes up the borehole, goes through the collar pipe and passes over a pulley at the top. The wire then goes down the outside of the pipe and is attached to a tensioning weight situated between two datum plates fixed to the collar pipe. A stainless steel tape attached to the bottom of the weight passes through a reading head attachment fixed to the lower datum plate.

To take a reading the spring tensioner micrometer, illustrated in Figure 7-5, is attached to the reading head below the lower datum plate and connected to the stainless steel tape. The tensioning device consists of a calibrated tension spring, the extension of which is monitored by a dial gauge. A screw feed tensions the monitoring wire via the spring, which is loaded to three specific extension levels (or loads). A micrometer built into the device is used to take readings at each tension level. This procedure is repeated three times on each monitoring wire, which results in a total of nine readings which are then averaged. The differences between the three tension levels can be used to check that the wire is free down to the anchor elevation, or to determine at which level it is trapped in the hole.

The collar pipe lower datum plate, rigidly attached to the collar of the hole, is the datum from which the readings are taken to each anchor elevation. From subsequent readings, displacement of the various anchors is detected and recorded. Problems associated with swelling and shrinkage of the surface soils, which can be of the order of tens of millimetres seasonally, are eliminated in the calculation of relative displacement between the anchors as each anchor is affected by the same amount.

The differential displacements between the various anchor elevations are used to determine the compression or tensile cracking and breaking up of the strata between the anchor elevations.

7.4 Underground Observations

The roof conditions in the test area were such that, under normal conditions, the only systematic support required was five 16 mm x 1.2 m full column resin bolts per intersection. Where slips or brows were encountered in the roof they were also supported using 16 mm x 1.2 m full column resin bolts. However, as a safety measure, prior to the start of the stooping operation, systematic support was installed throughout most of the area to be stooped, in the form of 16 mm x 1.8 m full column resin bolts, three in a row on a 2 m grid.

A mixture of sticks and roof bolt breaker lines was used during the stooping operation and both performed well. The roof bolt breaker lines consisted of two rows of 16 mm x 2 m full column resin bolts, five in a row with the rows 0.5 to 1 m apart.

The area was mapped by Ingwe Rock Engineering, the salient features being included in Figure 7-6.

Reduction in the size of the test pillar created large spans of between 11 m and 18 m, perpendicular to and diagonally across from the surrounding pillars. Once created, significant portions of the span in the proximity of the test pillar were unsupported. Because of safety implications regarding working under unsupported roof it was not possible to install sticks or packs around the test pillar to try and prevent any goaf material from coming into contact with the sides of the pillar. A photograph of the final reduced size test pillar is presented in Figure 7-7. The red and white strips of plastic tape hanging from the roof indicate the positions of the roof bolts in the original development. At the initial stage the pillar showed no signs of load as indicated in Figure 7-7.

From the extraction sequence shown in Figure 7-8 it can be seen that the reduction in size of the test pillar was carried out in two phases, starting before and ending after the extraction of pillar 2. Pillar 1 was then removed and in the stooping operation cuts No’s 11 and 12 had been extracted from pillar 4 when it was decided to leave the proposed cut No 13 intact, as this remaining portion of the pillar was observed to be highly stressed as a result of the extraction of the adjacent pillars. The Voest Alpine was trammed to pillar 3 to begin cut No 14.

On 17 January, the initial goaf fell in the area indicated in Figure 7-9, up against one side of the test pillar but stopping a short distance from the adjacent side. This goaf relieved some of the remaining load on pillar No 4 and it was subsequently extracted by cut No 13. The average height of this initial goaf was about 2.0 to 2.5 m and was less than the full mining height. As the stooping operation continued and further goafing occurred, increasing the overall goaf area, secondary goafing within the initial goaf area took place increasing the goaf height to an estimated 5 to 7 m.

Photographs of the primary and secondary goafing in the initial goaf area are presented in Figure 7-10.

The second goaf occurred on 20 January after pillars 3 and 6 had been removed and came close to the third side of the test pillar. The following day the goaf migrated into the area where pillar 9 had recently been extracted. This migration of the goaf area extended up to an estimated height of 5 to 7 m.

At the beginning of the stooping operation very small snooks were left standing. As the extracted area increased and the pillars became more highly loaded some large snooks were left. The approximate size and position of the snooks are shown in Figure 7-11. For comparison purposes photographs of the snooks left at pillars 1 and 7 are presented in Figure 7-12.

The final goaf occurred on 27 January 1997, five days after the last two pillars, 7 and 8, had been stooped. The test pillar was surrounded by the goaf. To what extent the goaf was applying confinement to the pillar is not known. A final underground visit was made to the site on 18 February 1997.

7.5 Extensometer Results

The first set of readings was taken on 13 January 1997. Monitoring continued up until 23 January 1997 with readings being taken in the morning on a daily basis, with the exception of Sunday 19 January. Although readings were also taken most afternoons, the morning readings are more comprehensive. On 27 January it was reported that large displacements had occurred, as a result of which the instrumentation had gone off scale and could not be read.

A visit to the site on 28 January revealed that a threaded stud in the monitoring linkage was loose and free to rotate, which could introduce a variation in the length of the No 4 anchor extensometer set-up. This suggests that the No 4 anchor monitoring results may not be as accurate as those for the other anchors, although displacement trends should be similar.

On 28 January, with the exception of anchor 5, all the weights had been pulled up against the top datum plate and were held there by the tension in the wires. By individually cutting the weights off monitoring wires 1, 2 and 4, it was estimated that each wire had been pulled down the hole by approximately 600 mm. [This figure excludes any stretching that may have occurred in the wires as a result of large displacements.] The monitoring wire from anchor 3 was lost as it sprang down the hole during the weight removal process.

By placing an additional 23 kg weight on monitoring wire 5 and measuring the induced extension, using a tape measure graduated down to 1 mm divisions, a load extension factor for the wire was

derived. After joining suitable lengths of wire on to wires 1, 2 and 4, the additional weight was added to each of the wires in turn. By measuring the individual induced extensions and using the factor calculated from wire No 5, the 'free' lengths of the wires were calculated and are given in Table 7-1.

Although the measuring device was relatively primitive, the above calculated 'free' wire lengths tended to indicate that each wire was still intact down to its attached anchor, even though they were passing through a region of relatively massive dislocation of the borehole somewhere in the super incumbent strata above the anchor 4 elevation.

Table 7-1 Calculated 'free' wire lengths 28 January 1997

Anchor	Installation depth	23 kg extension (mm)	'Free' wire length
1	105 m	65	102 m
2	102 m	64	100 m
4	93 m	60	94 m
5	55 m	35	

In order to check these results using a more accurate system, the site was revisited six days later on 3 February. The load extension tests were repeated using a spring tensioner micrometer, which is capable of measuring down to 0.01 mm. As previously mentioned, with this reading technique it is possible to calculate the two extension values between each set of three readings. By comparing the values, calculated from readings taken on 3 February, against the average of the values of the 10 sets of readings taken up to 23 January, it was possible to calculate a 'free' wire length for each monitoring wire including wire 5. These are included, along with the 'free' lengths calculated on 28 January, in Table 7-2.

Table 7-2 Calculated 'free' wire lengths 28 January & 3 February 1997

Anchor	Installation depth	28 January 'free' wire length	3 February 'free' wire length
1	105 m	102 m	95 m
2	102 m	100m	97 m
4	93 m	94 m	89 m
5	55 m		55.5 m

From the results presented in Table 7-2, there appears to have been a decrease in the lengths of all three 'free' wire lengths of between 3 m and 7 m although this could possibly be due to differences in the relative accuracies of the different systems used. The shortest 'free' wire length was No 4 which indicated that a restriction prevented it from moving below the 89 m elevation from

surface. The borehole log indicates the presence of a poor (weak) shale band extending from approximately 86 to 91 m below surface (approximately 7 m above the seam). It is therefore considered probable that crushing and or migration of material within this zone could be responsible for generating frictional holding forces of varying degrees on all the wires passing through this region.

7.6 Data Analysis

In Figure 7-13 the five anchors have been separated from one another for reasons of visual clarity and have been plotted relative to the surface using the borehole collar as the datum. Past experience has attributed the apparent downward movement of the anchor closest to the surface (anchor 5) to swelling within the upper weathered zone due to rain and an increase in the water table level. The dates on which the major goafs occurred have been included.

Anchor 4 exhibited an apparent upward movement between 20 and 21 January. This is not considered to be a real displacement and could either be a result of the loose stud being inadvertently unscrewed or anchor slippage, the latter being considered highly unlikely as it is anchored in sandstone.

Because the borehole collar on surface is used as the datum and is assumed not to move, any compression within the strata column manifests itself as the apparent upward movement of any anchors below the compressive zone.

The compression within the seam horizon can clearly be seen as anchors 2 and 3 are observed to be moving towards each other while anchor 1, below the seam, more or less duplicates the displacement pattern of anchor 2. This apparent upward movement indicates a shortening of the distance between the borehole collar and anchors 1 and 2.

The acceleration in the apparent downward movement of anchors 3 and 4, starting from 20 January suggests that the strata column above the pillar, which is under compressive loading conditions, has a section within it that is exhibiting tensile strain as anchors 3 and 4 are moving away from anchor 5. This could be interpreted as a dead weight loading situation with the top of the loading beam becoming detached from the overburden strata somewhere between anchors 4 and 5 (5 to 43 m above the seam).

In Figure 7-14 the swelling within the weathered zone has been eliminated as the displacements of anchors 2, 3, 4 and 5 have been plotted relative to the deepest anchor (anchor 1), which is below the seam and assumed to be stable. As is to be expected, the deformation values within the strata

column increase the higher the anchoring points are above the floor of the seam. However the largest compression is within the pillar (between anchors 2 and 3).

The anchor 4 readings are anomalous and show higher compressive values than anchor 5 situated 38 m above it. This could well be as a result of the previously mentioned loose stud, half a rotation of which would give an apparent displacement of the order of 1 mm. Since this particular installation is suspect, the finite readings should be treated with caution although most of the trends with time agree closely with the other anchor displacements.

Up until the time of the initial goaf on 17 January, the displacements measured at anchor elevations 2, 3, 4 and 5 were compressive but very small, 1 mm or less. From then until the second goaf on 20 January all four anchors exhibited similar trends as the respective compressive values increased. From 20 January until the final reading on the 23rd, there is a distinct acceleration in the displacement of anchor 3 in the immediate roof of the pillar as well as in the displacement of the anchors above it (anchors 4 and 5). The point of interest here is that the strata between anchors 3 and 5 switched from compression to relative tension only on 23 January, the day of the final reading, with an apparent elongation of less than 1 mm over the 38 m length of strata that separates these two anchors.

Relative tension is explained as follows: When the instrumentation was installed, the strata above the seam were already in a compressive loading regime. Any compressive increase, i.e. anchors moving towards each other, would easily be recognised as such. However, if the anchors returned to their original (installation) positions and then continued to move away from each other, the graphical interpretation would indicate tensile strain from the point where the original position was reached. In reality, however, the anchors would have to continue to move apart an unknown distance to fully unload the compressive bias in the system before the transition to tensile strain could take place.

The effects of the three main goafs appear to have acted as triggering mechanisms with regard to the overall rates of displacement of the majority of the anchors.

In Figure 7-15, the displacements of anchors 1 (1.5 m below the seam) and 2 (1.5m above the floor of the seam) are plotted relative to anchor 3. As is to be expected, they both follow similar displacement profiles with a small compressive strain, of about 0.5 millistrains, becoming apparent after the initial goaf on 17 January.

The readings that most closely reflect the deformation of the pillar are those between anchor 2 and 3 an interval of 3.2 m. These results are shown in Figure 7-16. This shows an increase in strain as surrounding pillars are extracted. The occurrence of the second goaf appears to have had the largest effect on the increase in the strain rate. On the day of the final readings, the strain value

was of the order of three millistrains. This value is generally considered insufficient to suggest that the pillar had failed at that time.

If we take the values presented in Figure 7-16 and extrapolate them using a best fit exponential curve, as illustrated in Figure 7-17, the indications are that displacement in excess of 60 mm, or approximately 20 millistrains, could have occurred before the visit of 27 January. At this strain value it is generally accepted that the pillar would have failed.

Further analysis of the results was carried out to investigate the possibility of the existence of another failure mechanism operating in unison with or independently of the pillar failure scenario.

If it had been possible to take a set of readings on anchors 1, 2, 3 and 4 on 28 January and plot them, all four would have shown an apparent downward movement of about 600 mm relative to anchor 5. As has earlier been suggested, this appears to have been as a result of some form of interference with the monitoring wires above the anchor 4 elevation. Anchor 5 was in the strata above this disturbance and was not affected by it. The displacements of anchors 3 and 4 plotted relative to anchor 5 are presented in Figure 7-18. The trend of anchor 3 until the second goaf on 20 January was a compressive movement with respect to anchor 5. Thereafter, there was an apparent dilation which had reached a value of approximately 2 mm by 23 January. Although the finite values indicated for anchor 4 are to be treated with caution, they followed the same trend as those for anchor 3 from the time of the third goaf on 21 January onwards.

These apparent dilations could possibly be attributed to a disturbance or dislocation occurring in the hole pulling on the monitoring wires. Since the anchored end is not free to move, any displacement would be transmitted to the free end of the monitoring wire on surface.

It is known that by 27 January there was some form of restriction in the hole just above the anchor 4 elevation. If what can be seen in Figure 7-18 is the onset of the ‘interference’ with monitoring wires 3 and 4, it could be assumed that monitoring wires 1 and 2, which passed through the same region, were also being affected in a similar manner.

In order to test the validity of this scenario, a data manipulation test was carried out. By taking the change in the recorded values of anchors 1, 2, 3 and 5 until 20 January, an average linear percentage increase applicable to each monitoring point was calculated and used to generate data until 23 January. Anchor No 4 was given an appropriate value to fit in with the rest. From 20 to 23 January a linear increment totalling 2 mm, similar to the actual apparent downward movement recorded on anchor 3, was introduced and used to adjust the readings of anchors 1, 2, 3 and 4. The results are presented in Figure 7-19.

Here the displacements of all five anchors relative to the borehole collar show similar trends to the recorded measurements up until 20 January. From 20 January onwards, anchors 3 and 4 moved down, away from anchor 5, while continuing compression took place between anchors 2 and 3. The change in the displacement rate is also noticeable on anchors 1 and 2 from 20 January onwards. The phenomenon was however not evident in the recorded readings presented in Figure 7-13. This subtle difference tends to reinforce the credibility of both the actual extensometer readings and the pillar failure scenario.

The surface borehole was last visited on 28 April. The weights on monitoring wires 1, 2 and 4 were again all up against the top datum plate, indicating that additional displacement / dislocation had occurred between the anchor 4 and anchor 5 elevations. The displacement of anchor 5, relative to the borehole collar, since the reading on 23 January had increased by approximately 8 mm and was in all probability due to swelling of the weathered zone. There was no evidence of the goaf having migrated past the anchor 5 elevation, 55 m from the surface. This data is included in the longer term monitoring results presented in Figure 7-20.

7.7 Conclusions

As a stooping operation the reduction in size of the test pillar and the extraction of the surrounding pillars was successful.

The monitoring of the surface borehole extensometer, which was carried out on a daily basis from 13 to 23 January, with the exception of the 19th, produced useful results. However, the most dramatic and important ground movements occurred during the weekend between 23 and 27 January during which time manual measurements were not taken.

In order to monitor displacements at the seam horizon with an accuracy of the order of 1.0 mm, it is necessary to use the manual micrometer loading device mentioned in the instrumentation section. If this exercise were to be repeated, a compromise between reading accuracy and continuous monitoring using a data logging system would have to be introduced to avoid losing very important, if not vital, information during the dynamic stages of the goafing operation.

The aim of this experiment was to load the pillar to failure and monitor the pillar and strata compression. This was achieved to an extent but the dynamic rate of loading was not captured by the monitoring system.

The intended/suggested methods of attempting to control the immediate roof and the area around the pillar proved to be impractical owing to the safety aspects and practicalities concerned with working under the unsupported roof, exposed as the test pillar was reduced in size. Goaf material

was observed to be up against at least one side of the test pillar which would have influenced its strength characteristics.

Having goafing heights estimated at 5 to 7 m close to the pillar could have reduced the confinement and degraded the stability of the 'weak' shale band approximately 7 m above the seam, causing the pillar to fail prematurely.

The monitoring did not prove beyond reasonable doubt that the pillar had failed. However, by extrapolation, using a best fit exponential curve, indications are that the test pillar would in all probability have failed before the visit of 23 January when the extensometer was found to be off scale.

7.8 Recommendations

Remote and continuous recording of the instrumentation is essential when monitoring a dynamic process such as the effects of goafing. A compromise must be reached between continuous recording and the capabilities of the manual readings as regards accuracy. Without such a compromise, it will not be possible to capture all the relevant data necessary to establish the 'full picture' of the behaviour of both the pillar and the surrounding strata.

The major outstanding problem is the control of the immediate roof and the area around the pillar to maintain the goaf at an acceptable distance to prevent confinement taking place. Further discussions with experienced practical mining personnel are required to find a workable solution. Without a practical solution, the chances of underground instrumentation remaining intact long enough to yield vital information are slim. Uncertainty as to whether the pillar has been confined by the goaf will inevitably cast doubt on the value of the data obtained.

7.9 Acknowledgements

The assistance of the colliery General Manager and staff as well as the rock engineering department of Ingwe is gratefully acknowledged.

7.10 References

Jack, B. W. and Prohaska, G. D. 1994 Observation and evaluation of a test pillar left intact in a stooping section. SIMRAC internal note (25/7/94).

Jack, B. W. and Prohaska, G. D. 1995 Number 2 seam pillar experiment. SIMRAC internal note (13/04/95).

Jack, B. W. and Prohaska, G. D. 1995 Observation and evaluation of the second test pillar at a colliery. SIMRAC internal note (20/06/95).

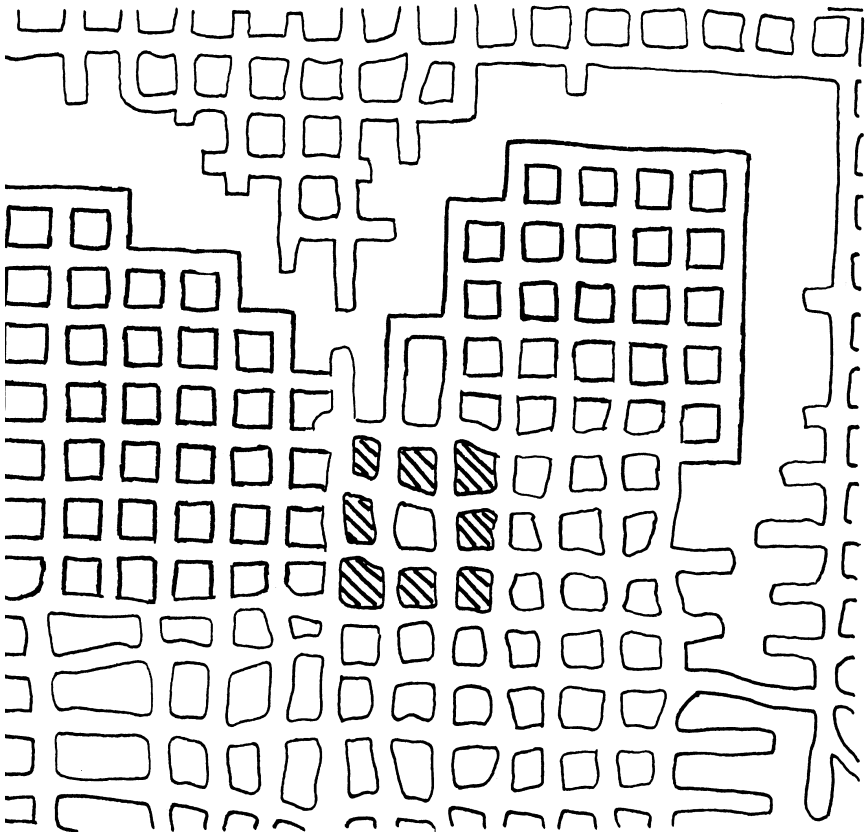

Figure 7-1 General layout of the area showing the eight pillars surrounding the test pillar.

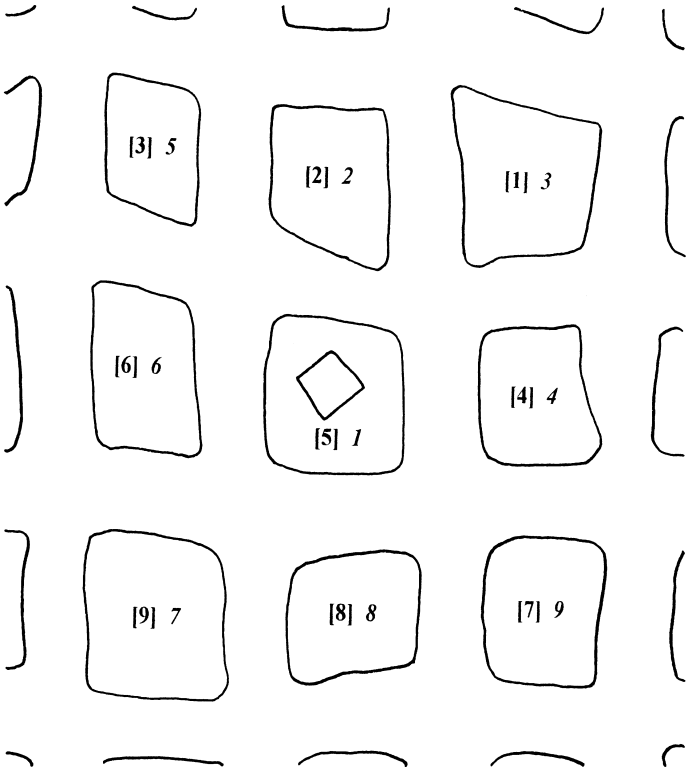

Figure 7-2 Pillar numbers [1] and extraction sequence, 1.

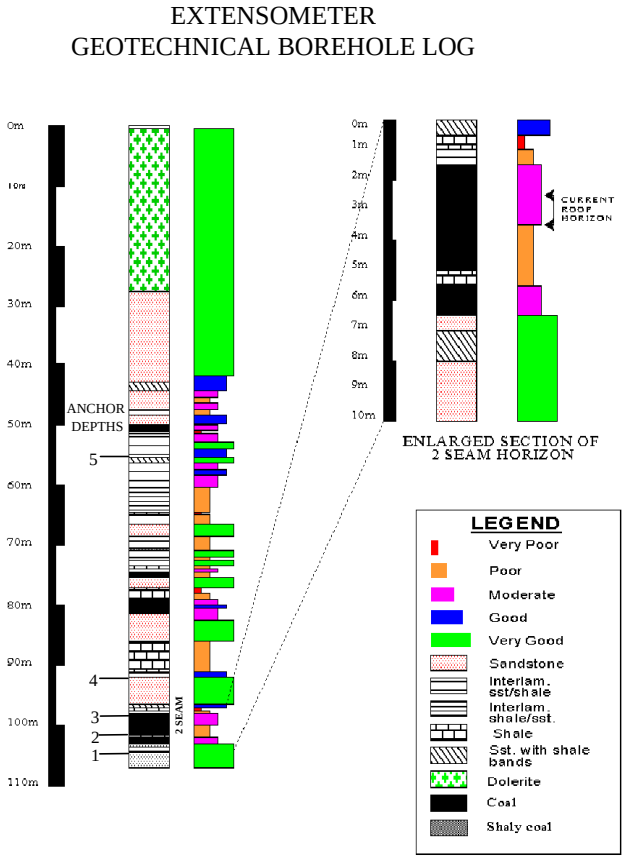

Figure 7-3 Geotechnical borehole log.

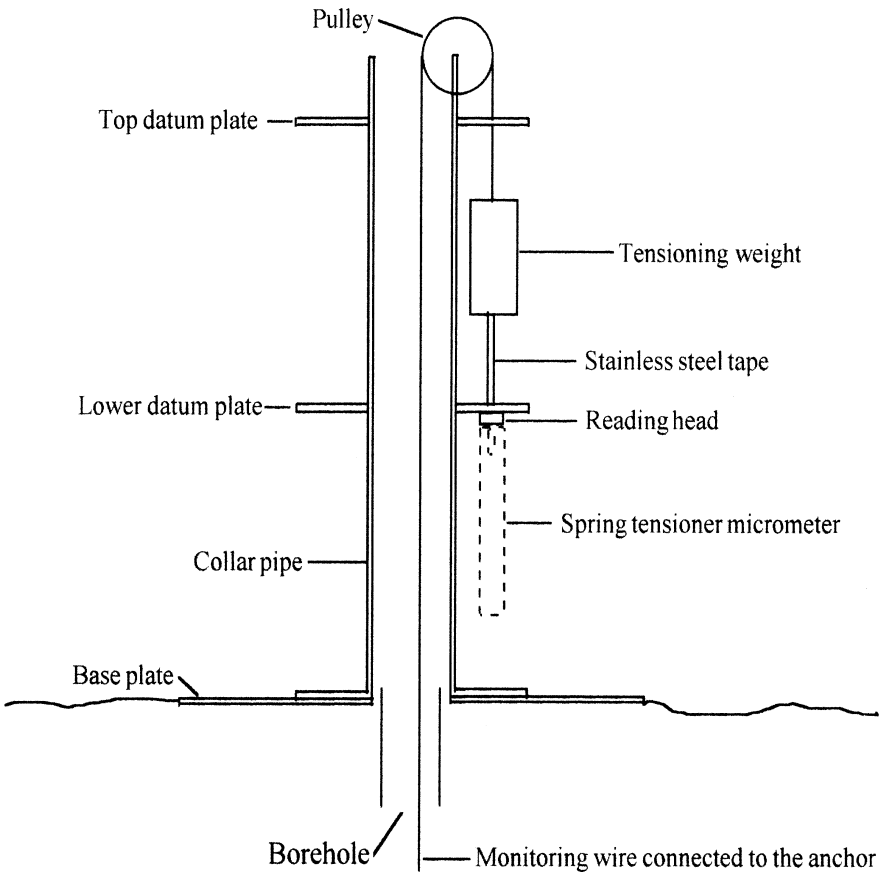

Figure 7-4 The collar pipe set-up.

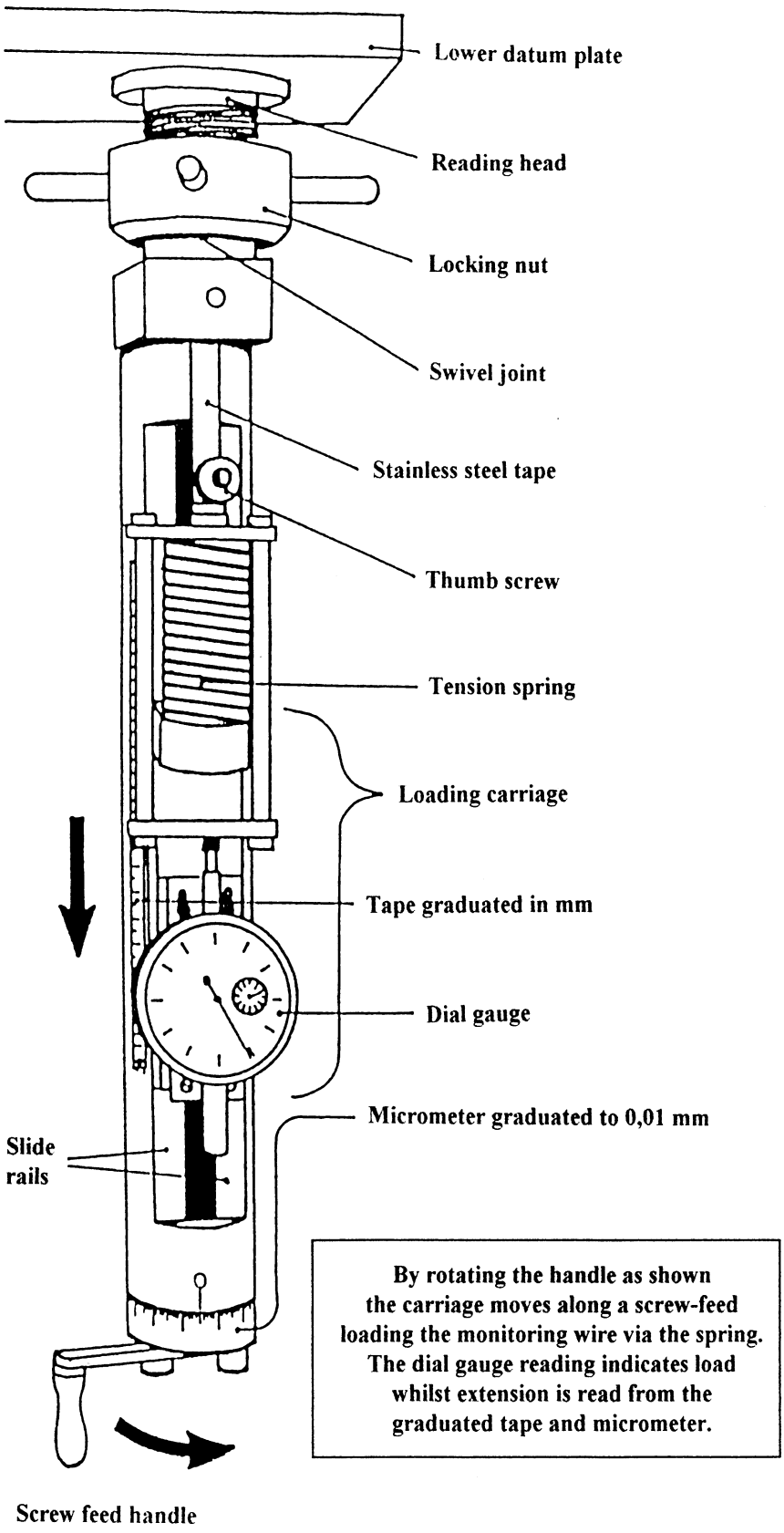

Figure 7-5 Extensometer loading device.

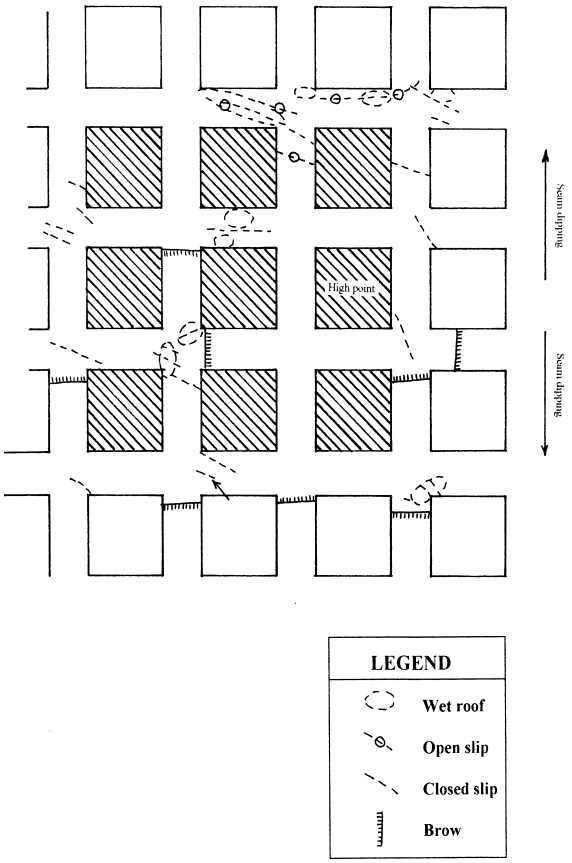

Figure 7-6 Roof features (after Ingwe Rock Engineering).

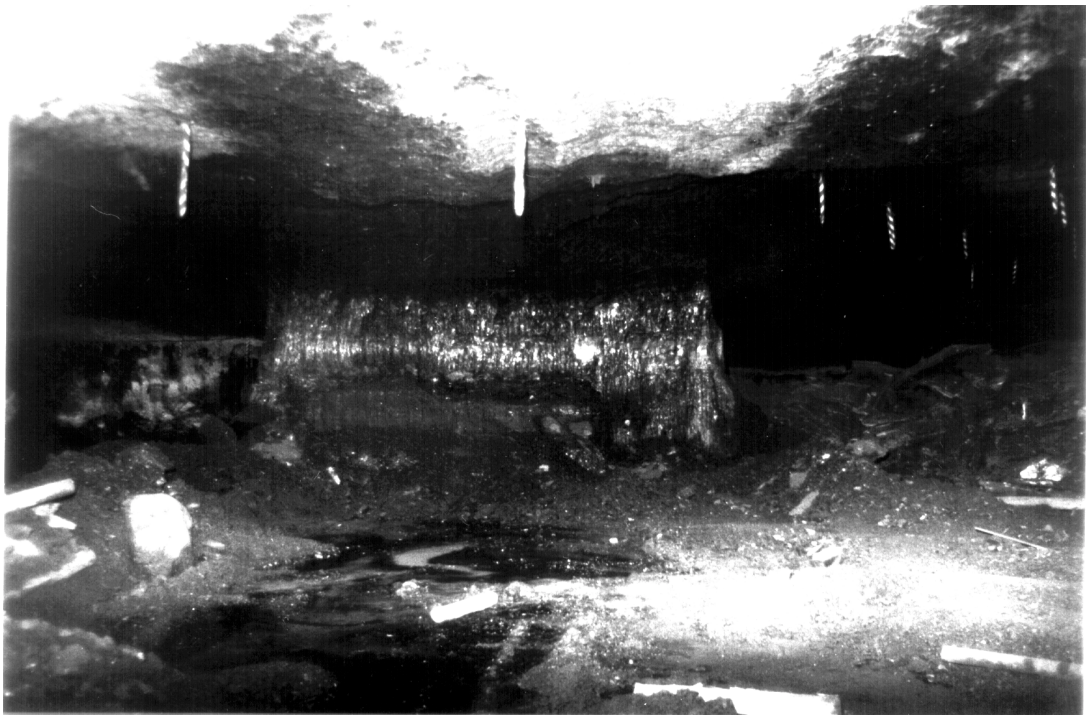

Figure 7-7 The test pillar after being reduced in size to 4 x 5 m.

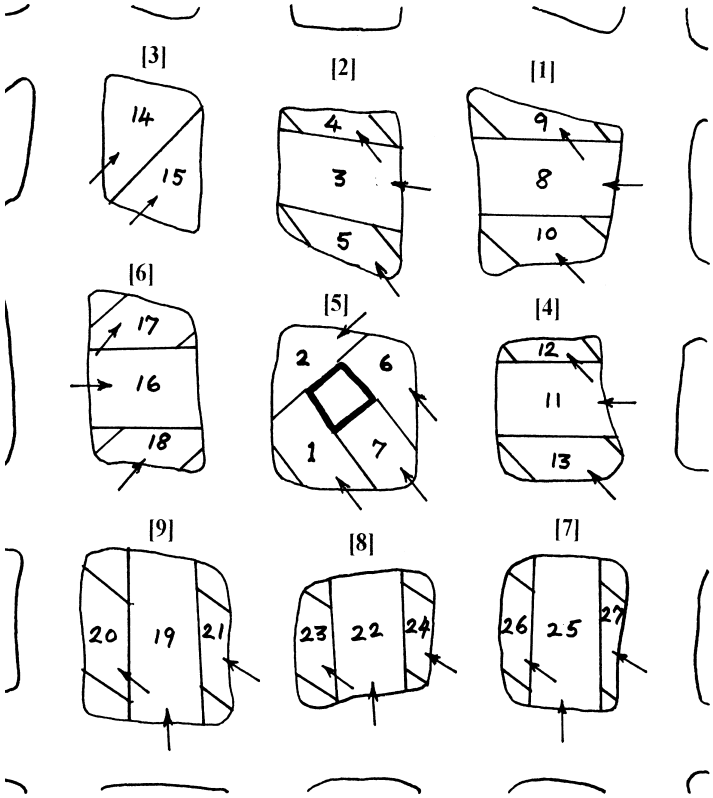

Figure 7-8 Cut extraction sequence.

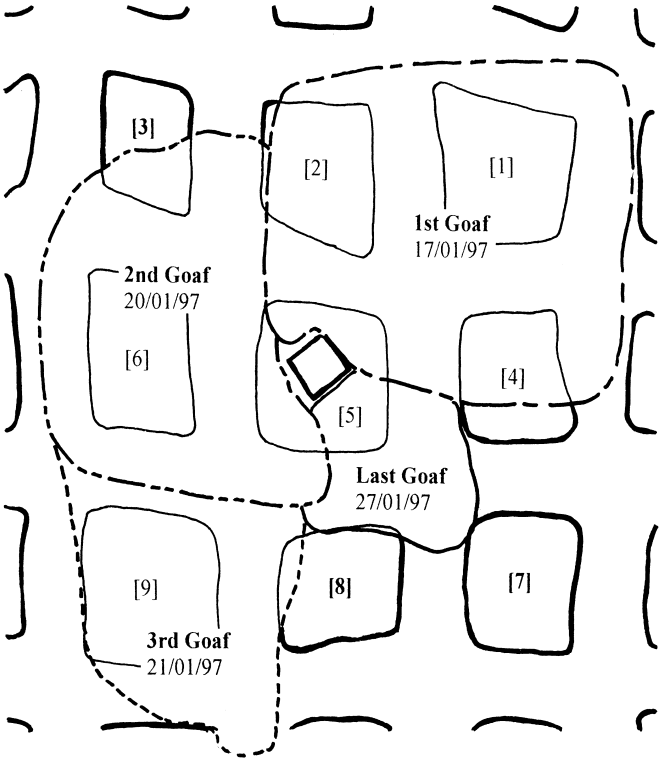

Figure 7-9 Goafing sequence.

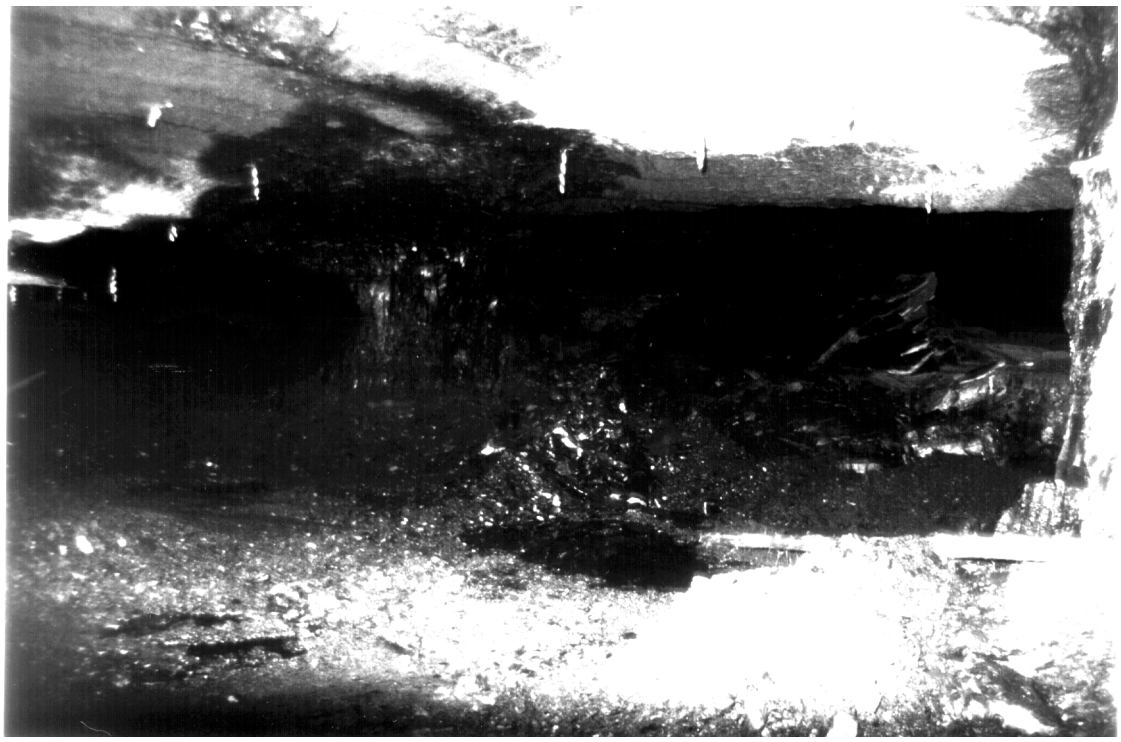

Primary goaf approximately 2 to 2.5 m in height

Secondary goaf approximately 5 to 7 m in height

Figure 7-10 Primary and secondary goafing of the initial goaf area.

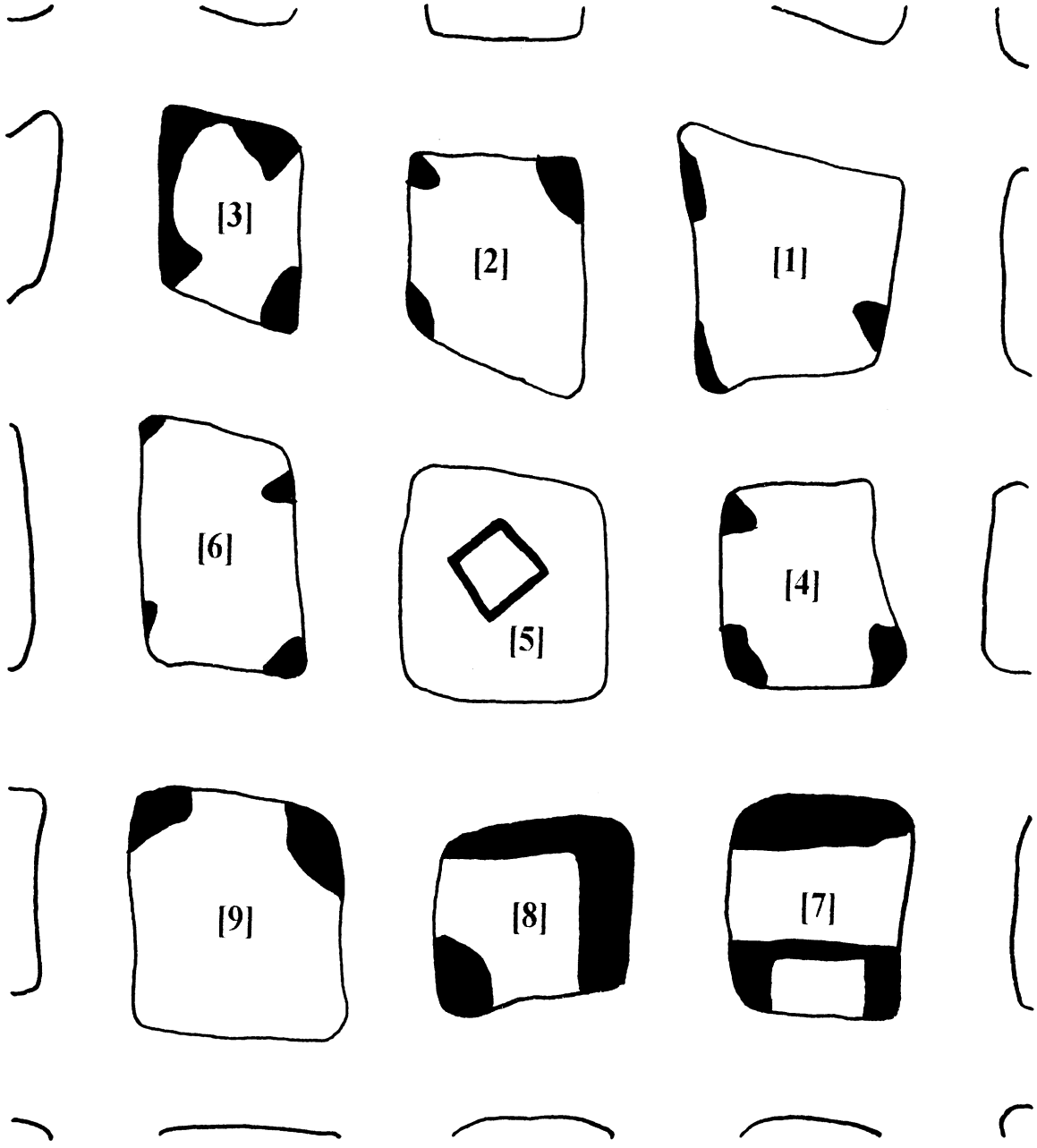

Figure 7-11 Approximate size and position of snooks.

Snooks left at pillar No 1

Snooks left at pillar No 7

Figure 7-12 Snooks left at pillars no 1 and no 7.

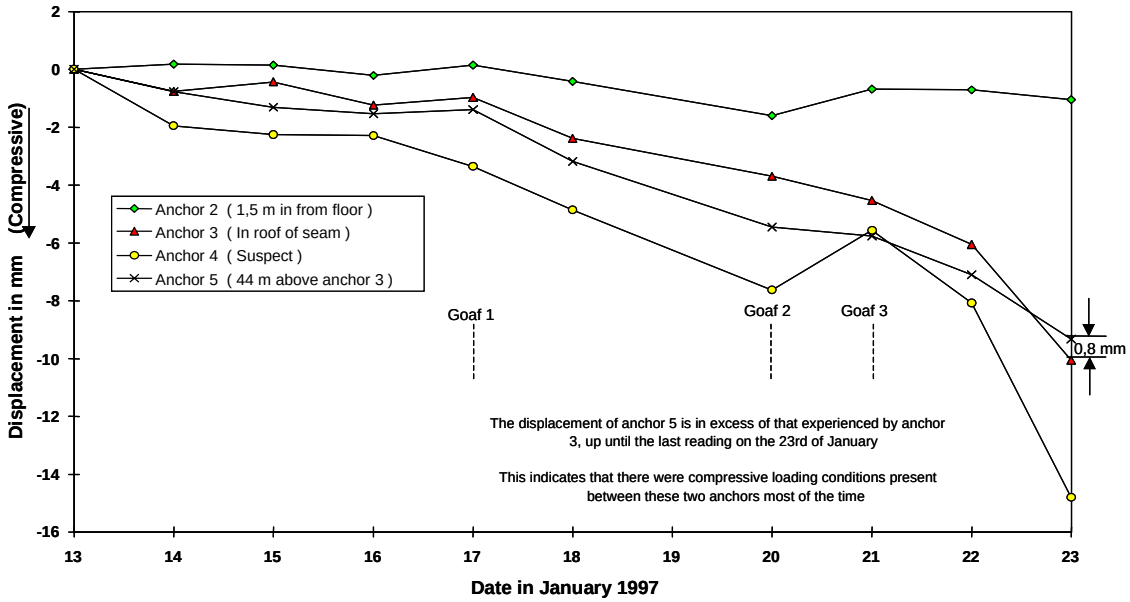

Figure 7-13 Anchor displacements relative to the borehole collar.

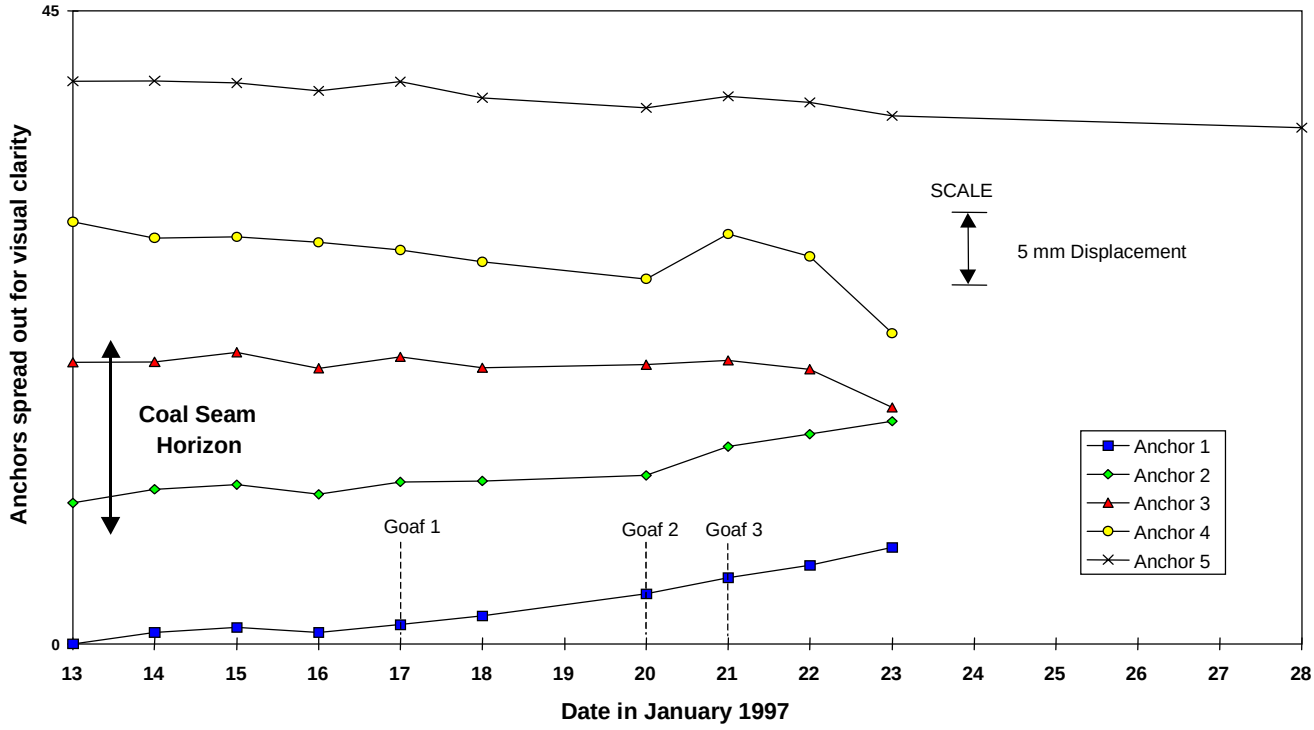

Figure 7-14 Anchor displacements relative to anchor 1.

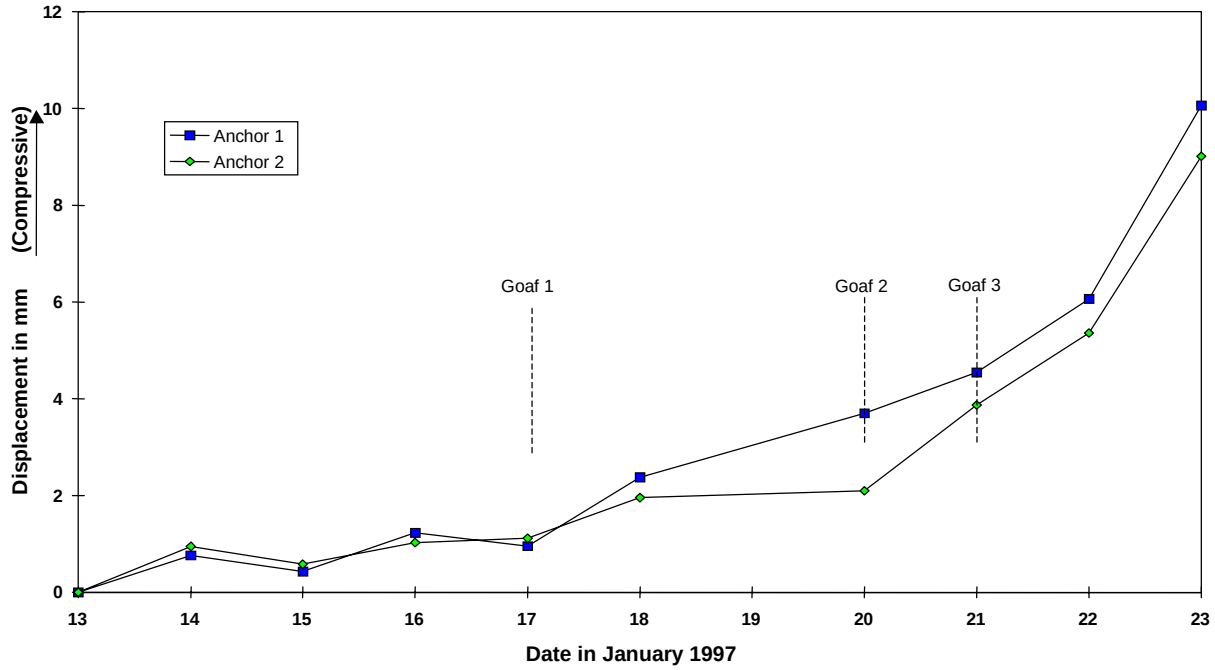

Figure 7-15 Displacement of anchors 1 and 2 relative to anchor 3.

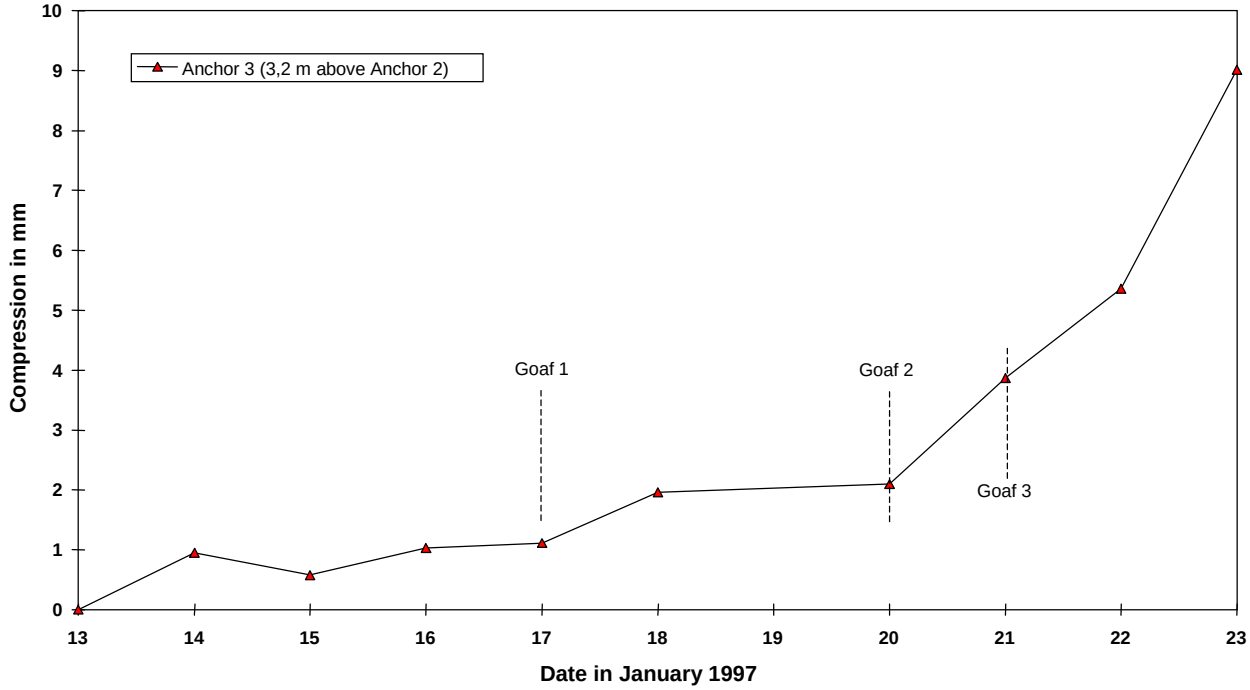

Figure 7-16 Compression of the coal seam between anchors 2 and 3.

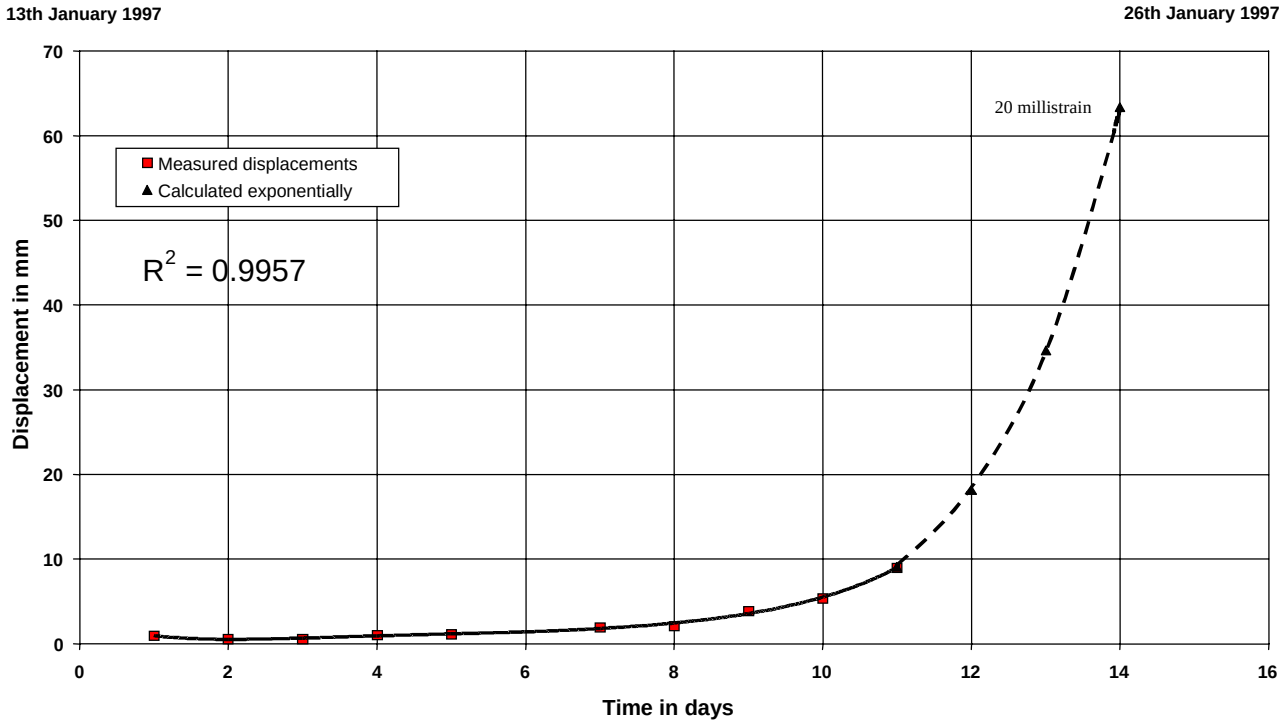

Figure 7-17 Exponential interpretation.

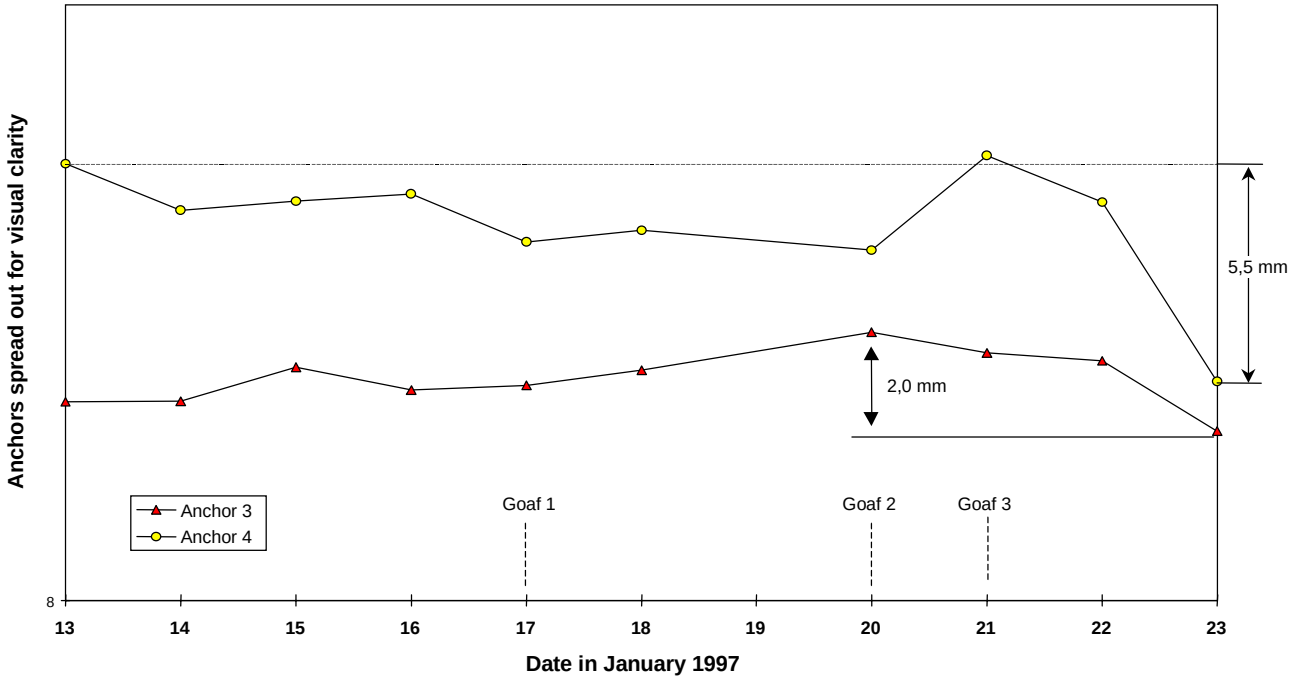

Figure 7-18 Displacement of anchors 3 and 4 relative to anchor 5.

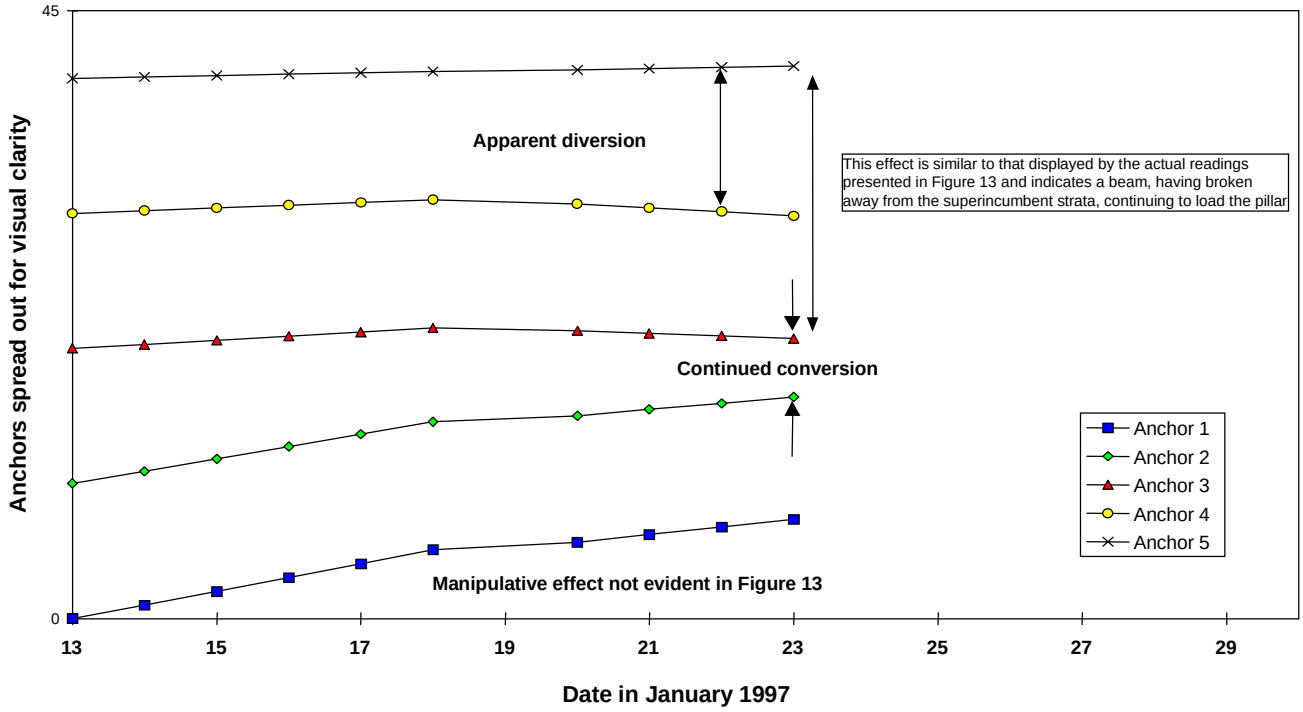

Figure 7-19 Result of the introduction of a progressive apparent downward interference on monitoring wires 1, 2, 3 and 4.

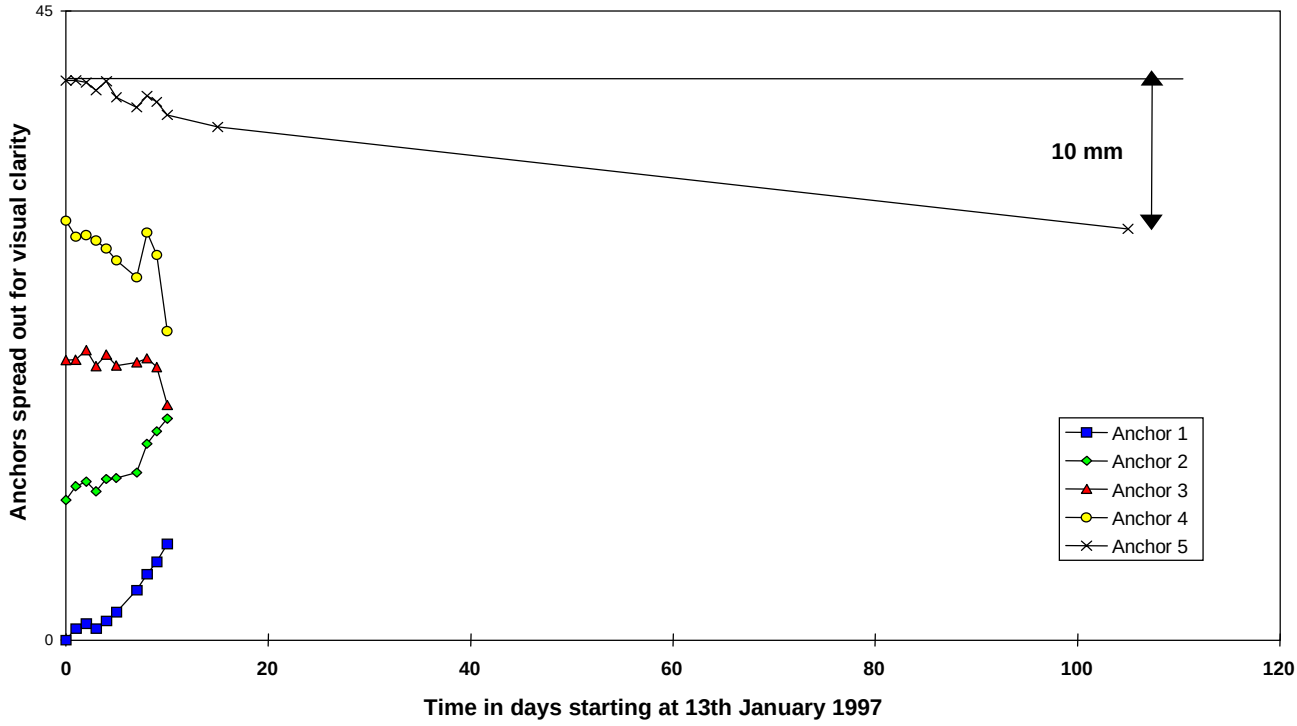

Figure 7-20 Longer term monitoring of anchor 5.

8 Identification of geotechnically similar areas

8.1 Introduction

The objective of this component of the project is to quantify the geotechnical characteristics of the most commonly exploited coal seams in South Africa and thus obtain a regional subdivision into geotechnical areas. This was achieved in areas where the range in values of parameters, which reduce pillar system stability, is the same as those encountered in the original area of investigation.

It is seen from analyses of pillar collapses that Salamon and Munro's empirically derived pillar strength formula works very well in areas where the original data was collected and in other areas where similar geotechnical conditions exist. However, several pillar collapses occurred where conditions are in one aspect or another significantly different to that from which Salamon's data set was collected.

Analysis of pillar collapses highlighted showed that in many cases that occurred after 1967, there is a dominant factor which caused the collapse. Therefore, in order to define the dominant factors affecting the pillar stability in different geotechnical areas where the critical parameters are outside the Salamon's range, pillar rating data collected as part of SIMCOL 021A project was analysed.

Geotechnical areas should be defined by specific combinations of geological factors comprising the rock mass, which in turn dictate the expected response of the rock mass to mining. Thus the crucial factor for discriminating such areas would be differences in the expected response of the rock mass to mining operations. Once this response is ascertained the ultimate aim would be to adopt appropriate rock engineering strategies to minimise potential rock related hazards.

8.2 Pillar rating database

In 1993, as part of SIMCOL 021A project, over 300 panels in 19 seams at nine different coalfields were visited in order to establish individual seam strength formulae and the roof, support, discontinuities and pillar conditions rated according to the system developed by Madden (1985).

Assessment of pillar performance was carried out in three stages. Firstly, the conditions of the pillar and the surrounding strata were described and recorded on a special form. Secondly, each observation was rated according to the relative importance of the parameters.

The classification process was based on detailed visual observations of bord and pillar conditions. A randomly chosen pillar in the centre of a bord and pillar panel is assumed to be representative of the area, is rated. The following parameters were taken into account in the rating system:

- Geology, including roof and floor thicknesses and overburden strata
- Mining dimensions (pillar and bord dimensions and panel width)
- Pillar performance (pillar fracturing and scaling)
- Roof performance (density and height of roof falls)
- Support performance (efficiency of the installed support)
- Effects of structural discontinuities on the pillar stability.

As many as 45 different parameters were included in the database. These parameters include the measurements taken underground and surveyor offsets, safety factors calculated from these measurements, geological information, as well as visual underground observations that enabled discontinuity, roof, support and pillar ratings to be determined. From all these parameters, only the discontinuity and roof ratings were thought to be relevant in identifying the different geotechnical areas. Therefore, these two ratings were used in this analysis. Subsequent to the data collection, it was realised that foundation failure, or a mechanism of pillar failure by splitting due to large lateral displacements in the foundation, is an important possible mechanism of pillar system failure. Therefore, foundation ratings are not included in this analysis. In addition, the geotechnical influences on foundation failure are not clear at his stage. This is an area of future work.

In the rating of the immediate roof, roof competence, density and the height of falls were considered, with a maximum rating of 200 points. Table 8-1 was used in the roof rating system.

Table 8-1 Roof rating components.

Point		Roof Competence
100		No Falls/cracks
75		No falls but cracks
50		Occasional cracks
25		Falls to a competent layer
0		Falls to an incompetent layer
		Occurrence of Falls
100		None
75		Occasional on a slip/dyke
50		Associated with slip/dyke
25		Intersections only
0		Intersections and bords
		Height of falls
1.00		None
0.75		Slight 0.1 m
0.50		Moderate 0.1 - 0.5 m
0.25		Severe 0.5 - 2.0 m
00.0		Very severe >2.0 m

If the thickness of falls to an incompetent layer are greater than 2.0 m in bords and intersections, then the roof is rated zero.

The performance of roof was calculated using the following equation:

Roof rating = Roof competence + (Density of falls x Height of falls).

The effect of structural discontinuities on the pillar strength was also investigated. Structural discontinuities such as slips, faults and dykes were mapped and their effects on pillar stability were rated. No effect is rated the highest (100). A severe effect where the discontinuities reduce the pillar area by approximately 30 % because of spalling, is rated zero. Table 8-2 was used to determine the effect of discontinuities on pillars.

The analyses of discontinuity and roof ratings showed that one of these ratings alone is not sufficient to identify different geotechnical areas. However, combinations of the two ratings can be used to identify different geotechnical areas in South African seams.

Table 8-2 Discontinuity rating components

point		**Effect on the pillar**	
100		None	
75		Slight	Minor effects on corners
50		Moderate	major effects on a corner or a sidewall
25		Severe	major effects on corners or sides
0		Very severe	feature reduces pillar area by 30%

The averages of these two ratings for different seams are plotted in Figure 8-1. Figure 8-1 also shows the data from Salmon and Munro (1967), Madden (1988) and 23 additional collapses as well as combinations of these three data sets for different coal seams. The seams shown in this figure do not represent the all database given in legend by the authors, but rather indicates one or more collapses in specific seams. For example, Salamon had only one collapse data in Witbank No 1 Seam, which is shown with a circular black dot in the figure, and there was no other collapses in this Seam. Similarly, all three databases had one or more collapses in Vereeniging No 2 and 3 Seams, this seam is represented with an open black circle in the figure.

This figure highlights that while in many seams the effect of discontinuities on pillar performance was similar, the roof rating can be significantly different which may determine the stability of the excavations and indicate relative support requirements.

Based on this figure, it was concluded that in South African seams 8 different geotechnical areas can be identified, which have a similar roof and discontinuity condition. These seams and the groups are detailed in Table 8-3.

Table 8-3 Identified geotechnical areas for South African coal seams.

Group No	Seam - Coalfield
1	Main - Zululand
2	Alfred - Utrecht
3	5 - Witbank 7 - Soutpansberg
4	2 - Witbank 4 - Highveld
5	Dundas - Utrecht 2 &3 - Vereeniging
6	Top-Bottom - Klip River 4 - Witbank
7	5 - Highveld Dundas - Vryheid Gus - Vryheid Alfred - Vryheid
8	Gus - Utrecht CU+CL - Eastern Transvaal 1 - Witbank 2 - Highveld

The data shown in Figure 8-1 is also given in Table 8-4 together with number of observation sites and the standard deviations of each seam for both discontinuity and roof ratings.

Table 8-4 Average discontinuity and roof rating results for each seam.

SEAM	COALFIELD	NUMBER OF SITES	ROOF RATING	DISCON. RATING	STDEV. ROOF RATING	STDEV. DISCON. RATING
2	Vereeniging	7.0	13.9	61.1	19.7	37.8
Dundas	Utrecht	10.0	48.8	61.4	54.8	17.5
Alfred	Utrecht	7.0	67.9	92.9	76.0	12.2
4	Highveld	50.0	118.3	90.9	79.8	20.1
Gus	Vryheid	10.0	128.8	100.0	75.2	0.0
2	Witbank	111.0	129.5	93.2	78.2	12.8
Alfred	Vryheid	10.0	130.0	100.0	75.3	0.0
Dundas	Vryheid	8.0	146.9	100.0	76.1	0.0
Top-Bottom	Klip River	24.0	154.7	92.7	73.2	20.4
5	Highveld	2.0	156.3	100.0	61.9	0.0
4	Witbank	25.0	166.7	93.0	61.4	18.4
Main	Zululand	11.0	178.4	45.5	38.7	18.8
7	Soutpansberg	10.0	185.0	87.5	47.4	13.2
5	Witbank	12.0	198.1	86.5	7.2	16.9
Gus	Utrecht	7.0	200.0	92.9	0.0	12.2
CU+CL	Eastern Transvaal	18.0	200.0	98.6	0.0	0.0
2	Highveld	6.0	200.0	100.0	0.0	0.0
1	Witbank	12.0	200.0	100.0	0.0	0.0

8.3 Conclusions

The analyses of discontinuity and roof ratings showed that one of these ratings alone is not sufficient to identify different geotechnical areas. However, a combination of them can be used to identify different geotechnical areas in South African seams. Based on the analysis of these two ratings eight different geotechnical areas which have similar roof and discontinuity conditions have been identified. These seams and the groups listed in order of relatively good to relatively poor conditions are as follows are shown in Figure 8-1. The inclusion of foundation failure in the characterisation of geotechnical areas is an area of future work.

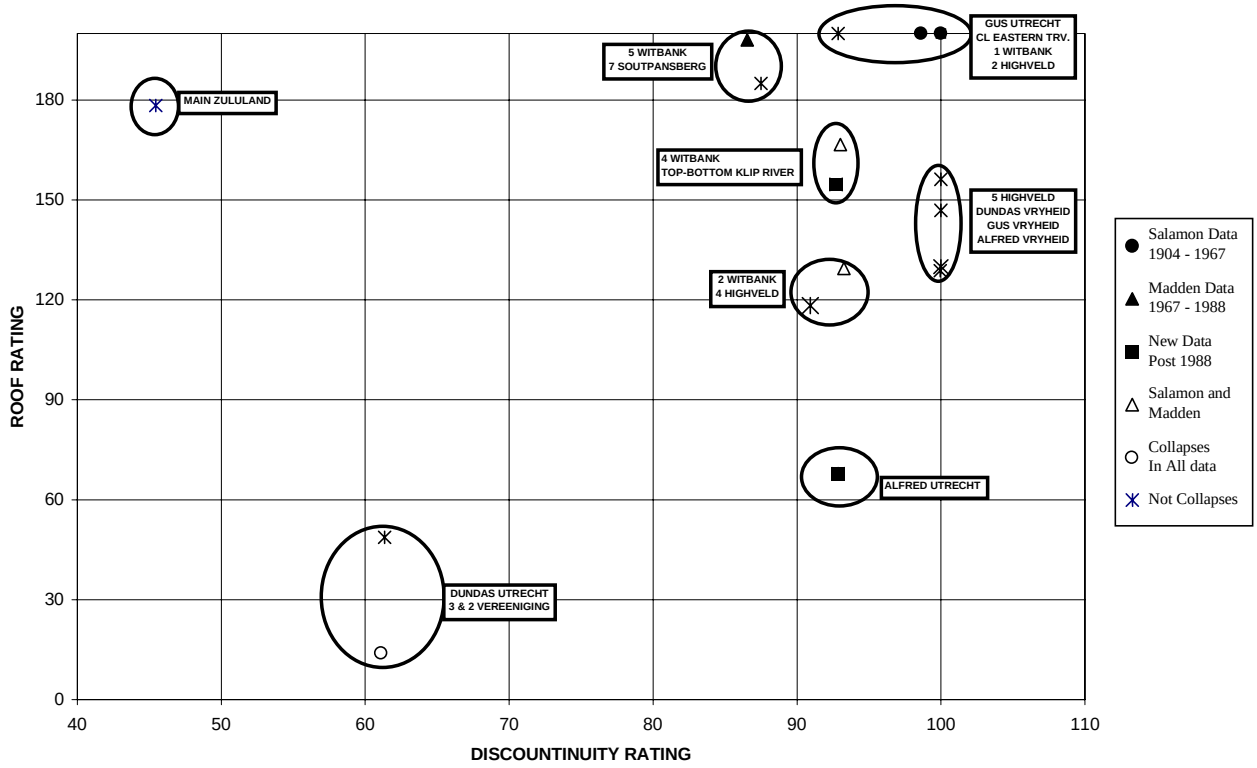

Figure 8-1 Geotechnical areas identified by discontinuity and roof ratings.